

JSCSEN 89(5)599-783(2024)

ISSN 1820-7421(Online)

Journal of the Serbian Chemical Society

Electronic
version

VOLUME 89

NO 5

BELGRADE 2024

Available on line at



www.shd.org.rs/JSCS/

The full search of JSCS
is available through

DOAJ DIRECTORY OF
OPEN ACCESS
JOURNALS

www.doaj.org

The **Journal of the Serbian Chemical Society** (formerly Glasnik Hemijskog društva Beograd), one volume (12 issues) per year, publishes articles from the fields of chemistry. The **Journal** is financially supported by the **Ministry of Education, Science and Technological Development of the Republic of Serbia**.

Articles published in the **Journal** are indexed in **Clarivate Analytics products: Science Citation Index-Expanded™** – accessed via **Web of Science®** and **Journal Citation Reports®**.

Impact Factor announced on 28 June, 2023: **1.000**; **5-year Impact Factor: 1.100**.

Articles appearing in the **Journal** are also abstracted by: **Scopus, Chemical Abstracts Plus (CAplusSM), Directory of Open Access Journals, Referativnii Zhurnal (VINITI), RSC Analytical Abstracts, EuroPub, Pro Quest and Asian Digital Library.**

Publisher:

Serbian Chemical Society, Karnegijeva 4/III, P. O. Box 36, 1120 Belgrade 35, Serbia
tel./fax: +381-11-3370-467, E-mails: **Society** – shd@shd.org.rs; **Journal** – jscs@shd.org.rs
Home Pages: **Society** – <http://www.shd.org.rs/>; **Journal** – <http://www.shd.org.rs/JSCS/>
Contents, Abstracts and full papers (from Vol 64, No. 1, 1999) are available in the electronic form at the Web Site of the **Journal** (<http://www.shd.org.rs/JSCS/>).

Internet Service:

Former Editors:

Nikola A. Pušin (1930–1947), **Aleksandar M. Leko** (1948–1954),
Panta S. Tutundžić (1955–1961), **Miloš K. Mladenović** (1962–1964),
Đorđe M. Dimitrijević (1965–1969), **Aleksandar R. Despić** (1969–1975),
Slobodan V. Ribnikar (1975–1985), **Dragutin M. Dražić** (1986–2006).

Editor-in-Chief:

BRANISLAV Ž. NIKOLIĆ, Serbian Chemical Society (E-mail: jscs-ed@shd.org.rs)

Deputy Editor:

DUŠAN SLADIĆ, Faculty of Chemistry, University of Belgrade

Sub editors:

Organic Chemistry

DEJAN OPSENICA, Institute of Chemistry, Technology and Metallurgy, University of Belgrade

Biochemistry and Biotechnology

JÁNOS CSANÁDI, Faculty of Science, University of Novi Sad
OLGICA NEDIĆ, INEP – Institute for the Application of Nuclear Energy, University of Belgrade

Inorganic Chemistry

BILJANA GLIŠIĆ, Faculty of Science, University of Kragujevac

Theoretical Chemistry

IVAN JURANIĆ, Serbian Chemical Society

Physical Chemistry

LJILJANA DAMJANOVIĆ-VASILJIĆ, Faculty of Physical Chemistry, University of Belgrade

Electrochemistry

SNEŽANA GOJKOVIĆ, Faculty of Technology and Metallurgy, University of Belgrade

Analytical Chemistry

RADA BAOŠIĆ, Faculty of Chemistry, University of Belgrade

Polymers

BRANKO DUNJIĆ, Faculty of Technology and Metallurgy, University of Belgrade

Thermodynamics

MIRJANA KIJEVCANIN, Faculty of Technology and Metallurgy, University of Belgrade

Chemical Engineering

TATJANA KALUĐEROVIĆ RADOIČIĆ, Faculty of Technology and Metallurgy, University of Belgrade

Materials

RADA PETROVIĆ, Faculty of Technology and Metallurgy, University of Belgrade

Metallic Materials and Metallurgy

ANA KOSTOV, Mining and Metallurgy Institute Bor, University of Belgrade

Environmental and Geochemistry

VESNA ANTIĆ, Faculty of Agriculture, University of Belgrade

History of and Education in Chemistry

DRAGICA TRIVIĆ, Faculty of Chemistry, University of Belgrade

English Language Editors:

LYNNE KATSIKAS, Serbian Chemical Society

VLATKA VAJS, Serbian Chemical Society

JASMINA NIKOLIĆ, Faculty of Technology and Metallurgy, University of Belgrade

Technical Editors:

VLADIMIR PANIĆ, Institute of Chemistry, Technology and Metallurgy, University of Belgrade

MARIO ZLATOVIĆ, Faculty of Chemistry, University of Belgrade

Journal Manager & Web Master:

MARIO ZLATOVIĆ, Faculty of Chemistry, University of Belgrade

Office:

VERA ČUŠIĆ, Serbian Chemical Society

Editorial Board

From abroad: **R. Adžić**, Brookhaven National Laboratory (USA); **A. Casini**, University of Groningen (The Netherlands); **G. Cobb**, Baylor University (USA); **D. Douglas**, University of British Columbia (Canada); **G. Inzelt**, Etvos Lorand University (Hungary); **J. Kenny**, University of Perugia (Italy); **Ya. I. Korenman**, Voronezh Academy of Technology (Russian Federation); **M. D. Lechner**, University of Osnabrueck (Germany); **S. Macura**, Mayo Clinic (USA); **M. Spiteller**, INFU, Technical University Dortmund (Germany); **M. Stratakis**, University of Crete (Greece); **M. Swart**, University de Girona (Cataluna, Spain); **G. Vunjak-Novaković**, Columbia University (USA); **P. Worsfold**, University of Plymouth (UK); **J. Zagal**, Universidad de Santiago de Chile (Chile).

From Serbia: **B. Abramović**, **V. Antić**, **R. Baošić**, **V. Bešković**, **J. Csanadi**, **Lj. Damjanović-Vasilić**, **A. Dekanski**, **V. Dondur**, **B. Dunjić**, **M. Đuran**, **B. Glišić**, **S. Gojković**, **I. Gutman**, **B. Jovančičević**, **I. Juranić**, **T. Kaluđerović**, **Radiočić**, **L. Katsikas**, **M. Kijevcanin**, **A. Kostov**, **V. Leovac**, **S. Milonjić**, **V.B. Mišković-Stanković**, **O. Nedić**, **B. Nikolić**, **J. Nikolić**, **D. Opsenica**, **V. Panić**, **M. Petkovska**, **R. Petrović**, **I. Popović**, **B. Radak**, **S. Ražić**, **D. Sladić**, **S. Sovilj**, **S. Šerbanović**, **B. Šolaja**, **Z. Tešić**, **D. Trivić**, **V. Vajs**, **M. Zlatović**.

Subscription: The annual subscription rate is **150.00 €** including postage (surface mail) and handling. For Society members from abroad rate is **50.00 €**. For the proforma invoice with the instruction for bank payment contact the Society Office (E-mail: shd@shd.org.rs) or see JSCS Web Site: <http://www.shd.org.rs/JSCS/>, option Subscription.

Godišnja pretplata: Za članove SHD: **2.500,00 RSD**, za penzionere i studente: **1000,00 RSD**, a za ostale: **3.500,00 RSD**; za organizacije i ustanove: **16.000,00 RSD**. Uplate se vrše na tekući račun Društva: **205-13815-62**, poziv na broj **320**, sa naznakom "pretplata za JSCS".

Nota: Radovi čiji su svi autori članovi SHD prioritetno se publikuju.

Odlukom Odbora za hemiju Republičkog fonda za nauku Srbije, br. 66788/1 od 22.11.1990. godine, koja je kasnije potvrđena odlukom Saveta Fonda, časopis je uvršten u kategoriju međunarodnih časopisa (**M-23**). Takođe, aktom Ministarstva za nauku i tehnologiju Republike Srbije, 413-00-247/2000-01 od 15.06.2000. godine, ovaj časopis je proglašen za publikaciju od posebnog interesa za nauku. **Impact Factor** časopisa objavljen 28. juna 2023. godine je **1,000**, a petogodišnji **Impact Factor 1,100**.

CONTENTS*

<i>Editorial</i>	599
<i>N. Živanović, N. Simin, M. Lesjak, D. Orčić, N. Mimica-Dukić and E. Svirčev</i> : Comparative study between homemade and commercial hawthorn (<i>Crataegus</i> spp.) extracts regarding their phenolic profile and antioxidant activity	603
<i>M. Jovanović, M. Vojinović Miloradov and L. Cvetičanin</i> : Effect of silver nanoparticles in treating and healing of burn wound	617
<i>V. Mišković-Stanković, A. Janković, S. Grujić, I. Matić-Bujagić, V. Radojević, M. Vukašinović-Sekulić, V. Kojić, M. Djošić and T. M. Atanacković</i> : Diffusion models of gentamicin released in poly(vinyl alcohol)/chitosan hydrogel	627
<i>J. K. Popović, D. J. Popović, K. J. Popović, D. Miljković, D. Lalošević, Z. Dolićanin and I. Čapo</i> : Immunohistochemical evidences of anticancer actions of metformin with other repurposed drug combinations and correlation with hamster fibrosarcoma tumor size	643
<i>M. Šunjević, D. Popović, S. Medić, M. Panjković and B. Gudurić</i> : A 7-year experience in core needle biopsy of breast lesions: Correlation between imaging and hematoxylin and eosin-stained sections	657
<i>Đ. M. Karanović, M. S. Hadnađev-Kostić, T. J. Vulić, M. M. Milanović, V. N. Rajaković-Ognjanović and R. P. Marinković-Nedućin</i> : The influence of the coprecipitation synthesis methods on photodegradation efficiency of ZnFe based photocatalysts	667
<i>L. Cvetičanin, M. Prica and S. Vujkov</i> : Influence of the elasticity variation of the 3D printed PMMA structure on the axial tooth vibration	679
<i>A. Bošković, M. Sremački, S. Vještica, A. Čavić, N. Marković and B. Borovac</i> : Sulphur hexafluoride in modern medium-voltage switchgear: Advantages, hazards and environmental impact	693
<i>O. Dokleštić, M. Vojinović Miloradov, N. Elezović, S. Kolaković and N. Simeunović</i> : Performance indicators model assessment for water system quality and supply in Montenegro	705
<i>N. Ž. Tošić, M. Z. Muhadinović, M. Z. Šunjević, I. P. Čosić and N. S. Stanisavljević</i> : Cadmium and lead flow analysis as a decisions support data for waste management	715
<i>R. Folić, D. Zenunović and Z. Brujić</i> : Effects of carbonation and chloride ingress on the durability of concrete structures	729
<i>M. Šunjević, D. Nedućin, R. Božović, M. Sremački, B. Obrovski and I. Subotić</i> : Effects of urban vegetation on PM mitigation: The case of a street in Novi Sad, Serbia	743
<i>Lj. Popović, N. Sremčev, D. Purković and I. Čosić</i> : Chemical engineering in technical and technological culture	757
<i>I. Subotić, V. Kisić and D. Nedućin</i> : Cultural heritage in the face of climate change: From protection to decolonisation	773

Published by the Serbian Chemical Society
Karnegijeva 4/III, P.O. Box 36, 11120 Belgrade, Serbia
Printed by the Faculty of Technology and Metallurgy
Karnegijeva 4, P.O. Box 35-03, 11120 Belgrade, Serbia

* For colored figures in this issue please see electronic version at the Journal Home Page:
<http://www.shd.org.rs/JSCS/>

**This issue is dedicated to the fifteenth anniversary of the election of
Professor Emeritus at the University in Novi Sad.**

Publication of this issue is financially supported by



the Provincial Secretariat for Higher Education and Scientific Research of the
Autonomous Province of Vojvodina

Editorial

This issue of the *Journal of the Serbian Chemical Society – JSCS* honors the jubilee anniversary, marking 15 years since the title Professor Emeritus of the University of Novi Sad was first bestowed. We express our sincere gratitude to the Editor-in-Chief and Editorial Team of JSCS for accepting the special concept of this issue, which aims to promote research results across multiple fields, with a particular emphasis on interdisciplinary collaboration.

The title of Professor Emeritus was established in Serbia in 2005 by the Law on Higher Education as a distinguished honor for exceptional achievements in academic career and contributions to affirming the home institution both nationally and internationally, mirroring a long-standing practice and tradition of universities worldwide. After the adoption of the University of Novi Sad Statute and the regulations outlining criteria and procedures, the title of Professor Emeritus of the University of Novi Sad was inaugurated in 2008, honoring six of our colleagues with remarkable academic careers. Since then, it has been bestowed upon 52 esteemed professors from 11 Faculties. The inclusion of all educational-scientific and artistic fields has fostered an innovative environment and catalyzed collaboration, facilitating the exchange of experiences, strengthening interdisciplinary bonds and underscoring a commitment to holistic research approaches.

Following the initiative of the professors emeriti, the Association of Professor Emeritus of the University of Novi Sad was founded in 2017 through the decision of the Senate and the Council of the University, with its activities commencing upon the election of the Presidency in 2018. In brief, its mission is defined by the following key objectives: evaluating curricula development and research trends at both national and international levels; promoting interdisciplinarity as a challenge of the modern era; facilitating the promotion and dissemination of scientific and artistic achievements within the academic and wider community; and fostering collaboration and networking between academic and other institutions on both national and international scales.

The five years of the Association's work are characterized by a myriad of activities. During this time, over 20 presentations and interactive workshops, led by distinguished national and international scientists and experts from various

fields, were organized, all open to the general public. Among the presenters and workshop moderators were many prominent members of the Serbian academic community, alongside colleagues from the USA, China, Germany, Slovenia, Great Britain, Portugal, Poland, Croatia, New Zealand, Italy and Canada, each possessing exceptional reputations and international experience. Additionally, six projects, supported by the Secretariat for Higher Education and Scientific Research of the Autonomous Province of Vojvodina, were undertaken, encompassing a variety of activities aimed at addressing key contemporary academic and research challenges and fostering institutional cooperation and networking. Undoubtedly, the unwavering support of the Rectorate and professional services of the University of Novi Sad and its Faculties significantly contributed to the realization of the Association's activities.

The publication of this special issue of the *Journal of the Serbian Chemical Society* marks a significant step toward accomplishing the Association's objectives. In conceptualizing its content, the experiences gained from activities aimed at acquainting a broader audience with scientific findings across various fields played a crucial role, further motivating the recognition of the importance of exchanging ideas and making connections between different professions to pave the way to pioneering new research avenues. This issue features papers spanning natural, technical-technological, medical, and social sciences, authored by colleagues who have embraced an interdisciplinary approach to their research. It constitutes a diverse compilation of scientific inquiries, firmly grounded in the fundamental scientific fields covered by the Journal and situated within an interdisciplinary context, thereby contributing to transcending conventional boundaries in the application of research findings. This issue also promotes the continual research engagement of professor emeriti, who co-authored the papers, and their collaboration with researchers of various backgrounds and expertise, including young scholars. The diverse authorship, representing numerous academic and research institutions, underscores the importance of fostering collaboration and knowledge exchange in tackling the contemporary challenge of rapid science and technology development.

Prof. Emerita Dr. Mirjana Vojinović Miloradov and Prof. Emerita Dr. Radmila Marinković-Nedučín, leading members of the Presidency of the Association of Professors Emeritus of the University of Novi Sad, have been appointed as guest editors for this issue, which was a special honor. We thank all contributors and young researcher supporting team for their efforts, as well as the Secretariat for Higher Education and Scientific Research of the Autonomous Province of Vojvodina for the financial support in realizing this issue.

Guest Editors

Prof. Emer. Dr. Mirjana Vojinović Miloradov
University of Novi Sad, Faculty of Technical Sciences

Prof. Emer. Dr. Radmila Marinković-Nedučín
University of Novi Sad, Faculty of Technology

Prof. Emerita Dr. Mirjana Vojinović Miloradov initiated this issue and played a pivotal role in shaping it with unparalleled dedication. With profound sadness, we bid farewell as she departed at the very end of its preparation, but her exceptional contribution will always be remembered. Being the first name on the list of elected professors' emeriti in 2008, her remarkable academic career, coupled with her steadfast adherence to the highest academic and ethical standards, epitomizes the noble ideals embodied by this title.

Prof. Emer. Dr. Radmila Marinković-Nedučín



J. Serb. Chem. Soc. 89 (5) 603–616 (2024)
JSCS–5742

Comparative study between homemade and commercial hawthorn (*Crataegus* spp.) extracts regarding their phenolic profile and antioxidant activity

NEMANJA ŽIVANOVIĆ, NATAŠA SIMIN*, MARIJA LESJAK, DEJAN ORČIĆ,
NEDA MIMICA-DUKIĆ and EMILIJA SVIRČEV

University of Novi Sad, Faculty of Sciences, Novi Sad, Serbia

(Received 30 November, revised 8 December 2023, accepted 23 January 2024)

Abstract: *Crataegus* species (hawthorn) have been commonly used in traditional medicine, especially for the treatment of congestive heart failure. Many studies confirmed that they are rich in polyphenols, thus exhibiting strong antioxidant activity, which contribute to the beneficial effects of hawthorn on the cardiovascular system. In the market, there are many herbal medicinal products based on hawthorn, which consumption as adjuvant therapy in heart-related issues is supported by European Medicines Agency. Since there is a global trend of making homemade herbal preparations, this study aimed to compare whether there is a difference in polyphenol profile and antioxidant potential between homemade and commercial ethanol extracts of hawthorn. Polyphenol profile was evaluated by determination of total phenolic and flavonoid contents, and by quantitative analysis of selected polyphenols by liquid chromatography–mass spectrometry/mass spectrometry. Antioxidant potential was examined by 2,2-diphenyl-1-picrylhydrazyl, ferric ion reducing antioxidant power and lipid peroxidation inhibition assays. The results of this study suggest that homemade ethanol extracts of hawthorn flowers, leaves and fruits are just as good source of polyphenols and antioxidants as commercial ones, and their utilization should be supported. Furthermore, hawthorn extracts made of leaves and flowers are better source of bioactive polyphenols and have higher antioxidant activity compared with the same of fruits, regardless of the method of preparation.

Keywords: polyphenols; LC-MS/MS; DPPH; FRAP; lipid peroxidation.

INTRODUCTION

Crataegus spp. are commonly known as hawthorn. It is a large genus of shrubs, belonging to the Rosaceae family, which comprises around 280 species. Hawthorn plants grow in areas with mild climate in Europe, Asia and North

* Corresponding author. E-mail: natasa.simin@dh.uns.ac.rs
<https://doi.org/10.2298/JSC231130006Z>

America.¹ In Europe and North America, the most common species are *Crataegus monogyna* Jacq, *C. laevigata* Poir (syn. *C. oxiacantha* L.) and *C. pentagyna* Waldst, while in China the most frequent species is *C. pinnatifida* Bge.²

Thanks to its medicinal properties, hawthorn species, particularly its flowers, leaves and fruits, have a long history of usage in the folk medicine of many countries. Traditionally, hawthorn preparations have been used to treat congestive heart failure, a disease defined by the inability of a weakened heart to pump blood well and to effectively provide oxygen and nutrients to peripheral tissues. Nowadays, numerous *in vivo* and *in vitro* studies confirmed different biological activities of *Crataegus* species, including antioxidant, antimutagenic, antimicrobial, hypolipidemic, hypoglycemic, immunostimulatory, hepatoprotective, cardiostimulant, antihypertensive, diuretic, *etc.*, which all can be associated with its traditionally recognized heart-protective benefits. The listed beneficial medicinal properties of hawthorn species can be attributed to a variety of bioactive compounds, including polyphenols, organic acids and amines, whose presence in hawthorn is confirmed in previous studies.^{1–5}

Numerous herbal medicinal products made from hawthorn, mainly for treating heart failure, are available on the worldwide market. Hawthorn flowers and leaves can be found in various herbal preparations, such as: comminuted or powdered herbal substance, dry or liquid extracts, tinctures or expressed juices from fresh herbal material.⁶ Also, different pharmaceutical forms of hawthorn preparations, including herbal teas or solid and liquid dosage forms for oral use are present. They may be sold as authorized prescription pharmaceuticals, over-the-counter (OTC) medications, authorized herbal medicinal items, dietary supplements or unregulated herbal remedies. They are often registered and sold as herbal or traditional herbal medicinal products, herbal dietary supplements or unregulated herbal remedies. Even though the products from hawthorn flowers & leaves have been granted a positive monograph by the European Medicines Agency (EMA), its latest guidelines strongly recommend against employing hawthorn preparations as monotherapy in heart failure. Instead, they should be used as an adjuvant therapy.⁷ Specifically, the Committee on Herbal Medicinal Products (HMPC) of the EMA concluded that hawthorn flower and leaf preparations can be used alone to ease symptoms of transitory cardiac complaints associated with anxiousness, such as palpitations, only once serious heart conditions have been excluded by a medical expert. They can also be applied to alleviate moderate symptoms of stress and to improve sleep.⁶ In addition, due to the rich occurrence of bioactive polyphenols, phytopreparations made of hawthorn could also be used as antioxidants for alleviating oxidative stress.⁸

One of the most popular products made of hawthorn use on the market are liquid herbal extracts, obtained from various plant parts (*e.g.* flower, leaf and

fruit) made by hydroalcoholic (methanol or ethanol) or water-based extraction. They are known as hawthorn tinctures or drops. According to the official European Pharmacopoeia, these liquid extracts can be made by extraction with ethanol (30–70 vol. %) and are standardized to a minimum of 0.8–3.0 % of flavonoids, expressed as hyperoside.^{9,10} On the other side, in the German Pharmacopoeia, the liquid extract (*Crataegi extractum fluidum*) is officinal preparation, standardized to 0.25–0.5 % of flavonoids, calculated to hyperoside.¹¹

Nowadays, trend of consuming herbal extracts, such as liquid herbal extracts, is growing. Namely, the global herbal extract market is forecasted to experience a compound annual growth rate (CAGR) of 6.63 % during the forecast period 2022–2027.¹² In parallel, a trend of making homemade products, including herbal preparations, is rising. Globally, do-it-yourself (DIY) culture is developing in many areas, due to different reasons such as: products costs rising, consumer mistrust in the quality of ingredients used in the industrial production processes as well as in medical approaches and health professionals, and a growing trend among consumers to turn to a more natural and simple way of life. Also, making one's own product can be a type of hobby that causes a feeling of joy upon preparing something beneficial for oneself.^{13,14} Bearing all the above mentioned in mind, the aim of this study was to reveal is there a difference in polyphenol quantitative and qualitative composition and antioxidant potential between homemade and commercially available hawthorn (*Crataegus* spp.) herbal ethanol extracts, made from hawthorn fruits or a mixture of flowers and leaves. The end purpose of this study was to conclude whether homemade hawthorn herbal ethanol extracts have sufficient quality and if their production by individuals should be encouraged and promoted.

EXPERIMENTAL

Extract preparation

A commercially available plant material of European origin was purchased in health food stores in Novi Sad, Serbia. The first material was a mixture of dried comminuted flowers and leaves, while the second one was dried hawthorn fruits. Each plant material was purchased from three different stores (different producers) and mixed in order to obtain composite sample, which was used for extracts preparation by maceration. On 30 g of dry flowers and leaves 150 mL of 70 % aqueous EtOH was added and maceration was performed overnight at room temperature. Afterwards, the extract was filtered and maceration was repeated one more time on plant leftovers following the same procedure. This extract is named homemade flowers and leaves extract (HMFL). For the purpose of further analysis, extract was evaporated to dryness *in vacuo* (35 °C), after which dry extract was dissolved in 50 % aqueous EtOH to the final concentrations of 200 mg/mL. The same procedure was repeated for preparation of fruit extract, except that 10 g of dry fruits was mixed with 50 mL of 70 % aqueous EtOH. This extract is named homemade fruit extract (HMF).

The samples of two types of commercial extracts of *Crataegus* spp., produced by Institute for medicinal plants research “Dr Josif Pančić”, were purchased in pharmacies in Novi

Sad, Serbia. The first type of extract was 56 % aqueous EtOH extract of flowers and leaves (labelled as CFL) and the second was aqueous-EtOH extract of fruits (CF). The commercial extracts were evaporated to dryness *in vacuo* (35 °C) and dry extracts were dissolved in 50 % aqueous EtOH to the final concentration of 200 mg/mL.

Chemical characterization of homemade and commercial hawthorn extracts

Chemical characterization of extracts was done by determination of total phenolic and flavonoid contents, as well as quantitative liquid chromatography–mass spectrometry/mass spectrometry (LC–MS/MS) analysis of 45 selected compounds. Total phenolic content was determined according to Lesjak *et al.* by the Folin–Ciocalteu method.¹⁵ Results were expressed as mg of gallic acid equivalents per g of dry weight (mg GAE/g dw). Total flavonoid content was determined according to Lesjak *et al.* using the colorimetric method and results were expressed as mg of quercetin equivalents per g of dry weight (mg QE/g dw).¹⁵

The content of quinic acid and other 44 selected phenolic compounds (14 phenolic acids, 25 flavonoids, 2 lignans and 3 coumarins) was determined by LC–MS/MS according to the previously reported method.¹⁶ Standards of the compounds were purchased from Sigma–Aldrich Chem, Fluka Chemie GmbH or from ChromaDex (Santa Ana, CA, USA). Samples and standards were analyzed using Agilent Technologies 1200 Series high-performance liquid chromatograph coupled with Agilent Technologies 6410A Triple Quad tandem mass spectrometer with electrospray ion source, and controlled by Agilent Technologies MassHunter Workstation software – Data Acquisition (ver. B.03.00). All extracts were diluted with 50 % aqueous MeOH to the concentrations of 20 and 0.1 mg/mL. The sample (5 µL) was injected into the system, and compounds were separated on Zorbax Eclipse XDB-C18 (50 mm × 4.6 mm, 1.8 µm) rapid resolution column. Data were acquired in dynamic multiple reaction monitoring (MRM) mode, peak areas were determined using Agilent MassHunter Workstation Software – Qualitative Analysis (ver. B.06.00). Calibration curves were plotted by OriginLabs Origin Pro (ver. 2019b) software and used for calculation of investigated compounds concentration in the extracts. Results are expressed as µg per g of dry weight (µg/g dw).

Determination of antioxidant potential of homemade and commercial hawthorn extracts

Antioxidant potential was evaluated by 2,2-diphenyl-1-picrylhydrazyl (DPPH) assay, ferric reducing power assay (FRAP) and inhibition of lipid peroxidation (LP) assay. DPPH assay was performed according to Lesjak *et al.* The results were expressed as IC_{50} (mg/mL).¹⁵ FRAP assay was performed according to Lesjak *et al.* and results were expressed as mg of ascorbic acid equivalents per g of dry weight (mg AAE/g dw).¹⁵ The ability of extracts to inhibit LP was determined by TBA assay according to Pintač *et al.*¹⁷ Results were expressed as IC_{50} (mg/mL).

Statistical analysis

The percent of inhibition achieved by different extract concentrations was calculated with the following equation: $I (\%) = 100(1 - A/A_0)$, where A was the absorbance of the investigated extracts corrected for the absorbance of the blank probe, and A_0 was the absorbance of the control. The IC_{50} values were determined by plotting inhibition–concentration curves in the OriginLabs Origin Pro (ver. 2019b) software. Results were expressed as mean ± standard deviation (SD) of three replicates. A comparison of the group means and the significant difference between the groups was verified by one-factor ANOVA followed by Tukey's HSD post-hoc test ($p \leq 0.05$). This was performed in Excel using the add-in Xrealstats from Real Statistics.

RESULTS AND DISCUSSION

Chemical composition of homemade and commercially available hawthorn extracts

Phenolic profile of hawthorn extracts was determined by measuring the total phenolic and flavonoid contents, as well as by quantitative LC–MS/MS analysis of selected compounds.

The total phenolic content was in the range of 17.0–190 mg GAE/g dw, while the total flavonoid content was in the range of 1.4–48.0 mg QE/g dw (Fig. 1). Flowers and leaves extracts had a significantly higher content of both total phenolic and flavonoid contents compared with fruit extracts, while homemade HMFL extract had the highest amount of both total phenolic and flavonoid contents among all examined samples. There was no significant difference in the contents of total phenolics and flavonoids between HMF and CF. The same conclusions can be made if TPC and TFC are calculated to a daily dose of the extracts (60 drops = 3 mL). If HMFL extract is consumed, TPC in a daily dose is 26.8 mg GAE, while with CFL extract it is 20.1 mg GAE. In the case of TFC, the daily intake through HMFL extract will be 6.77 mg QE, and through CFL extract 3.36 mg QE, which is twice lower. The TPC and TFC in a daily dose of fruit extracts were significantly higher in HMF compared to CF (2.98 mg GAE for HMF and 1.80 mg GAE for CF; 0.25 mg QE for HMF and 0.175 mg QE for CF).

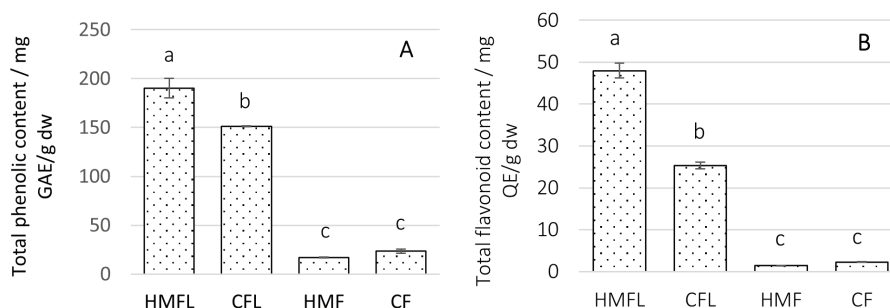


Fig. 1. Total phenolic (A) and flavonoid (B) contents in homemade and commercial hawthorn extracts. HMFL - homemade flowers and leaves extract, CFL - commercial flowers and leaves extract, HMF - homemade fruit extract, CF - commercial fruit extract.

Letters a–c denote a significant difference between samples ($p \leq 0.05$).

The results of the LC–MS/MS analysis revealed that 36, out of 45 analyzed compounds, were present in examined hawthorn extracts (Table I). Quinic acid, an intermediate in biosynthesis of chlorogenic acids, was the most abundant, especially in flowers and leaves extracts. Most phenolic acids and flavonoids were present in significantly higher amounts in flowers and leaves extracts compared with extracts of fruits. Analyzed but not detected compounds were: umbel-

liferon, *o*-coumaric acid, 3,4-dimethoxycinnamic acid, daidzein, genistein, mat-airesinol, secoisolariciresinol, baicalin, epigallocatechin gallate.

TABLE I. The content of selected phenolic compounds and quinic acid ($\mu\text{g/g dw}$) in homemade and commercially available hawthorn extracts analyzed by LC-MS/MS; abbreviations: HMFL – homemade flowers and leaves extract, CFL – commercial flowers and leaves extract, HMF – homemade fruit extract, CF – commercial fruit extract. Letters a–d denote a significant difference between samples ($p \leq 0.05$)

Compound	HMFL	CFL	HMF	CF
Quinic acid	60680±6068 ^b	75730±7573 ^a	22450±2245 ^c	23700±2370 ^c
Hydroxybenzoic acids				
<i>p</i> -Hydroxybenzoic acid	132.4±7.945 ^a	97.28±5.837 ^b	19.26±1.156 ^d	58.92±3.535 ^c
Gentisic acid	3.679±0.294 ^a	/ ^e	2.460±0.197 ^b	/
Protocatechuic acid	46.21±3.697 ^c	85.99±6.879 ^b	63.65±5.092 ^c	169.6±13.57 ^a
Gallic acid	2.811±0.253 ^c	7.338±0.660 ^a	<2.450 ^f	6.126±0.551 ^b
Vanillic acid	61.23±18.37 ^a	22.62±6.785 ^{bc}	43.79±13.14 ^{ab}	11.22±3.366 ^c
Syringic acid	4.557±0.911 ^c	4.935±0.987 ^c	14.89±2.978 ^b	23.75±4.750 ^a
Hydroxycinnamic acids				
Cinnamic acid	40.46±8.091 ^a	50.59±10.119 ^a	5.836±1.167 ^b	5.937±1.187 ^b
<i>p</i> -Coumaric acid	16.28±1.465 ^{bc}	75.52±6.796 ^a	11.64±1.048 ^c	23.34±2.100 ^b
Caffeic acid	20.65±1.446 ^b	57.45±4.021 ^a	4.949±0.346 ^d	11.27±0.789 ^c
Ferulic acid	7.629±0.763 ^b	12.94±1.294 ^a	4.899±0.490 ^c	11.08±1.108 ^a
Sinapic acid	/	0.852±0.085 ^c	1.481±0.148 ^b	2.363±0.236 ^a
5- <i>O</i> -Caffeoylquinic acid	14020±701 ^b	23500±1175 ^a	159.3±7.966 ^c	185.7±9.284 ^c
Coumarins				
Esculetin	2.303±0.138 ^c	4.087±0.245 ^a	0.495±0.030 ^d	3.599±0.216 ^b
Scopoletin	<0.600	<0.600	/	/
Flavonols				
Quercetin	104.6±31.38 ^b	245.2±73.56 ^a	39.26±11.78 ^d	47.62±14.29 ^d
Rutin	2309±69 ^b	3529±106 ^a	100.8±3.023 ^c	140.8±4.224 ^c
Quercetin 3- <i>O</i> -glucoside + quercetin 3- <i>O</i> -galactoside	13640±818 ^a	11040±663 ^b	1901±114 ^c	2931±176 ^c
Quercitrin	8.940±0.536 ^a	4.086±0.245 ^b	0.525±0.031 ^c	0.464±0.028 ^c
Isorhamnetin	3.534±0.212 ^b	6.385±0.383 ^a	2.039±0.122 ^c	3.545±0.213 ^d
Kaempferol	13.15±0.920 ^a	15.00±1.050 ^a	3.418±0.239 ^c	8.538±0.598 ^b
Kaempferol 3- <i>O</i> -glucoside	1227±086 ^a	951.7±66.62 ^b	66.23±4.636 ^c	109.5±7.665 ^c
Flavones				
Baicalein	2.068±0.621 ^a	2.616±0.785 ^a	/	/
Amentoflavone	<0.600	/	/	<0.600
Luteolin	8.268±0.413 ^b	21.31±1.066 ^a	1.213±0.061 ^c	2.356±0.118 ^c
Luteolin 7- <i>O</i> -glucoside	190.1±5.702 ^a	140.0±4.199 ^b	1.332±0.040 ^c	2.527±0.076 ^c
Apigenin	1.672±0.117 ^b	8.090±0.566 ^a	<0.075	0.146±0.010 ^c
Apigenin 7- <i>O</i> -glucoside	31.94±1.597 ^a	9.866±0.493 ^b	<0.075	0.198±0.010 ^c
Vitexin	88.77±4.438 ^a	93.93±4.696 ^a	5.978±0.299 ^b	13.02±0.651 ^b
Apiin	<0.075	0.698±0.035 ^a	<0.075	<0.075
Chrysoeriol	0.949±0.028 ^b	8.533±0.256 ^a	0.267±0.008 ^c	0.926±0.028 ^b

TABLE I. Continued

Compound	HMFL	CFL	HMF	CF
Flavones				
Myricetin	<9.750	<9.750	<9.750	<9.750
Flavanones				
Naringenin	46.42±3.249 ^b	72.42±5.070 ^a	1.756±0.123 ^c	3.784±0.265 ^c
Flavan-3-ols				
Catechin	18.10±1.810 ^a	/	8.686±0.869 ^b	8.818±0.882 ^b
Epicatechin	3426±343 ^a	1720±172 ^b	398.8±39.88 ^c	240.9±24.09 ^c

^aConcentration is below the instrument's limit of detection (LOD); ^bconcentration is below the limit of quantification (LOQ)

The amounts of selected polyphenols quantified by LC–MS/MS calculated to a daily dose of examined hawthorn extracts are available from authors upon request. The amount of examined phenolic acids and flavonoids in a daily dose of HMFL and CFL were significantly higher than the same in a daily dose of HMF and CF.

Antioxidant activity of homemade and commercially available hawthorn extracts

The antioxidant potential of hawthorn extracts was evaluated by DPPH, FRAP and LP assays, and the results are shown in Fig. 2.

From the results it can be seen that all samples displayed some level of antioxidant activity. Flowers and leaves extracts had significantly higher antioxidant potential compared to fruit extracts. In the FRAP assay, antioxidant activity was in the range of 10.1–100.8 mg AAE/g dw, with the highest activity shown by HMFL. In the DPPH assay, IC_{50} was in the range of 0.03–0.41 mg/mL, with the highest activity expressed by HMFL and CFL. Compared to the standard antioxidant butylated hydroxytoluene (BHT), with IC_{50} of 0.009 mg/mL¹⁷, hawthorn extracts were less potent quencher of DPPH radicals. All hawthorn samples inhibited LP, and IC_{50} was in the range of 0.14–1.56 mg/mL. The highest inhibitory activity towards LP was expressed by HMFL and CFL, while fruit extracts were significantly less potent inhibitors. Compared to BHT, with IC_{50} of 0.001 mg/mL,¹⁷ hawthorn extracts were significantly less potent inhibitors of LP. However, HMFL and CFL, but not HMF and CF, were more potent compared to propyl gallate (PG), with IC_{50} of 0.05 mg/mL.¹⁷

According to the results obtained in this study, homemade extract of flowers and leaves of hawthorn had the highest TPC and TFC, as well as content of individual polyphenols determined by LC–MS/MS, among all examined samples. Furthermore, both HMFL and CFL contained higher amounts of polyphenols than fruit extracts, which is in accordance with the findings of other researchers mentioned below. Also, even though extracts examined in this study can be regarded as rich sources of polyphenols, some other researchers reported higher con-

tents of total phenolics and flavonoids, as well as individual polyphenols. These differences could be a consequence of different geographical origin of the samples, different *Crataegus* species and chemotypes, or different extraction procedures. In addition, to our knowledge, there was no literature data regarding evaluation of polyphenol composition and antioxidant activity of commercial preparations made of hawthorn, just ones prepared in the laboratory.

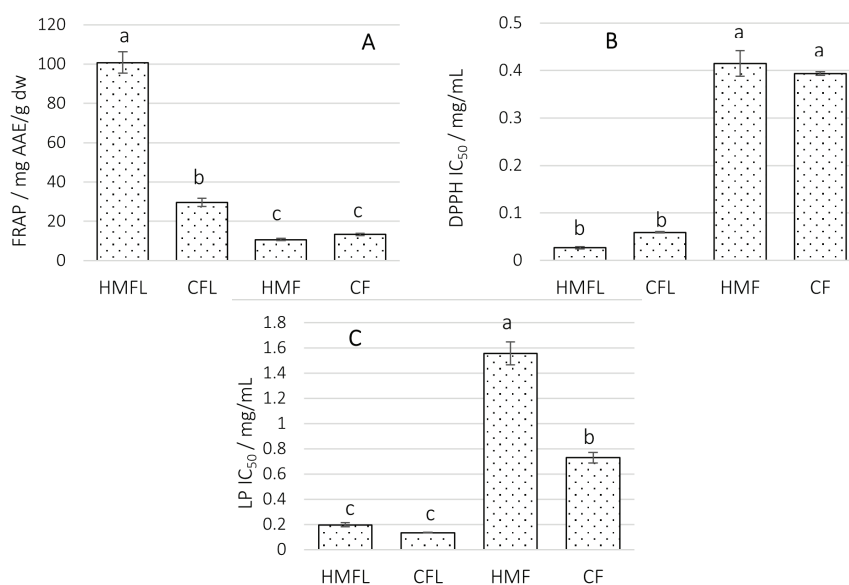


Fig. 2. Antioxidant activity of homemade and commercial hawthorn extracts; A – FRAP results, B – DPPH assay results and C – LP inhibition assay results. HMFL – homemade flowers and leaves extract, CFL – commercial flowers and leaves extract, HMF – homemade fruit extract and CF – commercial fruit extract. Letters a–c denote a significant difference between samples ($p \leq 0.05$).

Namely, in the available literature, there is abundance of data regarding the total phenolic and flavonoid contents of EtOH hawthorn extracts. Specifically, it was reported that leaf EtOH extract of *C. monogyna* contains 473.4 mg GAE/g dw of total phenols and 80.9 mg QE/g dw of total flavonoids.¹⁸ Also, it was determined that total phenolic content in fruit extracts of different *Crataegus* spp. grown in Turkey was in the range of 360–380 mg GAE/g of dried fruit, while total flavonoid content was in the range of 13–20 mg QE/g dw.³ Furthermore, the total phenolic content in EtOH extract made of mixture of *C. monogyna* and *C. oxyacantha* fruits grown in Serbia, was 35.4 mg GAE/g dw as published by Tadić *et al.*¹⁹ Zhang and collaborators determined that the total phenolic and flavonoids contents in ethanol extract of fruits of *C. pinnatifida* grown in China was 65 and 63 mg GAE/g dw, respectively,²⁰ while total phenolic content in methanol ext-

ract of dry aerial parts (flowering tops or flowers with young leaves) was 562.9 mg GAE/g dw and in dry fruit methanol extract 128.2 mg GAE/g dw, both from *C. monogyna* grown in France, as publishes by Froehlicher *et al.*²¹

LC–MS/MS analysis in the present study has shown that ethanolic flowers and leaves extracts, especially homemade extract, contain high amounts of chlorogenic acid, rutin, quercetin 3-*O*-glucoside and hyperoside, kaempferol 3-*O*-glucoside and epicatechin. Amounts of these compounds were significantly lower in fruit extracts. Also, different HPLC methods were performed for analysis of polyphenols in hawthorn extracts in previous studies. Specifically, Bardakci *et al.* detected epicatechin, vitexin, isoorientin, hyperoside, chlorogenic acid and quercetin in fruit extracts of different *Crataegus* species.³ Tadic *et al.* analyzed chemical composition of fruit extracts using HPLC-DAD method and determined chlorogenic acid, isoquercitrin, hyperosid and quercetin in higher concentrations, as well as rutin and vitexin in traces.¹⁹ Zhang and collaborators detected epicatechin and procyanidin B2 as the main components of methanolic extract of *C. pinnatifida* fruits in the concentrations of 2.816 and 2.435 mg/g dw, respectively,²⁰ which is lower than epicatechin determined in HMFL, and higher then epicatechin determined in CFL and fruit extracts from this study. Froehlicher *et al.* analyzed the content of chlorogenic acid, caffeic acid, hyperoside and epicatechin in extracts of fresh and dried fruits and dried aerial parts. Dry flowering tops (flowers with young leaves) extract contained the highest amounts of these compounds, followed by extracts of fresh and dried fruits,²¹ which is also in accordance with the results reported here.

Results of this study showed that flowers and leaves extracts had higher DPPH scavenging activity compared to fruit extract, whit the HMFL extract being the most potent among the examined extracts. Determined values in this study are in accordance with values reported by other researchers. Namely, DPPH radical scavenging activity of fruit hawthorn extracts of different *Crataegus* species expressed as IC_{50} published by other authors was in the range of 1.2–2.4 mg/mL,³ 1.4¹⁹ and 0.013 mg/mL.²² Froehlicher *et al.* evaluated the DPPH scavenging activity of dry aerial parts and dry fruit extracts of *C. monogyna*. The aerial parts extract was 5 times more active than fruit extract. However, these results were published in Trolox equivalents which cannot be compared with findings from this study.²¹ Furthermore, DPPH neutralization activity of mixed flower and leaf and fruit ethanol extract of *C. monogyna* collected in Italy, expressed as IC_{50} were 0.003 and 0.013 mg/mL, respectively,²² which is in accordance with results reported in this paper for flowers and leaves extracts. Furthermore, it was published that ethanol extract of *C. azarolus* leaves collected from Lebanon expressed IC_{50} value for DPPH 0.050 mg/mL, which is in accordance with results presented herein.²³

FRAP assay also showed that the flowers & leaves extracts had higher antioxidant capacity compared to the extracts of fruits, with the HMFL being the most potent among all examined extracts herein. Other authors also investigated hawthorn antioxidant potential using this assay. Namely, antioxidant activity determined by FRAP assay was 531.4 and 955.8 mg AAE/L for fruits and aerial parts extracts, respectively, prepared by traditional maceration, and 105.3 and 1630.9 mg AAE/L for fruits and aerial parts extracts, respectively, prepared by sonicated extraction, both with ethanol, for *C. monogyna* collected in Ireland,²⁴ which is in correlation with our results. Others evaluated the antioxidant activity of fruit extracts of different *Crataegus* spp. and they were in the range of 0.50–2.83 mM FeSO₄ eq per 1 g sample, showing good antioxidant activity but less potent than BHT which they used as a reference (4.24 mM FeSO₄ eq per 1 g of sample).³

Shortle *et al.* have examined the effects of hawthorn extracts on LP and found good inhibitory activity. The most active sample was the extract of aerial parts prepared by sonicated maceration, followed by aerial parts and fruit extracts obtained by traditional maceration, while the least active sample was fruit extract obtained by sonicated maceration.²⁴ These results are not fully comparable with the results of this study because of different methodologies applied, but in both studies aerial part extracts were more active than fruit extracts.

Hawthorn has been traditionally used for the treatment of heart conditions. Leaf and flower extracts possess inotropic and chronotropic effects on the heart and can enhance coronary blood flow. It is assumed that flavonoids present in examined extracts, such as epicatechin, catechin, rutin, quercetin, vitexin and hyperoside are responsible for these effects.²⁵ Namely, flavanols, including epicatechin and catechin, can reduce ROS and increase the bioavailability of NO, an important messenger for vasodilation which reduces hypertension.²⁶ Furthermore, rutin has the ability to improve ejection fraction, left ventricular systolic function and fractional shortening.²⁷ Rutin also exhibits strong antioxidant activity, like other flavonoids, which can greatly contribute to its cardioprotective activity.²⁸ Rutin and quercetin protect against cardiac hypertrophy but through different mechanisms of action. Both flavonoids modulate oxidative stress through the inhibition of Ang II-induced NADPH oxidase, a major source of superoxide radicals. They also act on ROS/NO axis, but only quercetin seems to act on MAPK pathways. Quercetin inhibits ERK1/2, JNK1/2 and p38, while rutin showed no significant inhibition toward ERK1/2 and p38.²⁹ Likewise, vitexin exhibits antioxidant, antitumor, antimetastatic, antimicrobial, neuroprotective, anti-inflammatory, hypotensive and cardioprotective activities.^{30,31} Attenuation of cardiac hypertrophy is achieved through the modulation of intracellular calcium concentration.³² Hyperoside also exhibits cardioprotective activity. It can increase left ventricular ejection fraction and reduce heart size. Additionally, it

has anti-hypertensive activity, which is achieved by influencing blood vessels.³³ Generally, the anti-hypertension activity of flavonoids can be exhibited through the inhibition of ET-1, a vasoconstriction factor produced by endothelium. It has been shown that an increase in flavonoid hydrophilicity and glycosylation can impair their anti-hypertensive activity. Another key element for this activity is the presence of the 4-keto group and flavonoids that do not possess it show low activity.³⁴

Hawthorn extracts made from flowers and leaves analyzed in this study, especially homemade extract, are rich in flavonoids, such as epicatechin and quercetin glycosides, and they also contain apigenin-*C*-glucoside (vitexin), which altogether affirm their use in the treatment of heart conditions. The examined extracts are also rich in other flavonoids and phenolic acids that can have other health benefits such as antioxidant, cardioprotective, anti-atherosclerotic, anti-inflammatory, anti-diabetic, anticancer and others.^{35–39} Considering that fruit extract contained lower amounts of these compounds, flowers and leaves extract usage should be favored. Furthermore, the preparation of flower and leaf extract in home conditions, using a simple extraction method with 70 % ethanol for 24 h at room temperature, in a ratio of 1:5 (dry plant material:70 % ethanol), could be considered as a suitable method, which may yield an extract of equal or even higher quality in terms of the quantity of biologically active phenolic compounds compared to commercial extracts.

CONCLUSION

Hawthorn flowers and leaves are a good source of phenolic compounds that have cardioprotective and other beneficial effects which supports its usage in herbal medicinal products. Flowers and leaves extract is a richer source of beneficial polyphenols than fruit extract. Furthermore, homemade flowers and leaves extract is richer in phenolic compounds responsible for its health-promoting effects, compared to commercial ones, which supports preparation of hawthorn flowers and leaves extract at home by individuals. However, safety issues (contraindications, special warnings and precautions for use and possible interactions with other medicinal products and other forms of interactions) and duration of use should be addressed when supporting homemade herbal preparations especially when used in therapeutic doses!

Acknowledgment. This study was financially supported by the Ministry of Science, Technological Development and Innovation of the Republic of Serbia (Grant No. 451-03-47/2023-01/200125).

ИЗВОД

УПОРЕДНА АНАЛИЗА ФЕНОЛНОГ ПРОФИЛА И АНТИОКСИДАНТНЕ АКТИВНОСТИ ДОМАЋИХ И КОМЕРЦИЈАЛНИХ ЕКСТРАКТА ГЛОГА (*Crataegus* SPP.)НЕМАЊА ЖИВАНОВИЋ, НАТАША СИМИН, МАРИЈА ЛЕСЈАК, ДЕЈАН ОРЧИЋ, НЕДА МИМИЦА-ДУКИЋ
И ЕМИЛИЈА СВИРЧЕВ*Универзитет у Новом Сагу, Природно-математички факултет, Нови Саг*

Врсте рода *Crataegus* (глог) се од давнина примењују у традиционалној медицини, нарочито за лечење конгестивне срчане инсуфицијенције. Резултати бројних истраживања потврдили су да су ове врсте богате биолошки активним молекулима, посебно из класе полифенола, који поседују снажну антиоксидантну активност, што доприноси кардиопротективним особинама глога. На светском тржишту могу се наћи бројни фитопрепарати на бази глога, чију употребу као допунске терапије срчаних обољења подржава Европска агенција за лекове. Терапеутски ефекат препарата глога условљен је његовим хемијским саставом на који утичу бројни генетски и еколошки фактори као и начин припреме препарата. С обзиром на све већу популарност припреме фитопрепарата у кућним условима, циљ овог истраживања био је да се упореди полифенолни профил и антиоксидативна активност комерцијалних препарата глога и препарата добијених једноставним методама екстракције прилагођених кућним условима. Хемијски профил полифенола је одређен мерењем садржаја укупних фенола и флавоноида, као и квантитативном анализом одабраних полифенола помоћу LC-MS/MS технике. Антиоксидантни потенцијал је испитан помоћу DPPH и FRAP теста и мерењем способности инхибиције липидне пероксидације. Добијени резултати показали су да не постоје значајније разлике у саставу полифенолних једињења и у антиоксидативној активности између етанолних екстракта цветова, листова и плодова глога који су припремљени једноставним методама екстракције (*home-made*) и комерцијалних фитопрепарата. Надаље, етанолни екстракти листова и цветова глога били су богатији полифенолима и показали јачу антиоксидативну активност у поређењу са екстрактима плодова, без обзира на начин припреме.

(Примљено 30. новембра, ревидирано 8. децембра 2023, прихваћено 23. јануара 2024)

REFERENCES

1. M. Wu, L. Liu, Y. Xing, S. Yang, H. Li, Y. Cao, *Front. Pharmacol.* **11** (2020) 118 (<https://doi.org/10.3389%2Ffphar.2020.00118>)
2. B. Yang, P. Liu, *J. Sci. Food Agric.* **92** (2012) 1578 (<https://doi.org/10.1002/jsfa.5671>)
3. H. Bardakci, E. Celep, T. Gözet, Y. Kan, H. Kırmızıbekmez, *S. Afr. J. Bot.* **124** (2019) 5 (<https://doi.org/10.1016/j.sajb.2019.04.012>)
4. J. Wang, X. Xiong, B. Feng, *Evid. Based Complement. Alternat. Med.* **2013** (2013) 149363 (<https://doi.org/10.1155/2013/149363>)
5. R. Guo, M. H. Pittler, E. Ernst, *Cochrane Database Syst. Rev.* **23** (2008) CD005312 (<https://doi.org/10.1002/14651858.CD005312.pub2>)
6. Committee on Herbal Medicinal Products (HMPC), *European Union herbal monograph on Crataegus spp., folium cum flore*, Report No.: EMA/HMPC/159075/2014, European Medicines Agency, London, 2016 (https://www.ema.europa.eu/en/documents/herbal-monograph/final-european-union-herbal-monograph-crataegus-spp-folium-cum-flore_en.pdf)

7. S. Đorđević, N. Čujić-Nikolić, *Med. Raw Mater.* **41** (2021) 63 (<https://doi.org/10.5937/leksir2141063D>) (in Serbian)
8. T. Li, S. Fu, X. Huang, X. Zhang, Y. Cui, Z. Zhang, Y. Ma, X. Zhang, Q. Yu, S. Yang, S. Li, *J. Funct. Foods* **90** (2022) 104988 (<https://doi.org/10.1016/j.jff.2022.104988>)
9. *European Pharmacopoeia*, Vol. 8.1, Council of Europe, Strasbourg, 2014a, 01/2010:1432 (ISBN 10: 9287175276)
10. *European Pharmacopoeia*, Vol. 8.1, Council of Europe, Strasbourg, 2014b, 04/2013:1220 (ISBN 10: 9287175276)
11. *Europäisches Arzneibuch*, 10. Ausgabe, 3. Nachtrag, Amtliche deutsche Ausgabe (Ph. Eur. 10.3), Deutscher Apotheker Verlag, Stuttgart, 2021 (ISBN-10:376927735X)
12. Mordor Intelligence, <https://www.mordorintelligence.com/industry-reports/botanicals-market> (accessed 22.06.2023)
13. D. Sarpong, G. Ofosu, D. Botchie, F. Clear, *Technol. Forecast. Soc. Change* **158** (2020) 120127 (<https://doi.org/10.1016/j.techfore.2020.120127>)
14. C. Couteau, H. Diarra, M. Lecoq, A. Ali, M. Bernet, L. Coiffard, *J. Clin. Aesthet. Dermatol.* **16** (2023) 18 (<https://www.ncbi.nlm.nih.gov/pmc/articles/PMC9891214>)
15. M. M. Lesjak, I. N. Beara, D. Z. Orčić, G. T. Anačkov, K. J. Balog, M. M. Francišković, N. M. Mimica-Dukić, *Food Chem.* **124** (2011) 850 (<https://doi.org/10.1016/j.foodchem.2010.07.006>)
16. D. Orčić, M. Francišković, K. Bekvalac, E. Svirčev, I. Beara, M. Lesjak, N. Mimica-Dukić, *Food Chem.* **143** (2014) 48 (<https://doi.org/10.1016/j.foodchem.2013.07.097>)
17. D. Pintać, D. Četojević-Simin, S. Berežni, D. Orčić, N. Mimica-Dukić, M. Lesjak, *Food Chem.* **286** (2019) 686 (<https://doi.org/10.1016/j.foodchem.2019.02.049>)
18. F. Belabdelli, N. Bekhti, A. Piras, F. M. Benhafs, M. Ilham, S. Adil, L. Anes, *Nat. Prod. Res.* **36** (2022) 3234 (<https://doi.org/10.1080/14786419.2021.1958215>)
19. V. M. Tadić, S. Dobrić, G. M. Marković, S. M. Đorđević, I. A. Arsić, N. R. Menković, T. Stević, *J. Agric. Food Chem.* **56** (2008) 7700 (<https://doi.org/10.1021/jf801668c>)
20. L.-L. Zhang, L.-F. Zhang, J.-G. Xu, *Sci. Rep.* **10** (2020) 8876 (<https://doi.org/10.1038/s41598-020-65802-7>)
21. T. Froehlicher, T. Hennebelle, F. Martin-Nizard, P. Cleenewerck, J.-L. Hilbert, F. Trotin, S. Grec, *Food Chem.* **115** (2009) 897 (<https://doi.org/10.1016/j.foodchem.2009.01.004>)
22. G. Lucconi, T. Chlapanidas, E. Martino, R. Gaggeri, S. Perteghella, D. Rossi, S. Faragò, D. Vigo, M. Faustini, S. Collina, M. L. Torre, *Pharm. Dev. Technol.* **19** (2014) 65 (<https://doi.org/10.3109/10837450.2012.752387>)
23. H. Kallassy, M. Fayyad-Kazan, R. Makki, Y. El-Makhour, E. Hamade, H. Rammal, D. Y. Leger, V. Sol, H. Fayyad-Kazan, B. Liagre, B. Badran, *Med. Sci. Monit. Basic Res.* **23** (2017) 270 (<https://doi.org/10.12659/msmbr.905066>)
24. E. Shortle, M. N. O'Grady, D. Gilroy, A. Furey, N. Quinn, J. P. Kerry, *Meat Sci.* **98** (2014) 828 (<https://doi.org/10.1016/j.meatsci.2014.07.001>)
25. World Health Organization (WHO), *WHO Monographs on Selected Medicinal Plants*, Vol. 2, WHO, Geneva, 2002, p. 66 (ISBN: 9241545372)
26. D. Grassi, G. Desideri, S. Necozone, F. Ruggieri, J. B. Blumberg, M. Stornello, C. Ferri, *Hypertension* **60** (2012) 827 (<https://doi.org/10.1161/HYPERTENSIONAHA.112.193995>)
27. H. N. Siti, J. Jalil, A. Y. Asmadi, Y. Kamisah, *J. Funct. Foods* **64** (2020) 103606 (<https://doi.org/10.1016/j.jff.2019.103606>)

28. K. Patel, D. K. Patel, in *Bioactive Food as Dietary Interventions for Arthritis and Related Inflammatory Diseases*, 2nd ed., R. R. Watson, V. R. Preedy, Eds., Academic Press, London, 2019, p. 457 (<https://doi.org/10.1016/B978-0-12-813820-5.00026-X>)
29. H. N. Siti, J. Jalil, A. Y. Asmadi, Y. Kamisah, *Int. J. Mol. Sci.* **22** (2021) 5063 (<https://doi.org/10.3390/ijms22105063>)
30. S.-H. Yang, P.-H. Liao, Y.-F. Pan, S.-L. Chen, S.-S. Chou, M.-Y. Chou, *Phytother. Res.* **27** (2013) 1154 (<https://doi.org/10.1002/ptr.4841>)
31. Y. Peng, R. Gan, H. Li, M. Yang, D. J. McClements, R. Gao, Q. Sun, *Crit. Rev. Food Sci. Nutr.* **61** (2021) 1049 (<https://doi.org/10.1080/10408398.2020.1753165>)
32. C. Lu, Y. Xu, J.-C. Wu, P. Hang, Y. Wang, C. Wang, J.-W. Wu, J. Qi, Y. Zhang, Z. Du, *Naunyn-Schmiedeberg's Arch. Pharmacol.* **386** (2013) 747 (<https://doi.org/10.1007/s00210-013-0873-0>)
33. S. Xu, S. Chen, W. Xia, H. Sui, X. Fu, *Molecules* **27** (2022) 3009 (<https://doi.org/10.3390/molecules27093009>)
34. G. Siasos, D. Tousoulis, V. Tsigkou, E. Kokkou, E. Oikonomou, M. Vavuranakis, E. K. Basdra, A. G. Papavassiliou, C. Stefanadis, *Curr. Med. Chem.* **20** (2013) 2641 (<https://doi.org/10.2174/0929867311320210003>)
35. M. Lilamand, E. Kelaiditi, S. Guyonnet, R. Antonelli Incalzi, A. Raynaud-Simon, B. Vellas, M. Cesari, *Nutr. Meta. Cardiovasc. Dis.* **24** (2014) 698 (<https://doi.org/10.1016/j.numecd.2014.01.015>)
36. A. Kozłowska, D. Szostak-Węgierek, in *Bioactive Molecules in Food. Reference Series in Phytochemistry*, J. M. Mérillon, K. Ramawat, Eds., Springer, Cham, 2019, p. 53 (https://doi.org/10.1007/978-3-319-78030-6_54)
37. A. Ekalu, J. D. Habila, *Beni-Suef Univ. J. Basic Appl. Sci.* **9** (2020) 45 (<https://doi.org/10.1186/s43088-020-00065-9>)
38. H. B. Rashmi, P. S. Negi, *Food Res. Int.* **136** (2020) 109298 (<https://doi.org/10.1016/j.foodres.2020.109298>)
39. A. Bento-Silva, V. M. Koistinen, P. Mena, M. R. Bronze, K. Hanhineva, S. Sahlström, V. Kitrytė, S. Moco, A.-M. Aura, *Eur. J. Nutr.* **59** (2020) 1275 (<https://doi.org/10.1007/s00394-019-01987-6>).



J. Serb. Chem. Soc. 89 (5) 617–626 (2024)
JSCS–5743

Effect of silver nanoparticles in treating and healing of burn wound

MLADEN JOVANOVIĆ¹, MIRJANA VOJINOVIĆ MILORADOV²
and LIVIJA CVETIČANIN^{2,3*}

¹Faculty of Medicine, University of Novi Sad, Serbia, ²Faculty of Technical Sciences, University of Novi Sad, Serbia and ³Obuda University, Budapest, Hungary

(Received 4 November, revised 24 November 2023, accepted 22 January 2024)

Abstract: The paper investigates the effect of silver nanoparticles preparations on the rate of burn healing and scar quality. Three preparations for burn treatment were considered: one with silver sulfadiazine and two with silver nanoparticles woven into two types of dressing: one, of polyethylene and second, carboxymethyl cellulose. The experiment was performed on pigs, due to anatomical and pathophysiological similarities with human skin. All three silver preparations have antimicrobial properties with a beneficial effect on the healing of burns. Preparations with silver nanoparticles proved to be the most effective, since they encourage very fast burn epithelialization, affect reduction of the level of matrix metalloproteinase-9 in the environment of the burn wound, lead to faster expression of vascular endothelial growth factor – VEGF, cause less thickening of the epidermis and contractility, and improve tension characteristics of the scar compared to the preparation with silver sulfadiazine. By comparing results of healing parameters and evaluation of the scar achieved with preparations with silver nanoparticles, it was evident that the best overall results of local treatment were achieved with silver nanoparticles in crystalline form. Due to quantum-mechanics, surface and chemical oxidation–reduction (reactive oxygen species) phenomenological characteristics Ag nanoparticles in crystalline form have unique ability to catalyze rate of healing.

Keywords: Ag nanoparticles; Ag sulfadiazine; carboxymethyl-cellulose dressing; polyethylene dressing; skin recovery; burn healing.

INTRODUCTION

Over the last few decades wound care technologies have extensively evolved.¹ For wound regeneration and wound-healing bioactive agents, such as: nanoparticles, cells and molecules, which enhance the performance are applied. These agents, incorporated into various dressings, inhibit bacterial growth and replic-

* Corresponding author. E-mail: cveticanin@uns.ac.rs
<https://doi.org/10.2298/JSC231104004J>

ation, give enhanced re-epithelialization, vascularization, improve recovery of the tissue functionality, and overall accelerate effective wound healing.

Research made on wounds show that Ag, as a bioactive chemical agent, has an important role in healing wounds.² Namely, thirty years ago it was found that the poorly soluble molecules such as the anti-infective Ag sulfadiazine aided to wound therapy. Further, it was shown that dressing with Ag sulfadiazine gives an accelerating skin wound healing effect.³ The effect of Ag sulfadiazine in wound healing compared to saline soaked dressing was researched.⁴ It was found that the healing is faster with the sulfadiazine and thus not allow the contraction of the wound. According to the fast progress in nanotechnology and nanomedicine, based on inclusion of unconventional materials, the idea to use the Ag nanoparticles in wound treatment was developed.⁵ However, the question was if the Ag nanoparticles are useful for treating also high-degree burns.⁶ It was found that a sandwich structure composite wound dressing with firmly anchored silver nanoparticles are appropriate for severe burn wound healing.⁷ Ag nanoparticle exhibits exceptional physical and chemical properties due to the high surface area to volume ratio. In the close contact with cell membrane Ag nanoparticles produce the increased concentration of reactive oxygen species and the metal ions permeate into the cytoplasm, thus induce quick death of bacteria. Nanocomposites with Ag nanoparticles are promising candidates in the antibacterial fields and wound treating even for infected skin burns.⁸

Kaler *et al.* investigated the *in vivo* wound healing activity of nano-silver-based gel, formulated on the biologically synthesized silver nanoparticles.⁹ The gel was obtained that has high efficiency in healing, has reduced side effect and enhanced curative activity in comparison to its counterpart (silver ions).¹⁰ Recently, a novel hydrogel film wound dressing composed of ulvan and Ag nanoparticles was developed. Ag nanoparticles are incorporated into the hydrogel film with the aim to improve antibacterial properties and provide a potential burn treatment. Ulvan is a polysaccharide from green algae that shows good hydrogel film dressing characteristics. The result of the research shows that the ulvan–silver nanoparticles hydrogel films have the ability to accelerate the healing of second-degree burns on rats skin and are potential candidates for wound dressings.¹¹

Wide research on antimicrobial effect of Ag nanoparticles in polyethylene based nanocomposites has been done.^{12–15} It is shown that even small amount of Ag nanoparticles, immobilized on the polyethylene surface, give high antibacterial and antiviral activities.¹⁶

The polyethylene terephthalate membrane (obtained from plastic waste) with Ag nanoparticles is suggested for a suitable wound dressing.¹⁷ Gels prepared from a combination of carboxymethyl cellulose and poloxamer incorporated with tea tree oil and lavender together with Ag nanoparticles also promise to be the convenient wound dressings.¹⁸ The polydopamine carboxy methyl cellulose Ag

nanoarticles composite hydrogel coating has good antibacterial and antiadhesion properties, too.¹⁹ The sodium carboxymethyl cellulose gels containing Ag nanoparticles improve antibacterial performance in general.²⁰ However, the advantage of one type of dressing over another remains to be investigated.

In the paper the effect of silver nanoparticles on treating burns is investigated. The research is done on pigs and their skin. Three dressings on burn injury are considered: one, with Ag-sulfadiazine, second, Ag nanoparticles in a carrier made of polyethylene and the third, Ag in a carrier made of carboxymethyl-cellulose. The aim was to compare the influence of the three dressings on burn wound and to obtain the optimal one which would substantially reduce the healing time, also reduce the risk of recurrent infections as well as costs associated.

EXPERIMENTAL

Plan of experiment

The experiment was done on 10 pigs of the age of 2 months and with weight of 20 kg. On the skin 8 burns were created: 4 on one and 4 on the other side of the backbone. Burns are of the same size, properly arranged and at the appropriate distance, at the same height, and equidistant from the spinal column, in order to have approximately the same thickness of the dermis. After shaving, the preparation of the operative field of skin was carried out by an aerosol and not by rubbing, in order not to cause hyperemia, which can affect the depth of the burn. The full-thickness burn wounds were created under anesthesia with the special equipment. The equipment consists of a heater (with voltage of 150–230 V), a thermo regulator (with accuracy 0.5 %) and a brass extension which is specially made with a smooth contact surface (of dimensions 47 mm×47 mm) with an integrated PT100 probe. Contact burns, with a surface area of 22.09 cm², were created with a brass attachment heated to a temperature of 92 °C for 15 s with uniform pressure.

Immediately, after the injury, various dressings with Ag were used for burn treatment and the research on effect of Ag on burn wound healing was done. For testing, the Ag was incorporated into various compress materials in elemental or ionic form. Two considered dressing materials applied in the experiment are: polyethylene and the carboxymethyl cellulose with Ag nanoparticles. For both dressings the incorporated silver is released gradually as an integral part of a certain material. Thus, one of them is the sandwich dressing with outside polyethylene layers and an absorbent inner core, made of artificial silk and polyester, in which silver in the form of nanocrystal, smaller than 20 nm, is woven (Acticoat – Smith & Nephew). Nanocrystalline silver protects the wound from bacterial contamination, and the inner core maintains optimal validity, which is essential for wound healing. At the other side, Ag nanoparticles are pressed into the carboxymethyl cellulose whose fibers absorb exudate, form a gel (Aquacel Ag, Convatec) and thereby maintain a moist wound environment. The silver ions are slowly released in this compression through hydration. These ions act as counterions in carboxymethyl cellulose. The third considered dressing is with sulfadiazine. In contrast to the aforementioned ones, Ag cations are counter-ions of deprotonated sulfadiazine anion.

Four groups were formed according to the utilized dressing:

- | | |
|-----------------|--|
| K control group | sterile saline-soaked dressing, |
| SSD group | dressing with 1% Ag-sulfadiazine, |
| NP group | dressing with Ag nanoparticles in crystalline form in polyethylene and |
| NKC group | dressing with Ag nanoparticles in carboxymethyl cellulose. |

Burns of each pig were randomly treated with 4 dressings: 2 with K, 2 with SSD, 2 with NP and 2 with NKC. It means, the total number of burns was 80 and each treatment was applied for two times on each pig, *i.e.*, 20 samples. The experiment lasted for 70 days at the Scientific Institute for Veterinary Medicine in Novi Sad, Serbia. In the postoperative course, the analgesic agent Diclofenac 50 mg was prescribed for the first ten days. The animals were kept in individual boxes with a surface area of 5 m² to prevent possible mutual injury. The feeding of pigs was standard. Dressing was carried out at regular intervals, using a standardized procedure with the same topical agent until complete healing. Sampling was done on 1, 4, 7, 11, 14, 18, 21, 24, 28, 32, 35 and 38 day. During this time the healing of the wound was monitored and the formed scar was analyzed using morphometric, histological, immune biochemical, microbiological and clinical parameters. On the 70th day after the experiment, the animals were sacrificed, and the skin samples were analyzed morpho-metrically, histologically and tensometrically.

Statistical procedures for data processing

For data processing the statistical package SPSS 14.0 for Windows was applied. Using the *T*-test, for comparison of 2 groups of data, and the one-way analysis of variance (ANOVA), for three or more groups of data, the average mean values were compared with the normal distribution for certain parameters. To check the differences in the distribution frequency of variables non-parametric tests were used. In addition, the Mann–Whitney test (for two independent samples) and the χ test are applied for comparing the frequencies of attributive features with a normal measurement scale. For all statistical tests it is accepted that there is a statistically significant difference if the probability of the null hypothesis is less than 0.05 ($p < 0.05$).

RESULTS AND DISCUSSION

Results of microbiological and histological wound swabs analysis

After application of dressing on burn, the quantitative and qualitative histological and microbiological analyses were done. The presence of bacteria on certain preparations only on the surface of the wound, and not inside the tissue was investigated. It was recorded that on the first day after the infliction of burns, the presence of bacteria was not observed in any group. On the 4th day, only a few individual cases of bacterial contamination were recorded in the control group. The highest contamination was found on the eleventh day after injury in all groups, except in the SSD group where it was on the fourteenth day. The presence of bacteria on the wound surface was in 40 % of the burns of the control group, 13 % of the burns of the SSD group, 12 % of the burns of the NCD group and 11 % of the burns of the NK group.

In addition, there was a significant statistical difference between the results of the control group in relation to all other groups ($\chi^2 = 9.267$, $p < 0.05$). In the control group, the number of histologically positive findings was significantly higher in all phases in which healing was monitored. When comparing the 3 remaining tested groups that were treated with different Ag preparations, no significant statistical differences were observed.

Analyzing and separating the bacteria types on the wound groups it was observed that in the group with saline-soaked dressing more types of bacteria are evident than in other groups (see Table I). Thus, in K there are 6, in SSD and NP there are 3 and in NKC only 2 types of bacteria. Comparing the control K group result with other ones, significant statistical differences was noted ($\chi^2 = 17.039$, $p < 0.01$). At the other side, the differences between the NP group, the SSD and NKC groups, in which burns were also treated with Ag-based preparations, is very small and does not show statistical significance ($\chi^2 = 1.625$, $p > 0.05$). For these three examined groups, the uniform diversity of bacterial strains is also a characteristic.

TABLE I. Bacteria isolated from variously treated burn wounds

Bacteria isolated from burn wounds	K	SSD	NP	NKC
<i>Staphylococcus sp. Coagulasa neg.</i>	+	+	+	+
<i>Staphylococcus saprophzticus</i>	+	+	+	-
<i>Enterobacter sp.</i>	+	-	-	-
<i>Escherichia coli</i>	+	-	-	+
<i>Proteus sp.</i>	+	+	-	-
<i>Klebsiella oxytoca</i>	+	-	-	+
Summary of positive counts, %	55	18	20	16

Clinical parameters on local infection

In all three groups of burns that were treated with different Ag preparations (SSD, NP, NKC), in most cases no indicators were recorded that would declare state of the presence of local infection. The condition of these burn wounds was characterized with a score of 1.

There was no statistically significant difference between these groups treated with different Ag preparations. However, greater number of burn wounds in the control K group, whose condition was characterized by a score of 2, differed statistically significantly compared to the other groups ($\chi^2 = 7.703$, $p < 0.05$).

Results of wound surface planimetric measurement during healing

The kinetic rate of healing of a burn wound is the most authoritative way to determine the effectiveness of the applied topical agent. Burns that were treated with Ag nanoparticles in ionic and crystalline form (NKC and NP) had, on average, a faster onset of healing compared to the other two groups. A statistically significant difference was observed when comparing the NP and K group and the NP and SSD group on the fourteenth day after injury.

In Table II, the re-epithelialization rate as the function of the date is shown. It is directly evident that there is the most significant difference in re-epithelialization during the eighteenth and twenty first day. The NP group had the best result, followed by the NKC group. A statistically significant difference was

manifested on the eighteenth day when comparing the NP and the NKC group with SSD and the K group. On the twenty first day, a significant difference in epithelialization was determined only in the NP group and the NKC group compared to the control K group. On the twenty fourth day the biochemical rate of re-epithelialization was still the best in the NP group and then, NKC, SSD and the control K group, but these differences did not have statistical significance. In the final healing phase, the differences between the groups were also not statistically significant. However, it is seen that 50 % of burnt is healed after 21 days, while the 75 % of re-epithelialization is after 28 days except the group K. For all groups the 100 % healing is in 38 days.

TABLE II. Re-epithelialization in time for all four groups

Re-epithelialization, %/day	K	SSD	NP	NKC
14	17	16	20	19
18	28	48	50	45
21	60	63	80	67
24	70	77	87	78
28	85	96	95	95
32	95	96	97	98
35	97	97	99	99
38	100	100	100	100

On the first day after inflicting injury, no expression of MMP-9 was observed. The first signs were evident on the fourth day in all groups. During the eleventh and fourteenth days a higher presence of MMP-9 was verified in the tissue of the burn wound in the K control, SSD and NKC groups compared to the NP group. The differences in expression were even more pronounced on eighteenth day. On the twenty fourth day a lower expression of MMP-9 was observed in the two groups treated with Ag nanoparticles compared to the other two groups. Finally, by monitoring of this protease from the first to twenty fourth day of burn treatment, the increase of the total expression of MMP-9 was observed.

Measured results of the scar surface and skin properties after burn treatment

By comparing the groups, it was observed that the highest percentage of contraction of the scar in relation to the surface of the skin before the injury was observed in the control group, where it was 38.3 %. In the group in which Ag-sulfadiazine was used, it was slightly lower (37.3 %), while the lowest percentage of contraction was recorded in the remaining two groups, in the NKC group it was 36 %, and in the NP group 35.2 %. A statistically significant difference (ANOVA, F.3.204, $p < 0.05$) was found when comparing the control K group with NKC ($t = 2.396$, $p < 0.05$), as well as when comparing the control K group with the NP group ($t = 2.485$, $p < 0.05$) which indicates that the topical treatment with Ag

nanoparticles in crystalline and ionic form had an effect on the reduction of the total contraction of the scar.

Thickness of epidermis

It was shown that the thickness of the epidermis in all examined groups was significantly greater in relation to healthy skin samples from the same region of the body where the cut thickness was 70 μm ($t = 2.664$, $p < 0.01$). A difference in the thickness of the epidermis can be observed in the burn groups that were treated with preparations with Ag nanoparticles compared to the control group and the one that was treated with Ag-sulfadiazine. A statistically significant difference was observed when comparing the results of the control and NKC groups ($t = 2.396$, $p < 0.05$), as well as the control and NP groups ($t = 2.485$, $p < 0.05$).

Thickness of dermis

The average total thickness of the dermis in the control group was 1000 μm , 980 μm in the SSD group, 960 μm in the NKC group, and 950 μm in the NP group. Hence, the average total thickness of the dermis in the studied groups was 970 μm . It differed minimally, that is, it was somewhat thicker than the average thickness of the dermis of healthy skin of the same region, which was 940 μm . These differences did not show statistical significance. (ANOVA, $F = 1.732$, $p > 0.05$).

Tensiometry results

Tensiometric analysis was performed on the seventieth day after the injury. It was observed that the scar tissue is on average 1.6 times weaker than intact skin, i.e. that it reached 63.9 % of the strength of healthy skin taken from the body region. The average ability to stretch the scarred skin when tearing was 3.7 times less compared to the intact skin, respectively, it reached only 27.3 % of the extension length of healthy skin of the same region.

By comparing the average values of the force required to tear the tissue between the groups, it was shown that the lowest force was reached by the control group, which was 8168 N, then the group treated with Ag-sulfadiazine 8644 N, the NP group 10330 N and the NKC group 11253 N. A statistically significant difference between the force was established tearing in healthy skin compared to these examined groups (ANOVA, $F = 91,980$, $p < 0.01$). In addition, a statistically significant difference ($p < 0.05$) was found when comparing the NKC and also the NP group with the control K group, and also of the NKC with SSD group.

The average values of the stretching limit of the skin were the least in the control K and SSD groups and amounted to 964 and 1070 μm respectively; while in the remaining two groups they were significantly higher and amounted to 1185 μm in the NP group and 1210 μm in the NKC group. A statistically significant difference was found between the extension of healthy skin in relation to all

examined groups (ANOVA, $F = 2715.205$, $p < 0.01$). A statistically significant difference ($p < 0.05$) was verified when comparing the NKC group and the NP group with the control C and SSD group.

CONCLUSIONS

The following is concluded:

1. All tested preparations with Ag in their composition had strong and approximately equal antimicrobial properties. By comparing histological, clinical and microbiological parameters, no statistically significant difference in antimicrobial action was observed between the groups of burns treated with Ag-sulfadiazine and Ag nanoparticles in crystalline or ionic form.

2. Nanocrystalline Ag has intensive anti-inflammatory properties and affect the reduction of MMP-9 levels in the environment of the burn wound. Burn epithelisation of 50, 75 and 100 % occurred faster in the group of burns treated with Ag nanoparticles in crystalline form than in ionic form. Ag nanoparticles in crystalline and ionic form showed proangiogenic properties and cause the increase of VEGF in burn already ten days after the injury. In addition, the reduction of the surface area of the open wound over time was the fastest in the group of burns treated with Ag nanoparticles in crystalline form, and then with Ag nanoparticles in carboxymethyl-cellulose.

3. Summarizing results related to the analysis of scars, it can be concluded that the groups in which Ag nanoparticles were used, showed the best research results as the catalyzer: significantly less thickening of the epidermis, less contractility of the scar, as well as better tension characteristics.

4. By comparing all the results of the examined parameters of healing and evaluation of scars, it was determined that the best overall results were obtained when using preparations with Ag nanoparticles in crystalline form. This result can be primarily explained by the surface high impact of Ag nanoparticles on the wound environment during healing and scar formation. Ag nanoparticles have unique quantum-mechanics, surface (nano size/amphiphilicity) and chemical oxidation–reduction (reactive oxygen species) properties permitting the antimicrobial and cytotoxicity catalytic characteristics.

Future research in burn wound treatment would be directed toward improving the considered dressing with Ag nanoparticles in crystalline form by adding substances which would have not only anti-inflammatory and anti-infective properties but also anesthetic effect. The recent research shows that the clove oil²¹ may be a good candidate.

ИЗВОД

УТИЦАЈ НАНОЧЕСТИЦА СРЕБРА НА ЛЕЧЕЊЕ И ЗАРАСТАЊЕ ОПЕКОТИНЕ

МЛАДЕН ЈОВАНОВИЋ¹, МИРЈАНА ВОЈИНОВИЋ МИЛОРАДОВ² и ЛИВИЈА ЦВЕТИЋАНИН^{2,3}¹Медицински факултет, Универзитет у Новом Сагу, ²Факултет техничких наука, Универзитет у Новом Сагу и ³Obuda University, Budapest, Hungary

У раду је истраживано деловање три препарата сребра, једног са сребро-сулфадиазиним и два са наночестицама сребра у јонском и кристалном облику, на брзину зарастање опекотине и квалитет насталог ожиљка. Експреимент је извршен на кожи свиња због анатомске и патофизиолошких сличности са људском кожом. Истраживања су показала да сва три препарата са сребром имају антимикуробне особине и благотворно делују на зарастање опекотина. Препарати са наночестицама сребра су се показали као високо ефикасни, јер каталишу врло брзу епителизацију опекотина, утичу на смањење нивоа матрикс маталопротеиназе-9 у окружењу опекотиинске ране и доводе до брже експресије васкуларног ендотелног фактора раста. Поред тога, изазивају мање задебљања епидерма, мању контрабилност и боље тензионе карактеристике ожиљка у односу на препарат са сребро-сулфадиазиним. Компарацијом резултата параметара зарастања и евалуације ожиљка остварених препаратима са наночестицама сребра утврђено је да су најбољи укупни резултати локалног лечења постигнути наночестицама сребра у кристалном облику као резултат квантно механичких, физичких, површинских, а посебно оксидоредуктивних (активне кисеоничне специје) карактеристика, а потом и у јонском облику.

(Примљено 4. новембра, ревидирано 24. новембра 2023, прихваћено 22. јануара 2024)

REFERENCES

1. M. H. Norahan, S. C. Pedroza-González, M. G. Sánchez-Salazar, M. M. Álvarez, G. T. de Santiago, *Bioact. Mater.* **24** (2023) 197 (<https://doi.org/10.1016/j.bioactmat.2022.11.019>)
2. M. J. Fresno, E. Selles, M. A. Camacho, *Acta Technol. Legis Medicam* **6** (1995) 220
3. M. C. Bonferoni, G. Sandri, S. Rossi, E. Delleria, A. Invernizzi, C. Boselli, B. Vigani, C. Caramella, F. Ferrari, A. I. Cornaglia, F. Riva, C. Del Fante, C. Perotti, *Mar. Drugs* **16** (2018) 56 (<https://doi.org/10.3390/md16020056>)
4. H. Maghsoudi, S. Monshidazadeh, M. Mrsgari. *Ind. J. Surg.* **73** (2011) 24 (<https://doi.org/10.1007/s12262-010-0169-2>)
5. H. M. Abdel-Mageed, N. Z. Abuelezz, R. A. Radwan, S. A. Mohamed, *J. Microencapsul.* **38** (2021) 414 (<https://doi.org/10.1080/02652048.2021.1942275>)
6. D. A. N. Moreno, M. S. Saladin, F. J. M. Viroel, M. M. J. Dini, T. B. Pickier, J. Amaral, C. A. dos Santos, V. M. Hanai-Yoshida, D. Grotto, M. Gerenutti, S. Hyslop, Y. Oshima-Franco, *Adv. Pharm. Bull.* **11** (2021) 130 (<https://doi.org/10.34172/apb.2021.014>)
7. J. M. Yang, Y. F. Huang, J. J. Dai, X. A. Shi, Y. Q. Zheng, *Regen. Biomater.* **8** (2021) rbab037 (<https://doi.org/10.1093/rb/rbab037>)
8. M. A. K. Ramadhan, A. N. Balasm, S. B. Kadhem, H. F. Al-Saedi, *Maced. Vet. Rev.* **44** (2021) 17 (<https://doi.org/10.2478/macvetrev-2020-0032>)
9. A. Kaler, A. K. Mittal, M. Katariya, H. Harde, A. K. Agrawal, S. Jain, U. C. Banarjee, *J. Nanopart. Res.* **16** (2014) 2605 (<https://doi.org/10.1007/s11051-014-2605-x>)

10. L. G. Wasef, H. M. Shaheen, Y. S. El-Sayed, T. I. A. Shalaby, D. H. Samak, M. E. Abd El-Hack, A. Al-Owaimer, I. M. Saadeldin, A. El-mleeh, H. Ba-Awadh, A. A. Swelum, *Biol. Trace Elem. Res.* **193** (2020) 456 (<https://doi.org/10.1007/s12011-019-01729-z>)
11. E. Sulastri, R. Lesmana, M. S. Zubair, A. F. A. Mohammed, K. M. Elamin, N. Wathoni, *Heliyon* **9** (2023) e18044 (<https://doi.org/10.1016/j.heliyon.2023.e18044>)
12. D. Olmos, G. M. Pontes-Quero, A. Corral, G. González-Gaitano, J. González-Benito, *Nanomaterials* **8** (2018) 60 (<https://doi.org/10.3390/nano8020060>)
13. M. Ashrafi, M. Hamadianian, A. R. Ghasemi, F. J. Kashi, *Polym. Compos.* **40** (2019) 3393 (<https://doi.org/10.1002/pc.25200>)
14. S. Dehghani, S. H. Peighambaroust, S. H. Fasihnia, S. J. Peighambaroust, N. K. Khosrowshahi, B. Gullón, J. M. Lorenzo, *Food Anal. Methods* **14** (2021) 98 (<https://doi.org/10.1007/s12161-020-01856-7>)
15. M. M. Mishyna, O. V. Hopta, G. O. Syrova, Y. A. Mozgova, S. G. Malanchuk, V. O. Makarov, V. L. Avramenko, I. A. Marchenko, O. S. Dubovyk, Y. M. Mishyn, *J. Educ. Health Sport* **11** (2021) 225 (<https://doi.org/10.12775/JEHS.2021.11.01.022>)
16. S. Seino, Y. Ohkubo, T. Magara, H. Enomoto, E. Nakajima, T. Nishida, Y. Imoto, T. Nakagawa, *Nanomaterials* **12** (2022) 3046 (<https://doi.org/10.3390/nano12173046>)
17. T. Soltanzakerin-Sorkhabi, M. Fallahi-Samberan, V. Kumaravel, *Molecules* **28** (2023) 5439 (<https://doi.org/10.3390/molecules28145439>)
18. S. Alven, S. A. Adeyemi, P. Ubanako, D. T. Ndinteh, Y. E. Choonara, B. A. Aderibigbe, *Ther. Deliv.* **14** (2023) 139 (<https://doi.org/10.4155/tde-2022-0054>)
19. Y. Cai, R. Gu, D., Yuhang, Z. Qi, Z. Ke, C. Cheng, H. Yang, J. Li, X. Yuan, *J. Biomater. Appl.* **38** (2023) 73 (<https://doi.org/10.1177/08853282231173576>)
20. C. Huang, M. Xiao, H. Cui, J. Wang, Y. Cai, Y. Ke, *Int. J. Biol. Macromol.* **252** (2023) 126495 (<https://doi.org/10.1016/j.ijbiomac.2023.126495>)
21. S. Perteghella, A. Garzoni, A. Invernizzi, M. Sorrenti, C. Boselli, A. Icaro Cornaglia, D. Dondi, S. Lazzaroni, G. Marrubini, C. Caramella, I. Catenacci, M. C. Bonferoni, *Antioxidants* **12** (2023) 273 (<https://doi.org/10.3390/antiox12020273>).



J. Serb. Chem. Soc. 89 (5) 627–641 (2024)
JSCS–5744

Diffusion models of gentamicin released in poly(vinyl alcohol)/chitosan hydrogel

VESNA MIŠKOVIĆ-STANKOVIĆ^{1#*}, ANA JANKOVIĆ^{2#}, SVETLANA GRUJIĆ²,
IVANA MATIĆ-BUJAGIĆ², VESNA RADOJEVIĆ^{2#}, MAJA VUKAŠINOVIĆ-SEKULIĆ²,
VESNA KOJIĆ³, MARIJA DJOŠIĆ^{4#} and TEODOR M. ATANACKOVIĆ⁵

¹Faculty of Ecology and Environmental Protection, University Union – Nikola Tesla, Cara Dusana 62–64, 11000 Belgrade, Serbia, ²Faculty of Technology and Metallurgy, University of Belgrade, Karnegijeva 4, 11000 Belgrade, Serbia, ³Oncology Institute of Vojvodina, University of Novi Sad, Put Dr Goldmana 4, 21204 Sremska Kamenica, Serbia, ⁴Institute for Technology of Nuclear and Other Mineral Raw Materials, Bulevar Franš d'Eperea 86, 11000, Belgrade, Serbia and ⁵Faculty of Technical Sciences, University of Novi Sad, 21000 Novi Sad, Serbia

(Received 7 December 2023, revised 15 January, accepted 22 January 2024)

Abstract: This study presents comparison of our recently formulated two compartmental model with General fractional derivative (GFD) and Korsmeyer–Peppas, Makoid–Banakar and Kopcha diffusion models. We have used our GFD model to study the release of gentamicin in poly(vinyl alcohol)/chitosan/gentamicin (PVA/CHI/Gent) hydrogel aimed for wound dressing in medical treatment of deep chronic wounds. The PVA/CHI/Gent hydrogel was prepared by physical cross linking of poly(vinyl alcohol)/chitosan dispersion using freezing-thawing method, and then was swollen for 48 h in gentamicin solution, at 37 °C. Different physicochemical (FTIR, SEM), mechanical and biological (cytotoxicity, antibacterial activity) properties have been determined. The concentration of released gentamicin was determined using a high-performance liquid chromatography (HPLC) coupled with mass spectrometry (MS). The ratio between concentration of released gentamicin and initial concentration of gentamicin in the hydrogel was monitored for the prolonged time period in order to obtain gentamicin release profile. It was proven that our novel diffusion GFD model better fitted to experimental data than other models, and enabled the determination of diffusion coefficient precisely for the entire time period.

Keywords: drug release; diffusion; pharmacokinetics; cytotoxicity; antibacterial activity; mechanical properties.

* Corresponding author. E-mail: vesna@tmf.bg.ac.rs

Serbian Chemical Society member.

<https://doi.org/10.2298/JSC231207010M>

INTRODUCTION

In pharmacokinetics, a popular choice is that of compartmental models, due to their implicit simplicity and ease of understanding in relation to the mass balance equations and assumptions for uniform distribution, homogeneous transient times and immediate response to drug bolus administration.¹ Numerous works and decades of research have tailored their applicability for optimal drug delivery assist devices in several domains of medical applications, *e.g.*, diabetes,² cancer,^{3,4} anaesthesia,^{5–7} immune deficiency, leukaemia⁸ and hormonal treatment.⁹ In this work we made an attempt to employ results of fractional derivative model, recently formulated^{10,11} for the study of drug release from hydrogel aimed for deep chronic wounds. Along with being a physical barrier for bacterial colonization, wound dressings often need to contain an antibacterial agent for active infection protection, which would be released gradually to maintain wound sterility.^{12–14} Generally, profiles of drug release from hydrogel matrices usually exhibit quick initial release – the so-called “burst release” effect, followed by a longer period of gradual release that eventually levels off as a plateau reaching 80–100 % release efficiency.^{15–17} There are several diffusion models used for evaluating the drug release profiles from hydrogel carriers, among which the most widespread are Korsmeyer–Peppas,¹⁸ Makoid–Banakar,¹⁹ Kopcha,²⁰ as well as the early-time approximations^{21,22}

The aim of this work was to synthesize and characterize poly(vinyl alcohol)/chitosan/gentamicin (PVA/CHI/Gent) hydrogel aimed for wound dressing and to predict the drug release behaviour using our two compartmental diffusion GFD model, as well as to compare GFD model with Korsmeyer–Peppas, Makoid–Banakar and Kopcha diffusion models.

EXPERIMENTAL

Materials

The following chemicals were utilized for preparation of PVA/CHI/Gent hydrogel: poly(vinyl alcohol) powder (fully hydrolysed, M_w , 70–100 kDa, Sigma Aldrich), chitosan powder (M_w , 190–310 kDa, deacetylation degree 75–85 %, Sigma Aldrich) and gentamicin sulfate solution (50 mg/ml in dH₂O, Sigma Aldrich). All solvents used for gentamicin release measurements were HPLC grade from J.T. Baker, USA, or Sigma Aldrich, gentamicin sulphate (50 mg/ml, Sigma Aldrich). Deionized water was obtained by passing the distilled water through a GenPure ultrapure water system (TKA, Germany). For antibacterial properties evaluation, monobasic (Centrohém, Serbia) and dibasic (Sigma Aldrich) potassium phosphates were used. Cell culture suspensions for cytotoxicity tests were prepared using MTT tetrazolium salt, EDTA, fetal calf serum and antibiotic–antimycotic solution (Sigma Aldrich).

Synthesis of PVA/CHI/Gent hydrogel

PVA colloid dispersion was prepared by dissolving PVA powder in hot distilled water at 90 °C for 2 h, under magnetic stirring. Chitosan was dissolved in 2 vol. % CH₃COOH under constant stirring at room temperature. After cooling of PVA, the CHI dispersion was added dropwise and the final dispersions (containing 10 wt. % PVA and 0.5 wt. % CHI) were homo-

genized by mixing at room temperature for 2–3 h. Further, the PVA/CHI hydrogels were prepared by physical cross linking of PVA/CHI dispersion using freezing–thawing method in 5 cycles. One cycle consisted of 16 h freezing at $-18\text{ }^{\circ}\text{C}$ followed by 8 h thawing at $4\text{ }^{\circ}\text{C}$. Finally, the hydrogels were swollen in 5.0 mg/ml gentamicin solution at $37\text{ }^{\circ}\text{C}$ during 48 h.

Physicochemical and mechanical characterization

Field-emission scanning electron microscopy (FE-SEM) was carried out on Mira3 XMU FEG-SEM (Tescan, Czech Rep.), operated at 7 kV, with SE detector. Fourier-transform infrared spectroscopy (FTIR) was carried out using the Nicolet iS10 FTIR spectrometer (Thermo Fisher Scientific, USA) between 4000 and 400 cm^{-1} . Tensile test of PVA, PVA/CHI and PVA/CHI/Gent films was performed at texture analyzer (Shimadzu, Japan) with load cell of 5 kN and test speed of 1 mm/min. The tensile strength (σ_{TS}) was determined as maximum on stress–strain curve, while Young's modulus of elasticity (E) was calculated as the slope of elastic part of stress–strain curve with Trapezium X software (Shimadzu, Japan). Specimens were prepared by cutting the films in long stripes (15×50) mm^2 . All measurements were performed in triplicates.

Gentamicin release studies

For the drug release assay, PVA/CHI/Gent hydrogel was immersed in deionized water and kept at $37\text{ }^{\circ}\text{C}$. Detailed experimental procedure is provided in the Supplementary material to this paper.

Evaluation of antibacterial properties

Antibacterial properties of PVA/CHI/Gent hydrogels were evaluated by quantitatively monitoring changes in the viable number of bacterial cells in suspensions that allowed for the direct contact with the material. In order to provide meaningful comparisons, tests were also run simultaneously on PVA, PVA/CHI and PVA/Gent. Two bacterial strains were used; *Staphylococcus aureus* TL (culture collection FTM, University of Belgrade, Serbia) and *Escherichia coli* ATCC 25922 (American Type Culture Collection). Detailed experimental procedure is provided in the Supplementary material.

Cytotoxicity

The 3-(4,5-dimethylthiazol-2-yl)-2,5-diphenyl tetrazolium bromide (MTT) test and dye exclusion test (DET) were employed to evaluate the toxicity of PVA, PVA/Gent, PVA/CHI and PVA/CHI/Gent hydrogels. Two fibroblast cell lines were used, a human (MRC-5) and a mice (L929) cell line. The experimental procedures for preparing cell cultures, MTT and DET tests are explained in the Supplementary material.

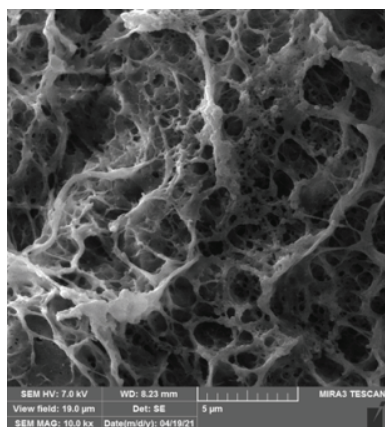
RESULTS AND DISCUSSION

Scanning electron microscopy (SEM)

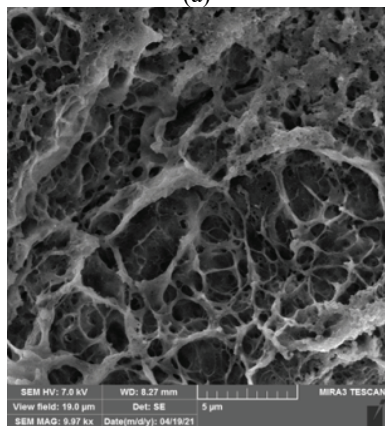
The microphotographs of PVA/CHI (Fig. 1a) and PVA/CHI/Gent hydrogels (Fig. 1b) revealed three-dimensional network structures with interconnected micropores evenly distributed through the hydrogels, suggesting that antibiotic has no influence on the hydrogels structure, confirming its homogeneous distribution through the polymer matrix.

Fourier-transform infrared spectroscopy (FTIR)

FTIR spectra for PVA/CHI and PVA/CHI/Gent hydrogels are represented in Fig. 2.



(a)



(b)

Fig. 1. SEM micrographs of PVA/CHI (a) and PVA/CHI/Gent (b) hydrogels.

The broad band observed at around 3260 cm^{-1} can be assigned to the stretching vibration of O–H participating in hydrogen bonding interactions.^{17,23} In comparison to the FTIR spectra of pure PVA hydrogel (data not shown), the shifting of this band to the lower wavenumbers indicated the interaction between hydrogen bonded –OH groups in PVA matrix and water molecules, along with hydrogen bond cross-linking between PVA hydroxyl groups and –NH₂ and –OH groups from gentamicin and chitosan. Bands at 2935 cm^{-1} and at around 2910 cm^{-1} can be assigned to the asymmetric stretching of CH₂ and symmetric stretching of C–H of the alkyl groups,²⁴ suggesting trans zigzag conformation of the polymers' hydrocarbon chains. The band at around 1650 cm^{-1} suggested the stretching of carbonyl bonds (C=O), most probably originated from the residue after hydrolysis of polyvinyl acetate during PVA production.^{17,24} The bands that appear at 1415 and 1416 cm^{-1} can be assigned to the –OH in plane coupling with C–H wagging in CH₂.^{17,25} In the case of PVA/CHI hydrogel (Fig. 1a), detected

bands at 1237 and 1326 cm^{-1} can be assigned to the C–H wagging, while band detected at 1376 cm^{-1} can be assigned to the $-\text{CH}_2$ wagging.²⁵ Almost the same bands' position for PVA/CHI/Gent hydrogel can be observed (Fig. 2b). Bands corresponding to symmetric stretching of C–O at 1142 cm^{-1} for both hydrogels, pointed to crystalline sequence of PVA.^{26,28} Bands detected at 1086, 916 and around 833 cm^{-1} , can be assigned to the C–O stretching in secondary alcohols (C–O–H),^{25,27} rocking of CH_2 vibration and C–C stretching in atactic form of PVA,^{23,24} respectively. Band at around 2850 cm^{-1} , represented the C–H stretching in chitosan structure.²⁵

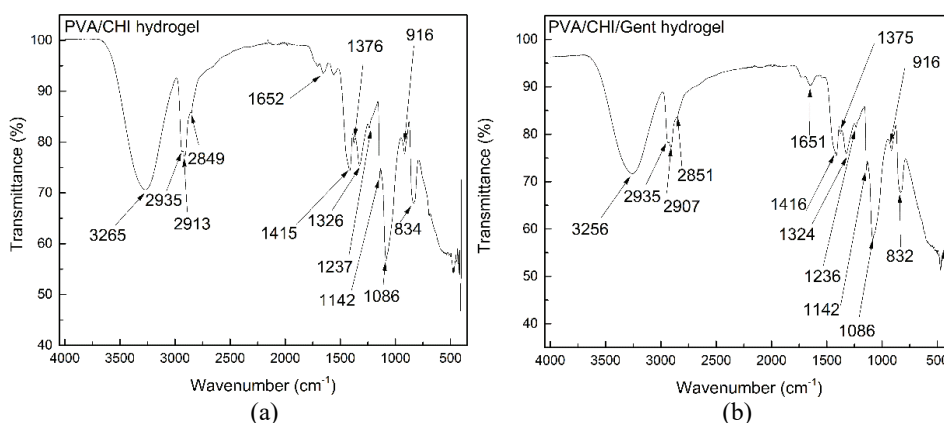


Fig. 2. FTIR spectra of PVA/CHI (a) and PVA/CHI/Gent (b) hydrogels.

Cytotoxicity

Fig. 3a and b display the results of cytotoxicity towards MRC-5 and L929 cells, based on the MTT test and the DET test, respectively.

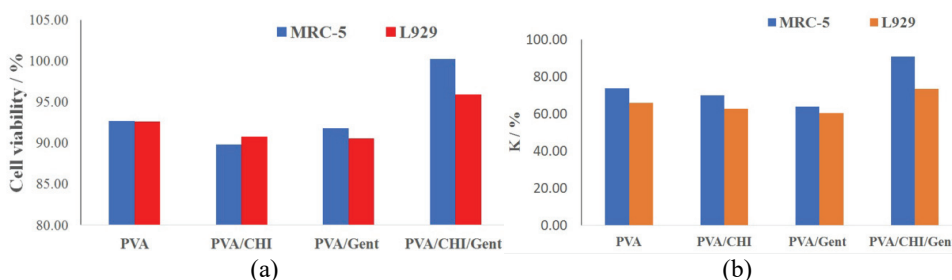


Fig. 3. Cytotoxicity of PVA, PVA/Gent, PVA/CHI and PVA/CHI/Gent hydrogels towards MRC-5 and L929 cell lines based on (a) MTT test and (b) DET test results.

The MTT test is based on the reduction of a water-soluble monotetrazolium salt to a violet-blue water-insoluble formazan. Only metabolically active cells are able to reduce the MTT salt that passes through the cell membrane and the inner

mitochondrial membrane into coloured formazan, thus providing insight into the metabolic activity of the cell.²⁹ Based on the material cytotoxicity scale proposed by Sjogren *et al.*³⁰ (S, cell viability >90 % – non-cytotoxic, 60–90 % – mildly cytotoxic, 30–60 % – moderately cytotoxic, ≤30 % – cytotoxic), according to which PVA, PVA/Gent, PVA/CHI and PVA/CHI/Gent could be considered as non-toxic materials and therefore are suitable for future *in vivo* testing. Trypan blue DET test is an efficient and simple method that is based on cell staining after their mixing with the solution of a dye. PVA/CHI/Gent hydrogel with active component did not provoke the inhibition of growth neither in the case of MRC-5 (91.11 %) nor for L929 (73.59 %), which is still within acceptable cytotoxicity limits. Slight drop in survival rate was attributed to the antibiotic presence similar to the recent study³¹ that described high concentrations of gentamicin (250–270 µg/mL), that were reached during the immersion of the antibiotic containing films, affected osteoblastic proliferation (MC3T3-E1 cells).

Antibacterial activity

The results obtained by examining the kinetics of antibacterial activity against *Escherichia coli* ATCC25922 and *Staphylococcus aureus* TL are shown in Fig. 4a and b, respectively. In the case of Gram-negative *E. coli*, PVA/Gent and PVA/CHI/Gent hydrogels show a bactericidal effect, since the reduction of the number of viable bacterial colonies was more than three orders of magnitude after only 15 min of incubation. After 1 h of inoculation, a sterile environment was achieved since there were no longer any alive *E. coli* cell present. For the Gram-positive *Staphylococcus aureus*, the absence of any living cells was observed after only 15 min. Interestingly, chitosan in PVA/CHI hydrogel exhibited bactericidal effect against *S. aureus*, because even after 15 min of incubation the number of living cells decreased by almost three orders of magnitude, and after 1 h it was established that there were no more living cells of *S. aureus* present.

Although it is very well known, from the literature, that chitosan possesses good antibacterial properties,³² it was obvious that in this case its initial concen-

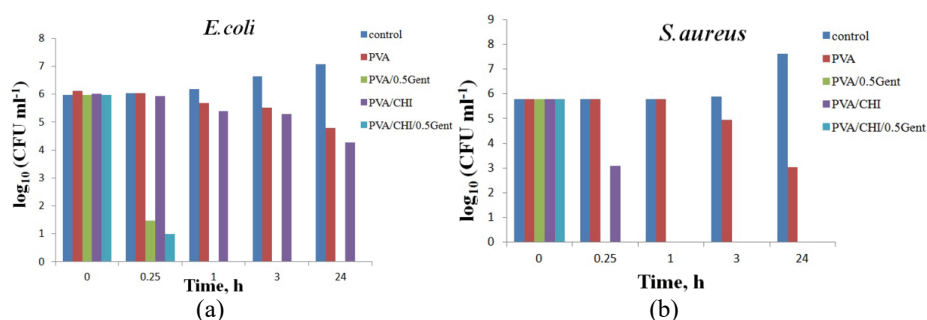


Fig. 4. Antibacterial activity of PVA, PVA/Gent, PVA/CHI and PVA/CHI/Gent hydrogels against: a) *Escherichia coli* and b) *Staphylococcus aureus*.

tration was too low to cause any effect on the tested *E. coli* strain. For the tested *S. aureus* (Fig 4b) sudden drop in the viable cells, only 1 h of post-incubation, agrees well with the documented³³ increased antibacterial effect of chitosan in the slightly acidic conditions.

Gentamicin release study and diffusion models

Mathematical properties as well as application of fractional derivatives of Riemann–Liouville and Caputo type are presented in the literature.^{34–37} Especially in Petráš³⁸ and Carvalho,³⁹ application of fractional calculus in biological systems is discussed. Here we recall the central result for the two compartmental model of drug diffusion, GFD model, presented by Miskovic-Stankovic.^{10,11} The amount of released gentamicin is determined from the following formula:

$$m_2(t) = m_1(0) \frac{k}{2\pi V_1} \int_{x_0 - i\infty}^{x_0 + i\infty} \frac{\exp(x_0 + ip)t / (x_0 + ip)}{a \frac{x_0 + ip}{(x_0 + ip + \lambda_1)^\alpha} + b \frac{x_0 + ip}{(x_0 + ip + \lambda_2)^\beta} + k \left(\frac{1}{V_1} + \frac{1}{V_2} \right)} dp \quad (1)$$

with $x_0 \geq 0$. Also:

$$m_1(t) = m_1(0) - m_2(t) \quad (2)$$

Parameters in the model are determined by least square method, *i.e.*, the sum squared residuals between measured and calculated values of m_2 at five measured points, Z , is minimized. Therefore, Z is given as:

$$Z(\alpha, \beta, \lambda_1, \lambda_2, a, b, k) = \sum_{j=1}^5 (m_2(t_j) - m_{2\text{measured}}(t_j))^2 \quad (3)$$

where $m_2(t_j)$ are values determined from Eq. (1) and $m_{2\text{measured}}(t_j)$ are measured values at time instant t_j .

The measured values of mass m_2 are divided by initial, total mass of gentamicin that in our experiments is $m_1(0) = 2.4551$ mg. Thus, we define relative mass of the gentamicin in hydrogel, q_1 , and relative mass of released gentamicin in deionized water surrounding hydrogel, q_2 , as:

$$q_1(t) = \frac{m_1(t)}{m_1(0)}; q_2(t) = \frac{m_2(t)}{m_1(0)} \quad (4)$$

We determined the parameters in Eq. (1), denoted as α^* , β^* , λ_1^* , λ_2^* , a^* , b^* , k^*) from the condition given by Eq. (2). Thus, the optimal values α^* , β^* , λ_1^* , λ_2^* , a^* , b^* , k^*) satisfy:

$$\min_{(\alpha, \beta, \lambda_1, \lambda_2, a, b, k)} Z(\alpha, \beta, \lambda_1, \lambda_2, a, b, k) = Z(\alpha^*, \beta^*, \lambda_1^*, \lambda_2^*, a^*, b^*, k^*) \quad (5)$$

In the minimization process we observed the restrictions that follow from the formulation of the model:

$$0 < \alpha \leq 1, 0 < \beta \leq 1, \lambda_1 \geq 0, \lambda_2 \geq 0, a \geq 0, b \geq 0, k \geq 0 \quad (6)$$

Experiments were performed with $V_1 = 254.5 \text{ mm}^3$, $V_2 = 1000 \text{ mm}^3$ and the area over which diffusion takes place $A = 2.40 \text{ cm}^2$. Condition given by Eq. (5) with Z given by Eq. (3) leads to $\alpha = 1$, $\beta = 0.001$, $\lambda_1 = 8.7 \times 10^{-7} \text{ s}^{-1}$, $\lambda_2 = 6.7562 \text{ s}^{-1}$, $a = 0.000898 \text{ s}$, $b = 0.037720 \text{ s}^{-0.999}$, $k = 0.005193 \text{ cm}^4/\text{day}$.

The corresponding diffusion coefficient, D , is calculated as follows. The shape of the hydrogel is cylinder with diameter 9 mm and the height (thickness) 4 mm. The area of the diffusion is calculated to be $A = 2.4 \text{ cm}^2$. Therefore, diffusion coefficient is $D = k/A = 2.50 \times 10^{-8} \text{ cm}^2 \text{ s}^{-1}$.

The obtained data (GFD model) were compared to several theoretical models in order to elucidate the diffusion parameters and to quantitatively compare gentamicin release behavior. The models applied were Makoid–Banakar,¹⁹ Korsmeyer–Peppas¹⁸ and Kopcha,²⁰ described by Eqs. (7)–(9), respectively.

$$C_t / C_0 = k_{\text{MB}} t^n \exp(-ct) \quad (7)$$

$$C_t / C_0 = k_{\text{KP}} t^n \quad (8)$$

$$C_t / C_0 = At^{1/2} + Bt \quad (9)$$

where C_t is the concentration of gentamicin released from hydrogel at time, t ; C_0 is the initial concentration of gentamicin inside the hydrogel; k_{MB} is the Makoid–Banakar constant; c is the Makoid–Banakar parameter; k_{KP} is the Korsmeyer–Peppas constant; n – coefficient which describes release transport mechanism, ($n < 0.5$ – Fickian diffusion, $n > 0.5$ – non-Fickian/anomalous diffusion, $n = 1$ – Case II transport,¹⁸ A and B – Kopcha's constants which depend on the dominant transport phenomenon during release. The models are depicted along with experimental profiles in Fig. 5 for Makoid–Banakar (Fig. 5a), Korsmeyer–Peppas (Fig. 5b) and Kopcha (Fig. 5c) models compared to GFD model. It should be noted that $m_2(t)$ in our GFD model Eq. (1) is proportional to the concentration C_t , while $m_1(0)$ is proportional to the concentration, C_0 . Gentamicin release profiles verified the initial burst release effect of gentamicin from the hydrogel, *i.e.*, 70 % loaded antibiotic was released within first 48 h which could be very useful in preventing biofilm formation, followed by slow release of gentamicin in a later time period. The calculated parameters and the fit quality evaluated using minimization of square residual, Z , for different models are listed in Table I.

It can be observed that GFD model provided the lowest value of Z , *i.e.*, notably better correlation with the experimental data in respect to the other models. The time exponent n is an indication of the dominant diffusion mechanism and, as its values were less than 0.5 (Table I), it can be concluded that the

release of gentamicin from hydrogel conformed to the Fickian diffusion behavior¹⁸ and was governed mainly by the concentration gradient of released gentamicin. This was also proved by Kopcha model, as the absolute values of the parameter A were higher compared to B , indicating that the predominant driving force for the release is the diffusion, and not the polymer matrix relaxation.⁴⁰

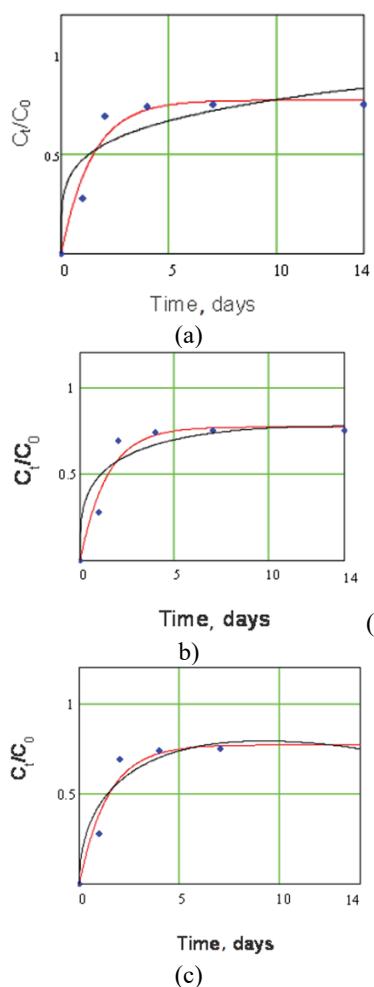


Fig. 5. Comparison between: a) Korsmeyer–Peppas (black line) and GFD model (red line), b) Makoid–Banakar (black line) and GFD model (red line) and c) Kopcha (black line) and GFD model (red line); ♦ experimental points.

In order to determine the value of diffusion coefficient of gentamicin, the early time approximation (ETA) model was applied and compared to diffusion coefficient calculated from GFD model. For ETA, two equations were used, standard ETA, Eq. (10), and a modified ETA, Eq. (11), proposed by Ritger and Peppas.²¹ According to Ritger and Peppas, the standard ETA is frequently misused, even though it only applies to very specific cases of swelling, and for spe-

cific geometries of thin films with very high aspect ratio (diameter divided by thickness; a thin film will typically have aspect ratio of the order of ~100, whereas for thick hydrogel discs it is closer to unity).²² In these equations, C_t/C_0 denotes the fraction of released gentamicin at the time t , D is the diffusion coefficient of gentamicin during the release, t – the time of release, δ is the hydrogel thickness and r is the radius of the hydrogel disc:

$$C_t / C_0 = 4\left(\frac{Dt}{\pi\delta^2}\right)^{1/2} \quad (10)$$

$$C_t / C_0 = 4\left(\frac{Dt}{\pi r^2}\right)^{1/2} - \pi\frac{Dt}{\pi r^2} - \frac{\pi}{3}\left(\frac{Dt}{\pi r^2}\right)^{3/2} + 4\left(\frac{Dt}{\pi\delta^2}\right)^{1/2} - \frac{2r}{\delta}\left(8\frac{Dt}{\pi r^2} - 2\pi\left(\frac{Dt}{\pi r^2}\right)^{3/2} - \frac{2\pi}{3}\left(\frac{Dt}{\pi r^2}\right)^2\right) \quad (11)$$

TABLE I. Fitting parameters for different models of gentamicin release from PVA/CHI/Gent hydrogel; GFD – GFD model; KP – Krosmeier–Peppas model; MB – Makoid–Banakar model; K – Kopcha model

Parameter	α	β	λ_1	λ_2	k cm ⁴ /day	D cm ² s ⁻¹	a	b	Z
GFD	1	0.001	8.7×10^{-3}	6.7562	5.193×10^{-3}	2.5042×10^{-8}	8.9×10^{-4}	0.0377	0.02564
Parameter	k_{KP} / s^{-n}	n							Z
KP	0.4737	0.2137							0.07735
Parameter	k_{MB} / s^{-n}	n	c						Z
MB	0.4956	0.2736	0.01972						0.06284
Parameter	$A / s^{-1/2}$	B / s^{-1}							Z
K	0.52356	-0.08643							0.04353

The ETA models represent the dependence of the fraction of released gentamicin on the square root of the release time (Fig. 6), while diffusion coefficient, D , of gentamicin release was determined from the slope of initial linear part of the experimental curve.

The value of D calculated by the standard ETA (5.53×10^{-8} cm² s⁻¹) is two times greater than value of D calculated by modified ETA (2.57×10^{-8} cm² s⁻¹) and GFD model (2.50×10^{-8} cm² s⁻¹). This implied that GFD model enabled the determination of D considering the gentamicin diffusion through the thick hydrogel where ratio between hydrogel diameter and thickness was about 2. Moreover, while ETA model extends the predictability of release up to 60 % and modified ETA up to 80–90 %, GFD model predicted the gentamicin release in the entire time period.

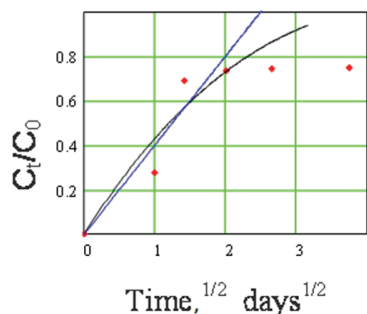


Fig. 6. Standard ETA (blue line) and modified ETA (black line) models, \blacklozenge experimental points.

Mechanical properties

Fig. 7 shows stress–strain curves for the PVA, PVA/CHI and PVA/CHI/Gent films, while tensile strength, modulus of elasticity and the strain corresponding to tensile strength (maximum of curve, when geometrical weakening of material starts), ε_m , are presented in Table II.

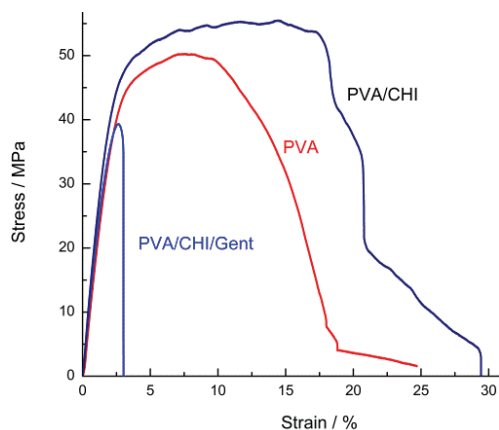


Fig. 7. Stress–strain curves from tensile test for PVA, PVA/CHI and PVA/CHI/Gent films.

TABLE II. Tensile strength (σ_{TS}), Young's modulus of elasticity (E) and tensile strain for maximum of tensile curves (ε_m)

Sample	σ_{TS} / MPa	SD / MPa	E / MPa	SD / MPa	ε_m / %	SD / %
PVA	47.25	4.3	1886.87	147	7.27	0.49
PVA/CHI	53.43	2.9	2223.67	211	13.31	1.57
PVA/CHI/Gent	36.50	4.0	1969.73	162	2.61	0.04

It could be seen that the tensile strength of PVA/CHI film increased by 13.1 %, Young's modulus by 18.0 % and tensile strain, ε_m , by 83.1 % compared to pure PVA film. This improvement in mechanical properties is a consequence of strong physical interactions and establishment of hydrogen bonds between PVA and CHI molecules.^{41,42} By comparing the mechanical properties of the PVA/CHI and PVA/CHI/Gent films, a decrease by 31.7 %, in tensile strength with the

addition of gentamicin, is observed. Young's modulus of elasticity by 11.4 %, while the tensile strain was even five times smaller. Also, from the shape of tensile curves it could be seen that the addition of gentamicin leads to an increase in the brittleness of the films.

CONCLUSION

In the course of this work we have synthesized poly(vinyl alcohol)/chitosan/gentamicin (PVA/CHI/Gent) hydrogel, non-toxic towards MRC-5 and L929 cell lines and with strong antibacterial activity against *Escherichia coli* and *Staphylococcus aureus*. Diffusion mechanism of gentamicin release from PVA/CHI/Gent hydrogel was studied by comparison of novel two compartmental models with general fractional derivative (GFD) and Korsmeyer–Peppas, Makoid–Banakar and Kopcha diffusion models. GFD model fitted the experimental gentamicin release profile better than other models and enabled the determination of the diffusion coefficient of gentamicin in entire time period.

SUPPLEMENTARY MATERIAL

Additional data and information are available electronically at the pages of journal website: <https://www.shd-pub.org.rs/index.php/JSCS/article/view/12722>, or from the corresponding author on request.

Acknowledgements. This research is supported by University Union – Nikola Tesla, Belgrade, Serbia (Vesna Miskovic-Stankovic) and Faculty of Technical Sciences, University of Novi Sad (Teodor Atanackovic); the Ministry of Science, Technological Development and Innovation, Republic of Serbia, Contracts No. 451-03-47/2023-01/200023 (Marija Djošić), 451-03-47/2023-01/200135 (Vesna Radojević, Maja Vukašinović-Sekulić, Svetlana Grujić, Ivana Matić-Bujagić), 451-03-47/2023-01/200287 (Ana Janković) and „Twinning to excel materials engineering for medical devices ExcellMater“, grant no. 952033, H2020-WIDESPREAD-2018-2020/H2020-WIDESPREAD-2020-5,2020-2023 (Ana Janković, Vesna Radojević).

ИЗВОД

ДИФУЗИОНИ МОДЕЛИ ОТПУСТАЊА ГЕНТАМИЦИНА ИЗ ПОЛИ(ВИНИЛ АЛКОХОЛ)/ХИТОЗАН ХИДРОГЕЛА

ВЕСНА МИШКОВИЋ-СТАНКОВИЋ¹, АНА ЈАНКОВИЋ², СВЕТЛАНА ГРУЈИЋ², ИВАНА МАТИЋ-БУЈАГИЋ²,
ВЕСНА РАДОЈЕВИЋ², МАЈА ВУКАШИНОВИЋ-СЕКУЛИЋ², ВЕСНА КОЈИЋ³, МАРИЈА ЂОШИЋ⁴
и ТЕОДОР М. АТАНАКОВИЋ⁵

¹Факултет за екологију и заштити животне средине, Универзитет Унион – Никола Тесла, Цара Душана 62–64, 11000 Београд, ²Технолошко–металурички факултет Универзитета у Београду, Карнегијева 4, 11000 Београд, ³Онколошки институт Војводине, Универзитет у Новом Саду, Пуш Др Голдмана 4, 21204 Сремска Каменица, ⁴Институт за технологију нуклеарних и других минералних сировина, Булевар Франц Ферера 86, 11000, Београд и ⁵Факултет техничких наука, Универзитет у Новом Саду, 21000 Нови Сад

Ова студија представља поређење нашег недавно формулисаног дво-компаратментског модела са општим фракционим изводима (GFD) и Корсмејер–Пепа-совим, Макоид–Банакаровим и Копча моделима дифузије. Користили смо наш

GFD модел за проучавање отпуштања гентамицина из поли(винил алкохол)/хитозан/гентамицин (PVA/CHI/Gent) хидрогела намењеног за третман дубоких хроничних рана. PVA/CHI/Gent хидрогел је припремљен физичким умрежавањем дисперзије поли(винил алкохол)/хитозан методом замрзавања и одмрзавања, а затим је бубрен 48 h у раствору гентамицина, на 37 °C. Испитивана су физичко–хемијска (FTIR, SEM), механичка и биолошка (цитотоксичност, антибактеријска активност) својства. Концентрација отпуштеног гентамицина је одређена коришћењем течне хроматографије високих перформанси (HPLC) у комбинацији са масеном спектрометријом (MS). Однос између концентрације отпуштеног гентамицина и почетне концентрације гентамицина у хидрогелу је праћен током дужег временског периода. Доказано је да је наш, нови дифузиони, GFD модел боље усклађен са експерименталним подацима од других модела и омогућава прецизно одређивање коефицијента дифузије за цео временски период.

(Примљено 7. децембра 2023, ревидирано 15. јануара, прихваћено 22. јануара 2024)

REFERENCES

1. D. Copot, R. L. Magin, R. De Keyser, C. Ionescu, *Chaos Solitons Fractals* **102** (2017) 441 (<http://dx.doi.org/10.1016/j.chaos.2017.03.031>)
2. L. Kovács, B. Benyó, J. Bokor, Z. Benyó, *Comput. Methods Programs Biomed.* **102** (2011) 105 (<http://dx.doi.org/10.1016/j.cmpb.2010.06.019>)
3. D. A. Drexler, L. Kovács, J. Sági, I. Harmati, Z. Benyó, *IFAC Proc.* **44** (2011) 3753 (<http://dx.doi.org/10.3182/20110828-6-IT-1002.02107>)
4. B. Kiss, J. Sági, L. Kovács, *SISY 2013 - IEEE 11th Int. Symp. Intell. Syst. Informatics Proc.* (2013) 271 (<http://dx.doi.org/10.1109/SISY.2013.6662584>)
5. D. Copot, C. M. Ionescu, *Conf. Proc. - IEEE Int. Conf. Syst. Man Cybern.* **2014** (2014) 2452 (<http://dx.doi.org/10.1109/smc.2014.6974294>)
6. C. Ionescu, A. Lopes, D. Copot, J. A. T. Machado, J. H. T. Bates, *Commun. Nonlinear Sci. Numer. Simul.* **51** (2017) 141 (<http://dx.doi.org/10.1016/j.cnsns.2017.04.001>)
7. C. M. Ionescu, D. Copot, R. De Keyser, *IFAC-PapersOnLine* **50** (2017) 15080 (<http://dx.doi.org/10.1016/j.ifacol.2017.08.2526>)
8. J. K. Popović, D. T. Spasić, J. Tošić, J. L. Kolarović, R. Malti, I. M. Mitić, S. Pilipović, T. M. Atanacković, *Commun. Nonlinear Sci. Numer. Simul.* **22** (2015) 451 (<http://dx.doi.org/10.1016/j.cnsns.2014.08.014>)
9. A. Churilov, A. Medvedev, A. Shepeljavyi, *Automatica* **45** (2009) 78 (<http://dx.doi.org/10.1016/j.automatica.2008.06.016>)
10. V. Miskovic-Stankovic, M. Janev, T. M. Atanackovic, *J. Pharmacokinet. Pharmacodyn.* **50** (2023) 79 (<http://dx.doi.org/10.1007/s10928-022-09834-8>)
11. V. Miskovic-Stankovic, T. M. Atanackovic, *Fractal Fract.* **7** (2023) 1 (<http://dx.doi.org/10.3390/fractalfract7070518>)
12. D. Simões, S. P. Miguel, M. P. Ribeiro, P. Coutinho, A. G. Mendonça, I. J. Correia, *Eur. J. Pharm. Biopharm.* **127** (2018) 130 (<http://dx.doi.org/10.1016/j.ejpb.2018.02.022>)
13. M. Naseri-Nosar, Z. M. Ziora, *Carbohydr. Polym.* **189** (2018) 379 (<http://dx.doi.org/10.1016/j.carbpol.2018.02.003>)
14. E. Caló, V. V. Khutoryanskiy, *Eur. Polym. J.* **65** (2015) 252 (<http://dx.doi.org/10.1016/j.eurpolymj.2014.11.024>)
15. K. Nešović, A. Janković, T. Radetić, M. Vukašinović-Sekulić, V. Kojić, L. Živković, A. Perić-Grujić, K. Y. K. Y. Rhee, V. Mišković-Stanković, *Eur. Polym. J.* **121** (2019) 109257 (<https://doi.org/10.1016/j.eurpolymj.2019.109257>)

16. K. Nešović, V. Mišković-Stanković, *Polym. Eng. Sci.* **60** (2020) 1393 (<http://dx.doi.org/10.1002/pen.25410>)
17. K. Nešović, V. B. Mišković-Stanković, *J. Vinyl Addit. Technol.* (2021) 1 (<http://dx.doi.org/10.1002/vnl.21882>)
18. R. W. Korsmeyer, R. Gurny, E. Doelker, P. Buri, N. A. Peppas, *Int. J. Pharm.* **15** (1983) 25 ([http://dx.doi.org/10.1016/0378-5173\(83\)90064-9](http://dx.doi.org/10.1016/0378-5173(83)90064-9))
19. M. C. Makoid, A. Dufour, U. V. Banakar, *S.T.P. Pharma Prat.* **3** (1993) 49
20. M. Kopcha, N. G. Lordi, K. J. Tojo, *J. Pharm. Pharmacol.* **43** (1991) 382 (<http://dx.doi.org/10.1111/j.2042-7158.1991.tb03493.x>)
21. P. L. Ritger, N. A. Peppas, *J. Control. Release* **5** (1987) 23
22. P. L. Ritger, N. A. Peppas, *J. Control. Rel.* **5** (1987) 37 ([http://dx.doi.org/10.1016/0168-3659\(87\)90035-6](http://dx.doi.org/10.1016/0168-3659(87)90035-6))
23. A. M. N. Santos, A. P. D. Moreira, C. W. P. Carvalho, R. Luchese, E. Ribeiro, G. B. McGuinness, M. F. Mendes, R. N. Oliveira, *Materials (Basel)* **12** (2019) 559 (<http://dx.doi.org/10.3390/ma12040559>)
24. S. Nkhwa, K. F. Lauriaga, E. Kemal, S. Deb, *Conf. Pap. Sci.* **2014** (2014) 403472 (<http://dx.doi.org/10.1155/2014/403472>)
25. M. Djošić, A. Janković, M. Stevanović, J. Stojanović, M. Vukašinović-Sekulić, V. Kojić, V. Mišković-Stanković, *Mater. Chem. Phys.* **303** (2023) 127766 (<http://dx.doi.org/10.1016/J.MATCHEMPHYS.2023.127766>)
26. A. Bernal-Ballen, J. Lopez-Garcia, M. A. Merchan-Merchan, M. Lehocky, *Molecules* **23** (2018) 3109 (<http://dx.doi.org/10.3390/molecules23123109>)
27. M. M. M. Abudabbus, I. Jevremović, A. Janković, A. Perić-Grujić, I. Matić, M. Vukašinović-Sekulić, D. Hui, K. Y. Y. Rhee, V. Mišković-Stanković, *Compos., B* **104** (2016) 26 (<http://dx.doi.org/10.1016/J.COMPOSITESB.2016.08.024>)
28. X. Xiong, J. Sun, D. Hu, C. Xiao, J. Wang, Q. Zhuo, C. Qin, L. Dai, *RSC Adv.* **10** (2020) 35226 (<http://dx.doi.org/10.1039/d0ra06053d>)
29. M. Ghasemi, T. Turnbull, S. Sebastian, I. Kempson, *Int. J. Mol. Sci.* **22** (2021) 12827 (<http://dx.doi.org/10.3390/ijms222312827>)
30. G. Sjögren, G. Sletten, E. J. Dahl, *J. Prosthet. Dent.* **84** (2000) 229 (<http://dx.doi.org/10.1067/mpr.2000.107227>)
31. E. S. Permyakova, A. M. Manakhov, P. V. Kiryukhantsev-Korneev, A. N. Sheveyko, K. Y. Gudzh, A. M. Kovalskii, J. Polčak, I. Y. Zhitnyak, N. A. Gloushankova, I. A. Dyatlov, S. G. Ignatov, S. Ershov, D. V. Shtansky, *Appl. Surf. Sci.* **556** (2021) 149751 (<http://dx.doi.org/10.1016/j.apsusc.2021.149751>)
32. J. Li, S. Zhuang, *Eur. Polym. J.* **138** (2020) 109984 (<http://dx.doi.org/10.1016/j.eurpolymj.2020.109984>)
33. Y. C. Chung, H. L. Wang, Y. M. Chen, S. L. Li, *Bioresour. Technol.* **88** (2003) 179 ([http://dx.doi.org/10.1016/S0960-8524\(03\)00002-6](http://dx.doi.org/10.1016/S0960-8524(03)00002-6))
34. K. Oldham, J. Spanier, *The Fractional Calculus*, Academic Press, New York, 1974
35. I. Podlubny, *Fractional Differential Equations*, Academic Press, San Diego, CA, 1999
36. A. A. Kilbas, H. M. Srivastava, J. J. Trujillo, *Theory and Applications of Fractional Differential Equations*, Elsevier, Amsterdam, 2006
37. T. M. Atanackovic, S. Pilipovic, B. Stankovic, D. Zorica, *Fractional Calculus with applications in Mechanics: Vibrations and Diffusion Processes*, ISTE, London, John Wiley & Sons, New York, 2014
38. I. Petráš, R. L. Magin, *Commun. Nonlinear Sci. Numer. Simul.* **16** (2011) 4588 (<http://dx.doi.org/10.1016/j.cnsns.2011.02.012>)

39. A. R. M. Carvalho, C. M. A. Pinto, *Commun. Nonlinear Sci. Numer. Simul.* **61** (2018) 104 (<http://dx.doi.org/10.1016/j.cnsns.2018.01.012>)
40. J. Krstić, J. Spasojević, A. Radosavljević, A. Perić-Grujić, M. Đurić, Z. Kačarević-Popović, S. Popović, *J. Appl. Polym. Sci.* **11** (2014) 40321 (<http://dx.doi.org/10.1002/app.40321>)
41. H. Chopra, S. Bibi, S. Kumar, M. S. Khan, P. Kumar, I. Singh, *Gels* **8** (2022) 111 (<http://dx.doi.org/10.3390/gels8020111>)
42. E. Olewnik-Kruszkowska, M. Gierszewska, E. Jakubowska, I. Tarach, V. Sedlarik, M. Pummerova, *Polymers (Basel)*. **11** (2019) 2093 (<http://dx.doi.org/10.3390/polym11122093>).



SUPPLEMENTARY MATERIAL TO
**Diffusion models of gentamicin released in
poly(vinyl alcohol)/chitosan hydrogel**

VESNA MIŠKOVIĆ-STANKOVIĆ^{1*}, ANA JANKOVIĆ², SVETLANA GRUJIĆ²,
IVANA MATIĆ-BUJAGIĆ², VESNA RADOJEVIĆ², MAJA VUKAŠINOVIĆ-SEKULIĆ²,
VESNA KOJIĆ³, MARIJA DJOŠIĆ⁴ and TEODOR M. ATANACKOVIĆ⁵

¹Faculty of Ecology and Environmental Protection, University Union – Nikola Tesla, Cara
Dusana 62–64, 11000 Belgrade, Serbia, ²Faculty of Technology and Metallurgy, University of
Belgrade, Karnegijeva 4, 11000 Belgrade, Serbia, ³Oncology Institute of Vojvodina,
University of Novi Sad, Put Dr Goldmana 4, 21204 Sremska Kamenica, Serbia, ⁴Institute for
Technology of Nuclear and Other Mineral Raw Materials, Bulevar Franš d'Eperea 86,
11000, Belgrade, Serbia and ⁵Faculty of Technical Sciences, University of Novi Sad,
21000 Novi Sad, Serbia

J. Serb. Chem. Soc. 89 (5) (2024) 627–641

Gentamicin release studies

High-performance liquid chromatography (HPLC) (Thermo Fisher Scientific, USA) was utilized for gentamicin components separation and the detection and quantitative analysis was done in an ion trap mass spectrometer (MS) (LCQ Advantage, Thermo Fisher Scientific). HPLC was equipped with a reverse-phase column (4.6 mm × 75 mm × 3.5 μm) Zorbax Eclipse® XDB-C18 (Agilent Technologies, USA), in front of which a precolumn (4.6 mm × 12.5 mm × 5 μm) was placed. Methanol (A), deionized water (B), and 10 % acetic acid (C) comprised the mobile phase. The optimized HPLC and MS operating parameters (mobile-phase gradient, analytes' precursor ions, fragmentation reactions used for quantification, and optimal collision energies) for the determination of gentamicin compounds were published in our previous paper.^{S1,S2}

The gentamicin mass spectra were collected in the *m/z* range of 50-1000. As expected, the MS spectrum revealed the three most abundant ions since gentamicin is composed of three compounds – gentamicin C1a, C2, and C1. These ions were further chosen as the precursor ions for each compound. Their most sensitive transitions were selected for quantification purposes. The presented gentamicin concentrations represent sums of the three determined gentamicin compounds.

* Corresponding author. E-mail: vesna@tmf.bg.ac.rs

Evaluation of antibacterial properties

The hydrogel samples were cut up to small pieces (~ 2 x 2 mm). Thus prepared samples were sterilized under UV light for 30 min in a laminar flow cabinet. The bacteria culture suspensions were prepared by resuspending overnight cultures in the phosphate buffer (the same buffer was used for the drug release and gel swelling studies). The initial cell numbers in the suspensions were $\sim 10^6$ CFU ml⁻¹. Approximately 2 g of each sample were added to the flasks with bacterial suspensions and incubated in the shaker water bath at 37 °C and 62 rpm. The controls were bacterial suspension in phosphate buffer, without any added samples. The cell numbers were monitored by sampling and serial dilution of the media aliquots after 15 min, 1 h, 3 h and 24 h of incubation. Nutrient agar base (1.5 wt %, 55 °C) was inoculated with 100 µl of culture medium and poured in sterile Petri dishes. The Petri dishes were incubated at 37 °C for 24 h, after which the viable cells were counted and expressed as colony forming units per ml (CFU ml⁻¹).

Cytotoxicity

Cell cultures. The cells were grown in Dulbecco's modified Eagle's medium with 4.5% glucose, supplemented with 10% fetal calf serum and antibiotic-antimycotic. The cells were sub-cultured twice a week and cell suspensions were prepared with 0.1% trypsin in EDTA. All cell lines were cultured in 25 cm² flasks at 37°C in atmosphere with 5% CO₂ (100% humidity). Viable cells were counted by 0.1% trypan blue exclusion, and exponentially growing cells were used for MTT assay. The viability of the cells used in the MTT assay was > 90%.

MTT assay. The viable cell cultures were seeded in 12-well plates with hydrogel samples (2 g), and control wells contained only the complete media with cells and without hydrogel samples. The incubation was conducted at 37°C for 48 h under air flow with 5% CO₂. After incubation, the cells were separated from the hydrogel samples by trypsinization treatment. Subsequently, 100 µl of the media with cells were cultured in 96-well microtiter plates at 5x10³ cells per well seeding density to ensure logarithmic growth rate throughout the assay. The microtiter plates were incubated for 48 h at 37°C. Three hours before the end of the incubation period, MTT solution (10 µl) was added in each well. Cells were incubated in the presence of MTT for 3 hours at 37°C, after which the medium and MTT were removed by suction. The blanks contained only media and MTT, without the cell cultures. The MTT test is based on the reduction of MTT dye to an insoluble formazan product inside the viable cells mitochondria, which causes the change of the medium color from blue to dark purple. After the media was discarded, the remaining solid precipitates with cells and purple formazan product were solubilized in 100 µl 0.04 M HCl isopropanol solution. After a few minutes at room temperature, the optical density (OD) at 540/690 nm was

measured using a Multiscan MCC340 spectrophotometer plate reader (Thermo Labsystems). Cell viability, S , is calculated using equation

$$S = 100A_u / A_c \quad (S1)$$

where A_u i A_c are absorbance of tested sample and control, respectively.

DET assay. Dye exclusion test (DET) towards two fibroblast cell lines was carried out according to the previously published protocols.^{S3} Viable cells were seeded in the 12-well plates (Costar) at concentration of 1×10^5 /mL, whereas the control wells did not contain samples, only the seeded cells. Plates were incubated at 37 °C under air flow with 5% CO₂, during the following 48 h. After the incubation, cells were separated from samples by trypsinization method i.e. by adding 0.1 % trypsin solution. The cell number and viability were further evaluated by the trypan blue exclusion method using a formula

$$K = 100N_s/N_k \quad (S2)$$

where K is growth inhibition expressed as a percent of control, N_k is the total number of cells (control) and N_s is the number of cells on the tested samples.

REFERENCES

- S1. M. Stevanović, M. Djošić, A. Janković, V. Kojić, J. Stojanović, S. Grujić, I. M. Bujagić, K. Y. Rhee, V. Mišković-Stanković, *J. Mater. Res. Technol.* **15** (2021) 4461 (<http://dx.doi.org/10.1016/j.jmrt.2021.10.072>)
- S2. M. Stevanović, M. Djošić, A. Janković, K. Nešović, V. Kojić, J. Stojanović, S. Grujić, I. Matić Bujagić, K. Y. Rhee, V. Mišković-Stanković, *ACS Omega* **5** (2020) 15433 (<http://dx.doi.org/10.1021/acsomega.0c01583>)
- S3. K. Nešović, A. Janković, V. Kojić, M. Vukašinović-Sekulić, A. Perić-Grujić, K. Y. Rhee, V. Mišković-Stanković, *Compos., B* **154** (2018) 175 (<http://dx.doi.org/10.1016/j.compositesb.2018.08.005>).



J. Serb. Chem. Soc. 89 (5) 643–656 (2024)
JSCS–5745

Immunohistochemical evidences of anticancer actions of metformin with other repurposed drug combinations and correlation with hamster fibrosarcoma tumor size

JOVAN K. POPOVIĆ^{1*}, DUŠICA J. POPOVIĆ², KOSTA J. POPOVIĆ³, DEJAN MILJKOVIĆ⁴, DUŠAN LALOŠEVIĆ⁴, ZANA DOLIĆANIN² and IVAN ČAPO⁴

¹Department of Pharmacology, Toxicology and Clinical Pharmacology, Faculty of Medicine, University of Novi Sad, Novi Sad, Serbia, ²Department of Biomedical Sciences, State University of Novi Pazar, Novi Pazar, Serbia, ³Department of Pharmacy, Faculty of Medicine, University of Novi Sad, Novi Sad, Serbia and ⁴Department of Histology and Embryology, Faculty of Medicine, University of Novi Sad, Novi Sad, Serbia

(Received 3 December, revised 13 December 2023, accepted 22 January 2024)

Abstract: The aim was to detect and correlate anticancer effects of metformin in combinations with other repurposed drugs, already registered for other indications, which may be immediately applied and clinically investigated in oncology, reducing the time and cost of research for new cancer treatments. Immunohistochemistry was performed for tumors treated by dual drug combinations containing metformin with deoxycholic acid, caffeine, itraconazole, nitroglycerin, disulfiram or diclofenac. The drugs were applied in Syrian golden hamsters (6 animals per group) with the inoculated BHK21/C13 fibrosarcoma in doses equivalent to usual human doses, <50 % LD_{50} . The anticancer effects were assessed by: p53 (mutational status); Ki-67 and PCNA (tumor proliferation); CD34 and CD31 (neoangiogenesis); GLUT1 (glucose metabolism); iNOS (NO metabolism); COX4, Cytochrome C and caspase 3 (apoptosis); immunohistochemical markers. Also, biophysical characteristics of fibrosarcoma, animal blood samples and the toxicity on main organs were analyzed. Treatments significantly ($P < 0.05$) reduced mutational status, tumor proliferation, neoangiogenesis, glucose metabolism, NO metabolism and modulated apoptosis, in correlation with tumor size, without toxicity and influence on biochemical blood and hematological tests. The administration of metformin in two-drug combination with deoxycholic acid, caffeine, itraconazole, nitroglycerin, disulfiram or diclofenac may be recommended for further clinical investigations in oncology.

Keywords: tumour markers; fibrosarcoma; metformin; repurposed drugs; hamsters.

* Corresponding author. E-mail: jovapopmf@gmail.com; jovan.popovic@mf.uns.ac.rs
<https://doi.org/10.2298/JSC231203007P>



INTRODUCTION

Anticancer effects of some pleiotropic low cost non-oncological, marketed drugs, such as metformin, deoxycholic acid, caffeine, itraconazole, nitroglycerin, disulfiram or diclofenac are reported *in vitro* (cell lines), but investigations *in vivo* (experimental animals) and clinical investigations, especially of their certain combinations, are not yet conducted.

The activation of NF- κ B (Nuclear factor kappa-light-chain-enhancer of activated B cells) signaling has been found in many types of tumors, including breast, colon, prostate, skin and lymphoid tumors.¹ NF- κ B, as the master stimulator of cancer development and maintenance, stimulates proliferation, angiogenesis and modulates apoptosis (inhibits apoptosis in cancer cell lines).

Metformin inhibited proliferation and stimulated apoptosis of various cancer cell lines by suppression of NF- κ B in lung,² human ovarian,³ human gastric adenocarcinoma⁴ and prostate cancer cells.⁵

It has been shown that deoxycholic acid inhibited NF- κ B activity, limited cancer cell proliferation, invasion and induced apoptosis *in vitro*: in human pancreatic cancer cells,⁶ gastric carcinoma cells,⁷ lung cancer cells,⁸ prostate cancer cells,⁸ breast cancer cells,⁸ colon cancer cells,^{9,10} gastric carcinoma cells¹¹ and hepatic carcinoma cells.¹²

Caffeine inhibits NF- κ B and induces apoptosis in many human cancer cell lines (lung, pancreatic, leukemia) *in vitro*.^{13,14}

Itraconazole exhibits significant anticancer effects in various cancer cell lines *in vitro* via inhibition of NF- κ B, angiogenesis, folate, autophagy and cholesterol transportation.^{15,16} The same as metformin, itraconazole inhibits protein synthesis, cell growth, proliferation and stimulates apoptosis.¹⁷

Nitroglycerin liberates nitric oxide (NO) in the tissues, which modifies tumor cell metabolism by modulating the Warburg effect in cancer therapy.¹⁸ Similarly to metformin,¹⁹ NO from nitroglycerin causes folate and B₁₂ deficiency.^{20,21} Nitroglycerin inhibits NF- κ B, downstream related proteins and stimulates apoptosis *in vitro*.²²

Disulfiram inhibits proliferation and stimulated apoptosis of various cell lines *in vitro* by NF- κ B suppression: leukemia,²³ endometriotic,²⁴ lymphoid,²⁵ glioblastoma,²⁶ colorectal,²⁷ non-small cell lung²⁸ and gastric cancer cells.²⁹

Diclofenac inhibits NF- κ B in human and mouse hepatoma cells *in vitro*.^{30,31} Diclofenac also inhibits NF- κ B activation, inhibited proliferation and stimulated apoptosis in various tumour cells *in vitro*.³²

The opposite functional crosstalk between NF- κ B and p53 has a key role in the pathogenesis of most tumours. p53, a tumour suppressor protein, nuclear transcription factor described as “the guardian of the genom”, stops the formation of tumours and prevents mutation. p53 is associated with cell cycle arrest, angio-

genesis inhibition and apoptosis modulation (induces apoptosis in cancer cell lines).

We screened non-oncological pleiotropic drugs (inhibitors of NF- κ B) with approved anticancer characteristics *in vitro*, and their combinations on experimental BHK-21/C13 fibrosarcoma in hamsters and correlated indicators of tumour growth (tumour weight and immunohistochemical parameters expression).

Frequently used mouse models offer an attractive system for cancer therapy research. However, there are important limitations: firstly, concerning the immune mediated rejection of cancer xenograft and secondly, models that use the immune deficient mice (in order to avoid the rejection) can produce metastases.³³ Cell lines were the main component of any experimental model. BHK-21/C13 cells are able to undergo malignant transformation when they are subcutaneously injected into hamsters.³³

A model of BHK-21/C13 cell culture induced sarcoma in Syrian hamsters is easy reproducible, tumour is solitary, big enough in short time, never produced metastases and without influence of the host immune mechanisms. Immunologically, hamsters do not recognize BHK-21/C13 cells as tumorigenic and tumour is enormously growing. The tumour is locally infiltrative. BHK-21/C13 cells are tumorigenic only for hamsters (except nude mice). Only whole live cells are tumorigenic, not DNA, or cell extracts. This model is excellent for the pharmacological examination of antitumor agents, because the tumour never produces metastases and is not influenced by immune rejection, in contrast with some other animal tumour models (Fig. 1).

EXPERIMENTAL

Animal model

The study was performed on Syrian golden hamsters (6 hamsters per group; males only; age, 12–15 weeks; weight, ~80 g). The animals were obtained from the Pasteur Institute and were maintained under standard animal housing conditions at 25±2 °C and 60±2 % humidity under a 12-h light/dark cycle. The animals had ad libitum access to food and water.

BHK-21/C13 cells were subcutaneously inoculated (1ml, 2×10⁶ cells/ml) into the back of all hamsters by the same researcher (Fig. 1). After the tumour inoculation, the following characteristics were monitored: general condition; general clinical signs (diarrhoea, breathing disorders, neurological signs); behaviour; body weight (measured daily); tumour diameter, location and ulceration; appearance of multiple tumours.

Our study followed internationally recognized guidelines on animal welfare, as well as local and national regulations (ARRIVE guidelines; Law on animal welfare of the Republic of Serbia; University of Novi Sad Rules for work with experimental animals). All animals were subjected to protocols approved by the University of Novi Sad Animal Ethics Committee (Novi Sad, Serbia): Doc. No. EK: II-E-2020-07; Doc. No. EK: I-2022-01; No. 04-150/15; Doc. No. EK: I-2022-02; and approved by the Ministry of Agriculture, Forestry and Water Management – Veterinary Directorate (Belgrade, Serbia): No. 323-07-09359/2020-05; No. 323-07-03995/2022-05; No. 323-07-03996/2022-05; No. 323-07-03997/2022-05.

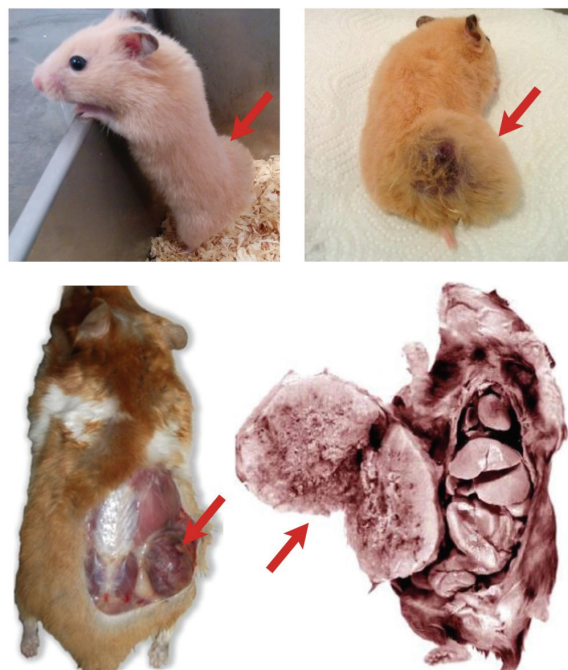


Fig. 1. Syrian hamster with BHK-21/C13 cell culture inoculated subcutaneously. Large tumor on the inoculation site, without spreading on internal organs.

The treatments were initiated after the subcutaneous inoculation of 1 ml of BHK-21/C13 cell suspension (2×10^6 cells/ml) into the back for the development of a subcutaneous fibrosarcoma tumour. Single metformin, deoxycholic acid, caffeine, itraconazole, nitroglycerin, disulfiram or diclofenac and dual combinations with metformin (all from Galenika a. d.) were applied perorally in 1–2 ml of fluid (saline), according hamster body mass, *via* a gastric probe, in daily doses equivalent to usual human doses by normalization to body surface area, < 50 % of hamster oral median lethal dose LD_{50} (Table I).

BHK-21/C13 cells were produced in DMEM substrate with 4.5 g/L glucose, with 10 % foetal bovine serum (FBS), 2 mM glutamine and 1 % penicillin/streptomycin (all from Capricorn Scientific), at 37 °C, in a 5 % CO_2 humidified atmosphere. BHK-21/C13 cells were subcultured twice a week once they reached a confluency of 70–80 %.

Immunohistochemistry

Immunohistochemical p53, Ki-67, PCNA, CD34, CD31, GLUT1, iNOS, COX4, cytochrome C and caspase 3 staining was performed to assess tumour mutational status (p53), proliferation (Ki-67, PCNA), neoangiogenesis (CD34, CD31), glucose metabolism (GLUT1), NO metabolism (iNOS) and apoptosis (COX4, Cytochrome C, caspase 3). COX4 is a mitochondrial cytochrome C oxidase marker of apoptosis (overexpressed in cancer cells), cytochrome C is a useful marker of mitochondrial and cellular damage and apoptosis in tumours and caspase 3 is a crucial mediator of apoptosis (frequently activated death protease, detects endogenous levels of cleaved caspase 3). In immunohistochemical staining, the following primary antibodies were used: p53 (Thermo Fisher Scientific, Inc.; DO-7; Product # MA5-12557;

1:100), Ki-67 (Thermo Fisher Scientific, Inc.; cat. no. RB-9043-P0, 1:300), PCNA (Thermo Fisher Scientific, Inc.; cat. no. RB-9055-P, 1:300), CD34 (Abcam; cat. no. ab81289; 1:200), CD31 (Abcam; cat. no. ab28364; 1:200), GLUT1 (Thermo Fisher Scientific, Inc.; cat. no. RB-9052-P0; 1:200), iNOS (Thermo Fisher Scientific, Inc.; RB-9242-P0; 1:100), COX4 (Abcam; cat. no. ab185056; 1:1,000), Cytochrome C (Abcam; cat. no. ab133504; 1:200) and caspase 3 (Abcam; cat. no. ab13847; 1:200). Briefly, sections (5 μ m) were deparaffinized in xylene (100 %) and rehydrated in descending ethanol series (100 % twice for 3 min; 95 % for 3 min and 70 % for 3 min). For antigen retrieval, the sections were microwaved (850 W; -98 °C) for 20 min in Tris-EDTA buffer (10 mM Tris Base, 1 mM EDTA solution, 0.05 % Tween 20, pH 9.0), washed twice for 5 min with TBS plus 0.025 % Triton X-100 (with agitation) and blocked by immersion in 10 % goat serum (cat. no. G6767; Sigma–Aldrich; Merck KGaA) in TBS with 1 % BSA (cat. no. T6789; Sigma–Aldrich; Merck KGaA) for 2 h at room temperature. Primary antibodies dissolved in TBS with 1 % BSA were incubated at 4 °C overnight. The sections were washed twice for 5 min with TBS plus 0.025 % Triton X-100 (with agitation) and incubated with 0.3 % H₂O₂ in TBS for 15 min at room temperature. Horseradish peroxidase-conjugated goat polyclonal rabbit immunoglobulin G secondary antibody (cat. no. ab6721; Abcam) dissolved in TBS with 1 % BSA was added to the sections for 2 h at room temperature. The sections were washed three times for 5 min with TBS. For visualization, the chromogen 3,3-diaminobenzidine tetrahydrochloride (cat. no. K3468; Liquid DAB + Substrate-Chromogen System; Dako; Agilent Technologies, Inc.) was added and incubated for 10 min at room temperature. The sections were washed with water for 5 min and were stained with Mayer's hematoxylin for 5 min at room temperature. The stained tumour slices were assessed using Leica DMLB 100T (Leica Microsystems GmbH) microscope at 400 \times magnification. Images were captured using a Leica MC190 HD camera (Leica Microsystems GmbH). Immunorexpression was evaluated based on the positive cells counts (stained /total number of cells) or on the stained portions of surface area (stained surface/whole surface) in the tumour sections (mean of 10 measurements) using UTHSCSA Image Tools for Windows version 3.00.

Blood biochemical tests and haematological analyses

2–3 ml of the total collected blood was used for standard laboratory analyses: glucose, serum proteins, albumins haemoglobin, sedimentation, erythrocytes, leucocytes, lymphocytes, monocytes, granulocytes, platelets, haematocrit, mean corpuscular volume, mean corpuscular haemoglobin and mean corpuscular haemoglobin concentration, in all three experiments. The serum, obtained from the blood samples by centrifugation at 2,000 \times g for 10 min, was analysed using an auto chemistry analyser (Rayto Life and Analytical Sciences Co., Ltd.). Commercial tests for the determination of glucose concentration (cat. no. 21503), serum proteins (cat. no. 11500) and albumins (cat. no. 11547; BioSystems S.A.) were used. An auto haematology analyser (Abacus Junior Vet; Diatron; Stratec SE) was used for enumeration of blood cells.

Statistical analysis

Mean \pm SD or \pm SE and correlation analysis were determined and one-way ANOVA followed by a Student–Newman–Keuls post hoc test were performed using TIBCO Statistica 13.3.1 software (TIBCO Software, Inc.). P values less than 0.05 were regarded statistically significant. To check significances obtained by parametric testing (comparing the means), the two-sided Mann–Whitney *U* tests (comparing the medians) were additionally performed.

RESULTS AND DISCUSSION

After inoculation of BHK-21/C13 cells, fibrosarcoma was developed in all hamsters (Fig. 2). Animals had isolated, well-demarcated solid tumours without any adverse effects on general health and well-being. The maximal tumour diameters after sacrifice, were <3.5 cm in all experiments. The maximal tumour burdens after sacrifice were much below 10 % of the animal body weight in all experiments. Pathological, histopathological and toxicological analysis following autopsy revealed no signs of toxicity on main organs (heart, lungs, stomach, intestine, liver, kidneys and brain), nor metastases or ascites.

TABLE I. Weights \pm SD (g) and control/treatment difference *P*-values of extirpated hamster fibrosarcomas treated with single drug and various combinations of metformin 500 mg/day with another repurposed drug

Drugs/dose, mg/kg	Control	Single 1.	Single 2.	Combination	Control/Single 1. <i>P</i> -values	Control/Single 2. <i>P</i> -values	Control/Combin. <i>P</i> -values
1. Metformin/500	2.90	2.45	3.06	1.36	0.61375	0.89427	0.04501
2. Deoxycholic acid/100	\pm 1.39	\pm 1.28	\pm 2.11	\pm 0.61			
1. Metformin/500	2.54	1.10	2.32	0.42	0.30021	0.78122	0.04110
2. Caffeine/100	\pm 2.30	\pm 0.77	\pm 1.31	\pm 0.32			
1. Metformin/500	4.85	3.20	3.99	1.13	0.39604	0.55283	0.02921
2. Itraconazole/250	\pm 3.35	\pm 1.65	\pm 0.98	\pm 0.41			
1. Metformin/500	2.67	2.42	1.97	1.44	0.59372	0.13005	0.01542
2. Nitroglycerin/25	\pm 1.05	\pm 0.98	\pm 1.02	\pm 0.75			
1. Metformin/500	4.38	4.01	4.22	0.65	0.39856	0.60277	0.00013
2. Disulfiram/50	\pm 0.50	\pm 0.69	\pm 0.99	\pm 0.27			
1. Metformin/500	3.80	3.10	2.80	0.19	0.30005	0.16483	0.00080
2. Diclofenac/60	\pm 0.77	\pm 0.89	\pm 1.16	\pm 0.15			

The experimental and control groups were statistically compared for glucose levels, haemoglobin levels, haematocrit levels, serum proteins, sedimentation, red and white blood cell counts, platelet number, but no significant differences were observed among the groups in all experiments ($P < 0.05$).

Peroral co-treatment with dual drug combinations containing metformin with deoxycholic acid, caffeine, itraconazole, nitroglycerin, disulfiram or diclofenac significantly inhibited tumour growth as indicated by significant decreases in tumour weight, compared with the control group and the single treatment groups (Table I).

The immunohistochemical evaluation (Fig. 3) revealed significantly ($P < 0.05$) decreased tumour mutational status, as demonstrated by p53; significantly ($P < 0.05$) decreased proliferation status of tumour cells, as demonstrated by Ki-67 and PCNA; significant ($P < 0.05$) inhibition of tumour vasculature, as demonstrated by CD31 and CD34; significant ($P < 0.05$) inhibition of glucose metabolism, as demonstrated by GLUT1; significant ($P < 0.05$) inhibition of NO meta-

bolism, as demonstrated by iNOS staining; and significant ($P < 0.05$) decrease in apoptosis intensity, as demonstrated by COX4, cytochrom C and caspase 3, in all analysed slices of tumours from animals treated with the combinations, compared with the control group and the single treatment groups. Furthermore, captivating correlation were obtained between tumour weight (g) and all analysed immunohistochemical parameters expression (Table II).

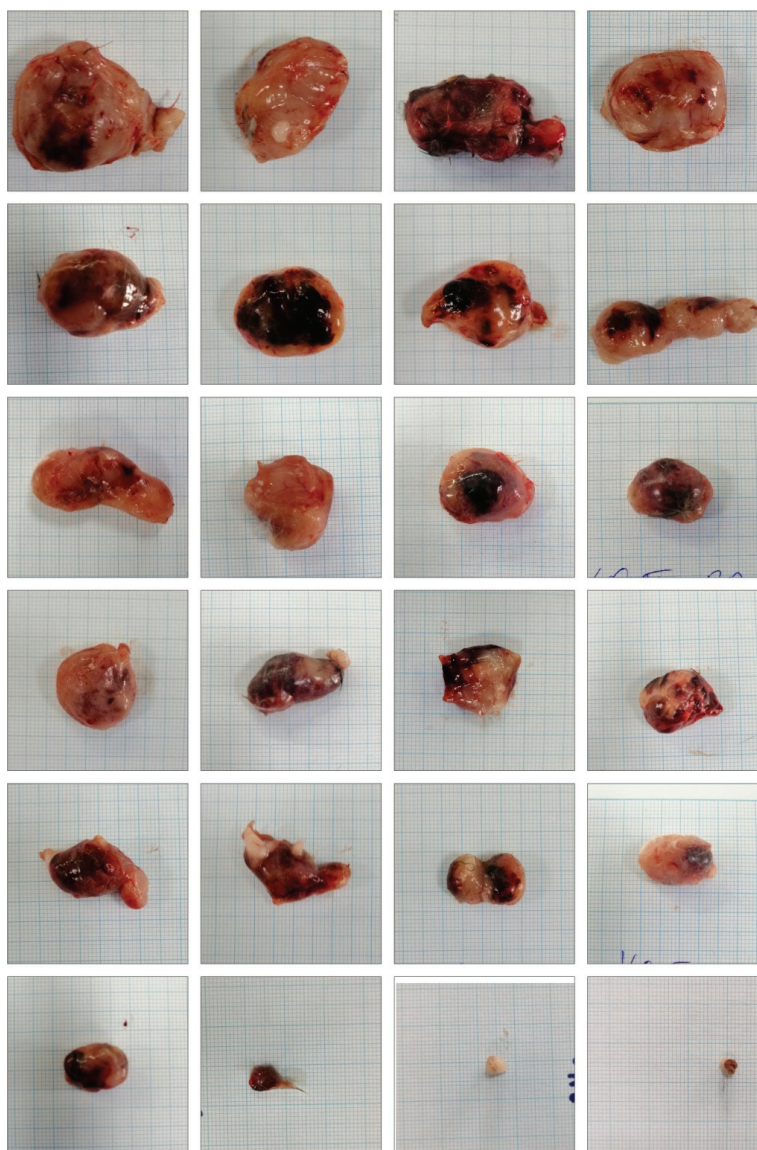


Fig. 2. Extirpated hamster fibrosarcomas placed on one-millimeter grid paper.

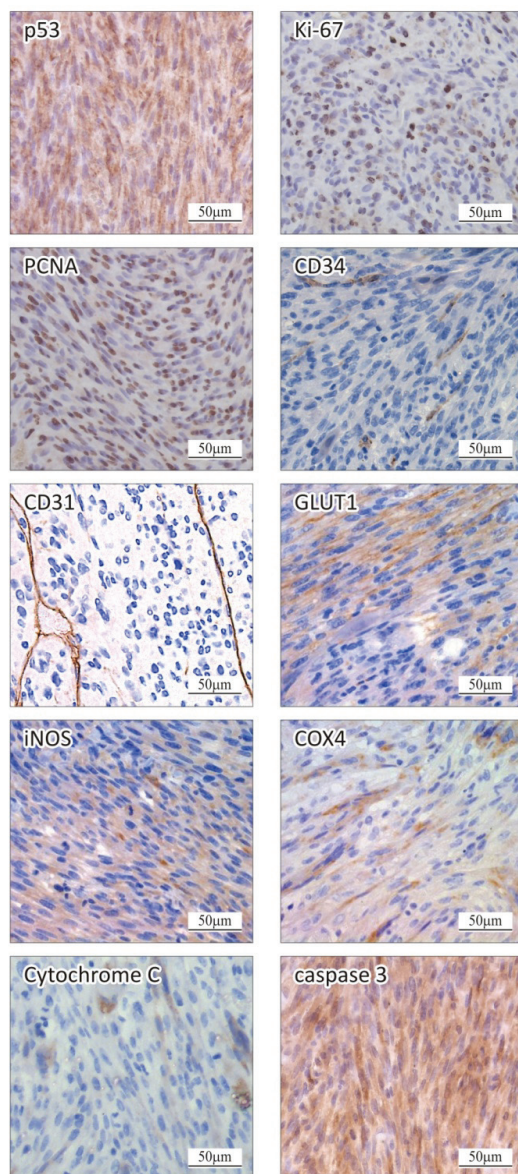


Fig 3. Extirpated hamster fibrosarcoma immunohistochemical staining images (examples from the control groups); illustration for used immunohistochemical stainings (p53, Ki-67, PCNA, CD34, CD31, GLUT1, iNOS, COX4, cytochrome C and caspase 3).

The results (Table I) confirmed the significant ($P < 0.05$) synergistic anticancer effects of all examined drug combinations on hamster fibrosarcoma, with significant correlation ($P < 0.05$) between decrease in tumour weight and immunohistochemical staining grade (Table II), without toxicity on main organs (based on the gross and microscopic standard pathological examination of organs, tis-

sues and whole bodies), influence on body weight, biochemical and haematological blood tests.

TABLE II. Correlation of tumour weight (g) and immunohistochemical expression (intensity)

Immunohistochemical parameter	Line fit plot	Pearson correlation coefficient (<i>r</i>)	<i>P</i> -value×10 ⁷
p53	$y = 8.095x + 1.597$	0.98511	2.1600
Ki-67	$y = 8.630x + 1.522$	0.98501	2.1672
PCNA	$y = 8.367x + 1.664$	0.98506	2.1622
CD34	$y = 1.002x + 0.576$	0.96396	0.70657
CD31	$y = 1.326x + 0.328$	0.95803	0.012902
GLUT1	$y = 0.091x + 0.050$	0.95784	0.013131
iNOS	$y = 0.080x + 0.031$	0.98646	1.4477
COX4	$y = 0.940x + 0.278$	0.96552	0.59297
Cytochrome C	$y = 0.925x - 0.221$	0.97395	0.19512
Caspase 3	$y = 7.791x + 1.782$	0.94972	0.021730

Findings of significant correlation between the significantly reduced tumour weight and immunohistochemical markers expression validate the anticancer effects of the investigated repurposed drug combinations.

Our explanation of the positive correlation between the tumour weight and the used immunohistochemical staining markers intensity, or more precisely, the explanation of the treated tumour weight decrease and the correlated p53 (“the guardian of the genom”) staining decrease (what seems contrary to the usual expectation); the reduced expression of proliferation indicators Ki-67 and PCNA (as expected); the reduced expression of neoangiogenesis indicators CD34 and CD31 (as expected); reduced expression of glucose metabolism indicator GLUT1 (as expected); the reduced expression of NO metabolism indicator iNOS (as expected); and the reduced expression of apoptosis indicators COX4, cytochrome C, caspase 3 (what seems contrary to usual expectation), based on recent literature, is as follows.

The tumour suppressor protein p53 is overexpressed in a large fraction of human tumours, including sarcomas.³⁴ It has been found that: 1) p53 abnormalities may be an early event that contributes to the neoplastic transformation; 2) p53 overexpression may be related to the progression toward more aggressive tumour forms.³⁴ The p53 protein is frequently mutated in many human cancers.³⁴ The mutant p53 protein has a much longer half-life than the wild-type protein and accumulates in large amounts in the nuclei of transformed cells. In contrast, the levels of the wild-type p53 protein are normally so low that they cannot be detected by immunohistochemistry.³⁴ Immunohistochemical detection of p53: 1) strong homogeneous staining pattern (aggressive tumor); 2) rare scattered positive nuclei (treated tumour). p53 protein overexpression (mutated) was significantly associated with parameters of biological aggressiveness. Mutant p53 pro-

tein may be unable to perform the normal p53 function of suppressing cell proliferation.³⁴ p53 is the most commonly mutated gene in cancer, including soft tissue sarcoma in humans.³⁵

Ki-67 and PCNA proteins – cellular markers for proliferation, CD34 – a marker of endothelial cells and vascular differentiation, CD31 – a useful specific adjunctive marker for tumour vasculature endothelial differentiation (more specific and sensitive than CD34), GLUT1 – associated with glucose transport across membranes (overexpressed in cancer), iNOS – marker of NO metabolism in the cytoplasm, associated with the tumour progression, proliferation and angiogenesis (overexpressed in various neoplastic processes) were in our experiments positively correlated to tumour weight. This could be expected, since the tumour cell proliferation, neoangiogenesis and glucose or NO metabolism intensity are involved in the tumour biological outcomes, such as tumour weight.¹

COX4, Cytochrome C and caspase 3 – markers of apoptosis, were in our study also directly correlated with tumour weight. Disregulation of apoptosis is a hallmark of cancer, enabling tumour cells to evade cell death and promote uncontrolled growth. In cancer cells increased levels of cleaved caspase 3 have been observed, indicating ongoing apoptotic events that might be ineffective or stopped by pro-survival pathways.³⁶ Rate of apoptosis, as measured by both caspase 3 activation or by other methods and nucleosome release are higher in breast cancer than in non-malignant breast tissue.³⁷ This finding would appear to conflict with the widely held belief that apoptosis is reduced in malignancy. The proliferation/apoptosis ratio, however, may be higher in carcinomas than in the corresponding normal tissue.³⁷ Tumour growth is the result of cell proliferation and cell loss by apoptosis.³⁸ By the comparison with non-neoplastic breast tissue, caspase 3 appeared to be upregulated in malignant breast tissue (> 75 % of the specimens).³⁸ The caspase-3 protein overexpression appears to be involved in the apoptotic pathways influenced by wild-type p53 (mutated p53).³⁸ The caspase 3 expression correlates with poor prognostic parameters such as higher histologic grade and high proliferation in breast carcinoma patients.³⁹ The caspase 3 expression could be linked with malignancy progression and correlates with the malignancy of head and neck cancer in humans.⁴⁰

Repurposing approved non-oncology drugs can significantly expedite the process of identifying effective anticancer treatments overcoming drug resistance in cancer and improve patient outcomes in a cost-effective manner.⁴¹ A good illustration of relevance and importance of drug repurposing for cancer treatment are clinical investigations available up to 2024 from multiple resources (PubMed, Google Scholar, ClinicalTrials.gov, Drug Bank database, ReDo database and the National Institutes of Health).⁴² The antidiabetic agents contribute to 52 clinical trials: metformin (37 trials/Phase I– III), pioglitazone (10 trials/Phase I and II), desmopressin (2 trial Phase I and II), dapaglifozin (1 trial/Phase I), epalrestat (1

trial/Phase II), acarbose (1 trial/Phase II) against different cancer types (*e.g.*, in clinical trial Phase III: breast, colorectal, endometrial, prostate and non-small cell lung cancer).⁴²

CONCLUSION

The results of our experiments confirmed the significant anticancer effects of the metformin co-treatments with deoxycholic acid, caffeine, itraconazole, nitroglycerin, disulfiram or diclofenac on hamster fibrosarcoma, without toxicity. The anticancer properties of the examined two-drug combinations in hamsters, documented by significant decrease in tumour weight and immunohistochemical staining grade, further supported by the significant correlation between the two, with used doses equivalent to standard human doses, suggest that the effective nontoxic oncological therapies in humans and prevention of cancer relapse using these drug combinations may be achievable. The administration of metformin in combination with deoxycholic acid, caffeine, itraconazole, nitroglycerin, disulfiram or diclofenac might be an effective and safe approach in novel nontoxic adjuvant anticancer treatment and can be recommended for further clinical investigations.

Acknowledgements. This study was supported by the Republic of Serbia, Autonomous Province of Vojvodina, Provincial Secretariat for High Education and Scientific Research, grants nos. 142-451-2498/2021-03 (DP), 142-451-2676/2021 (JM), 142-451-2626/2021 (DL) and Republic of Serbia, Ministry of Education, Science and Technological Development, grant no. 451-03-68/2022-14/200114. The authors would like to gratefully acknowledge Mrs. Vesna Popović for her expert technical assistance and suggestions during the preparation of this study.

ИЗВОД

ИМУНОХИСТОХЕМИЈСКИ ПОКАЗАТЕЉИ АНТИКАНЦЕРСКОГ ДЕЛОВАЊА КОМБИНАЦИЈА МЕТФОРМИНА СА ДРУГИМ ПРЕНАМЕЊЕНИМ ЛЕКОМ И КОРЕЛАЦИЈА СА ВЕЛИЧИНОМ ТУМОРА НА ФИБРОСАРКОМУ ХРЧКА

ЛОВАН К. ПОПОВИЋ¹, ДУШИЦА Ј. ПОПОВИЋ², КОСТА Ј. ПОПОВИЋ³, ДЕЈАН МИЉКОВИЋ⁴, ДУШАН ЛАЛОШЕВИЋ⁴, ЗАНА ДОЛИЋАНИН² И ИВАН ЧАПО⁴

¹Завод за фармакологију, титоксикологију и клиничку фармакологију, Медицински факултет, Универзитет у Новом Саду, Нови Сад, ²Департаман за биомедицинске науке, Државни универзитет у Новом Пазару, Нови Пазар, ³Завод за фармацију, Медицински факултет, Универзитет у Новом Саду, Нови Сад и ⁴Завод за хистологију и ембриологију, Медицински факултет, Универзитет у Новом Саду, Нови Сад

Циљ је био откривање и корелација антиканцерских ефеката метформина у комбинацији са другим пренамењеним лековима, већ регистрованим за друге индикације, који се могу одмах применити и клинички испитати у онкологији, што смањује време и трошкове истраживања нових терапија канцера. Имунохистохемија је урађена за туморе лечене комбинацијама два лека, које садрже метформин са деоксихолном киселином, кофеином, итраконазолом, нитроглицерином, дисулфирамом или диклофенаком. Лекови су примењени код сиријских златних хрчака

(6 животиња по групи) са инокулисаним ВНК21/С13 фибросаркомом, у дозама еквивалентним уобичајеним дозама за људе, <50 % LD_{50} . Антиканцерска дејства су процењена помоћу имунохистохемијских маркера: p53 (мутациони статус); Ki-67 и PCNA (пролиферација тумора); CD34 и CD31 (неоангиогенеза); GLUT1 (метаболизам глукозе); iNOS (NO метаболизам); COX4, cytochrome C и caspase 3 (апоптоза). Такође, анализирани су биофизичке карактеристике фибросаркома, узорци крви животиња и токсичност за главне органе. Третмани су значајно ($P < 0,05$) смањили мутациони статус, пролиферацију тумора, неоангиогенезу, метаболизам глукозе, метаболизам NO и модулирали апоптозу, у корелацији са величином тумора, без токсичности и утицаја на биохемијске крвне и хематолошке тестове. Примена комбинација два лека – метформина са: деоксихолном киселином, кофеином, итраконазолом, нитроглицерином, дисулфирамом или диклофенаком, може се препоручити за даља клиничка испитивања у онкологији.

(Примљено 3. децембра, ревидирано 13. децембра 2023, прихваћено 22. јануара 2024)

REFERENCES

1. D. Verzella, A. Pescatore, D. Capece, D. Vecchiotti, M. V. Ursini, G. Franzoso, E. Alesse, F. Zazzeroni, *Cell Death Dis.* **11** (2020) 210 (<https://doi.org/10.1038/s41419-020-2399-y>)
2. L. Li, T. Wang, M. Hu, Y. Zhang, H. Chen, L. Xu, *Front. Oncol.* **10** (2020) 1605 (<https://doi.org/10.3389/fonc.2020.01605>)
3. L. Ma, J. Wei, J. Wan, W. Wang, L. Wang, Y. Yuan, Z. Yang, X. Liu, L. Ming, *J. Exp. Clin. Cancer Res.* **38** (2019) 77 (<https://doi.org/10.1186/s13046-019-1090-6>)
4. C. C. Lu, J. H. Chiang, F. J. Tsai, Y. M. Hsu, Y. N. Juan, J. S. Yang, H. Y. Chiu, *Int. J. Oncol.* **54** (2019) 1271 (<https://doi.org/10.3892/ijco.2019.4704>)
5. J. Yang, J. Wei, Y. Wu, Z. Wang, Y. Guo, P. Lee, X. Li, *Oncogenesis* **4** (2015) e158 (<https://doi.org/10.1038/oncsis.2015.18>)
6. Z. Wu, Y. Lü, B. Wang, C. Liu, Z. R. Wang, *World J Gastroenterol.* **9** (2003) 2759 (<http://dx.doi.org/10.3748/wjg.v9.i12.2759>)
7. J. S. Pyo, Y. S. Ko, G. Kang, D. H. Kim, W. H. Kim, B. L. Lee, J. H. Sohn, *J. Cancer Res. Clin. Oncol.* **141** (2015) 1181 (<https://doi.org/10.1007/s00432-014-1890-1>)
8. J. P. Phelan, F. J. Reen, N. Dunphy, R. O'Connor, F. O'Gara, *BMC Cancer* **16** (2016) 476 (<https://doi.org/10.1186/s12885-016-2528-2>)
9. S. Yui, R. Kanamoto, T. Saeki, *Nutr. Cancer* **60** (2008) 91 (<https://doi.org/10.1080/01635580701525893>)
10. J. Ignacio Barrasa, N. Olmo, P. Pérez-Ramos, A. Santiago-Gómez, E. Lecona, J. Turnay, M. Antonia Lizarbe, *Apoptosis* **16** (2011) 1054 (<https://doi.org/10.1007/s10495-011-0633-x>)
11. H. B. Yang, W. Song, M. D. Cheng, H. F. Fan, X. Gu, Y. Qiao, X. Lu, R. H. Yu, L. Y. Chen, *Mol. Med. Rep.* **11** (2015) 2749 (<https://doi.org/10.3892/mmr.2014.3004>)
12. P. M. Rodrigues, M. B. Afonso, A. L. Simão, P. M. Borralho, C. M. P. Rodrigues, R. E. Castro, *Sci. Rep.* **5** (2015) 17528 (<https://doi.org/10.1038/srep17528>); *Erratum in: Sci. Rep.* **6** (2016) 27828 (<https://doi.org/10.1038/srep27828>)
13. M. Hałas, M. Izdebska, A. Klimaszewska-Wiśniewska, M. Gagat, D. Radciniewska, A. Glińska, K. Gizler, E. Bielińska, A. Grzanka, *Open Life Sci.* **9** (2014) 727 (<https://doi.org/10.2478/s11535-014-0315-0>)

14. E. D. Osarieme, D. T. Modupe, O. P. Oluchukwu, *Arch. Clin. Biomed. Res.* **3** (2019) 326 (<https://doi.org/10.26502/acbr.50170077>)
15. H. Tsubamoto, T. Ueda, K. Inoue, K. Sakata, H. Shibahara, T. Sonoda, *Oncol. Lett.* **14** (2017) 1240 (<https://doi.org/10.3892/ol.2017.6325>)
16. M. D. Navarro-Martínez, J. Cabezas-Herrera, J. N. Rodríguez-López, *Int. J. Antimicrob. Agents* **28** (2006) 560 (<https://doi.org/10.1016/j.ijantimicag.2006.07.012>)
17. C. L. Li, Z. X. Fang, Z. Wu, Y. Y. Hou, H. T. Wu, J. Liu, *Biomed. Pharmacother.* **154** (2022) 113616 (<https://doi.org/10.1016/j.biopha.2022.113616>)
18. J. Mintz, A. Vedenko, O. Rosete, K. Shah, G. Goldstein, J. M. Hare, R. Ramasamy, H. Arora, *Vaccines* **9** (2021) 94 (<https://doi.org/10.3390/vaccines9020094>)
19. A. Garcia, G. Tisman, *J. Clin. Oncol.* **28** (2010) e19 (<https://doi.org/10.1200/jco.2009.25.7857>)
20. M. A. Erkurt, İ. Aydoğdu, N. Bayraktar, İ. Kuku, E. Kaya, *Turk. J. Hematol.* **26** (2009) 197 (<https://pubmed.ncbi.nlm.nih.gov/27265632/>)
21. P. Pradhan, *J. Vector. Borne. Dis.* **46** (2009) 100 (<https://pubmed.ncbi.nlm.nih.gov/19502689/>)
22. V. Sukhatme, G. Bouche, L. Meheus, V. P. Sukhatme, P. Pantziarka, *Ecancer* **9** (2015) 568 (<https://doi.org/10.3332/ecancer.2015.568>)
23. B. Xu, S. Wang, R. Li, K. Chen, L. He, M. Deng, V. Kannappan, J. Zha, H. Dong, W. Wang, *Cell. Death. Dis.* **8** (2017) e2797 (<https://doi.org/10.1038/cddis.2017.176>)
24. O. Celik, A. Ersahin, M. Acet, N. Celik, Y. Baykus, R. Deniz, E. Ozerol, I. Ozerol, *Eur. Rev. Med. Pharmacol. Sci.* **20** (2016) 4380 (<https://pubmed.ncbi.nlm.nih.gov/27831632/>)
25. J. Zha, F. Chen, H. Dong, P. Shi, Y. Yao, Y. Zhang, R. Li, S. Wang, P. Li, W. Wang, B. Xu, *J. Transl. Med.* **12** (2014) 163 (<https://doi.org/10.1186/1479-5876-12-163>)
26. M. A. Westhoff, S. Zhou, L. Nonnenmacher, G. Karpel-Massler, C. Jennewein, M. Schneider, M. E. Halatsch, N. O. Carragher, B. Baumann, A. Krause, T. Simmet, M. G. Bachem, C. R. Wirtz, K. M. Debatin, *Mol. Cancer. Res.* **11** (2013) 1611 (<https://doi.org/10.1158/1541-7786.mcr-13-0435-t>)
27. W. Wang, H. L. McLeod, J. Cassidy, *Int. J. Cancer.* **104** (2003) 504 (<https://doi.org/10.1002/ijc.10972>)
28. K. Butcher, V. Kannappan, R. S. Kilari, M. R. Morris, C. McConville, A. L. Armesilla, W. Wang, *BMC Cancer* **18** (2018) 753 (<https://doi.org/10.1186/s12885-018-4617-x>)
29. J. Zhang, K. Pu, S. Bai, Y. Peng, F. Li, R. Ji, Q. Guo, W. Sun, Y. Wang, *J. Int. Med. Res.* **48** (2020) 300060520925996 (<https://doi.org/10.1177/0300060520925996>)
30. B. Herpers, S. Wink, L. Fredriksson, Z. Di, G. Hendriks, H. Vrieling, H. de Bont, B. van de Water, *Arch. Toxicol.* **90** (2016) 1163 (<https://doi.org/10.1007/s00204-015-1536-3>)
31. L. Fredriksson, B. Herpers, G. Benedetti, Q. Matadin, J. C. Puigvert, H. de Bont, S. Dragovic, N. P. Vermeulen, J. N. Commandeur, E. Danen, M. de Graauw, B. van de Water, *Hepatology* **53** (2011) 2027 (<https://doi.org/10.1002/hep.24314>)
32. Y. Takada, A. Bhardwaj, P. D. Potdar, B. Aggarwal, *Oncogene* **23** (2004) 9247 (<https://doi.org/10.1038/sj.onc.1208169>)
33. A. M. Cimpean, D. Lalošević, V. Lalošević, P. Banović, M. Raica, O. A. Mederle, *In Vivo* **32** (2018): 791 (<https://doi.org/10.21873/invivo.11309>)
34. G. Toffoli, C. Doglioni, C. Cernigoi, S. Frustaci, T. Perin, B. Canal, M. Boiocchi, *Ann. Oncol.* **5** (1994) 167 (<https://doi.org/10.1093/oxfordjournals.annonc.a058771>)

35. P. Das, D. Kotilingam, B. Korchin, J. Liu, D. Yu, A. J. Lazar, R. E. Pollock, D. Lev, *Cancer* **109** (2007) 2323 (<https://doi.org/10.1002/cncr.22680>)
36. L. Flanagan, M. Meyer, J. Fay, S. Curry, O. Bacon, H. Duesmann, K. John, K. C. Boland, D. A. McNamara, E. W. Kay, H. Bantel, H. Schulze-Bergkamen, J. H. Prehn, *Cell Death Dis.* **7** (2016) e2087 (<https://doi.org/10.1038/cddis.2016.7>)
37. N. O'Donovan, J. Crown, H. Stunell, A. D. Hill, E. McDermott, N. O'Higgins, M. J. Duffy, *Clin. Cancer Res.* **9** (2003) 738 (<https://pubmed.ncbi.nlm.nih.gov/12576443/>)
38. L. Nakopoulou, P. Alexandrou, K. Stefanaki, E. Panayotopoulou, A. C. Lazaris, P. S. Davaris, *Pathobiology* **69** (2001) 266 (<https://doi.org/10.1159/000064337>)
39. A. Nassar, D. Lawson, G. Cotsonis, C. Cohen, *Appl. Immunohistochem. Mol. Morphol.* (2008) **16** 113 (<https://doi.org/10.1097/PAI.0b013e318032ea73>)
40. F. F. V. E. Silva, M. E. Padín-Iruegas, V. C. A. Caponio, A. I. Lorenzo-Pouso, P. Saavedra-Nieves, C. M. Chamorro-Petronacci, J. Suárez-Peñaranda, M. Pérez-Sayáns, *Int. J. Mol. Sci.* **23** (2022) 11937 (<https://doi.org/10.3390/ijms231911937>)
41. R. Mohi-ud-din, A. Chawla, P. Sharma, Prince A. Mir, F. H. Potoo, Ž. Reiner, I. Reiner, D. A. Ateşşahin, J. Sharifi-Rad, R. H. Mir, D. Calina, *Eur. J. Med. Res.* **28** (2023) 345 (<https://doi.org/10.1186/s40001-023-01275-4>)
42. M. A. Hijazi, A. Gessner, N. El-Najjar, *Cancers* **15** (2023) 3199 (<https://doi.org/10.3390/cancers15123199>).



J. Serb. Chem. Soc. 89 (5) 657–665 (2024)
JSCS–5746

A 7-year experience in core needle biopsy of breast lesions: Correlation between imaging and hematoxylin and eosin-stained sections

MILENA ŠUNJEVIĆ^{1,2*}, DUNJA POPOVIĆ^{1,3}, SARA MEDIC¹, MILANA PANJKOVIĆ^{1,2}
and BRANIMIR GUDURIĆ¹

¹University of Novi Sad, Faculty of Medicine, Novi Sad, Serbia, ²University Clinical Centre of Vojvodina, Centre for Pathology and Histology, Novi Sad, Serbia and ³University Clinical Centre of Vojvodina, Medical Rehabilitation Clinic, Novi Sad, Serbia

(Received 11 November, revised 24 November 2023, accepted 7 March 2024)

Abstract: Screening mammography is an imaging procedure which allows breast cancer detection in its early stage. The Breast Imaging and Reporting Data System (BI-RADS) determined six radiological categories for describing lesions. The core needle biopsy (CNB) is minimally invasive procedure that provides pathohistological samples. *Via* microscopic analysis, samples are categorized into five groups according to the B system for pathohistological report. The aim of the study was to follow the spectrum of pathohistological diagnoses; to define which BI-RADS and core categories are most commonly expressed in certain age groups; and to determine the incidence of histological diagnoses in different BI-RADS categories. The study included 631 patients and data was analysed in order to localise the lesion, BI-RADS and core category and pathohistological diagnosis. Within 631 biopsies, 33 diagnoses were given. In each age group, the findings indicating a high risk for malignancy were the most common (>2 %). The highest percentage of malignant categories was found in patients over the age of 61. Final diagnoses showed a deviation compared to the radiological categories, especially in BI-RADS4 category. Pathohistological diagnosis is always a definite confirmation of a breast lesion type and it has significant contribution to the evaluation of CNB quality.

Keywords: mammography; BI-RADS; histology; breast.

INTRODUCTION

Breast cancer is the second most common cause of death due to malignancy in women worldwide. Mortality rate is estimated to be 6.6 %, with the global incidence being 11.6 %. In East Europe, the incidence is 54.5 % and mortality rate peaks 15.5 % in women aged 40–60 years.^{1,2} National guidelines for malig-

* Corresponding author. E-mail: milena.sunjevic@mf.uns.ac.rs
<https://doi.org/10.2298/JSC231111026S>



nancy prevention in primary health services give following propositions: guide for self-examination in women who are up to 30 years old, once-a-year clinical examination for women older than 40 and the screening mammography for women aged 45–69 years once in two years.^{3–5} Screening mammography is an imaging technique based on use of low energy X-rays, which provides the detection of breast cancer in its earliest stage of growth, before the disease is clinically manifested. This procedure gives the opportunity to detect lesions smaller than 2 cm in diameter, for both *in situ* and invasive carcinoma.^{4–6} The advantage of this method is its ability to detect microcalcifications which are often the only sign of *in situ* carcinoma. On the other hand, the sensitivity of mammography is 85 % and only 65 % in women with high breast density. Specificity of the method is about 90 %, however, the reproducibility is limited because of radiation that needs to be reduced to lower values.⁷ The Breast Imaging Reporting and Data System (BI-RADS), established by the American College of Radiology (ACR), defined the categories of mammography results, marked as BI-RADS 0–6. BI-RADS4 category was further subcategorized into A, B and C (with 2–10 %; 11–50 and 51–95 % malignance probability, respectively).⁸ In the case of palpable lesions suspicious of malignancy during the clinical examination (categories K3, K4 and K5) or the mammography results suspicious of malignancy, patients are suggested to undergo following methods: fine needle aspiration biopsy (FNAB), vacuum assisted biopsy (VAB) or core needle biopsy (CNB). These procedures are performed for the purpose of definite pathohistological diagnosis. The percutaneous biopsy methods of non-palpable lesions could be conducted with the navigation of imaging methods such as ultrasonography, stereotaxic mammography or MRI.⁹ The core needle biopsy is minimally invasive procedure which allows the tissue sampling through the incision of small diameter made by radiologist. The sensitivity of CNB is 97–99 %. The CNB categories are defined as B1–B5, where B5 category is further subcategorized into: B5a (*in situ*), B5b (invasive carcinoma), B5c (invasion cannot be determined) and B5d (malignant phyllodes tumours, lymphoma, sarcoma and metastases).¹⁰

The aim of this study was to define the spectre of pathohistological diagnoses in the Centre for Pathology and Histology in the University Clinical Centre of Vojvodina after a radiological diagnostic procedure in a 7-year period, to emphasize the most common BI-RADS and CNB categories in certain age groups, and to make a preview of specific diagnoses which were preliminary defined by the BI-RADS system.

EXPERIMENTAL

In a 7-year period, the cases of 631 patient were reviewed in this retrospective study. The study was conducted in the University Clinical Centre of Vojvodina and approved by the Research Ethics Committee of this institution. The study obtained radiology reports categorized as BI-RADS 0–5, and based on age, anamnestic data and clinical examination, the pre-

cise indications for CNB were stated. The exclusion criteria used in this study referred to patients with VAB samples, metastatic lesions and lesions without neoplastic predisposition. Tissue samples were fixed by 10 % neutral formalin, then routinely paraffin-embedded and cut at approximately 5-mm intervals, sliced to 4- μ m-thick sections and stained with hematoxylin and eosin (H&E). The lesions were categorized according to the European Society of Breast Cancer Specialists and Biopsy reporting the category system as B0 (inadequate sample), B1 (normal breast tissue), B2 (benign), B3 (uncertain malignant potential), B4 (suspicious of malignancy) or B5 (malignant). Histologic grade (1, 2 or 3), nuclear pleomorphism (1, 2 or 3) and mitoses per 10 high power fields (HPF) were counted and defined in cases of malignant neoplasm. The grade of malignant lesions was determined according to the Nottingham prognostic index as: Grade I = summary result 3, 4 or 5, Grade II = summary result 6 or 7 and Grade III = summary result 8 or 9.⁸ The data was processed in the Microsoft Excel 2016 and the results were presented in tables through percentages.

RESULTS AND DISCUSSION

Based on age distribution, 631 patient was divided into 6 categories with different percentage presentation: <30 (1.11 %), 31–40 (5.86 %), 41–50 (12.20 %), 51–60 (31.22%), 61–70 (44.06%) and >70 years of age (5.55 %). The presentation of certain BI-RADS categories in different age groups was shown in Table I. The most common BI-RADS categories were 4a, 4b and 5. The predominant categories within age groups were: <30: BI-RADS4a; 31–40: BI-RADS3; 41–50: BI-RADS4a; 51–60: BI-RADS4b; 61–70: BI-RADS4b; >70: BI-RADS4b and 5.

TABLE I. BI-RADS categories in different age groups given as presentation in certain age groups in %

BI-RADS	Summary presentation, %	Group					
		<30	31–40	41–50	51–60	61–70	>70
0	0.95	0	0	0	0.48	0.32	0.16
1	0	0	0	0	0	0	0
2	4.28	0	0.32	0.63	0.9	1.27	0.16
3	8.87	0.16	2.22	1.58	2.38	2.22	0.32
4a	30.12	0.53	1.53	4.44	9.50	13.21	0.90
4b	30.59	0.21	0.9	3.01	10.14	14.47	1.85
4c	9.83	0.21	0.42	1.27	2.85	4.33	0.74
5	1.37	0	0.48	1.27	3.96	8.24	1.85

Table II shows the frequency of CNB categories and the presentation in different age groups. The predominant categories within age groups were: <30: B4; 31–40: B2; 41–50: B2; 51–60: B2; 61–70: B5; >70: B5.

Tables III and IV present all histological diagnoses after the core needle biopsy and their percentage within BI-RADS categories which indicated the biopsy at the first place.

The breast morphology changes from early adolescence to menopause under the influence of sex hormones. The breast structure significantly influences the inter-

TABLE II. Frequency of CNB categories and presentation in certain age groups given as representation of CNB categories in specific age groups in %

CNB	Representation of CNB categories in summary results, %	Group					
		<30	31–40	41–50	51–60	61–70	>70
B1	11.41	0.79	0.79	0.95	3.80	5.71	0.16
B2	47.86	3.02	3.80	7.13	17.12	18.07	1.74
B3	1.90	0.16	0.16	0	0.63	0.95	0.16
B4	0	0	0	0	0	0	0
B5	38.19	0.48	1.11	4.12	9.67	19.33	3.49

TABLE III. Diagnostic specter in the preliminary determined BI-RADS categories 0, 2 and 3

BI-RADS 0	BI-RADS 2	BI-RADS 3
B1: No morphological changes or cell atypia (0.48 %)	B1: No morphological changes or cell atypia (0.79 %)	B1: No morphological changes or cell atypia (1.43 %)
B5: DCIS (0.16 %)	B2: Adenosis (0.16 %)	B2: Adenosis (0.48 %)
	Apocrine metaplasia (0.48 %)	Sclerosis and microcalcifications (0.32 %)
	Fibrosis (0.32 %)	
	Fibrocystic change (0.48 %)	
	Fibroadenoma (1.11 %)	
	Gynecomastia (0.16 %)	
	Ductal hyperplasia (0.16 %)	
	Steatonecrosis (0.16 %)	
	B3: Uncertain malignant potential (0.16 %)	B5: DCIS (0.64 %)
		Invasive lobular carcinoma (0.16 %)
		Invasive carcinoma of no special type (0.16 %)
	B5: Invasive ductal carcinoma (0.16 %)	

pretation of mammographic results and fibroglandular breast composition aggravates further BI-RADS classification, thus also the indications for CNB. From the total number of newly ill, 30 % of patients is younger than 50, and approximately 33 % are from 50 to 64 years of age.^{11–13} In our regional centre, mammography was most commonly performed in women from 51 to 70 years of age (75.27 %), and the most common categories were BI-RADS4 and BI-RADS5 (76.08 %). CNB is the method of choice in diagnosis of papillary lesions, but it is unreliable for differentiating fibroadenoma from phyllodes tumour (B3) in cases of fibroepithelial lesions.¹³ The tissue volume obtained during CNB is smaller than the volume obtained during VAB.¹⁴ The number of false negative CNB results compared to open excision biopsy (OEB) is 1.4 % for biopsies performed with 16G and 18G needles. The biggest concordance is proven in the cases of diagnosing lesions larger than 10 mm. The sensitivity of CNB method rises with the size of specimen, number of calcifications and it is dependent of tumour type.¹⁵ It is better to opt for CNB in cases of palpable lesions or those with micro-

TABLE IV. Diagnostic specter in the preliminary determined BI-RADS categories 4 and 5

BI-RADS 4a BI-RADS 4b BI-RADS 4c	BI-RADS 5
B1: No morphological changes or cell atypia (8.72 %)	B1: No morphological changes or cell atypia (0.16 %)
B2: Adenosis (2.85 %)	B2: Adenosis (0.16 %)
Pseudoangiomatous stromal hyperplasia (0.16 %)	
Mastitis (1.43 %)	
Papillomatosis (0.32 %)	
Intraductal papilloma (1.27 %)	
Steatonecrosis (1.11 %)	
Sclerosis and microcalcifications (3.64 %)	
Postradiation stromal atypia (0.16 %)	
B3: Uncertain malignant potential (0.95 %)	B5: LCIS (0.16 %)
Phyllodes tumor (0.32 %)	Invasive ductal carcinoma (10.94 %)
	Invasive lobular carcinoma (1.11 %)
	Micropapillary carcinoma (0.16 %)
	Mucinous carcinoma (0.16 %)
	Mixed carcinoma (0.16 %)
	Cribriform carcinoma (0.16 %)
	Tubulolobular carcinoma (0.16 %)
	Invasive carcinoma of no special type (0.48 %)
B5: DCIS (0.95 %)	
Invasive ductal carcinoma (16.48 %)	
Invasive lobular carcinoma (3.01 %)	
Micropapillary carcinoma (0.32 %)	
Mixed carcinoma (0.32 %)	
Mucinous carcinoma (0.64 %)	
Metaplastic carcinoma (0.16 %)	
Invasive carcinoma of no special type (0.48 %)	
Neuroendocrine carcinoma (0.16 %)	

calcifications. If a clinical or radiological assessment indicates cystic lesion, a better approach is through the fine needle aspiration cytology (FNAC).¹⁶ In a systematic meta-analysis from Wang *et al.*, the results pointed to a better sensitivity of CNB than FNAC in the evaluation of suspicious breast lesions.¹⁷ Even though FNAC is a less invasive and easily reproducible modality, the differentiation of fibroadenoma and *in situ* carcinoma cannot be made by this method.¹⁶ The indicative radiological field for BI-RADS3 category encompasses the circumscribed palpable lesions, complicated cysts and cluster microcysts. The prevalence of various histological findings showed that the most commonly found are atypical ductal hyperplasia, flat epithelial atypia, lobular neoplasia, papillary changes and radial scarring. Histology after the excision points to the higher fre-

quency of benign than malignant changes (74 vs. 26 %).^{13–16} The alternative approach to these lesions is its removal by VAB technique, in order to avoid the open surgical excision due to the significant number of benign lesions. B3 category was presented in 1.59 % of all cases in our institution. Even though CNB is less specific in differentiating phyllodes tumour from fibroepithelial changes (69.2 %), its specificity is higher than FNAB (21.6 %). This tumour is most commonly described as BI-RADS4 category.¹⁷ Ultrasound is more precise in the detection of phyllodes tumour than mammography, and due to its variations in clinical behaviour, it is appropriate to mark it as B3 lesion.¹⁷ The occurrence of phyllodes tumour among diagnoses in the Centre for Pathology and Histology was 0.32 %. According to the literature, the BI-RADS3 category lesions, identified by ultrasound, present a risk of malignancy <2 %. For these lesions, a close instrumental follow-up every 6 months, then every 6–12 months for 2 years, is suggested in literature.^{13–16} A study by Pistolese *et al.* shows that 4.7 % of cases underwent histological verification, and the malignancy rate was 5.7 % – higher than expected.¹⁸ In the 7-year study from USA on 9068 CNB samples, the frequency of benign lesions was 64.2 %, of high-risk lesions 3.5 % and of malignant lesions 32.3 %. After the surgical excision or VAB, the breast carcinoma was confirmed in 3.2 % benign, 26.3 % high-risk and 100 % malignant lesions. In OEB samples, the percentage of underestimated DCIS was 33.6 and 24.5 % for high-risk lesions, such as atypical ductal hyperplasia, flat epithelial atypia and lobular neoplasia.¹⁹ The discordance between radiological and pathohistological diagnoses in the context of benign and malignant nature of breast lesions is particularly noticeable in BI-RADS4 category. Based on our data, 59.97 % of CNB specimens showed no morphological changes or cellular atypia, which leads us to a wide area of biopsy indications in our institution. According to the National Guideline of Good Clinical Practice for diagnosing and treating breast cancer, a biopsy is not indicated in the cases of BI-RADS0-2 category.¹⁶ Within the analysed data, the frequency of these categories further undergoing pathohistological analysis was 5.23 %. The course of core needle biopsy requires a good communication and the accordance between the radiologist, surgeon and pathologist. The specialists in the field of radiology are following BI-RADS system since 2003, which is established on the risk assessment for malignant lesions considering the perennial comparison of numerous imaging findings.¹⁷ Even though there are frequent discrepancies between the radiological and the pathohistological findings, invasive and more expensive surgical procedure and possible complications are generally avoided by histologically defining the benign nature of breast lesions. It is recommended to revise BI-RADS2 category in case of a malignant pathohistological features – B5, in order to avoid overlooking significant breast changes.^{16–19} The pathohistological diagnosis is always a definite confirmation of a breast lesion and it has cardinal contribution to the evaluation of CNB qual-

ity. The computer modelling of breast carcinoma represents a new trend in diagnosing breast lesions, which is based on mathematical functions – the artificial neurons. The computer-aided diagnosis was presented in a 2018 study, which showed the relation between mammographic and pathohistological phenotypes and revealed a new model of diagnostic approach: the mammography-histology phenotype, a binding model that allows mapping and connecting the mammographic features with the pathohistological presentation of breast lesions. The reduced unnecessary indications for the biopsy contribution to a simpler and a more accurate clinical decision making about the prognosis and a further clinical approach is expected. The expectations reach the ability of identifying the sub-cellular models of the expressed genes characteristic of cancer and non-cancer cells, determining the factors responsible for the high-grade lesions, modelling the time progression of first-appearing change, the better prediction of lesion aggressiveness and the possible outcomes for patients.²⁰ For the purpose of prosper in automatic, digital classification of the verified changes by H&E method, the grand challenge on breast cancer histology images (a BACH challenge) was set and the main goal was to classify and localize the histologically relevant categories based on a large amount of data grouped and published in a specific way.²¹

CONCLUSION

The following is included:

1. The breast cancer is the most common female malignancy in both the developing and developed world and is the primary cause of death among women globally. The risk of breast cancer increases with age and it is assumed that the number of older women living with breast cancer will quadruple by 2040.
2. The core needle biopsy (CNB) is the preferred pathological method for breast cancer diagnosis, compared to the fine-needle aspiration cytology or the surgical excision. The tissue obtained by CNB gives the information regarding the tumour type, the grade and the expression of biomarkers, if needed.
3. Discrepancies between the radiological and the pathohistological findings are frequent, but invasive and more expensive surgical procedure and possible complications can be generally avoided by the histologically defining benign nature of breast lesions.

ИЗВОД

СЕДМОГОДИШЊЕ ИСКУСТВО СА ИГЛЕНИМ БИОПСИЈАМА ЛЕЗИЈА ДОЈКЕ:
КОРЕЛАЦИЈА ИЗМЕЂУ ИМИЦИНГА И ХЕМАТОКСИЛИН–ЕОЗИН БОЈЕНИХ
ПРЕПАРАТА

МИЛЕНА ШУЊЕВИЋ^{1,2}, ДУЊА ПОПОВИЋ^{1,3}, САРА МЕДИЋ¹, МИЛАНА ПАЊКОВИЋ^{1,2} И БРАНИМИР ГУДУРИЋ¹

¹Универзитет у Новом Сагу, Медицински факултет, Нови Сад, ²Универзитетски клинички центар Војводине, Центар за патолозију и хистолозију, Нови Сад и ³Универзитетски клинички центар Војводине, Клиника за медицинску рехабилитацију, Нови Сад

Мамографија представља радиолошку процедуру која омогућава детекцију карцинома дојке у раној фази. BI-RADS систем класификације је детерминисао шест радиолошких категорија за опис лезија присутних у дојци. Иглена биопсија је минимално инвазивна процедура која омогућава добијање узорака за микроскопску анализу, који су надаље подељени у пет група према Б систему класификације. Циљ студије био је сагледање спектра патохистолошких дијагноза, дефинисање најчешће BI-RADS и Б категорије у различитим добним групама и детерминисање заступљености хистолошких дијагноза у различитим BI-RADS категоријама. Студија је обухватила 631 пацијента и подаци су анализирани у односу на локализацију лезије, радиолошке категорије и хистолошке дијагнозе. У свакој доброј групи, налаз везан за висок ризик од малигнитета је био најзаступљенији (>2 %). Највећи проценат малигне категорије је био заступљен код пацијенткиња старијих од 61 годину. Крајње дијагнозе показале су девијацију у односу на радиолошку категорију, посебно у категорији BI-RADS 4. Патохистолошка дијагноза је једина дефинитивна потврда типа лезије дојке и има огроман допринос у евалуацији квалитета иглених биопсија.

(Примљено 11. новембра, ревидирано 24. новембра 2023, прихваћено 7. марта 2024)

REFERENCES

1. F. Bray, J. Ferlay, I. Soerjomataram, R. L. Siegel, L. A. Torre, A. Jemal, *CA. Cancer. J. Clin.* **68** (2018) 394 (<https://dx.doi.org/10.3322/caac.21492>)
2. H. G. Welch, C. P. Prorok, A. J. O'Malley, B. S. Kramer, *N. Engl. J. Med.* **375** (2016) 1438 (<https://dx.doi.org/10.1056/NEJMoa1600249>)
3. A.A. Mohamed, Y. Luo, H. Peng, R. C. Jankowitz, S. Wu, *J. Digit. Imag.* **31** (2018) 387 (<https://dx.doi.org/10.1007/s10278-017-0022-2>)
4. H. Pu, J. Peng, F. Xu, N. Liu, F. Wang, X. Huang, Y. Jia, *Clin. Breast. Cancer.* **20** (2020) 317 (<https://dx.doi.org/10.1016/j.clbc.2020.02.009>)
5. N. Houssami, D. Bernardi, F. Caumo, S. Brunelli, C. Fantò, M. Valentini, G. Romanucci, M. A. Gentilini, M. P. Macaskill, *Breast* **38** (2018) 150 (<https://dx.doi.org/10.1016/j.breast.2018.01.002>)
6. R. R. Winkel, M. Euler-Chelpin, E. Lynge, P. Diao, M. Lillholm, M. Kallenberg, J. L. Forman, M. B. Nielsen, W. Y. Uldall, M. Nielsen, I. Vejborg, *Cancer. Epidemiol.* **49** (2017) 53 (<https://dx.doi.org/10.1016/j.canep.2017.05.006>)
7. A. A. Mohamed, W. A. Berg, H. Peng, Y. Luo, R. C. Jankowitz, S. Wu, *Med. Phys.* **45** (2018) 314 (<https://dx.doi.org/10.1002/mp.12683>)
8. M. Wang, X. He, Y. Chang, G. Sun, L. Thabane, *Breast* **31** (2017) 157 (<https://dx.doi.org/10.1016/j.breast.2016.11.009>)

9. M. Von Euler-Chelpin, M. Lillholm, I. Vejborg, M. Nielsen, E. Lynge, *Breast. Cancer. Res.* **21** (2019) 111 (<https://dx.doi.org/10.1186/s13058-019-1203-3>)
10. S. D. Raj, V. Fein-Zachary, P. J. Slanetz, *Semin. Ultrasound CT. MR.* **39** (2018) 16 (<https://dx.doi.org/10.1053/j.sult.2017.08.001>)
11. M. Sirous, S. P. Shahnani, A. Sirous, *Adv. Biomed. Res.* **7** (2018) 56 (https://dx.doi.org/10.4103%2Fabr.abr_161_17)
12. A. Gastouniotti, E. F. Conant, D. Kontos, *Breast. Cancer. Res.* **18** (2016) 91 (<https://dx.doi.org/10.1186/s13058-016-0755-8>)
13. E. Łukasiewicz, A. Ziemiecka, W. Jakubowski, J. Vojinovic, M. Bogucevska. *J. Ultrason.* **17** (2017) 267 (<https://dx.doi.org/10.15557/jou.2017.0039>)
14. I. Chakrabarti, *J. Cytol.* **35** (2018) 176 (https://dx.doi.org/10.4103%2FJOC.JOC_35_18)
15. C. E. Edmonds, L. R. Lamb, S. F. Mercaldo, D. A. Sippo, K. S. Burk, C. D. Lehman, *Am. J. Roentgenol.* **214** (2020) 240 (<https://dx.doi.org/10.2214/AJR.19.21778>)
16. S. Kulkarni, S. Murchite, A. Patil, *J. Surg. Res.* **5** (2022) 221 (<https://dx.doi.org/10.26502/jsr.10020215>)
17. J. C. Litherland, *Clin. Radiol.* **57** (2002) 81 (<https://dx.doi.org/10.1053/crad.2001.0875>)
18. C. A. Pistolese, D. Tosti, D. Citraro, F. Ricci, C. Di Stefano, F. Lamacchia, D. Ferrari, R. Floris, *Ultrason Med Biol.* **45** (2019) 78 (<https://dx.doi.org/10.1016/j.ultrasmedbio.2018.09.004>)
19. W. A. Berg, *J. Breast Imag.* **3** (2021) 527 (<https://dx.doi.org/10.1093/jbi/wbab060>)
20. A. Hamidinekoo, E. Denton, A. Rampun, K. Honnor, R. Zwigelaar, *Med. Imag. Anal.* **47** (2018) 45 (<https://dx.doi.org/10.1016/j.media.2018.03.006>)
21. G. Aresta, T. Araujo, S. Kwok, S. S. Chennamsetty, M. Safwan, V. Alex, *Med. Imag. Anal.* **56** (2019) 122 (<https://dx.doi.org/10.1016/j.media.2019.05.010>).



J. Serb. Chem. Soc. 89 (5) 667–678 (2024)
JSCS–5747

The influence of the coprecipitation synthesis methods on photodegradation efficiency of ZnFe based photocatalysts

DURĐICA M. KARANOVIĆ^{1*}, MILICA S. HADNAĐEV-KOŠTIĆ¹, TATJANA J. VULIĆ¹, MARIJA M. MILANOVIĆ¹, VLADANA N. RAJAKOVIĆ-OGNJANOVIĆ² and RADMILA P. MARINKOVIĆ-NEDUČIN^{1#}

¹Faculty of Technology Novi Sad, University of Novi Sad, Bulevar Cara Lazara 1, 21000 Novi Sad, Serbia and ²Faculty of Civil Engineering, University of Belgrade, Bulevar Kralja Aleksandra 73, 11000 Beograd, Serbia

(Received 6 November, revised 15 November 2023, accepted 22 January 2024)

Abstract: Organic dye pollutants that are progressively used in modern chemical industries, emerged as a major source of water contamination. A promising eco-friendly and simple approach to water purification is the heterogeneous photocatalytic process that uses various metal oxide semiconductors in the presence of light, initiating the oxidation-reduction reactions resulting in dye degradation. The aim of this study was to investigate the influence of coprecipitation synthesis methods on photodegradation efficiency. The ZnFe based photocatalysts were synthesized using two different methods: low (LS) supersaturation and high (HS) supersaturation coprecipitation and thermally activated at 100, 300, 500 and 700 °C. Structural and textural characterisation were carried out and their efficiency in methylene blue photodegradation test reaction was studied. LS samples treated at 100 and 300 °C exhibited very low photodegradation efficiency (less than 10 %) when compared to HS samples treated at the same temperatures (75 and 85 %). The efficiency of LS 500 and LS 700 samples improved (67 and 75 %) with the increase in thermal treatment temperature and the photodegradation efficiency difference between LS and HS samples decreased. Such behaviour of LS and HS samples could be explained by structural and textural properties that originated from different synthesis methods.

Keywords: mixed metal oxides; photocatalysis; methylene blue.

INTRODUCTION

Rapid industrial growth over past few decades had immense negative influence on water eco-systems due to the presence of organic and inorganic con-

* Corresponding author. E-mail: djurdjicakaranovic@uns.ac.rs

Serbian Chemical Society member.

<https://doi.org/10.2298/JSC231106005K>



taminants such as synthetic dyes,^{1,2} antibiotics,³ pesticides,⁴ *etc.* These micro-contaminants raised concerns due to their excessive use in various industries and their discharge to aquatic environment. Organic and inorganic dyes have the ability to persist in the water environment for a significant amount of time, because of their stability. Textile industry was reported to lose up to 200,000 tons of dyes to effluents due to inefficiency of the dyeing process.⁵ Methylene blue (MB) is one of the organic dyes commonly used in industry and its presence in aquatic environment proved to be toxic.^{6,7} Methods of purification of wastewater before its discharge in environment have been researched over the past few decades, and some of them include adsorption, membrane filtration, oxidation, bioremediation, ion-exchange and heterogenous photocatalysis.^{8,9} The main disadvantage of many methods for water purification is the lack of capability to completely degrade hazardous pollutants.¹⁰ Photocatalytic purification of wastewater using semiconductive oxides, such as TiO₂, ZnO and Fe₂O₃, received substantial attention since it could use free and sustainable solar energy, it is simple, rapid, environmentally friendly and leads to complete degradation of organic and inorganic contaminants.^{11–14} The possible additional application of these photocatalytic materials could be in the infrastructure design introducing added-value to porous pavements for managing pluvial floods resulting in the reduction of water pollution.¹⁵ Layered double hydroxides (LDHs) are described as anionic clays with layered structure, with metal cations uniformly distributed in the hydroxide layers. Their versatility brought about significant attention in the field of photocatalytic degradation of dyes. Upon thermal treatment of LDHs, their layered structure collapses, hydroxyls and interlayer water transition to gaseous phase, triggering the formation of mixed metal oxides.¹⁶ The use of mixed metal oxides in photocatalytic purification of wastewater became very popular field of research, due to their reported ability to degrade various dyes,¹⁷ pesticides,¹⁸ antibiotics.³ Mixed metal oxides are promising for the application in photocatalytic treatment of wastewater because of their favourable properties, such as strong oxidation ability, good photocatalytic properties and coupling with semiconductors.¹⁹ For example, zinc oxide exhibited favourable photocatalytic properties, such as high stability, non-toxicity and, due to its large band gap of 3.37 eV, possible coupling with semiconductors with narrow energy band gap in order to ameliorate its photocatalytic performance.^{20,21} ZnO could also be used as antibacterial agent, since it has been reported to have antibacterial influence on both Gram-positive and Gram-negative bacteria.²² Furthermore, iron and its oxides are suitable for the photocatalytic application because of their stability, non-toxicity, magnetic and optical properties, abundance and low cost.²³ ZnFe mixed metal oxides obtained by thermal degradation of LDHs received much attention due to the possibility to tailor their functional properties during the synthesis

procedure resulting in the formation of nonstoichiometric mixed oxides with different additional phases, favourable for photocatalytic application.¹⁶

Various synthesis methods have been researched, including coprecipitation, sol–gel, hydrothermal, layer deposition and calcination of metal hydroxide precursor.^{2,24,26} The coprecipitation synthesis method was selected taking into consideration that the synthesis path should be simple, cost-effective and environmentally friendly. The motivation behind this study was to apply a simple synthesis route that will enable the formation of photocatalysts with suitable properties for efficient photocatalytic application. Taking all of the above into account, the influence of synthesis method and thermal treatment on structural, textural and photocatalytic properties of obtained ZnFe photocatalysts was studied.

EXPERIMENTAL

Preparation of photocatalysts

Photocatalysts were synthesized using two synthesis methods: low supersaturation coprecipitation (LS) method at constant pH and high supersaturation (HS) coprecipitation method. For both synthesis methods the same base solution (0.67 M Na_2CO_3 ; 2.25 M NaOH) and metal precursors were used: $(\text{Fe}(\text{NO}_3)_3 \cdot 9\text{H}_2\text{O})$ and $\text{Zn}(\text{NO}_3)_2 \cdot 6\text{H}_2\text{O}$ dissolved in 1 M solution containing 30 mol % of Fe and 70 mol % of Zn. In the LS method, the precursor solutions and the base solution were continuously added ($4 \text{ cm}^3 \text{ min}^{-1}$) at constant temperature (40°C) maintaining the constant pH of 9.4 in the reaction mixture (Fig. 1a). In the HS method (Fig. 1b), the precursor solutions were quickly added to the base solution and vigorously stirred at constant temperature (40°C). The precipitation products obtained from both synthesis methods were aged (12 h), washed with distilled water until pH 7, dried (24 h; 100°C) and thermally treated at different temperatures ($300, 500, 700^\circ\text{C}$) for 5 h in air. The synthesized samples were denoted as follows: ZnFe LS 100, ZnFe LS 300, ZnFe LS 500, ZnFe LS 700, ZnFe HS 100, ZnFe HS 300, ZnFe HS 500, ZnFe HS 700.

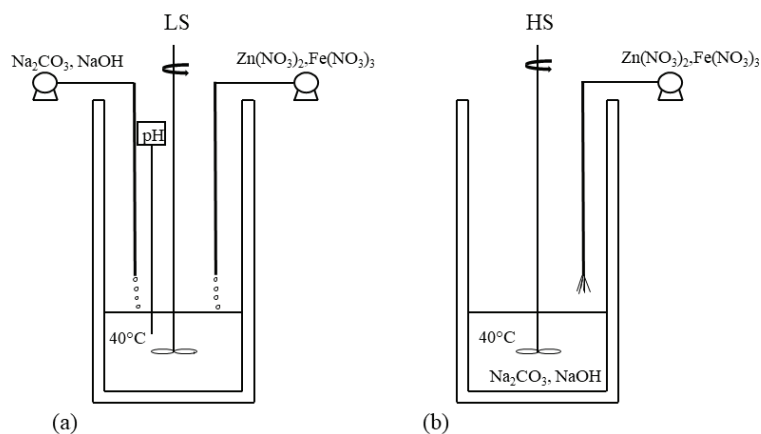


Fig. 1. Schemes of experimental set-ups for: a) LS and b) HS synthesis method.

Characterization of photocatalysts

X-ray powder diffraction (XRD) was used for the identification of crystalline phases. XRD analysis was conducted with Rigaku MiniFlex 600 with Cu-K α radiation ($\lambda = 0.15406$ nm; 2θ range from 10 to 70°; scan rate = 0.02 s⁻¹). The crystallite size was calculated using the Scherrer formula:

$$D = k \frac{\lambda}{\beta \cos \theta} \quad (1)$$

where D , nm, is the crystallite size, k is the shape function (0.9), λ , nm, is X-ray wavelength, θ is angle of diffraction and β full width at half maximum of the most intense peak.

Textural analysis was performed by low temperature nitrogen adsorption at -196 °C (Microtrac Belsorp Max II). The surface area was calculated using the Brunauer–Emmer–Teller (BET) method. The pore size distribution and the cumulative pore volume were determined by Brunauer–Joyner–Hallenda (BJH) method applied to the desorption branch of the isotherm. The external surface area, which represented the mesopore surface area without micropores, was calculated using the t -plot method.

Photodegradation experiments

Photocatalytic tests were performed in an open cylindrical Pyrex vessel. Prior to the irradiation, all of the mixtures (100 ml of MB solution and 50 mg of photocatalyst) were stirred in the dark. The MB concentration was measured at defined time intervals using the UV–Vis spectrophotometer (Cecil2000) at maximum absorption length of 664 nm. The adsorption/desorption equilibrium was reached after 30 min. These tests were performed in order to ensure that photocatalytic efficiency of investigated samples was solely attributed to the photocatalytic reaction.

When the equilibrium was established, reaction mixtures were irradiated by the light source (Osram Ultra Vitalux 300 W lamp with the emission spectrum that simulates the solar light placed 45 cm above the top surface of MB solution) and aliquots were analysed at defined time intervals. The decrease in MB concentration was used to calculate the efficiency of MB photodegradation:^{27,28}

$$E_{\text{eff}} = 100 \frac{c_0 - c}{c} \quad (2)$$

E_{eff} , %, is the photodegradation efficiency, c_0 , mg dm⁻³, and c , mg dm⁻³, are the initial and measured MB concentration.

Kinetics of the photocatalytic reaction

The kinetics of MB photodegradation reaction were evaluated using the pseudo-first-order reaction that follows the Langmuir–Hinshelwood kinetic model:²⁹

$$\ln \left(\frac{c_0}{c_t} \right) = k_{\text{app}} t \quad (1)$$

The MB concentration at defined time t was denoted as c_t and k_{app} is the apparent first order reaction rate constant, obtained from the slope of linear function $\ln(c_0/c_t)$ vs. time.

The half-time of the reaction, $t_{1/2}$, was calculated as follows:

$$t_{1/2} = \frac{\ln 2}{k_{\text{app}}} \quad (4)$$

RESULTS AND DISCUSSION

Structural characterization

XRD diffraction peaks of all synthesized and thermally treated photocatalysts, presented in Fig. 2, can be correlated with the series of Bragg reflections corresponding to the standard JCPDS. XRD patterns of ZnFe LS 100 in Fig. 2a exhibited low intensity broad peaks characteristic for the layered structure (2θ values of 13.18, 23.97, 32.72 and 59.27°) which correspond to (003), (006), (009) and (110) planes,³⁰ with additional low intensity broad peaks (32.6 and 36.2°) that could be attributed to the ZnO phase. XRD analysis of the dried sample obtained by the HS method (ZnFe HS 100) revealed the presence of sharp, intense peaks of dominant (31.8, 34.4, 47.5, 56.6, 62.8°) zincite ZnO phase. Considering that the dominant phase of LS sample was typical for the layered structure, it can be concluded that the LS synthesis method triggered the formation of ZnFe layered double hydroxide, whereas the HS method led to formation of non-stoichiometric mixed metal oxides.

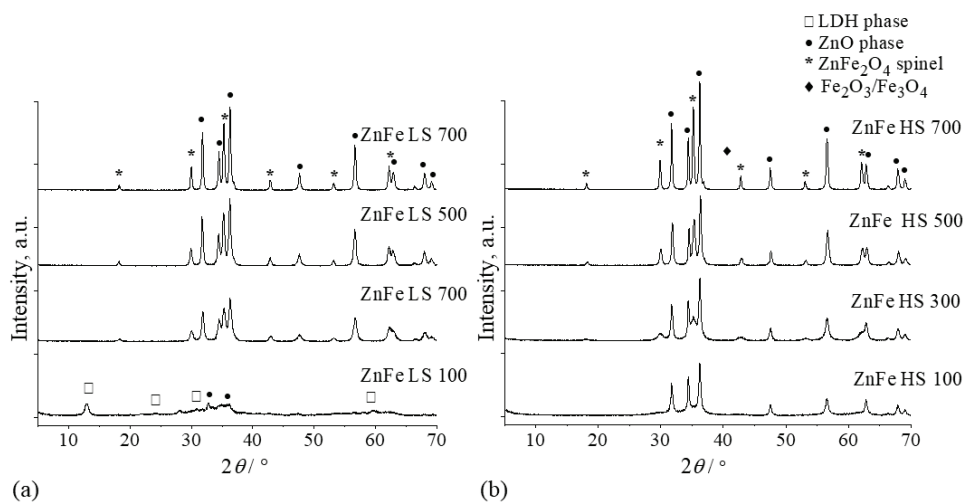


Fig. 2. XRD pattern of photocatalysts: a) LS samples and b) HS samples.

After thermal treatment of LS samples at temperatures above 300 °C (ZnFe LS 300), the layered structure collapsed and intense, sharp peaks were detected corresponding to the zincite ZnO phase (JCPDS File no. 79-2205). Additionally, new, lower intensity peaks (30, 35.4, 42.8 and 52.9°) were detected in both LS and HS samples treated at 300 °C that confirmed the formation of ZnFe₂O₄ spinel phase (JCPDS file no. 89-1012). For samples obtained by both LS and HS method the increase in thermal treatment temperature (500 and 700 °C) intensified the crystallisation of the phases detected by the presence of sharp, more

intense and distinctive peaks of both, dominant zincite ZnO phase and additional ZnFe₂O₄ spinel phase. Additionally, in both LS and HS samples thermally treated at 700 °C the appearance of low-intensity peak was detected at 2θ value of around 37° that could be correlated to the Fe₂O₃ or Fe₃O₄ phase (JCPDS file no. 87-2334).^{31,32} The crystallite size calculated for the dominant phase (Table I), also confirmed the increase of crystallite size with the rise of thermal treatment temperature, considering that the temperature increase generally results in the grain growth and consequently in greater crystallite size.^{16,31,32} When compared with the HS samples, LS samples exhibited similar crystal structure at higher temperatures with lower peak intensities, indicating lower crystallinity of LS samples. The XRD analysis results showed significant influence of synthesis method on the crystal structure of studied samples.

TABLE I. Structural and textural parameters of analysed samples

Sample	D / nm	$S / \text{m}^2 \text{g}^{-1}$	d_p / nm	$V_p / \text{cm}^3 \text{g}^{-1}$	$S_{tp} / \text{m}^2 \text{g}^{-1}$
ZnFe LS 100	9.6	82	14.9	0.36	80.8
ZnFe LS 300	15.8	28.5	46.9	0.32	28
ZnFe LS 500	22.6	27	40.5	0.26	25.4
ZnFe LS 700	28.1	12.6	80.7	0.22	12.6
ZnFe HS 100	20.7	147	4.8	0.16	145.1
ZnFe HS 300	22.4	108	5.1	0.17	107.4
ZnFe HS 500	25.5	16.3	22.7	0.11	16
ZnFe HS 700	33.7	7.8	39.22	0.08	7.5

Textural characterization

The results of textural analysis are given in Fig. 3 and Table I. The adsorption isotherms and pore size distribution of all studied samples are presented in Fig. 3. BET surface area, S , average pore diameter, d_p , pore volume, V_p , and external surface area obtained from t -plot method, S_{tp} , are given in Table I. The isotherms of LS samples (Fig. 3a) corresponded to type II isotherm from IUPAC classification. This type of isotherm is characteristic for non-porous or macroporous adsorbents and it represented unrestricted monolayer/multilayer adsorption. Type IV isotherms correspond to HS samples (Fig. 3b) and are characterized by the finite multi-layer formation that corresponds to complete filling of capillaries in an adsorbent. The mesoporous isotherms should be classified in more details if the hysteresis loop (where adsorption and desorption curves do not overlay) is present. LS samples exhibited H3 hysteresis loop type, indicating that LS samples had mesoporous structure with wedge shaped pores formed by the loose stacking of flaky particles.³³ Whereas for HS samples, hysteresis loops correspond to combination of H1/H3 types formed at relative pressure range of 0.4–1, concluding that present mesopores have non uniform shape.³¹

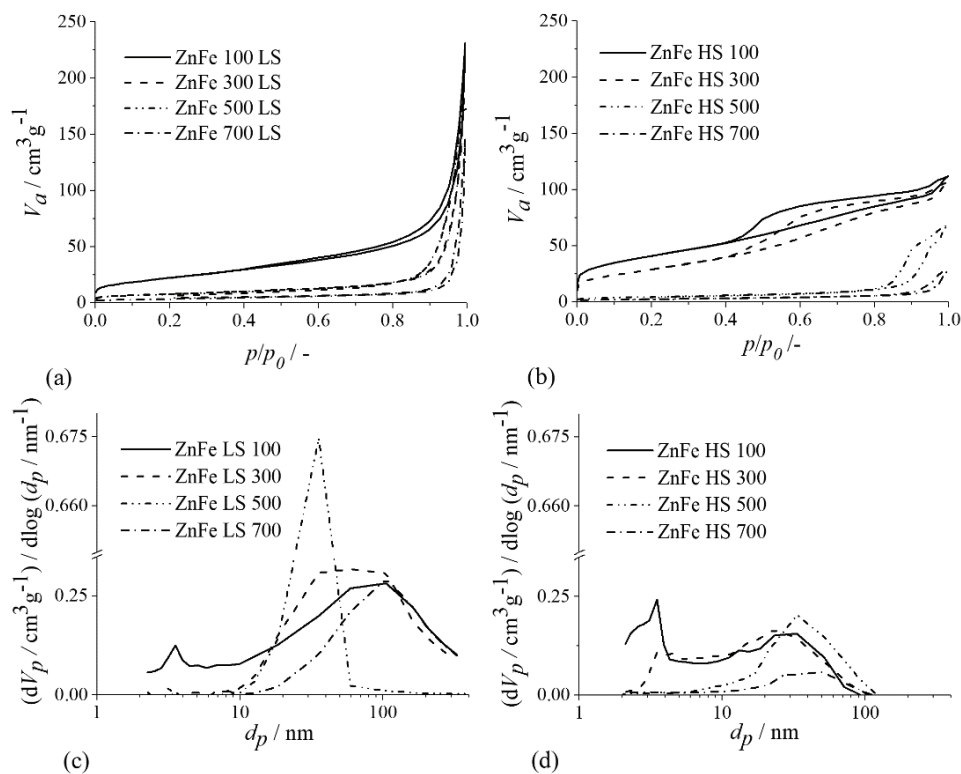


Fig. 3. Textural analysis results: a) adsorption isotherms for LS samples; b) adsorption isotherms for HS samples; c) pore size distribution for LS samples; d) pore size distribution for HS samples.

From Fig. 3c it was observed that the ZnFe LS 100 sample had a developed pore size distribution with an intense peak at around 3 nm that is in good agreement with the detected high surface area (Table I) and a wide peak at higher values of pore diameters (40–110 nm). ZnFe LS 300 sample exhibited a broad peak in the region of pore diameters from 30 to 100 nm. Upon the thermal treatment at 500 °C, sample ZnFe LS 500 showed monomodal pore size distribution with one intense peak at around 35 nm, whereas the sharp peak at 3 nm completely disappeared, which is in correlation with smaller measured pore volume.³¹ The pore size distribution of sample ZnFe LS 700 shifted towards higher pore diameter values (> 50 nm), also in correlation to the significantly low surface area (Table I).

The pore size distribution of HS samples (Fig. 3d) was similar to LS samples, with a larger amount of smaller mesopores resulting in the much larger surface area. With the increase in the temperature of the HS sample thermal treatment, the presence of both, smaller and larger mesopores decreased, especially

for the samples treated at 500 and 700 °C BET surface area of LS samples treated at lower temperatures (100 and 300 °C), when compared to the corresponding HS samples, was significantly lower since it originated from the presence of mainly larger pores in those samples.¹³ Pore size distribution and its change with temperature indicated that the increase in thermal treatment temperature shifted the pore size distribution towards higher values of pore diameters, which is in good correlation with measured parameters (a decrease in pore volume and BET surface area and an increase in average pore diameter).

The results obtained from textural analysis were also analysed by *t*-plot method.³⁴ The calculated external surface area is in good agreement with the calculated BET surface area, since it represented the surface area only from mesopores. These results confirmed that there were no micropores present in any of the samples.

Photodegradation of methylene blue

The results of the MB photodegradation (Fig. 4) showed that all the HS samples have significant photodegradation efficiency higher than the corresponding LS samples. Besides that, the LS samples treated at lower temperatures (100 and 300 °C) had very low efficiency (< 10 %). The results also indicate that the increase in thermal treatment temperature increased the photodegradation efficiency for samples obtained by both coprecipitation methods. Photocatalytic behaviour could be explained by the presence of photocatalytic active phases. All HS samples have photocatalytic active ZnO phase, whereas the samples treated at higher temperatures (ZnFe HS 300, ZnFe HS 500 and ZnFe HS 700) also have an additional ZnFe₂O₄ phase. The coupling of ZnO and ZnFe₂O₄ phases with energy bands from 2.1 to 2.3 eV, enhanced the MB photodegradation in the solar light spectrum.³¹ Lower photodegradation efficiency of LS samples could be

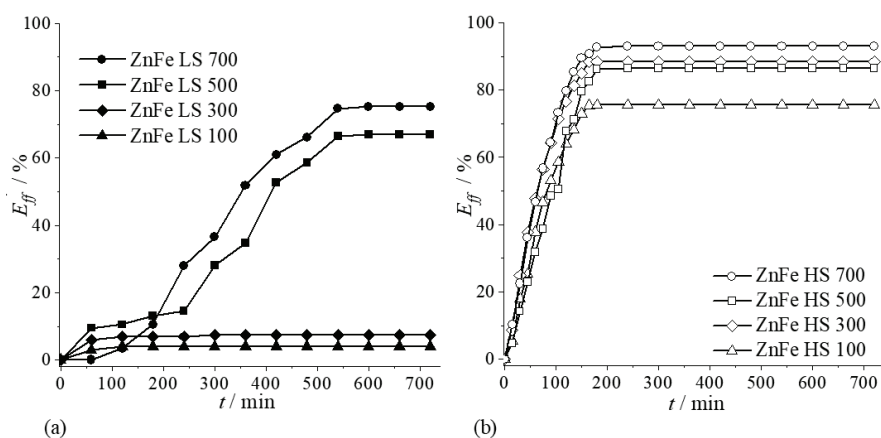


Fig. 4. Photodegradation efficiency of: a) LS photocatalysts and b) HS photocatalysts.

attributed to the lower presence and lower crystallinity of active phases, when compared to the corresponding HS samples, especially for the ZnFe LS 100 sample being the only sample with the LDH phase and the lowest amount of ZnO phase. Higher photodegradation efficiency (67 and 75 %) was observed for LS samples thermally treated at 500 and 700 °C probably due to the higher amount of ZnFe₂O₄ spinel phase. The enhanced photodegradation efficiency of ZnFe HS 700 (96 %), when compared to the corresponding LS sample, could be assigned to the higher amount of photocatalytic active ZnO, ZnFe₂O₄ phase and Fe₂O₃ phase which could allow easier transport of photo-induced electrons from ZnFe₂O₄.¹⁴ It could be concluded that the favourable textural properties without the presence of adequate active phases did not have great impact on the photocatalytic behaviour.

Kinetics of photocatalytic reaction

The results of the kinetic study indicated that the experimental data obtained from MB photodegradation experiments were best fitted with the linear fit and followed the pseudo-first-order reaction model. The correlation coefficient was proposed as the best criteria for selection of kinetic model. The calculated values of the rate constant (Table II), as well as the half time of the reaction, for HS samples treated at 500 and 700 were approximately 5 times higher than rate constant values for LS samples treated at same temperatures, which confirmed that ZnFe HS 500 and 700 samples participated in faster reactions. The obtained results from the kinetic study showed that MB photodegradation followed Langmuir–Hinshelwood kinetic model, since photodegradation reactions with single substrate usually follow this model.³⁵

TABLE II. Kinetic parameters of analysed samples

Sample	$k_{app} / \text{min}^{-1}$	$t_{1/2} / \text{min}$	R^2	Sample	$k_{app} / \text{min}^{-1}$	$t_{1/2} / \text{min}$	R^2
ZnFe LS 100	–	–	–	ZnFe HS 100	0.0084	82.5	1
ZnFe LS 300	–	–	–	ZnFe HS 300	0.0120	57.8	1
ZnFe LS 500	0.0022	315.1	0.96	ZnFe HS 500	0.0094	73.7	0.97
ZnFe LS 700	0.0017	407.7	0.95	ZnFe HS 700	0.0136	51.0	1

Since Langmuir–Hinshelwood kinetic model can be used under the following assumptions: *i*) limited amount of adsorption sites on photocatalyst surface, *ii*) monolayer coverage, *iii*) reversible adsorption reaction and *iv*) homogenous surface of photocatalysts; it could be concluded that the nature of active sites and their distribution had great influence on the rate of photocatalytic reaction and the rate of the entire process depended on the reaction carried out on the surface active sites.²⁹

CONCLUSION

The mixed metal oxides obtained by low and high supersaturation co-precipitation methods were analysed and their efficiency was evaluated in MB photodegradation reaction. Both HS and LS samples exhibited desirable photocatalytic properties when thermally treated at higher temperatures due to the favourable structural and textural properties. It could be concluded that the photocatalytic active phases and the high crystallinity detected by XRD were responsible for good photocatalytic behaviour of HS samples. Furthermore, it could be concluded that the favourable textural properties without the presence of the adequate active phases did not have great impact on the photocatalytic behaviour. The study revealed that the HS sample treated at 700 °C had the highest efficiency in MB removal, probably due to the largest amount of active phases (ZnO, ZnFe₂O₄ and Fe₂O₃/Fe₃O₄). The reaction kinetics corresponded to the Langmuir–Hinshelwood pseudo-first order model. This study demonstrated that the synthesis path had a significant influence on the photocatalytic active phase formation and consequently on the MB photodegradation efficiency.

Acknowledgement. This research was supported by the Science Fund of the Republic of Serbia, Grant No. 7737365, Zero-Waste Concept for Flood Resilient Cities – Ø-Waste-Water and by the Ministry of Science, Technological Development and Innovation of the Republic of Serbia (Grant No. 451-03-47/2023-01/ 200134).

ИЗВОД

УТИЦАЈ КОПРЕЦИПИТАЦИОНЕ МЕТОДЕ СИНТЕЗЕ НА ЕФИКАСНОСТ
ФОТОКАТАЛИЗАТОРА НА БАЗИ ZnFe

ЂУРЂИЦА М. КАРАНОВИЋ¹, МИЛИЦА С. ХАДНАЂЕВ-КОСТИЋ¹, ТАТЈАНА Ј. ВУЛИЋ¹, МАРИЈА М. МИЛАНОВИЋ¹, ВЛАДАНА Н. РАЈАКОВИЋ-ОГЊАНОВИЋ² и РАДМИЛА П. МАРИНКОВИЋ-НЕДУЧИН³

¹Технолошки факултет Нови Сад, Универзитет у Новом Саду, Булевар цара Лазара 1, 21000 Нови Сад, ²Грађевински факултет, Универзитет у Београду, Булевар Краља Александра 73, Београд и ³Универзитет у Новом Саду, Др Зорана Ђинђића 1, 21000 Нови Сад

Органски полутанти, попут боја, су веома заступљени у савременој хемијској индустрији, због чега су постали велик извор загађења. Хетерогена фотокатализа представља једноставан и еколошки повољан процес пречишћавања отпадних вода. Као фотокатализатори користе се различити полупроводници у виду металних оксида који у присуству светлости разграђују полутанте низом оксидо-редукционих реакција. Циљ овог истраживања је испитивање утицаја копреципитационе методе на ефикасност фоторазградње. Фотокатализатори на бази ZnFe су синтетисани користећи две копреципитационе методе: методу малог (LS) и великог (HS) презасићења и термички активирани на температурама од 100, 300, 500 and 700 °C. Анализиране су њихове структурне и текстуралне особине, као и ефикасност фотокаталитичке разградње метиленског плавог. LS узорци термички третирани на 100 и 300 °C су показали веома малу ефикасност разградње боје (< 10 %) у поређењу са HS узорцима третираним на истим температурама (75 и 85 %). Са порастом температуре термичке активације повећала се ефикасност LS 500 и LS 700 узорка (67 и 75 %), а разлика у ефикасности LS и HS узорка се смањила.

Овакво понашање LS и HS узорака се може објаснити разликама у текстуалним и структурним особинама које потичу од различитих метода синтезе.

(Примљено 6. новембра, ревидирано 15. новембра 2023, прихваћено 22. јануара 2024)

REFERENCES

1. L. Mohapatra, K. M. Parida, *Sep. Purif. Technol.* **91** (2012) 73 (<https://doi.org/10.1016/j.seppur.2011.10.028>)
2. Z. Meng, M. Wu, Y. Yu, F. Meng, A. Liu, S. Komarneni, Q. Zhang, *Appl. Clay Sci.* **161** (2018) 1 (<https://doi.org/10.1016/j.clay.2018.04.008>)
3. R. Langbehn, C. Michels, H. Moreira Soares, *Environ. Pollut.* **275** (2021) 116603 (<https://doi.org/10.1016/j.envpol.2021.116603>)
4. I. A. Saleh, N. Zouari, M. A. Al-Ghouti, *Environ. Technol. Innov.* **19** (2020) 101026 (<https://doi.org/10.1016/j.eti.2020.101026>)
5. C. J. Ogugbue, T. Sawidis, *Biotechnol. Res. Int.* **2011** (2011) 967925 (<https://doi.org/10.4061/2011/967925>)
6. C. Srinivas, C. Nagamani, M. Gangadhar, M. Raja Sekhar, *Asian J. Chem.* **22** (2010) 5045 (https://asianjournalofchemistry.co.in/user/journal/viewarticle.aspx?ArticleID=22_7_11)
7. S. Pandey, J. Y. Do, J. Kim, M. Kang, *Int. J. Biol. Macromol.* **143** (2020) 60 (<https://doi.org/10.1016/j.ijbiomac.2019.12.002>)
8. M. Hadnadjev-Kostic, T. Vulic, Dj. Karanovic, M. Milanovic, *J. Serb. Chem. Soc.* **87** (2022) 1011 (<https://doi.org/10.2298/JSC220228034H>)
9. B. G. Ankamwar, V. B. Kamble, J. I. Annsi, L. S. Sarma, C. M. Mahajan, *J. Nanosci. Nanotechnol.* **17** (2017) 1185 (<https://doi.org/10.1166/jnn.2017.12579>)
10. G. Zhao, L. Liu, C. Li, T. Zhang, T. Yan, J. Yu, X. Jiang, F. Jiao, *J. Photochem. Photobiol., A* **367** (2018) 302 (<https://doi.org/10.1016/j.jphotochem.2018.08.048>)
11. K. Abderrazek, F.S. Najoua, E. Srasra, *Appl. Clay Sci.* **119** (2016) 229 (<https://doi.org/10.1016/j.clay.2015.10.014>)
12. I. Ahmad, S.B. Khan, T. Kamal, A.M. Asiri, *J. Mol. Liq* **229** (2017) 429 (<https://doi.org/10.1016/j.molliq.2016.12.061>)
13. M. Hadnadjev-Kostic, T. Vulic, R. Marinkovic-Neducin, D. Lončarević, J. Dostanić, S. Markov, D. Jovanović, *J. Clean Prod.* **164** (2017) 1 (<https://doi.org/10.1016/j.jclepro.2017.06.091>)
14. S. Sun, X. Yang, Y. Zhang, F. Zhang, J. Ding, J. Bao, C. Gao, *Prog. Nat. Sci. Mater.* **22** (2012) 639 (<http://dx.doi.org/10.1016/j.pnsc.2012.11.008>)
15. O. Govedarica, M. Aškrabic, M. Hadnadev-Kostic, T. Vulic, B. Lekic, V. Rajakovic-Ognjanovic, D. Zakic, *Materials* **15** (2022) 4919 (<https://doi.org/10.3390/ma15144919>)
16. B. Kim, D. Lee, G. Gwak, Y. Han, J. Oh, *J. Solid State Chem.* **269** (2019) 454 (<https://doi.org/10.1016/j.jssc.2018.10.013>)
17. M. Sánchez-Cantú, M.E. Hernández-Torres, A. Castillo-Navarro, E. Cadena-Torres, E. Rubio-Rosas, E., Gracia-Jiménez, J.M., Tzompantzi, F., *Appl. Clay Sci.* **135** (2017) 1 (<https://doi.org/10.1016/j.clay.2016.08.028>)
18. E.S. da Silva, V. Prevot, C. Forano, P. Wong-Wah-Chung, H.D. Burrows, M. Sarakha, *Environ. Sci. Pollut. Res.* **21** (2014) 11218 (<https://doi.org/10.1007/s11356-014-2971-z>)
19. S. B. Jaffri, K. S. Ahmad, *Green Process Synth.* **8** (2019) 172 (<https://doi.org/10.1515/gps-2018-0058>)

20. J. Gajendiran, V. Rajendran, *Mater. Lett.* **116** (2014) 311 (<https://doi.org/10.1016/j.matlet.2013.11.063>)
21. C. Han, M.Q. Yang, B. Weng, Y. Xu, *Phys. Chem. Chem. Phys.* **16** (2014) 16891 (<https://doi.org/10.1039/c4cp02189d>)
22. A. E. A. Yagoub, G. M. Al-Shammari, L. N. Al-Harbi, P. Subash-Babu, R. Elsayim, M. A. Mohammed, M. A. Yahya, *Appl. Sci.* **12** (2022) 11613 (<https://doi.org/10.3390/app122211613>)
23. M. Afkari, S. M. Masoudpanah, M. Hasheminasari, S. Alamolhoda, *Sci. Rep.* **13** (2023) 6203 (<https://doi.org/10.1038/s41598-023-33338-1>)
24. M. T. Uddin, Y. Nicolas, C. Olivier, T. Toupance, L. Servant, M. M. Müller, H. J. Kleebe, J. Ziegler, W. Jaegermann, *Inorg. Chem.* **51** (2012) 7764 (<https://doi.org/10.1021/ic300794j>)
25. A. M. Tripathi, R. G. Nair, S. K. Samdarshi, *Sol. Energy Mater. Sol. Cells* **94** (2010) 2379 (<https://doi.org/10.1016/j.solmat.2010.08.022>)
26. Y. Shen, T. R. B. Foong, X. Hu, *Appl. Catal., A* **409–410** (2011) 87 (<https://doi.org/10.1016/j.apcata.2011.09.033>)
27. S. Kurajica, I. Minga, R. Blazic, K. Muzina, P. Tominac, *Athens J. Sci.* **5** (2018) 7 (<https://doi.org/10.30958/ajs.5-1-1>)
28. I. Raheb, M. S. Manlla, *Heliyon* **7** (2021) (<https://doi.org/10.1016/j.heliyon.2021.e07427>)
29. M. Hadnadjev-Kostic, T. Vulic, R. Marinkovic-Neducin, *Adv. Powder Technol.* **25** (2014) 1624 (<https://doi.org/10.1016/j.apt.2014.05.015>)
30. D. Moustafa, R. Mahmoud, H. M. A. El Salam, N. Shehata, *Appl. Nanosci.* **11** (2021) 709 (<https://doi.org/10.1007/s13204-020-01632-3>)
31. M. Hadnadjev-Kostic, Dj. Karanovic, T. Vulic, J. Dostanić, D. Lončarević, *Green Process. Synth.* **12** (2023) 20228153 (<https://doi.org/10.1515/gps-2022-8153>)
32. X. Liu, F. Zhu, W. Wang, J. Lei, G. Yin, *Int. J. Electrochem. Sci.* **11** (2016) 9696 (<https://doi.org/10.20964/2016.11.62>)
33. Z. Wang, X. Jiang, M. Pan, Y. Shi, *Minerals* **10** (2020) 377 (<https://doi.org/10.3390/min10040377>)
34. A. Galarnau, F. Villemot, J. Rodriguez, F. Fajula, B. Coasne, *Langmuir* **30** (2014) 13266 (<https://doi.org/10.1021/la5026679>)
35. L. el Mersly, E. M. el Mouchtari, E. M. Moujahid, C. Forano, M. el Haddad, S. Briche, A. Alaoui Tahiri, S. Rafqah, *J. Sci-Adv. Mater. Dev.* **6** (2021) 118 (<https://doi.org/10.1016/j.jsamd.2020.08.002>).



J. Serb. Chem. Soc. 89 (5) 679–692 (2024)
JSCS–5748

Influence of the elasticity variation of the 3D printed PMMA structure on the axial tooth vibration

LIVIJA CVETICANIN^{1,2*}, MILJANA PRICA¹ and SANJA VUJKOV³

¹University of Novi Sad, Faculty of Technical Sciences, Novi Sad, Serbia, ²Obuda University, Budapest, Hungary and ³University of Novi Sad, Faculty of Medicine, Department of Dentistry, Novi Sad, Serbia

(Received 18 January, revised 15 February, accepted 7 March 2024)

Abstract: Recently, 3D printing with poly methyl methacrylate (PMMA) has been widely used in dentistry: 3D printing is a suitable method for producing any complex three-dimensional shape, and PMMA is a material that has suitable properties in the oral cavity environment. That is why 3D printing is very often used to make PMMA teeth. There is the impact between teeth during chewing that causes shape variation and tooth vibration. As cyclic vibrations adversely affect the durability of PMMA teeth, they must be eliminated. The object of this work is to study the axial vibrations of a 3D printed tooth, as well as to give recommendations for modifying the PMMA structure with the aim of vibration damping. Tooth vibration is mathematically modeled and analytically solved. The obtained result provides a link between the vibrational properties and the elasticity variation of the PMMA material. The function that defines the change in elasticity of PMMA depends on the “slow time”. (The term “slow time” implies a product of time and a parameter that is less than one). For a decreasing elasticity function, the vibration is of damped type: for higher is the elasticity reduction, the faster is the vibration decay. Based on the determined elasticity function, the modification of the PMMA structure can be realized. Authors propose the application of the obtained elasticity variation function for programming 4D printing with modified PMMA.

Keywords: 3D printing; PMMA in dentistry; variable modulus of elasticity; axial vibration in tooth; analytic solving method; planning of 4D printing.

INTRODUCTION

In modern dentistry, new technologies and especially new materials are the drivers of development. One of the new techniques for making complex shaped three-dimensional objects in dentistry, like teeth, bridges, implants, bone supplements, *etc.*, is the so-called 3D printing. It is the procedure for fabrication of a

* Corresponding author. E-mail: cveticanin@uns.ac.rs
<https://doi.org/10.2298/JSC240118029C>

three-dimensional object based on the 3D CAD or digital model. During the process of creating an object with 3D printing, under computer control, “layer by layer” of material is applied until the final structure is formed. The advantages of digital manufacturing is speed and efficiency. For 3D printing the so called “3D printing materials” are applied. There is the special technology on a 3D printer which produces the material from chemical components that enter into a chemical reaction under the influence of liquid, heat, radiation, *etc.* In dentistry, it is important the material to be close to those of living beings or most acceptable for the human body. In the last ten years materials for 3D printing attract research interest.

In general, materials applied in dentistry can be classified into 4 groups: polymers, metals, ceramics and biomaterials.¹ By comparing the 4 materials it is found that the chemical and physical properties of polymers are better than those of ceramics and metals. Polymers have advantage due to elasticity and tensile strength which provide high performance and durability feature and are applied for denture bases, artificial teeth, temporary crowns, bridge and crown facings and implants.² Polymers are used in polymeric resins for replacing tooth structure and missing tooth. Advantage of these resins is their ability to bond with other resins directly to the tooth structure. According to these founding the 3D printing material is usually assumed to be of polymer type. Synthetic and natural bio polymers are applied in 3D printing.³ The applied synthetic polymers are: poly capro-lactone (PCL), polymethyl methacrylate (PMMA), polylactic acid (PLA), acrylonitrile butadiene styrene (ABS), polyvinyl alcohol (PVA), polylactic-co-glycolic acid (PLGA) and ultraviolet (UV) resins. The following three natural biopolymers are also used: hyaluronic acid (HA), chitosan and alginate. However, one of the most often used polymers in dentistry which support long-term dental applications is the PMMA.^{4,5}

Chemical construction and property definition

PMMA (IUPAC name: poly(methyl 2-methylpropenoate)) is a synthetic polymer prepared by the free radical addition and polymerization of methyl methacrylate ($C_5O_2H_8$) to polymethyl methacrylate ($C_5O_2H_8$)_n. The polymerization reaction is initiated and activated by generating a free radical either chemically or with energy (such as heat, light, microwaves). In the propagation stage, the activated polymerization continues *via* the binding of monomers followed by termination through shifting of the free electrons to the chain end. The majority of PMMA are supplied as polymeric powders and monomer liquids.

The basic component of the liquid is the methyl methacrylate (MMA), the methyl ester of methyl 2-methylpropenoate. In this colorless liquid an accelerator, inhibitor, plasticizer, as cross-linking agent are added. MMA is the highest-volume compound among lower methacrylates used for polymer synthesis.

Unlike acrylic acid (AA), MAA and its alkyl esters have a methyl group adjacent to the double bond in the acyl component, hindering nucleophile addition at this site. This nucleophile addition is correlated with decreased cytotoxicity and genotoxicity of methacrylates compared to the acrylates. The powder consists of acrylic or copolymer heads, an initiator (benzoyl peroxide pigments – mercury sulfide, cadmium sulfide or dyes), opacifiers (titanium dioxide) and in addition – dyed synthetic fibers, plasticizers, inorganic particles (glass fibers, zirconium silicate).

To avoid any discrepancies, it is necessary to use the recommended ratio of PMMA powder and liquid (2.5:1 or 3–3.5:1, volume ratio). In the case of a high powder-to-liquid ratio, this means that not all of the PMMA beads will be wet, leading to a granular texture, while a low powder-to-liquid ratio.

In 3D printing the exothermic chemical reaction starts upon mixing of the PMMA powder and liquid, which harden either chemically (cold cure) or *via* energy application in the case of heat-cured PMMA materials.⁶ The phases of process of PMMA polymerization are initiation, activation, propagations and termination.

Finally, although numerous new alloplastic materials show promise, the versatility and reliability of PMMA cause it to remain a popular and frequently used material.⁷ The main advantage of the PMMA material is its long durability, low cost and high performance. In addition the material is non-toxic, biocompatible, inert, and has no color change in time. Due to these characteristics PMMA is material for temporary crowns and bridges, artificial teeth, implants, to manufacture surgical guides, custom trays, working casts and temporary restorations.⁸

Comparison of PMMA produced with 3D printing with CAD/CAM milling and conventional procedure

In dentistry the PMMA parts are made with 3D printing, computer-aided designing/computer-aided manufacturing (CAD/CAM) milling or with conventional procedure. For comparing the mentioned methods, let us consider the physical and mechanical properties of a PMMA provisional crown produced using the previously mentioned three procedures.⁹ The following mechanical characteristics were compared: fracture strength, flexural strength, elastic modulus, toughness, peak strain, resilience, micro-hardness, surface roughness, wear resistance, and also the following physical properties: color change, water sorption and solubility. It is found that the fracture strength, flexural strength, peak stress, elastic modulus, and wear resistance are some of the mechanical properties better for 3D printed PMMA structure compared to other two ones. However, it was not the case for toughness, resilience, and micro-hardness. In addition, 3D printed PMMA provisional crown had inferior physical properties. In spite of disadvantages, the 3D printed PMMA structure was suggested to be

used as an alternative to conventional and CAD/CAM milled materials.⁹ Namely, 3D printing made available a number of PMMA dental models to be easily fabricated, polished and repaired using the 3D printers. 3D printers reduce the production time and allow the production of multiple 3D copies.¹⁰ In addition, the 3D printing available the production of any shape due to the fact that three-dimensionally printed materials are fabricated by a layering technique. Conventional fabrication using PMMA with a mixture of self-polymerising powder and liquid requires longer cure times than it is in 3D printing. However, the disadvantages of 3D printing PMMA require to be investigated and eliminated.¹¹

Mechanical and physical properties of PMMA in dentistry

Measurements done on the 3D printed PMMA parts revealed that the tensile strength is 2.91 MPa and a modulus of elasticity of 223 MPa.¹² Comparing the values with those obtained for the same parts produced by traditional methods show that the first are worse. It was the reason to develop methods to improve properties of 3D printed parts in dentistry and they are as follows:

1. To improve the mechanical properties in 3D printed PMMA the thickness of layers during the printing process has to be controlled: the lower the layer thickness of printing the more layer-to-layer interfaces will be available; thus, each layer will be polymerized in a better way, which will increase the mechanical properties of these materials. The materials display superior mechanical properties if the build orientation for layers is deposited perpendicular to the direction of the applied load.

2. Improvement of mechanical properties in 3D printing is possible by infiltration of epoxy and smaller particles which may influence the qualities of the final products. To obtain better dimensional accuracy and resiliency, but also longer term application PMMA has to be mixed with some additional components. Modifications of PMMA involving chemical or mechanical reinforcement using supplementary materials (fibers, nanofillers, nanotubes and hybrid materials) have resulted in remarkable improvements in the mechanical (impact strength, cyclic fatigue, flexural strength, and wear resistance), physical (thermal conductivity, water sorption, solubility and dimensional stability), and biological (antimicrobial activity, biocompatibility) properties.⁶ Nanodiamonds in low concentrations can be added as reinforcement to improve the overall properties of PMMA-based fixed interim prostheses.¹³ The tensile strength is up to 26.6 MPa and the modulus of elasticity is 1184 MPa. Increasing the content of nanodiamonds the modulus of elasticity reaches its highest value of 2084 MPa. PMMA composites printed with three different reinforcements: aluminum nitride, titanium oxide and barium titanate have the tensile strength even 3200–4000 MPa¹⁴ and elastic modulus of 1075 MPa.¹⁵

3. After fabrication, 3D-printed materials may be subjected to post-treatments, which would increase the degree of conversion and lead to lower residual monomers and increased mechanical properties. To improve physical and mechanical properties such as density, elasticity and strength of material the polymerization process through heat and press has to be applied. It gives the PMMA material to be dimensionally stable but chemically unstable in the oral cavity and is sensitive on water sorption or dehydration.⁶ The conclusion is that the post-treatment of PMMA for dental application is not recommended.

During chewing process each tooth is dynamically loaded with the impact force acting along the tooth's vertical axis. The force causes tooth deformation which is extreme small, as the property of natural tooth material is rigid. As previously mentioned, the PMMA material, which is suggested for tooth substitution, has certain elastic property differing from that of the natural tooth. During each chewing the PMMA tooth undergoes some deformation and shape variation which is periodically repeated. The impact force in chewing causes axial vibration in the elastic 3D printed PMMA tooth. This vibration is unwilling as it dissipate the useful chewing energy and also shortens the lifetime of the PMMA tooth.

The aim of the paper is to analyze the axial vibration of the artificial PMMA tooth caused by impact and to define the time variable elasticity function of the modified PMMA structure as to eliminate or reduce the vibration.

The research result is suggested to be the basis for programming of the 4D printed modified PMMA tooth. Namely, 4D printing is the technology in which manufacturers can produce materials with self-folding interactions.¹⁶ The 3D printing is extended with the fourth dimension which includes the time variation of the parameter.¹⁷ The prescribed elasticity time variable function, would be incorporated into concept of microstructure of the 3D printed material. Although the 4D printing procedure is equal to that in 3D process through computer-programmed deposition of material in successive layers, in the 4D printing in PMMA the so called "smart" or "programmable" material would be included. The elasticity variation in PMMA would be activated only due to action of the external chewing force. The input from the 3D printed item would become another structure *via* the impact of external energy source. Thus, the 4D printing would have the capacity to alter shape over time and to eliminate the axial vibration.

ANALYTIC PROCEDURE FOR DYNAMIC ANALYSIS OF THE 3D PRINTED PMMA TOOTH MODEL

For dynamic analysis the 3D printing PMMA tooth is modeled as a clamped-free rod with circle cross-section and length which is approximately equal to diameter. The impact force, which lasts for a short time τ and acts along the rod, causes axial vibration.

Model of the 3D printed PMMA tooth

Due to chewing, the force which acts on the tooth causes axial vibration. The aim of the paper is to consider the effect of the impact force on the tooth made of PMMA material.

The shape of the tooth is designed as a clamped-free (fixed at one end and free at the other) short circular rod (Fig. 1). Three types of models are considered: one, of barrel type (Fig. 1a), the second, of cylindrical type (Fig. 1b) and the third is of hollow type (Fig. 1c).

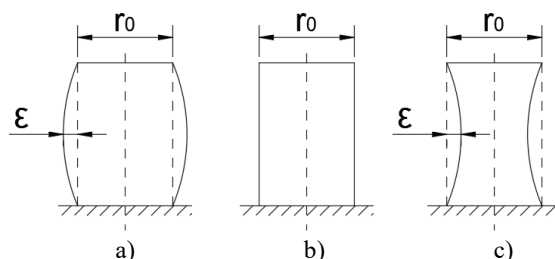


Fig. 1. Models of tooth: a) barrel type model ($\varepsilon > 0$), b) constant cylindrical model ($\varepsilon = 0$), c) concave model ($\varepsilon < 0$).

For the first and third model the cross-section is varying along the rod axis and the radius function $r(x)$ is:

$$r(x) = r_0 \pm \varepsilon \left(\sin \frac{\pi x}{l} \right) \quad (1)$$

where r_0 is the initial radius, $\varepsilon \ll 1$ is the small perturbation value, l is the length of the model, x is the axial coordinate, sign + is for the barrel type model in Fig. 1a and sign - is for concave model in Fig. 1c. For the cylindrical model (Fig. 1b) the radius is constant and $\varepsilon = 0$, i.e., $r = r_0 = \text{const}$.

Remark. In the following text the Eq. (1) with sign + is considered.

Let us consider the equilibrium of the elementary part of the rod. The element has the mass dm and the high is dx (Fig. 2). The element is in equilibrium if the following equation is satisfied:

$$\frac{\partial}{\partial t} \left(dm \frac{\partial u}{\partial t} \right) + F = F + \frac{\partial F}{\partial x} dx \quad (2)$$

where F is the force which acts in axial direction, u is the deflection and t is time.

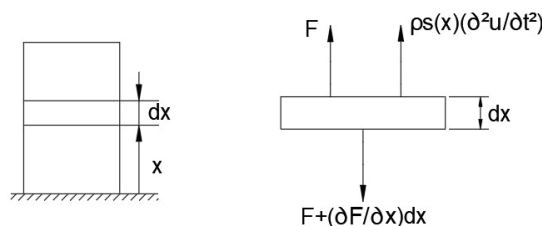


Fig. 2. Equilibrium of an elementary section of the model.

The axial force is the product of the stress σ and the cross section S :

$$F = S(x)\sigma \quad (3)$$

where $S(x) = r^2(x)\pi$. The stress-strain rheological model is assumed to be of linear Kelvin-Voigt type:

$$\sigma = E \frac{\partial u}{\partial x} + \frac{\partial}{\partial t} \left(b \frac{\partial u}{\partial x} \right) \quad (4)$$

where E is the Young's modulus of elasticity and b is the parameter of the deformation velocity. Analyzing the experimentally obtained elasticity values it is obtained that it is varying slowly in time. So, the parameter b is described as a function of "slow time" τ , *i.e.*, $b = b(\tau)$ where $\tau = \nu t$ and $\nu \ll 1$ is a small parameter. Substituting Eq. (3) with Eq. (4) into Eq. (2) it is obtained:

$$\frac{\partial}{\partial t} \left(\rho S(x) \frac{\partial u}{\partial t} \right) = \frac{\partial}{\partial x} \left(ES(x) \frac{\partial u}{\partial x} + S(x) \frac{\partial}{\partial t} \left(b(\tau) \frac{\partial u}{\partial x} \right) \right) \quad (5)$$

The relation (5) is the mathematical expression of the vibration model. It is a linear partial differential equation with time and coordinate variable parameters. For the boundary conditions:

$$u(0,t) = 0, \quad \frac{\partial u}{\partial x}(l,t) = 0 \quad (6)$$

the solution of Eq. (5) is assumed in the form:

$$u(x,t) = T(\tau) \sin \left(\frac{\pi x}{2l} \right) \quad (7)$$

Substituting Eq. (7) into Eq. (5) it is obtained:

$$\begin{aligned} S(x) \ddot{T} \sin \left(\frac{\pi x}{2l} \right) + (\omega^2 T + \frac{b(\tau)}{\rho} \dot{T}) [S(x) \left(\frac{\pi}{2l} \right)^2 \sin \left(\frac{\pi x}{2l} \right) - \frac{\partial S(x)}{\partial x} \left(\frac{\pi}{2l} \right) \cos \left(\frac{\pi x}{2l} \right)] = \\ = -T \frac{1}{\rho} \frac{\partial b(\tau)}{\partial t} [S(x) \left(\frac{\pi}{2l} \right)^2 \sin \left(\frac{\pi x}{2l} \right) - \frac{\partial S(x)}{\partial x} \left(\frac{\pi}{2l} \right) \cos \left(\frac{\pi x}{2l} \right)] \end{aligned} \quad (8)$$

Averaging the periodic functions over the length of the rod l :

$$\begin{aligned} \frac{1}{l} \int_0^l S(x) \sin \left(\frac{\pi x}{2l} \right) dx = \frac{1}{l} \int_0^l (r_0^2 \pi \sin \left(\frac{\pi x}{2l} \right) + 2\varepsilon_0 r_0 \pi \sin \left(\frac{\pi x}{l} \right) \sin \left(\frac{\pi x}{2l} \right)) dx = 2r_0^2 + \frac{8}{3} \varepsilon_0 r_0 \\ \frac{1}{l} \int_0^l \left(\frac{\partial S(x)}{\partial x} \cos \left(\frac{\pi x}{2l} \right) \right) dx = 4\varepsilon_0 r_0 \pi \frac{\pi}{2l} \cos \left(\frac{\pi x}{l} \right) \cos \left(\frac{\pi x}{2l} \right) = \frac{8}{3} \varepsilon_0 r_0 \frac{\pi}{2l} \end{aligned} \quad (9)$$

and using Eq. (8) after some modification it follows:

$$\left(1 + \frac{4\varepsilon}{3r_0} \right) \ddot{T} + \left(\frac{\pi}{2l} \right)^2 (\omega^2 T + \frac{b(\tau)}{\rho} \dot{T}) = T \frac{1}{\rho} \frac{\partial b(\tau)}{\partial t} \left(\frac{\pi x}{2l} \right)^2 \quad (10)$$

where $\omega^2 = E/\rho$. Using the series expansion for small parameter $\varepsilon/r_0 \ll 1$ and neglecting the terms higher than $O((\varepsilon/r_0)^2)$, the Eq. (10) is:

$$\ddot{T} + \frac{\varepsilon_1 b(\tau)}{\rho} \dot{T} + \omega_1^2 T = -\nu \frac{\varepsilon_1}{\rho} \frac{\partial b(\tau)}{\partial t} T \quad (11)$$

where $\varepsilon_1 = (\pi/2l)^2 (1 - (4\varepsilon/(3r_0)))$ and $\omega_1^2 = \varepsilon_1 \omega^2$. The relation (11) is a second order ordinary differential equation with slow time variable parameters. Unfortunately, to find the exact solution for Eq. (11) is impossible. The approximate method based on time variable amplitude and phase is applied.¹⁸ For $\nu = 0$ and $\tau = 0$ the relation (11) transforms into the equation with constant parameter:

$$\ddot{T} + \frac{\varepsilon_1 b_0}{\rho} \dot{T} + \omega_1^2 T = 0 \quad (12)$$

where $b(0) = b_0$. Solution of Eq. (12) is:

$$T = A \exp(-\delta t) \cos(\Omega t + \theta) \quad (13)$$

where A and θ are arbitrary amplitude and phase, and:

$$\delta = \frac{\varepsilon_1 b_0}{2\rho}, \quad \Omega = \sqrt{\omega_1^2 - \left(\frac{\varepsilon_1 b_0}{2\rho}\right)^2} \quad (14)$$

Comparing Eqs. (11) and (12) it is seen that Eq. (11) is the perturbed version of Eq. (12). According to this conclusion the solution of Eq. (11) is assumed in the form:

$$T = A \exp\left(-\int \delta(\tau) dt\right) \cos \psi \quad (15)$$

and time derivative:

$$\dot{T} = -A\delta \exp\left(-\int \delta(\tau) dt\right) \cos \psi - A\Omega \exp\left(-\int \delta(\tau) dt\right) \sin \psi \quad (16)$$

where $A = A(t)$, $\theta = \theta(t)$, and:

$$\dot{\psi} = \Omega(\tau) + \dot{\theta} \quad (17)$$

$$\delta(\tau) = \frac{\varepsilon_1 b(\tau)}{2\rho}, \quad \Omega(\tau) = \sqrt{\omega_1^2 - \left(\frac{\varepsilon_1 b(\tau)}{2\rho}\right)^2} \quad (18)$$

Comparing the time derivative of Eq. (15) with the assumed one (see Eq. (16)) the constraint follows as:

$$\dot{A} \cos \psi - A \dot{\theta} \sin \psi = 0 \quad (19)$$

Substituting the time derivative of Eq. (16) and the relations (15) and (16) into Eq. (11) it yields:

$$-\dot{A}(\delta \cos \psi + \Omega \sin \psi) + A\dot{\theta}(\delta \sin \psi + \Omega \cos \psi) = Av \left(\left(\frac{\partial \delta(\tau)}{\partial t} - \frac{\varepsilon_1 b(\tau)}{\rho} \right) \cos \psi + \frac{\partial \Omega(\tau)}{\partial t} \sin \psi \right) \quad (20)$$

By rewriting Eqs. (19) and (20) we obtain:

$$\dot{A} = -\frac{1}{\Omega} \left(\left(\frac{\partial \delta(\tau)}{\partial t} - \frac{\varepsilon_1}{\rho} \frac{\partial b(\tau)}{\partial \tau} \right) \cos \psi + \frac{\partial \Omega(\tau)}{\partial t} \sin \psi \right) Av \sin \psi \quad (21)$$

$$\dot{\theta} A = -\frac{1}{\Omega} \left(\left(\frac{\partial \delta(\tau)}{\partial t} - \frac{\varepsilon_1}{\rho} \frac{\partial b(\tau)}{\partial \tau} \right) \cos \psi + \frac{\partial \Omega(\tau)}{\partial t} \sin \psi \right) Av \cos \psi \quad (22)$$

It is at this point the averaging of periodical function ψ is introduced. The averaged equations are:

$$\dot{A} = -\frac{Av}{2\Omega} \frac{\partial \Omega(\tau)}{\partial t} \quad (23)$$

$$\dot{\theta} = -\frac{v}{2\Omega} \left(\frac{\partial \delta(\tau)}{\partial t} - \frac{\varepsilon_1}{\rho} \frac{\partial b(\tau)}{\partial \tau} \right) \quad (24)$$

Integrating Eq. (23) for the initial condition $A(0) = A_0$ the amplitude variation is:

$$A = A_0 \sqrt{\frac{\Omega}{\Omega(\tau)}} \quad (25)$$

Substituting Eq. (25) into Eq. (24) it is:

$$\dot{\theta} = \frac{\nu}{4\Omega} \frac{\varepsilon_1}{\rho} \frac{\partial b(\tau)}{\partial \tau} \quad (26)$$

Finally, the averaged solution of Eq. (15) is:

$$T = A_0 \sqrt{\frac{\Omega}{\Omega(\tau)}} \exp\left(-\int \frac{\varepsilon_1 b(\tau)}{2\rho} dt\right) \cos\left(\theta_0 + \int \left(\sqrt{\omega_1^2 - \left(\frac{\varepsilon_1 b(\tau)}{2\rho}\right)^2} + \frac{\nu}{4\Omega} \frac{\varepsilon_1}{\rho} \frac{\partial b(\tau)}{\partial \tau}\right) dt\right) \quad (27)$$

where $\theta(0) = \theta_0$. After some simplification the approximate solution is:

$$T = A_0 \sqrt{\frac{\Omega}{\Omega(\tau)}} \exp\left(-\int \frac{\varepsilon_1 b(\tau)}{2\rho} dt\right) \cos\left(\theta_0 + \Omega t + \frac{\varepsilon_1(b(\tau) - b_0)}{4\Omega\rho}\right) \quad (28)$$

Finally, in general, the vibration is:

$$u = \sum_{n=1}^{\infty} A_{0n} \sqrt{\frac{\Omega}{\Omega(\tau)}} \exp\left(-\int \frac{\varepsilon_1 b(\tau)}{2\rho} dt\right) \cos\left(\theta_{0n} + \Omega t + \frac{\varepsilon_1(b(\tau) - b_0)}{4\Omega\rho}\right) \sin\left(\frac{n\pi x}{2l}\right) \quad (29)$$

where A_{0n} and θ_{0n} satisfy the initial conditions. For initial conditions:

$$u(0, x) = P, \quad \frac{\partial u(0, x)}{\partial t} = 0 \quad (30)$$

where P is the chewing force which causes the vibration, the amplitude A_0 and the first term of Eq. (29), u_1 , follows as:

$$A_0 = P\left(1 + \left(\frac{\delta}{\Omega}\right)^2\right), \quad \tan \theta_0 = \frac{\delta}{\Omega} \quad (31)$$

$$u_1 = P\left(1 + \left(\frac{\delta}{\Omega}\right)^2\right) \sqrt{\frac{\Omega}{\Omega(\tau)}} \exp\left(-\int \frac{\varepsilon_1 b(\tau)}{2\rho} dt\right) \cos\left(\tan^{-1}\left(\frac{\delta}{\Omega}\right) + \Omega t + \frac{\varepsilon_1(b(\tau) - b_0)}{4\Omega\rho}\right) \sin\left(\frac{\pi x}{2l}\right) \quad (32)$$

Vibration in the tooth depends on the initial shape of the tooth (parameter ε) and on the material property ($b(\tau)$ function). For the decreasing slow time function ($b(\tau)$ vibration is of damping type, Eq. (32)). The energy dissipation is faster for faster decrease of $b(\tau)$. Namely, in Eq. (32) both terms:

$$\sqrt{\frac{\Omega}{\Omega(\tau)}} \text{ and } \exp\left(-\int \frac{\varepsilon_1 b(\tau)}{2\rho} dt\right)$$

have the same tendency: if $b(\tau)$ increases, the both terms increase and also their product.

RESULTS AND DISCUSSION

Let us assume the model, with modified PMMA material, with slow time elasticity variation:

$$b(\tau) = \frac{b_0}{1 + \tau} \quad (33)$$

The Eq. (32) transforms into:

$$u_1 = P \left(1 + \left(\frac{\delta}{\Omega}\right)^2\right) \left(\frac{\omega_1^2 - \delta^2}{\omega_1^2 - \delta^2 / (1 + \tau)^2}\right)^{1/4} (1 + \tau)^{-\delta/\nu} \times \cos\left(\tan^{-1}\left(\frac{\delta}{\Omega}\right) + \Omega t + \frac{\delta}{2\Omega} \frac{1}{1 + \tau}\right) \sin\left(\frac{\pi x}{2l}\right) \quad (34)$$

For numerical data: $\omega = 1.18 \times 10^9 \text{ s}^{-1}$, $b_0 = 10^3 \text{ N s m}^{-2}$, $\rho = 1170 \text{ kg m}^{-3}$, $E = 223 \text{ MPa}$, $\nu = 0.1 \text{ s}^{-1}$, the temporal vibration expression (28) is treated as:

$$T = A_0 \left(\frac{\omega_1^2 - \delta^2}{\omega_1^2 - \delta^2 / (1 + \tau)^2}\right)^{1/4} (1 + \tau)^{-\delta/\nu} \cos\left(\tan^{-1}\left(\frac{\delta}{\Omega}\right) + \Omega t + \frac{\delta}{2\Omega} \frac{1}{1 + \tau}\right) \quad (35)$$

In Fig. 3 the axial vibrations of the upper surface of three tooth models (Fig. 1) are plotted: $\mu = 0$ is the model with constant circular cross-section, $\mu = 0.5$ is the parameter of barrel type (convex) model, $\mu = -0.1$ is of the concave model, where $\mu = 4\varepsilon/3r_0$. In Fig. 3 it is seen that for all three models the amplitude of vibration has the tendency of decrease. The velocity of vibration amplitude decrease is faster for the concave than for the convex model and even for that with constant cross-section. The period of vibration is also shorter for the concave model than for the model with constant radius and for the convex model.

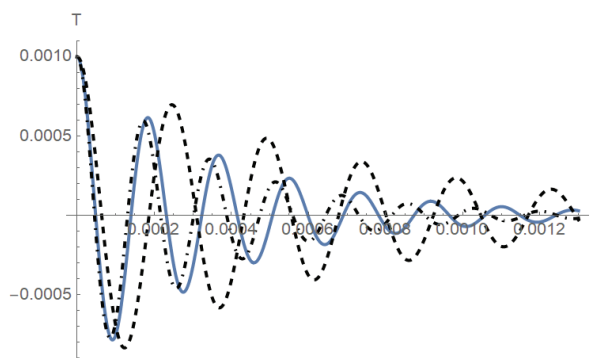


Fig. 3. Temporal time function for various values of parameter μ : $\mu = 0$ (full line), $\mu = 0.5$ (dashed line), $\mu = -0.1$ (dash-dot line).

To determine the total time necessary for vibration delimitation it is necessary to know that the chewing rate varies in the interval 0.94–2.5 chewings/s.¹⁹ Namely, vibration elimination has to be finished in the maximal time interval between two chewings which is approximately 0.4 seconds. It is obvious from the Fig. 2 that the 4D printed model, made of PMMA material with stored energy and programmed according to Eq. (33), is able to eliminate the vibration in the corresponding time interval.

In Fig. 4 the influence of the modulus of elasticity E on the vibration properties is tested. For $\mu = 0$ and modulus of elasticity is $E = 1190$ MPa and $E = 2084$ MPa the temporal function is plotted. It is obtained that the elasticity value has the influence on the frequency of vibration, but the influence on the amplitude vibration is not significant. For higher is the value of the modulus E , the period of vibration is shorter.

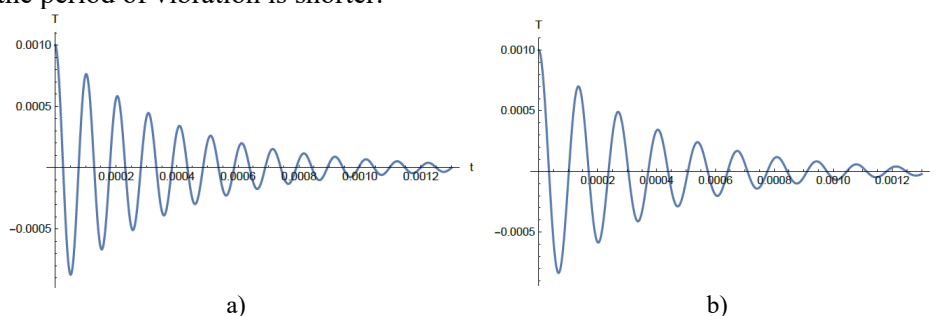


Fig. 4. Axial vibration for various elasticity modulus: a) $E = 1190$ MPa, b) $E = 2084$ MPa.

In Fig. 5 the influence of parameter ν on vibration properties of the model are considered. The parameter values are $\nu = 0$ and $\nu = 1$. It is obtained that for higher value of parameter ν the amplitude of vibration is higher, The influence of ν on the period of vibration is negligible.

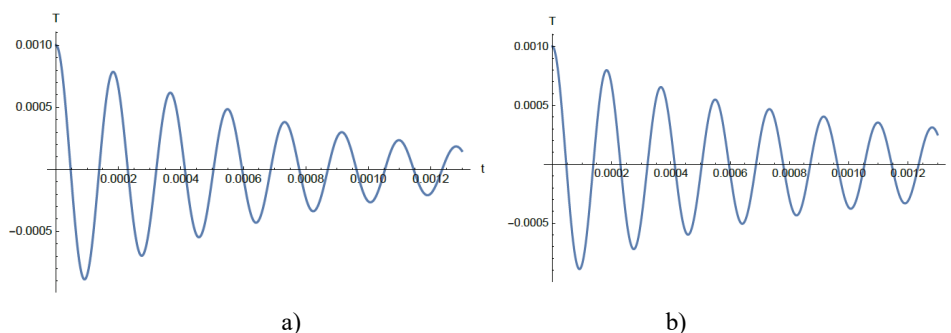


Fig. 5. Temporal time function for various values of ν : a) $\nu = 0$, b) $\nu = 1$ s⁻¹.

In Fig. 6 the $T-t$ diagrams for $b_0 = 10^3$ N s m⁻² and $b_0 = 500$ N s m⁻² are plotted. It is obtained that for higher value of the parameter b_0 the velocity of amplitude decay is slower than for smaller parameter value. The parameter b_0 has the influence on the frequency of vibration.

CONCLUSIONS

It is concluded:

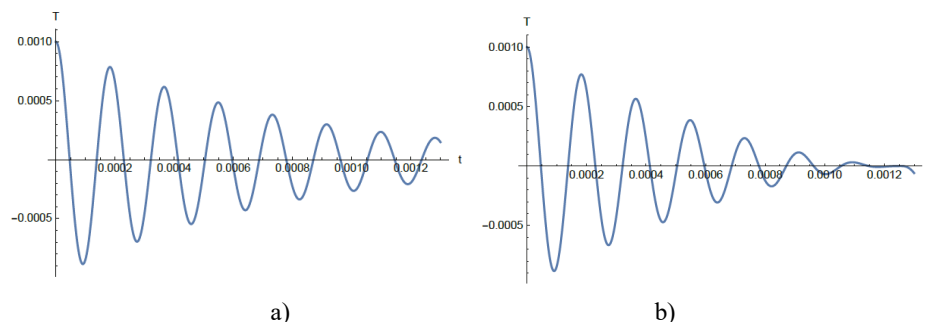


Fig. 6. The $T-t$ diagrams for avariable b_0 a) $b_0 = 10^3 \text{ N s m}^{-2}$; $b_0 = 500 \text{ N s m}^{-2}$.

1. Impact force in chewing causes axial vibration of the 3D printed PMMA elastic tooth.

2. Vibration of the tooth depends on the tooth shape. The vibration amplitude and phase variation is more intensive for barrel formed tooth than for the tooth with constant circular cross section and is the smallest for the tooth of concave form. Namely, the tooth with concave form behaves like the unit in auxetic structure. The deformation and vibration along the axial axis for this 3D printed PMMA model is smaller than for the model with constant cross section and is suggested to be applied in the 4D printing of the tooth,

3. Decay of axial vibration is obtained by using the PMMA modified material with slow time variable elastic property. Damping of vibration is more intensive if the elasticity of the modified PMMA material is decreasing in time.

4. The elasticity property of 3D printed PMMA tooth has the influence on the frequency of axial vibration: the higher is the value of modulus of elasticity, the period of vibration is shorter.

5. Based on the axial vibration time function, the elasticity variation of the 3D printed PMMA material is prescribed. In the tooth, designed with this elasticity – slow time function, elimination or reduction of the axial vibration is expected.

Future research has to be oriented toward 4D printing of PMMA tooth where a new material assembly (a combination of multiple materials, for example) has to be created under stress that becomes “stored” within the material. This stress can later be released, causing an overall material shape change according to elasticity variation as suggested in the result of the paper. To realize tooth, with time variable elastic function, the PMMA has to be modified to be the smart material. It would be the programmable matter, wherein after the fabrication process, the printed tooth reacts with force parameters within the environment and changes its form accordingly.

Acknowledgement. We have to thank Dr Miljan Sunjevic for his help in preparing the Graphical Abstract and Figures.

ИЗВОД

УТИЦАЈ ВАРИЈАЦИЈЕ ЕЛАСТИЧНОСТИ 3Д ШТАМПАНЕ ПММА СТРУКТУРЕ НА АКСИЈАЛНЕ ВИБРАЦИЈЕ ЗУБА

ЛИВИЈА ЦВЕТИЋАНИН^{1,2}, МИЉАНА ПРИЦА¹ и САЊА ВУЈКОВ³¹Универзитет у Новом Сагу, Факултет техничких наука, Нови Саг, ²Obuda University, Budapest, Hungary и ³Универзитет у Новом Сагу, Медицински факултет, Департаман за стоматологију, Нови Саг

Од недавно, 3Д штампање са поли метил метакрилатом (РММА) има широку примену у стоматологији: 3Д штампа је погодна метода за производњу било ког сложеног тродимензионалног облика, а РММА је материјал који има погодна својства у окружењу усне шупљине. Због тога се 3Д штампа веома често примењује за израду РММА зуба. Ови зуби у току жвакања долазе у контакт, јавља се између њих удар који доводи до промене облика и вибрације зуба. Како цикличне вибрације лоше утичу на издржљивост РММА зуба, оне се морају елиминисати. Циљ овог рада је проучавање аксијалних вибрација 3Д штампаног зуба као и давање препорука за модификацију структуре РММА са циљем пригушивања вибрација. Вибрације зуба су математички моделоване и аналитички решене. Добијени резултат даје везу између вибрационих својстава и варијације еластичности РММА материјала. Функција која дефинише промену еластичности РММА зависи од „спорог времена“. (Израз „споро време“ подразумева производ времена и параметра који је мањи од један). За опадајућу функцију еластичности, вибрација је пригушена: што је интензивније смањење еластичности, то је брже опадање вибрација. На основу утврђене функције еластичности може се реализовати модификација структуре РММА. Аутори предлажу примену добијене функције варијације еластичности за програмирање 4Д штампе са модификованим РММА.

(Примљено 18. јануара, ревидирано 15. фебруара, прихваћено 7. марта 2024)

REFERENCES

1. T. K. Vaidyanathan, J. Vaidyanathan, D. Arghavani, *Acta Biomater. Odontol. Scand.* **2** (2016) 108 (<http://dx.doi.org/10.1080/23337931.2016.1219664>)
2. G. Oberoi, S. Nitsch, M. Edelmayr, K. Janjic, A. S. Müller, H. Agis, *Front. Bioeng. Biotechnol.* **6** (2018) 172 (<http://dx.doi.org/10.3389/fbioe.2018.00172>)
3. H. Cai, X. Xu, X. Lu, M. Zhao, Q. Jia, H.-B., Jiang, J.-S. Kwon, *Polymers* **15** (2023) 2405 (<https://doi.org/10.3390/polym15102405>)
4. L. Peñate, J. Basilio, M. Roig, M. Mercadé, *J. Prosthet. Dent.* **114** (2015) 248 (<https://doi.org/10.1016/j.prosdent.2014.12.023>)
5. A. Nulty, *Clin. Dent.* **2** (2022) 44 (<http://doi.org/10.20944/preprints202105.0316.v1>)
6. M. S. Zafar, *Polymers* **12** (2020) 2299 (<http://dx.doi.org/10.3390/polym12102299>)
7. R. Q. Frazer, R. T. Byron, P. B. Osborne, K. P. West, *J. Long-Term Eff. Med. Implant* **15** (2005) 629 (<http://doi.org/10.1615/jlongtermeffmedimplants.v15.i6.60>)
8. S. M. Pituru, M. Greabu, A. Totan, M. Imre, M. Pantea, T. Spinu, A. M. C. Tancu, N. O. Popoviciu, I.-I. Stanescu, E. Ionescu, *Materials* **13** (2020) 2894 (<http://dx.doi.org/10.3390/ma13132894>)
9. S. Jain, M. E. Sayed, M. Shetty, S. M. Alqahtani, M. H. D. Al Wadei, S. G. Gupta, A. A. A. Othman, A. H. Alshehri, H. Alqarni, A. H.; Mobarki, *Polymers* **14** (2022) 2691 (<https://doi.org/10.3390/polym14132691>)

10. G. Alp, S. Murat, B. Yilmaz, *J. Prosthodont.* **28** (2018) e491 (<http://doi.org/10.1111/jopr.12755>)
11. M. Petras, O. Naka, S. Doukoudakis, A. Pissiotis, *J Esthet Restor Dent* **24** (2012) 26 (<http://doi:10.1111/j.1708-8240.2011.00467.x>)
12. C. Polzin, S. Spath, H. Seitz, *Rapid Prototyp. J.* **19** (2013) 37 (<http://dx.doi.org/10.1108/13552541311292718>)
13. P. Protopapa, E. Kontonasaki, D. Bikiaris, K. M. Paraskevopoulos, P. Koidis, *Dent. Mater. J.* **30** (2011) 222 (<http://dx.doi.org/10.4012/dmj.2010-135>)
14. K. Afaf, B. Serier, K. Kaddouri, M. Belhouari, *Fratt. Ed. Integrità Strutt.* **53** (2020) 66 (<http://dx.doi.org/10.3221/IGF-ESIS.53.06>)
15. M. Wieckiewicz, V. Opitz, G. Richter, K. W. Boening, *Biomed Res. Int.* **2014** (2014) 150298 (<http://dx.doi.org/10.1155/2014/150298>)
16. H. Hamza, *Innovation* **1** (2018) e17 (<http://dx.doi.org/10.30771/2018.4>)
17. M. Javaid, A. Haleem, R. P. Singh, S. Rab, R. Suman, L. Kumar, *J. Oral Biol. Craniofac. Res.* **12** (2022) 388 (<https://doi.org/10.1016/j.jobcr.2022.05.002>)
18. L. Cveticanin, *Strong Nonlinear Oscillators – Analytical Solutions, Mathematical Engineering*, 2nd ed., Springer, Berlin, 2018 (ISBN 978-3-319-58825-4)
19. M. Farooq, E. Sazonov, *Electronics (Basel)* **5** (2016) (<https://doi.org.10.3390/electronics5040062>).



J. Serb. Chem. Soc. 89 (5) 693–704 (2024)
JSCS–5749

Sulphur hexafluoride in modern medium-voltage switchgear: Advantages, hazards and environmental impact

ALEKSANDAR BOŠKOVIĆ¹, MAJA SREMAČKI^{1*}, SUNČICA VJEŠTICA²,
ALEKSANDRA ČAVIĆ³, NADA MARKOVIĆ¹ and BRANISLAV BOROVAC¹

¹University of Novi Sad, Faculty of Technical Sciences, Trg Dositeja Obradovića 6, 21000 Novi Sad, Serbia, ²Metropolitan University, Faculty of Applied Ecology Futura, Požeška 83a, 11000 Belgrade, Serbia and ³Faculty of Economics and Engineering Management, FIMEK, Cvećarska 2, 21000 Novi Sad, Serbia

(Received 3 December, revised 8 December 2023, accepted 2 February 2024)

Abstract: Sulphur hexafluoride is synthesised as a persistent and non-toxic gas with an exceptional dielectric strength. In contemporary medium-voltage switchgear within power distribution systems, SF₆ gas is used for the insulation and the extinction of electric arc. The application of SF₆ has advantages in terms of gas physicochemical characteristics and performance; the dimensions, the cost-effectiveness, the reliability of the switchgear equipment and the duration, as well as the cost of maintenance were significantly reduced. SF₆ is a known greenhouse gas, which tends to accumulate in the lungs, inducing oxygen depletion and respiratory complications. The by-products of SF₆ formed during the electric arc can be harmful and toxic. The equipment containing SF₆ is being replaced in the EU and worldwide. Using ALOHA[®] software the scenarios of leakage for SF₆ and by-products were modelled in urban areas, where the switchgear is frequently placed. In areas where the circulation of wind is lower (urban areas), in hazardous situations, it is not possible to depend on high dispersion levels or minimisation of concentration and threat. The models have shown that SF₆ poses an environmental problem and its by-products cause a serious health hazard in the case of leakage in urban areas, rendering red threat zones from 10 to 60 m in radius.

Keywords: greenhouse gas; switching device; persistence; toxicity; ALOHA[®] software.

INTRODUCTION

In the light of predominant effects of climate change that are becoming more evident every day, it is necessary to discuss and research the application of the greenhouse gases (GHG) produced, used, and abused in anthropogenic processes.

* Corresponding author. E-mail: majasremacki@uns.ac.rs
<https://doi.org/10.2298/JSC231203008B>

GHGs have a significant role in the phenomenon recognized as a plethora of anthropogenically prompted climate change.

The substance proven to be a potent GHG chemical is sulphur hexafluoride. Sulphur hexafluoride (sulphur (VI) fluoride – SF₆), is a versatile and highly potent chemical compound with a broad range of applications. This inorganic compound has a unique and stable molecular structure, made up of one sulphur atom coupled to six fluorine atoms. SF₆ has found use in a variety of commercial and scientific practices due to its exceptional qualities.^{1,2}

Because of the SF₆ electrical insulating characteristics, sulphur hexafluoride is a crucial component in high-voltage electrical equipment such as transformers, circuit breakers and switchgear.^{3,4} SF₆ possesses the capacity of efficiently extinguishing the electrical arc, as well as non-reactivity to most common materials.

Sulphur hexafluoride also possesses prominent advantages and distinctive properties that render it highly useful in the vast variety of industrial practices, which make it an exceptionally versatile greenhouse gas (GHG). The key properties of SF₆ are its remarkable insulating properties, high thermal stability and non-flammability, effectively minimizing the risks of fires during use and applications. Additionally, SF₆ exhibits electronegativity nearly three times that of air, thus enhancing its performance significantly. One of the benefits is superior arc-extinguishing capabilities, which enable SF₆ switchgear to be designed in a more compact and robust manner. This, in turn, enables minimal maintenance, ultimately making SF₆ a highly cost-effective solution for various applications.^{1,5,6}

Sulphur hexafluoride is also used in the manufacturing of semiconductors as a dielectric gas; as blanketing gas in the production of electronic devices, and it also finds applications in the medical field as a contrast agent for ultrasound imaging and ophthalmology, particularly during retinal detachment surgery (retinal ablation).^{1,7,8}

Furthermore, SF₆ is widely used in environmental research and communal systems maintenance and diagnostics, as a tracer gas (flow patterns, leak detection), particularly in the research on air and atmosphere, due to its low reactivity and long atmospheric lifetime.¹

However, the prominent disadvantage of SF₆ lies in its environmental impact, as it is a GHG with the highest global warming potential (GWP). The imminent and proven impact that SF₆ and its by-products have on the environment and health, prompted actions for its replacement, as it has been listed in the Kyoto Protocol, as a potent GHG. Corresponding to the European F-gas Regulation (EC 517/2014), which aims at cutting the EU's fluorine gas emissions to at least one-third by 2030, the replacement of switchgear using SF₆ as insulation gas has already begun.^{1,9,10}

However, in Serbia, the electro-distribution industry regards switchgear equipment (SGE) that uses SF₆ as an insulating gas as the best available tech-

nology (BAT). In Vojvodina, approximately 5 % of all switchgear devices are the ones using SF₆. However, SF₆ SGE has been used in this region only since 2005, as it is characterised in this region as a BAT. Until then, devices insulation based on air, oil, low oil, and vacuum were used, so this percentage is expected to steadily increase over time, especially due to the automation and digitalisation of the power distribution network. This preference can be considered controversial and contradictory to EU practices, given the increasing trend of installing SGEs containing SF₆.

The recent decision of the United Nations Framework Convention on Climate Change (UNFCCC), from 2022, requires the use of 100-year monitoring values for GHGs to calculate the GWP of a chemical as a CO₂ equivalent.¹¹ According to the EPA and Intergovernmental Panel on Climate Change (IPCC), it is the most potent GHG known to date, with the astonishing 23,5 thousand times higher potential for global warming than an equivalent amount of CO₂ (Table I).

TABLE I. GHG properties in the atmosphere (lifetime in the atmosphere, global warming potential and approximate concentration in air)^{12,13}

GHG compound	<i>t</i> / year	<i>GWP</i> / kg CO ₂ m ⁻²	<i>c</i> / ppm; ppb; ppt
CO ₂	– ^a	1	400 ppm
CH ₄	12	28	1800 ppb
N ₂ O	109	265	320 ppb
PFCs	≤100	11,100	≤ 600 ppt
HFCs	≤15	12,400	≤ 80 ppt
NF ₃	500	16,100	≤ 1 ppt
SF ₆	3,200	23,500	8 ppt

^aIs not provided, as it is a component of the atmosphere

The switchgear (SG) refers to the combination of electrical switches, fuses or circuit breakers used to control, protect and isolate electrical equipment. The switchgear controls the electrical system by switching on/off, regulating, and providing protection against abnormal conditions. SGs are used in substations, industrial setups, buildings and other places where electrical equipment is needed.¹⁴ There are several points of classification of switchgear, medium voltage switchgear (MVSG) with SF₆ as the insulation gas was selected for the purpose of this research because of the physicochemical properties and environmental impacts of SF₆. In Serbia, about 5 % of all switchgear devices are the ones using SF₆ as insulation gas. In the examined area MVSG equipment is in urban and living areas, making the possibility of SF₆ and its by-products leakage plausible and an important issue to investigate.

The occurrence of an electric arc is advantageous in terms of managing over-voltage. However, when the arc is active, it generates a considerable amount of thermal energy, leading to substantial thermal and mechanical stresses. These

stresses may include contact burning or combustion, insulation damage, and an elevation in internal pressure.¹⁵

During the arc, SF₆ will decompose and form SF₆ arc plasma, while forming many sulphur fluoride species. While arc temperature decreases, sulphur fluoride species will recombine into SF₆ molecules. However, if H₂O, O₂ and other vapours (nitrogen, helium, argon, hydrogen, *etc.*) are present in MVSG, the production of toxic by-products of SF₆ is inevitable.^{1,9,16,17}

The inhalation of large quantities of SF₆ displaces oxygen in the lungs and can lead to asphyxiation. Furthermore, when arcs occur in switchgear, toxic by-products form, such as (hydrogen fluoride, sulfuryl fluoride, sulphur tetrafluoride, sulphur pentafluoride, sulphur(IV) oxide, among others), which may trigger a plethora of health problems, and in extreme cases can be life-threatening.^{1,12,18}

Hydrogen fluoride is highly corrosive and toxic, causing severe chemical burns and respiratory damage upon exposure. It contributes to the formation of acid rain and has detrimental effects on aquatic life and vegetation when released into the environment.^{1,19}

Sulfuryl fluoride is primarily a respiratory hazard and can cause severe lung damage and irritation to the eyes and skin. While sulfuryl fluoride is less persistent in the environment, its high global warming potential makes it a concern for climate change impacts.^{1,20}

Sulphur tetrafluoride is extremely toxic, because the exposure to it leads to severe respiratory tract and skin irritation. SF₄ can decompose to form highly toxic and corrosive by-products, posing risks to wildlife and ecosystems.¹

There is limited information on sulphur pentafluoride, but it is expected to be highly reactive and potentially toxic, similar to other sulphur fluorides. As with other fluorinated compounds, SF₅ could contribute to atmospheric and environmental degradation if released. SF₅ is particularly interesting as it can form highly toxic disulphur decafluoride (S₂F₁₀) in the appropriate conditions.²¹

Sulphur dioxide is a significant respiratory irritant, affecting lung function and exacerbating respiratory diseases. It is a major air pollutant, contributing to acid rain and causing harm to ecosystems and plant life.^{1,22}

To address these problems, efforts are being made to reduce its emission into the atmosphere and create more ecologically friendly alternatives. Due to the previously mentioned environmental and safety issues and concerns, numerous countries and international bodies have implemented strict controls and regulations on the use, handling and disposal of SF₆.

The aim of this paper is to perform the risk assessment *via* ALOHA[®] software of the possibility of SF₆ and its by-products leakage from MVSG. It has been observed that the current energy system layout in Serbia does not have any plans in place for the evacuation of people in the event of an accidental release of SF₆ and its byproducts. Additionally, there are no early warning systems that can

detect any leakage, except for the pressure control in the chamber where SF₆ is stored. However, this can only be monitored through the network surveillance system and not on the site of the leakage itself. This type of modelling can improve the preparation and security by enabling the creation of evacuation and minimization plans and improving the system as a whole.

EXPERIMENTAL

Areal Locations of Hazardous Atmospheres, ALOHA[®], open-source software was used to provide risk assessment for accidental leakage of SF₆ from MVSG in transformation substations. ALOHA[®] is the hazard modelling program, based on Gaussian plume, for the Computer-Aided Management of Emergency Operations, CAMEO[®], software suite, which is used widely to plan for and respond to chemical emergencies, developed by USEPA. The Gaussian plume-based models have the lowest resource demand and, thus, are suitable for fast decision-making in emergencies.²³

ALOHA is a computer program that helps develop plans and responses to chemical releases and prepare for emergencies. It deals with chemicals that become airborne and includes two air dispersion models – the Gaussian model for lighter gases and the heavy gas model for denser gases. ALOHA has a decision algorithm to choose between these models and includes a chemical library with important data required as input for modelling scenarios. ALOHA can help model various release scenarios, including toxic gas clouds, BLEVEs, jet fires, vapour cloud explosions, pool fires and flammable areas. The output results include threat zones, graphs of source strength, and specific location threats. It's important to note that ALOHA provides estimates, not precise results, and the accuracy of the results depends on the input data accuracy and interpretation of the results. ALOHA has limitations, such as the inability to estimate distances greater than 10 km, unreliability of results under very stable atmospheric conditions or during wind speeds of less than 1 m/s, *etc.* However, since ALOHA has been compared to similar models and verified against field data, it is considered reliable and is used for the simulations conducted within this research.²³

Several different but similar programs can be used for the modelling of hazardous and accidental situations, process hazard analysis software tool (PHASt) were compared with the Korea off-site risk assessment supporting tool (KORA), but ALOHA is the most precise assessment open-source tool, according to the vast number of literature sources. This was the reason for selecting ALOHA as the most viable option for this research.^{23–25}

The methodology used for this research is in detail available in the literature.^{24,25} The parameters for ALOHA[®] were selected according to the real location and position of the substation located in the outdoor urban environment. The input data required for modelling, physical and chemical properties, can be found in the ALOHA[®] chemical library (CAMEO[®] Chemicals) which comprehends hundreds of substances and solutions.

While using ALOHA[®] software, it's necessary to select a chemical and source type, specify the location and time, and input weather-related parameters including atmospheric stability class, varying terrain, cloud coverage, air temperature, humidity, speed and direction of the wind. With the required inputs and integrated equations, ALOHA[®] can perform simulations of various release scenarios, including toxic gas clouds, boiling liquid expanding vapor explosions (BLEVEs), jet fires, vapour cloud explosions, pool fires and areas prone to flammability. The software generates output that comprises scenario-specific danger zones, threats at locations, and graphs showing source strength. These results are displayed both graphically and in a text summary.²⁵

Methodology

To manage disaster risks in inhabited areas, the hazard and exposure parameters must be assessed. This helps decision-makers understand the problem and develop an effective risk management strategy. The hazard context is analysed based on the physical nature of the accident and its impact on people and the environment. Atmospheric temperature, wind speed, relative humidity, atmospheric stability, cloud coverage, terrain profile and urbanisation level, substance properties and release quantity for hazard are defined as necessary variables for hazard definition and modelling, as well as location and impacted population are defined as necessary variables for modelling scenarios in the context of exposure.

The atmospheric parameters were fixed throughout all the modelled scenarios. The average and/or predominant conditions for selected locations were observed for environmental parameters that apply to selected locations – air temperature (11.6 °C), wind velocity (7 m s⁻¹) and direction (north-west), terrain (urban/forest), cloud coverage (40 %), atmospheric stability class (D), temperature inversion (no) and relative humidity (50 %).^{26,27}

While varying the source parameters and chemicals (SF₆, HF, SO₂, SF₄, SF₅ and SO₂F₂) the analysis was performed for parameters incorporated into the ALOHA[®] concerning acute exposure guideline level (AEGL) or protective action criteria (PAC) values for outdoor stationed MVSGs (Table II).

TABLE II. The concentration of AEGL and/or PAC 1, 2 and 3 values and density in the gaseous state for SF₆ and its by-products²⁸⁻³⁰; c_1 – concentration of substance for AEGL1 or PAC1, c_2 – concentration of substance for AEGL2 or PAC2, c_3 – concentration of substance for AEGL3 or PAC3

Parameter	HF	SO ₂	SF ₄	SF ₅	SO ₂ F ₂	SF ₆
c_1 / ppm	1	0.2	0.01	0.001	1	3,000
c_2 / ppm	24	0.75	0.1	0.1	21	33,000
c_3 / ppm	44	30	0.82	1	64	-
ρ / kg m ⁻³	0.69	2.62	3.78	5.38	3.72	6.5

When establishing a model, ALOHA[®] uses values from Table II to render a visualization of the data for inserted parameter values as 3 threat zones (TZ) as levels of concern (LOCs) – red, orange and yellow. The red LOC represents the worst hazard level; the orange and yellow LOC represent the areas of decreasing hazards.

RESULTS AND DISCUSSION

After conducting an analysis involving 60 distinct scenarios using the ALOHA[®] software, a crucial deduction has emerged. For 1 g of SF₆, there are no threat zones generated, the first mass of SF₆ that gets only yellow threat zones (TZ) generated for the average conditions is 114 kg with a 17 m radius. The first mass of SF₆ released that generates orange and yellow threat zones for the average conditions is 5 t with a 37 and 129 m radius, respectively. The release of 10 t of SF₆ generates red, orange, and yellow threat zones of 19, 54 and 184 m in radius, respectively. It has come to light that to pose a genuine threat to human health and overall well-being, an approximate release of 5 to 10 metric tons of SF₆ gas into the atmosphere is required, which is neither a realistic nor possible

scenario. Interestingly, when we shift our focus to ambient air conditions, this threshold drops significantly to a mere 5 kg of SF₆. To put this into perspective, 5 kg is roughly half the volume of SF₆ typically found within a single medium voltage switchgear (MVSG).

Upon the evaluation of this data, it is determined that SF₆, when used as an insulation medium, emerges not as a direct health and safety concern, but rather as a prominent environmental issue. This concern, however, comes with a caution, that it primarily relates to situations where MVSGs are not enclosed within confined spaces.

According to the results of 60 different scenarios in ALOHA[®] software, it has been determined that to pose a danger to human health and well-being it is necessary to release approximately 5 to 10 t of SF₆ gas in the air, for the ambient air it is 5 kg of SF₆ which is approximately half the volume of SF₆ in one MVSG. Therefore, evaluating the obtained data, SF₆ as an insulation medium is clearly an environmental problem, not a health and safety concern when the MVSGs are not in closed spaces.

In a typical MVSG, there is approximately 10 L of sulphur hexafluoride, and a typical urban location usually houses about 3 to 5 devices. Considering SF₆ has a density in the range from 6 to 6.5 kg m⁻³, this means that each litre of the gas has a mass from 6 to 6.5 g. The insulating gas is under a pressure of 20 kPa, with an estimated leak rate of 0.011 atm* cm³ h⁻¹. In Table II the densities of all observed SF₆ by-products are shown.²⁸⁻³⁰

The results of the most relevant scenarios that were modelled are shown in Table III.

TABLE III. Results of threat zone radiuses, r / m, for modelled scenarios for each compound

Compound	Treat zone		
	Red	Orange	Yellow
HF	19	26	112
SO ₂	13	79	133
SF ₄	60	141	335
SF ₅	36	240	562
SO ₂ F ₂	<10	13	18

On the other hand, the by-products of the SF₆ that are formed if SF₆ is in contact with a spark or direct flame render a completely different outcome with only 1 g of substance. Grams are used in ALOHA[®] software as a unit of measure to perform the risk assessment. For HF, a quantity of 1 gram (1449 cm³) of the gas produces a red TZ (RTZ) spanning 19 m in radius, while for SO₂, the same mass (381.7 cm³) of gas results in an RTZ of 13 m in radius. In the case of SF₄, 264.5 cm³ amounts to an RTZ of 60 m in radius, while the SF₅, with volume of

* 1 atm = 101325 Pa

only 185.9 cm^3 , creates an RTZ of 36 m in radius. Lastly, for SO_2F_2 , 1 g (268.8 cm^3) creates a red threat zone of less than 10 m in radius.

The stations and substations housing MVSG filled with SF_6 are strategically located in urban areas, often in close proximity to densely populated areas, a compelling concern emerges. This concern revolves around the potential and, in many cases, well-justified risk of exposure in the unfortunate event of SF_6 and its by-products leakage. The urban setting amplifies the seriousness of the situation, as any release of this insulating gas and by-products can directly impact the nearby populace. In such circumstances, the paramount security measure in place remains the continuous monitoring of the pressure levels within the insulating system.

Fig. 1 shows a preview of the red threat zone radiuses for every SF_6 by-product discussed in this research for a specific realistic layout of an urban area. The possible source of SF_6 and its by-products is on the ground level, surrounded by 8 to 10-storey buildings (approximately 25 to 36 m). In this figure, a real location has been observed and the obtained RTZ have been shown on the selected real location. The spacing of the buildings and the location of streets, as well as the playground portray the real location in one city in Serbia.

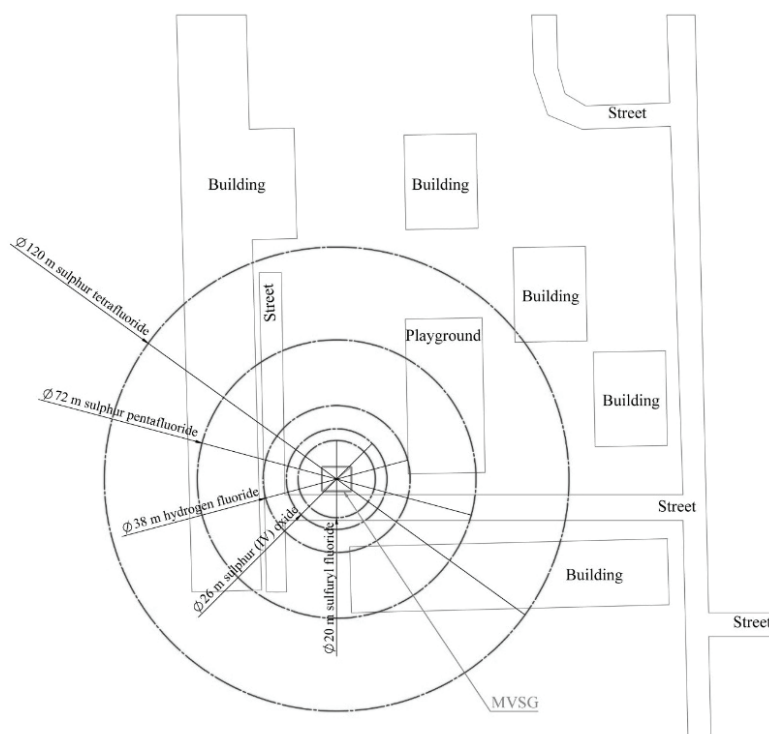


Fig. 1. A preview of the generated red threat zones (RTZ) for all SF_6 by-products in the urban area without impact of wind parameters (velocity and direction).

This type of research is the first in the area of MVSG using SF₆ as insulation gas and the potential risks to health and the environment in the Republic of Serbia. It opens the question and inquiry into the characteristics and the implications of SF₆ in this specific domain.

CONCLUSION

While SF₆ has several benefits that have helped it become a fixture in medium-voltage switchgear, its proven environmental effects, and risks, as well as the risk considering population, should not be neither underestimated nor ignored. Based on 60 scenarios in ALOHA[®] software, it's found that releasing 5–10 t of SF₆ gas poses a threat to human health. In open air, just 5 kg of SF₆ (half of a typical MVSG's volume) is enough to cause concern. This highlights SF₆ as an environmental issue, but not a health and safety hazard when MVSGs are outdoors. A typical MVSG has about 10 L of SF₆ in urban areas with 3–5 devices. SF₆ density ranges from 6–6.5 kg m⁻³. It's pressurized at 20 kPa, with a leak rate of 0.011 cm³ h⁻¹. In case of a spark or flame, SF₆ produces different by-products of only 1 gram in quantity. The ALOHA[®] software uses grams for the risk assessment. For example, 1 g of HF spans a 19 m radius RTZ, SO₂ a 13 m radius, SF₄ a 60 m radius, SF₅ a 36 m radius, and SO₂F₂ a <10 m radius.

The purpose of this paper is to conduct a risk assessment using the ALOHA[®] software to determine the likelihood and the possible effects of SF₆ and its by-products leaking from the medium-voltage switchgear. It has been observed that the current energy system layout in Serbia does not have any evacuation plans in place in case of an accidental release of SF₆ and its by-products. Furthermore, there are no early warning systems to detect any leakage, except for the pressure control in the chamber where SF₆ is stored. However, this can only be monitored through the network surveillance system and not on the site of the leakage itself.

This type of modelling can enhance the preparation and security by allowing the development of the evacuation and the minimization plans, as well as the improvement of the entire system.

The urban medium-voltage switchgear installations introduce a prominent element of concern due to the potential leakage. In response to this concern, a central security measure takes precedence: the continuous monitoring of pressure levels within the insulating system. This responsible surveillance acts as the first line of defence, mitigating risks associated with SF₆ in these urban settings, as well as serious and compulsory responses and guidelines for conduct, protection, and actions in the case of leaks. Consequently, a growing resolve has emerged within the industry to explore viable alternatives to SF₆. There is an increasing determination to investigate SF₆ alternatives that might deliver the benefits of SF₆, while avoiding the related hazards and risks. Meanwhile, stringent regul-

ations and routine maintenance can reduce many of the dangers connected with its usage. The only eco-efficient SF₆ alternative that shows promise to this date, other than air, which is already in use, is the HFO1234zeE (trans-1,3,3,3-tetrafluoropropene), as it has low, but more importantly, known toxicity and is not carcinogenic, mutagenic or reprotoxic.³¹ As the environmental issues of SF₆ properties are more prominent (*GWP* = 23,500), it seems promising that the new generation of environment-friendly gas insulation, like HFO1234zeE has extremely low *GWP* (6) and ozone depletion potential (*ODP* = 0).

Acknowledgement. The work was partially supported by the Ministry of Education, Science and Technological Development through project no. 451-03-68/2020-14/200156: “Innovative scientific and artistic research from the FTS (activity) domain”.

ИЗВОД

СУМПОР-ХЕКСАФЛУОРИД У МОДЕРНИМ СРЕДЊЕНАПОНСКИМ ПРЕКИДАЧИМА: ПРЕДНОСТИ, ОПАСНОСТИ И УТИЦАЈ НА ЖИВОТНУ СРЕДИНУ

АЛЕКСАНДАР БОШКОВИЋ¹, МАЈА СРЕМАЧКИ¹, СУНЧИЦА ВЈЕШТИЦА², АЛЕКСАНДРА ЧАВИЋ³,
НАДА МАРКОВИЋ¹ и БРАНИСЛАВ БОРОВАЦ¹

¹Универзитет у Новом Саду, Факултет техничких наука, Трт Доситејева Обрадовића 6, 21000 Нови Сад, ²Универзитет Метрополисен, Факултет за примењену екологију Фушера, Пожешка 83а, 11000 Београд и ³Факултет за економију и инжењерски менаџмент, ФИМЕК, Цветарска 2, 21000, Нови Сад

Сумпор-хексафлуорид синтетиче се као постојан и нетоксичан гас са изузетном диелектричном чврстином. У савременим средњенапонским прекидачима система за дистрибуцију електричне енергије, SF₆ се користи за изолацију и гашење електричног лука. Примена SF₆ има предности у погледу физичко-хемијских карактеристика и перформанси гаса; димензијама, економичности и поузданости опреме прекидача, те у трајању и трошковима одржавања који су значајно умањени. SF₆ је познат као гас стаклене баште који има тенденцију да се акумулира у плућима, изазивајући смањење концентрације кисеоника и узрокује респираторне компликације. Нуспроизводи SF₆ могу настати током електричног лука и могу бити штетни и токсични. У ЕУ и широм света опрема која садржи SF₆ као изолациони гас је у процесу замене. Користећи софтвер ALOHA[®] моделирани су сценарији за неконтролисано испуштање за SF₆ и нуспродукте у урбаним подручјима, где се најчешће постављају прекидачи. У подручјима где је циркулација ветра слаба (урбана подручја) у опасним ситуацијама није могуће ослонити се на висок ниво дисперзије или минимизацију концентрације и претње. Модели су показали да SF₆ представља опасност по животну средину, а његови нуспродукти и озбиљан hazard по здравље ако се неконтролисано испусте у урбаним срединама, стварајући црвену зону опасности од 10 до 60 m у полупречнику.

(Примљено 3. децембра, ревидирано 8. децембра 2023, прихваћено 2. фебруара 2024)

REFERENCES

1. W. T. Tsai, *J. Fluor. Chem.* **128** (2007) 1345
(<https://doi.org/10.1016/j.jfluchem.2007.06.008>)

2. C. T. Dervos, P. Vassiliou, *J. Air Waste Manage. Assoc.* **50** (2011) 137 (<https://doi.org/10.1080/10473289.2000.10463996>)
3. M. Maiss, C. A. M. Brenninkmeijer, *Environ. Sci. Technol.* **32** (1998) 3077 (<https://doi.org/10.1021/es9802807>)
4. *IPCC Task Force on National Greenhouse Gas Inventories*, <https://www.ipcc-nggip.iges.or.jp/public/gp/english/> (accessed 29.10.2023)
5. S. Kumar, S. Sanjay, B. P. Yadav, N. A. Siddiqui, S. Varadharajan, in *Advances in Industrial Safety. Springer Transactions in Civil and Environmental Engineering*. F. I. Khan, N. A. Siddiqui, S. M. Tauseef, B. P. Yadav, Eds., Springer, Singapore, 2020, p. 310 (https://doi.org/10.1007/978-981-15-6852-7_21)
6. Y. S. Son, S.J. Lee, C. Y. Choi, J. H. Park, T. H. Kim, I. H. Jung, *Radiat. Phys. Chem.* **124** (2016) 220 (<https://doi.org/10.1016/j.radphyschem.2015.11.016>)
7. A. Mete, P. Türkçüoğlu, S. Kimyon, K. Güngör, *Int. Ophthalmol.* **37** (2017) 1057 (<https://doi.org/10.1007/s10792-016-0336-y>)
8. M. N. Elmohamady, M. T. I. Khalil, A. S. M. Bayoumy, M. Rateb, H. M. Faramawi, *Eye* **35** (2021) 441 (<https://doi.org/10.1038/s41433-020-0867-3>)
9. R. Yang, M. Xu, J. Yan, M. Yang, Y. Geng, Z. Liu, J. Wang, *Energies* **14** (2021) 414 (<https://doi.org/10.3390/en14020414>)
10. *EUR-Lex, Access to European Union law*, <https://eur-lex.europa.eu/legal-content/EN/TXT/PDF/?uri=CELEX:32014R0517> (accessed 11.11.2023)
11. *UNCC Report of the Conference of the Parties on its twenty-seventh session*, <https://unfccc.int/documents/626564> (accessed 29.10.2023)
12. P. Forster, T. Storelvmo, in *Climate Change 2021: The Physical Science Basis*, V. Masson-Delmotte, P. Zhai, A. Pirani, S.L. Connors, C. Péan, S. Berger, N. Caud, Y. Chen, L. Goldfarb, M.I. Gomis, M. Huang, K. Leitzell, E. Lonnoy, J.B.R. Matthews, T.K. Maycock, T. Waterfield, O. Yelekçi, R. Yu, B. Zhou, Eds., Cambridge University Press, Cambridge, 2021, p. 2391 (<https://doi.org/10.1017/9781009157896.009>)
13. R. F. Weiss, J. Mühle, P. K. Salameh, C. M. Harth, *Geophys. Res. Lett.* **35** (2008) L20821 (<https://doi.org/10.1029/2008GL035913>)
14. Y.A. M. Alsumaidae, C. T. Yaw, S. P. Koh, S. K. Tiong, C. P. Chen, K. Ali, *Energies* **15** (2022) 6762 <https://doi.org/10.3390/en15186762>
15. N. Dorraki, K. Niayesh, *J. Phys. D: Appl. Phys.* **54** (2021) 255503 (<https://doi.org/10.1088/1361-6463/abf25a>)
16. Y. Fu, A. Yang, X. Wang, A.B. Murphy, X. Li, D. Liu, Y. Wu, M. Rong, *J. Phys., D* **49** (2016) 385203 (<https://doi.org/10.1088/0022-3727/49/38/385203>)
17. M. Xu, J. Yan, M. Yang, Y. Geng, Z. Liu, J. Wang, *AIP Adv.* **10** (2020) 095214 (<https://doi.org/10.1063/5.0018972>)
18. *USEPA Inventory of U.S. Greenhouse Gas Emissions and Sinks: 1990–2021*, <https://www.epa.gov/ghgemissions/inventory-us-greenhouse-gas-emissions-and-sinks-1990-2020> (accessed 11.11.2023.)
19. M. Meldrum, *Regul. Toxicol. Pharmacol.* **30** (1999) 110 (<https://doi.org/10.1006/rtph.1999.1342>)
20. W. T. Tsai, *J. Environ. Sci. Health, C* **28** (2010) 125 (<https://doi.org/10.1080/10590501.2010.481806>)
21. C. T. Dervos, P. Vassiliou, *J. Air Waste Manage. Assoc.* **50** (2000) 137 (<https://doi.org/10.1080/10473289.2000.10463996>)

22. C. Heaviside, C. Witham, S. Vardoulakis, *Sci. Total Environ.* **774** (2021) 145549 (<https://doi.org/10.1016/j.scitotenv.2021.145549>)
23. P. Füle, G. Kristóf, *J. Wind. Eng. Ind. Aerodyn.* **179** (2018) 407 (<https://doi.org/10.1016/j.jweia.2018.06.015>)
24. R. Yadav, S. Chaudhary, B. P. Yadav, S. Varadharajan, S. M. Tauseef, in *Advances in Industrial Safety, Springer Transactions in Civil and Environmental Engineering*, F.I. Khan, N.A. Siddiqui, S.M. Tauseef, B.P. Yadav, Eds., Springer, Singapore, 2020, p. 310 (https://doi.org/10.1007/978-981-15-6852-7_14)
25. J. Bondžić, M. Sremački, S. Popov, I. Mihajlović, B. Vujić, M. Petrović, *J. Environ. Manage.* **293** (2021) 112941 (<https://doi.org/10.1016/j.jenvman.2021.112941>)
26. World Weather, https://world-weather.info/archive/serbia/novi_sad/ (accessed 09.11.2023.)
27. Weather Atlas, <https://www.weather-atlas.com/en/serbia/novi-sad-climate> (accessed 09.11.2023.)
28. CAMEO[®] Chemicals, <https://cameochemicals.noaa.gov/> (accessed 09.11.2023.)
29. NIST Chemistry WebBook, SRD 69, <https://webbook.nist.gov/chemistry/> (accessed 12.11.2023.)
30. National Library of Medicine, PubChem, <https://pubchem.ncbi.nlm.nih.gov/> (accessed 12.11.2023.)
31. J. Wang, Q. Li, H. Liu, X. Huang, J. Wang, *J. Mol. Graph. Model.* **100** (2020) 107671 (<https://doi.org/10.1016/j.jmglm.2020.107671>).



J. Serb. Chem. Soc. 89 (5) 705–714 (2024)
JSCS–5750

Performance indicators model assessment for water system quality and supply in Montenegro

OLIVERA DOKLESTIĆ^{1,2}, MIRJANA VOJINOVIĆ MILORADOV¹, NATAŠA ELEZOVIĆ³, SRĐAN KOLAKOVIĆ^{1*} and NENAD SIMEUNOVIĆ¹

¹Faculty of Technical Sciences, University of Novi Sad, Trg Dositeja Obradovića 6, 21000 Novi Sad, Serbia, ²Ekoboka project ltd., Herceg Novi, Montenegro, Kralja Tvrtka no. 3, 85340 Herceg Novi, Montenegro and ³Faculty of Technical Sciences, University of Priština in Kosovska Mitrovica, Knjaza Miloša 7, 38220 Kosovska Mitrovica, Serbia

(Received 6 December, revised 13 December 2023, accepted 2 February 2024)

Abstract: The paper researches water quality, supply and management system assessment problems of the Montenegrin coastal region. A significant problem is generated by seasonal tourism, the main branch of Montenegrin coastal economy. The selected performance indicators model has been tested in the water supply system of the city Herceg Novi, as a representative experimental system for the Montenegrin coastal area. The city Herceg Novi has 33.000 permanent residents and around 80.000 individual consumers during the summer touristic season. The research activities are based on the seasonal parameters defined by the monitored performance indicators of the water supply system. The study depicts the developed indicators performance model based on the obtained experimental monitoring data. Within the experimental analytical research performance an indicator matrix was established. The coastal area of Montenegro is experiencing over 50 % of water loss. Structure developed in the model applies the performance indicators and results in systematic losses reduction. The model takes into account the principle of seasonality, and the existence of two completely different periods of the year. This type of the experimental research with testing *in situ* was for the first time performed and implemented in the coastal Adriatic region of Montenegro.

Keywords: water quality; aquatic system model; model assessment.

INTRODUCTION

The management of water supply systems in Europe and developed countries has been constantly improving through the last three decades. The development has been predominately focused on the rational use of natural water resources, and water losses using different methods and mechanisms, technical and

* Corresponding author. E-mail: kolak@uns.ac.rs
<https://doi.org/10.2298/JSC231206009D>

administrative nature. The experimental activities apply a performance indicator matrix to the management of water supply systems, or systems in one region with similar basic parameters, starting from natural environmental conditions, through technical elements, to relations with other industries on which water production and consumption depend.

Tourism industry must be taken into account when planning water supply system in coastal regions. In water project management it is obligatory to keep in mind that the touristic activities are a very demanding and fluctuations in the required continuous water supply are the primary factors affecting beneficial economic development. The lack of regular water supply to consumers can have significant and large repercussions on the development of the tourism economy. The primary task in the tourist environment is the continuous supply of water all 365 days of the year, considering the peaks of high consumption, which occur at least twice a day.

The control assessment of the water supply companies in coastal regions implies the responsibilities for overcoming complex situation between the produced and the needed quantities of water. The solution for the complex interdisciplinary problem is of interest to many experts and institutions in the Mediterranean region, particularly where tourism is the dominant industry. Experiences from practice and studies in the Adriatic basin, as well as in the Mediterranean countries, such as the coastal parts of Spain, Italy, Portugal, regions similar to Montenegrin coast, were applied. In the "Water Management Strategy of Montenegro" new and modern approach to water resources management was applied, harmonizing laws with the legislation of the European Union and ratified international conventions and declarations.¹ The operational aspect of the "Water Management Strategy of Montenegro" has been set for 2035, with the main strategy to reduce losses in public water supply systems to less than 30 %. In the Coastal Region of Montenegro, water supply systems are characterized by a high percentage of unaccounted water losses (non-revenue water, NRW), above 50 %. The percentage of unaccounted water is in agreement with the administrative and technology management policy.

The matrix performance indicators have been established as the optimal algorithm and mechanism to control the operation of the water supply system. Performance indicators (*PI*) provide a set of measures to monitor and improve water supply services to consumers (developed theory of the *PI* use in water systems).²⁻⁴ In the last twenty years, the significant progress has been made in the application of *PI* research. *PI* knowledge has been significantly expanded as the water supply system has been implemented in Mediterranean countries.⁵ The system has proven that it can be adapted and used in very different contexts and for a variety of purposes.⁶⁻⁹

In the technological, economic and ecomanagement field of water supply systems, *PI* model classifies types in the sphere of losses, defines methodology for detection and reduction in the system. In coastal regions the highlight and emphasize is on seasonal fluctuations in available water resources and water consumption.

Remarkable experiences from the Italian practice for urban areas in the case of insufficient water or in the case of climatic arid areas (town Ferragina) are valuable, with focus on the terms which included the loss analysis and applicable calculation.^{5,9} To analyse the losses in the system, it is significant to recognize the water balance with all structural components of the system.^{8,10} The components of the water balance, on the other hand, must be determined in volumetric form before beginning any loss reduction activities. The conserving water in local conditions usually means reducing the volume of water for one or more purposes. The concept of “water conservation” improves quality and capitalizes social, touristic, technological, public, economic and environmental benefits.^{6,8}

The research aims to determine the model for adaptability and improvement of water quality and supply systems in the coastal region, where high technical water losses are evident. The *PI* model has been tested in the coastal area of Montenegro with six selected corresponding municipalities. The regional water supply system of the Montenegrin coast reimburses insufficient quantities in local water resources when required.

The experimental research is oriented on the water quality and supply system management with increasing efficiency, reduction of the unaccounted water percentage, and rational use of water resources.

EXPERIMENTAL

The assessment of water supply, supplementary conditions and problems was conducted for the coastal region of Montenegro in six municipalities: Herceg Novi, Kotor, Tivat, Budva, Bar and Ulcinj including about 140000 permanent residents. In 2019, a total of 14.45 million overnight stays were registered for the entire territory of Montenegro, in various types of accommodation services, of which 85 % stayed in the coastal region. The number of tourists and the number of overnight stays, is growing from year to year.

In the research activities, data for comparative analysis, assessment and modelling was obtained from local water supply companies of the coastal region of Montenegro. All the data is collected through the monthly reports and edited by “Vodacom”, a joint management enterprise for six water supply companies in the coast. The state Energy Regulatory Agency is in charge of monitoring the water supply companies in Montenegro, and the data is provided by yearly reports.¹¹⁻¹⁵ Apart from statistical data, which are published by both institutions in a monthly or annual summary report, there are no available information and research papers dealing with analysis of parameters, performance indicators, considering causes and consequences, as well as the of specific chemical and environmental characteristics in management system assessment.

PI model design

The *PI* model was prepared for the water supply system based on the assessment of positive and negative factors in the operational phase of existing structures in the coastal region, with two highly differentiated periods of the year. The research included the SWAT analyses.¹⁶ The model creates approximate representation of the system and process management, with a goal to improve the performance of the active water supply system. Modelling comprises the creation of the basic *PIs* matrix with more than 50 *PIs*. The decisive *PIs* for the water supply systems management are covered in Table I.

TABLE I. Performance indicators for application in the water system management

<i>PI</i> No.	Description of the indicator
<i>PI1</i>	Coverage of water supply service by number of connections (%)
<i>PI3</i>	Water production per consumer (m ³ /consumer/month)
<i>PI4</i>	Water production per connection (m ³ /connection/month)
<i>PI5</i>	Water consumption per user (m ³ /consumer/month)
<i>PI6</i>	Water consumption - households (l/s/d)
<i>PI7</i>	Water consumption-households (m ³ /consumer - households/month)
<i>PI8</i>	Water consumption - economy (m ³ /consumer/month)
<i>PI9</i>	Percentage of reported water consumption for households in relation to the total measured amount of water consumed (%)
<i>PI10</i>	Percentage of water consumption for the economy in relation to the total measured amount of water consumed (%)
<i>PI13</i>	Percentage of non-revenue water in the total amount of water produced (%)
<i>PI14</i>	Volume of non-revenue water expressed per user per day (m ³ /p/m)
<i>PI15</i>	Non-revenue water per km of network per day (m ³ /km/day)
<i>PI16</i>	Unit electricity consumption per m ³ of invoiced water (kWh/m ³)
<i>PI19</i>	Number of failures per 1000 consumers
<i>PI20</i>	Number of failures per km of water supply network (breakdowns/km)
<i>PI21</i>	Average duration of failures (number of hours spent/total number of failures)

The water supply system model is defined by the expert system and experience from practice and application of the abstraction mechanism. The abstraction provides elements, variables, parameters and characteristics crucial for achieving the objective, while all other are neglected. The experience contributes in expanding the theoretical platform with known parameters by applying performance indicators. After theoretical consideration, the model should provide directions and guidelines for improving the practical operational state of the water supply system. The model expresses the complex and physical reality in mathematical system quantifying calculations in order to recognize risks and uncertainties. The application of the model minimize uncertainties and risks by replicating real circumstances and adjusting theoretical and practical parameters. Water supply systems are highly dynamic, variable in both spatial and temporal parameters and constantly adjusting the extent and the scope. The only constant in the system is volume of the tank, with the fluctuating water level, which adds another variable in system. Network extensions on the basis of newly built pipelines are part of the extrapolation of the network, as well as new water supply facilities. The changes in the pipeline network are in smaller strokes, considering the time intervals of the change. The quantities of water entering and leaving the system, number of failures, water gauges, interventions and other activities are considered as variables in the model. Selected variables

arrange a basic parameters matrix as a structural component of the water supply system mathematical model. Seasonal disproportion is an imperative characteristic of the coastal region, the starting point in performance indicators model.

The water supply system is modeled in the mathematical correlation $VS = \{E, V, F\}$ where VS is water supply system, E is a set of the most important elements of the system, V is set of connections and F is a function of the target system. E is defined as a set of primarily important elements consists of variables and constants in the water supply system: the length of water supply network, number of consumers, number of water gauges, number of tourists, quantity of produced water, quantity of consumed water, number of network failures. V is determined by set of connections of key performance indicators ($PI1, PI3, PI4, \dots, PI21$). F indicates the function of the system to reduce losses, *i.e.*, the percentage of unaccounted for water, and to provide sufficient and necessary amount of water (in the tourist season).

Essential premise of the model is the observation of the water supply system and functioning through two periods of the year (winter and summer).

Very complex and dynamic structure of the mathematical management model depicted in Fig. 1 with two distinguished annual periods, suggests the introduction of two operational subsystems for winter and summer. Both subsystems introduce fundamental characteristics: the amount of water produced and consumed, and the number of network failures and technical water losses. System is defined by variables: the amount of produced and consumed water in system, and the number of failures as a multiplier (n), which has a value of $n > 1$. Summer variables are compared to the variables of the winter functional system. Total water losses in the system are technically lower in summer than in winter, defining the multiplier as summer/winter, $n < 1$. In general, the characteristic of the entire Montenegrin coast is that the amount or volume of water produced in local resources in winter is much higher than in summer, and inversely proportional to water needs. The multiplier of produced water, for the amount available for entering the system, is: $V_{winter}/V_{summer} > 1$.

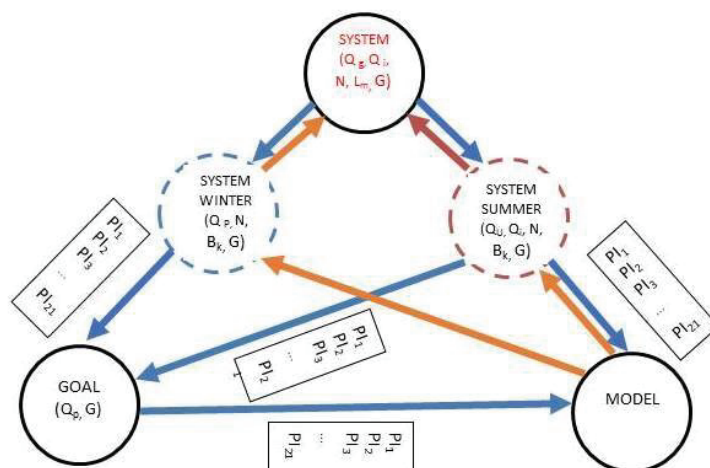


Fig. 1. Schematic mathematical model of a water supply system.

The system performance indicators, as indicators of status and change, indicate the functionality of the system, and their comparison in time frames identifies monthly and seasonal

changes. The mathematical model was reduced on the matrix of seventeen key indicators: *PI1*, *PI3*, *PI4*, *PI5*, *PI6*, *PI7*, *PI8*, *PI9*, *PI10*, *PI13*, *PI14*, *PI15*, *PI16*, *PI19*, *PI20* and *PI21*. Indicators are a relation that organizes pulsing signal, pointing out what needs to be corrected in order to improve the functionality and efficiency of the system.

Each subsystem aspires to a defined objective, and the status is analytically expressed by PIs. The function of the model is to modify the subsystems, based on the facts, ignoring problems from the real system, which often neglect crucial information. The flow of system dynamics is defined based on the real structure, from the intent to the model, and then modifying the elements again, for the next iterative cycle, which reduces losses in the system. The objective is transformed into a time function of reducing technical losses to an acceptable level of up to 30 % during the summer, since everything in the tourist region is subordinated to the summer and the supply of touristic facilities.

Technical losses in the winter are a completely different in comparison with the summer. Winter season characteristics are too much water, not enough consumers, pressures increased to high levels. In winter period, the operation of the maintenance teams on the network is important for repairing failures and damage to pipelines, installation of valves to reduce pressures, and discharging out of the system all unnecessary quantities before entering the distribution system. It is vital to reduce the technical losses in the winter as well, as the ratio of produced and consumed water.

RESULTS AND DISCUSSION

The key indicators for analysing the state of the water supply system, defined in Table I are: *PI1*, *PI3*, *PI4*, up to *PI20* and *PI21*. *PIs* are related to water production and consumption, grid failures, non-revenue water and electricity consumption. WSM benchmarking, as a set of performance indicators, provides relevant data for the system. Table II defines the key *PI* for the period between 2015–2019 with seasonal identification, for winter, W, and summer, S, period. Water consumption is growing yearly (*PI5*, *PI6*, *PI7*, *PI8*) indicating the tourism industry and household consumption twice higher in the summer than in the winter.

The significant seasonal deviations are evident in the Table II showing that seasonal observation is justified. Indicators differ from each other in almost all elements of the water supply network functioning, in the entire water supply system. Very differentiated indicator values are obtained: *PI13*, *PI14* and *PI15* for unaccounted water and network losses by season (winter 81.81 and summer 71.79).

The percentages of the unaccounted water from 2015 to 2019, imply a declining trend, as 2019 is with more favourable coefficients for the winter 80.76, and for the summer 69.06 period.

The ratio of unaccounted water summer:winter is calculated as 0.86 and is adopted as the index of seasonal balance in unaccounted water. The correlation is used in calculations when designing pipelines, and when adopting the relevant diameters in the sizing of pipelines, starting from the fact that in the summer, when consumption is higher, more water is in circulation and less pressure.

TABLE II. Key performance indicators, observed by season for 2015–2019 for the water supply system of Herceg Novi

<i>PI</i>	2015		2016		2017		2018		2019	
	W	S	W	S	W	S	W	S	W	S
<i>PI1</i>	95.63	95.76	96.04	96.04	96.16	96.16	96.21	96.27	96.39	96.39
<i>PI3</i>	51.66	54.35	44.37	56.32	46.73	57.02	42.08	52.17	42.36	53.06
<i>PI4</i>	84.00	88.54	72.00	91.37	72.28	94.37	66.12	81.77	67.51	84.56
<i>PI5</i>	16.69	15.27	7.58	15.30	7.51	15.66	10.38	21.05	7.83	16.25
<i>PI6</i>	143.02	280.47	138.16	278.30	137.51	292.83	145.23	297.18	139.65	284.65
<i>PI7</i>	6.56	12.81	6.32	12.58	6.29	13.31	11.09	17.15	6.26	12.87
<i>PI8</i>	25.70	48.94	24.72	52.71	22.66	41.89	42.93	80.66	29.97	63.82
<i>PI9</i>	77.89	78.22	78.03	76.77	79.24	78.63	78.67	76.71	74.41	73.61
<i>PI10</i>	22.11	21.78	21.97	23.23	20.76	21.37	21.33	23.29	25.59	26.39
<i>PI13</i>	84.45	71.10	82.67	73.26	83.80	73.06	82.05	69.77	81.50	69.06
<i>PI14</i>	43.79	39.08	36.80	41.02	38.83	42.22	60.82	42.26	34.52	36.78
<i>PI15</i>	103.65	92.08	88.38	98.16	93.72	101.76	81.74	85.40	82.90	88.25
<i>PI16</i>	0.86	0.80	0.79	0.68	0.84	0.72	0.67	0.41	0.45	0.54
<i>PI19</i>	4.75	9.48	5.14	7.29	5.26	8.70	5.19	8.59	5.14	7.78
<i>PI20</i>	0.33	0.66	0.36	0.51	0.37	0.62	0.39	0.61	0.38	0.56
<i>PI21</i>	4.54	3.68	5.12	3.82	4.58	3.87	5.25	6.07	4.68	4.26

The *PI* Table II displays that the amount of water lost is significantly lower in summer than in winter. In the experimentally tested coastal region of Montenegro it is evident that the development of water supply systems happens mostly spontaneously and deteriorated over time, pipes are very damaged or remained trapped by subsequently built facilities. Interpolations and extrapolations of the water supply network were not accompanied by the adequate hydraulic checks of the pipeline network parameters, which is reflected in high network pressures (between 6 and 12 bar) and frequent cracks and occurrences of various damages in the network.

Indicator *PI3* and *PI5* are the basic seasonality indicators for the water supply system. The ratio of available (produced) and required (consumed) water in the system indicates the unused amount of water. Indicator *PI13* (percentage of non-revenue water in the total amount of water produced) is an indicator of the lost amount of water, which did not reach the consumer, *i.e.*, which is not registered on water gauges. In 2015 and 2016, there were regular restrictions on water supply, during the summer months, June–August, while this was not the case in 2018–2020, although the amount of water available in the system was the same. However, the difference was made by the increased degree of intervention in the repair of network failures, increased mobility, throughout the year, continuously, which was not the practice previously. *PI15* has a downward trend, with a difference from 2015–2019 of $103.65 - 82.90 = 20.75 \text{ m}^3 \text{ km}^{-1}$ per day in summer. The significant reduction is also noteworthy in winter $13.51 \text{ m}^3 \text{ km}^{-1}$ per day.

The scheme presented in Fig. 1 provides a simplified methodology for the application of indicators, with the greater the number of indicators included in the analysis, the closer the results are to the real situation, and thus the easier it is to achieve the goal of improvement.

The indicators *PI19*, *PI20* and *PI21* deal with the number of network failures per 1000 consumers, the number of failures per km of water supply network and the average duration of fault repair. Construction works performed over the pipelines are the most common reason for damage.

Indicators are not just criterion of the current state of the water supply system, but imperative for the necessary changes in the system through management.

In the Coastal region of Montenegro, parameter of water losses in the system are much less important in the off-season. The available amount of water in all local water system exceeds the needs of consumers. Non-revenue water is important because of the electricity consumption in pressure subsystems, while the fact of losing the amount of water is not important. The separation of indicators by seasons demands rational needs of water production, electricity consumption, the necessary design of water supply network with accompanying facilities: pumping and hydrophore stations and reservoirs, different profiles, for summer and winter period. The *PIs* indicate need for circular, extensive design, with two pipelines (for winter and summer supply) as rational and beneficial solution.

CONCLUSION

The coastal area of the Montenegro is a challenging tourist region with distinct peaks in water consumption in the summer season compared to the rest of the year. *PI* model matrix is assembled on the experimental data for water supply systems (summer and winter) and includes parameters of water production and consumption, number of grid failures, unaccounted for water losses. The WMS benchmarking defines necessity to introduce seasonal analyses, the ratio of touristic and off season, when water resources are at minimum and maximum. Since the tourist season is not year-round, but lasts intensively in the period May–September, when water resources are at a minimum and consumption is at a maximum. The period is representative for analysing the system and observing the matrix of performance indicators. The treatment of water loss issues is different from the aspect of seasonality.

Current Montenegrin coastal region practice in water supply, neglect the issues and significance of seasonality concept, while the *PI* model through the research indicates importance for use.

The indicators performance model assessment for water system management in the coastal region of Montenegro was for the first time effectively performed with the depiction of unique and effective management plan.

ИЗВОД

ПРОЦЕНА МОДЕЛА ИНДИКАТОРА ПЕРФОРМАНСИ КВАЛИТЕТА И ВОДОСНАБДЕВАЊА У ЦРНОЈ ГОРИ

ОЛИВЕРА ДОКЛЕСТИЋ^{1,2}, МИРЈАНА ВОЈИНОВИЋ МИЛОРАДОВ¹, НАТАША ЕЛЕЗОВИЋ³,
СРЂАН КОЛАКОВИЋ¹ и НЕНАД СИМЕУНОВИЋ¹

¹Факултет техничких наука Универзитета у Новом Саду, Трт Доситејева Обрадовића 6, 21000 Нови Саг, ²Екобока пројекат лнд, Краља Тврђика 3, 85340 Херцег Нови, Црна Гора и ³Факултет техничких наука, Универзитета у Приштини са привременим седиштем у Косовској Митровици, Књаза Милоша 7, 38220 Косовска Митровица

Истраживање приказује проблеме квалитета и управљања у систему водоснабдевања црногорског приморја. Значајан проблем је сезонски туризам, главна грана црногорске приморске привреде. Примењени модел индикатора перформанси тестиран је у систему водоснабдевања града Херцег Новог, као репрезентативног експерименталног примера за црногорско приморје. Град Херцег Нови има 33.000 сталних становника и око 80.000 индивидуалних потрошача током летње туристичке сезоне. Истраживачке активности су засноване на сезонским параметрима дефинисаним праћеним индикаторима перформанси система водоснабдевања. Рад приказује модел индикатора перформанси развијен на реалној матрици, а тестиран на примеру водовода у Херцег Новом. У оквиру експерименталног аналитичког истраживања креирана је матрица индикатора перформанси. Услед сезонских варијација, бележи се преко 50 % губитака воде у приморју Црне Горе. Структура развијена у моделу примењује индикаторе перформанси и резултира систематским смањењем губитака. Модел се базира на принципу сезонских варијација, два потпуно различита периода у години. Експериментално истраживање са тестирањем *in situ* први пут је спроведено у приморском јадранском региону Црне Горе.

(Примљено 6. децембра, ревидирано 13. децембра 2023, прихваћено 2. фебруара 2024)

REFERENCES

1. M. of A. and R. D. Government of Montenegro, *Water Management Strategy of Montenegro*, Ministry of Agriculture and Rural Development, Podgorica, 2017 (in Montenegrin)
2. H. Alegre, M. do Céu Almeida, *Strategic Asset Management of Water Supply and Wastewater Infrastructures*, IWA Publishing, London, 2009, (<https://doi.org/10.2166/9781780401720>)
3. H. Alegre, J. M. Baptista, E. Cabrera, F. Cubillo, P. Duarte, W. Hirner, W. Merkel, R. Parena, *Performance indicators for water supply services*, IWA Publishing, London, 2006
4. R. Parena, *Performance Indicators for Water Supply Services*, IWA Publishing, London, 2000
5. M. Scoullou, E. Ferragina, C. Narbona, *Environ. Sustain. Dev. Mediterr.* (2010) 53 (http://www.iemed.org/observatori-es/arees-danalisi/arxiu-adjunts/10-papers-for-barcelona-2010/8-environmental-and-sustainable-development-in-the-mediterranean/ferragina_8.pdf)
6. M. Oberascher, M. Möderl, R. Sitzenfrei, *Water* **12** (2020) 3446 (<https://doi.org/10.3390/w12123446>)

7. A. O. Lambert, T. G. Brown, M. Takizawa, D. Weimer, *J. Water Supply Res. Technol.* **48** (1999) 227 (<https://doi.org/10.2166/aqua.1999.0025>)
8. H. E. Mutikanga, S. K. Sharma, K. Vairavamoorthy, *J. Water Resour. Plan. Manag.* **139** (2013) 166 ([https://doi.org/10.1061/\(ASCE\)WR.1943-5452.0000245](https://doi.org/10.1061/(ASCE)WR.1943-5452.0000245))
9. H. Mutikanga, S. Sharma, K. Vairavamoorthy, E. Cabrera, *J. Water Supply Res. Technol.* **59** (2010) 471 (<https://dx.doi.org/10.2166/aqua.2010.066>)
10. C. Bozkurt, M. Firat, A. Ates, S. Yilmaz, O. Ozdemir, *Sigma J. Eng. Nat. Sci. – Sigma Mühendislik ve Fen Bilim. Derg.* **40** (2022) 310 (<https://doi.org/10.14744/sigma.2022.00035>)
11. Vodacom, *Annual report on business indicators of water supply and sewerage companies, report for 2017*, 2018
12. Vodacom, *Annual report on business indicators of water supply and sewerage companies, report for 2018*, 2019
13. Vodacom, *Monthly Report on Performance Indicators of Water Supply and Sewerage Companies for February 2018*, 2018
14. Vodacom, *Annual report on business indicators of water supply and sewerage companies, report for 2019*, 2020
15. Vodacom, *Monthly Report on Business Indicators of Water Supply and Sewerage Companies for August 2018*, 2018
16. N. Elezovic, D. Komatina Ilic, I. Dervisevic, S. Ketin, P. Dasic, *Fresenius Environ. Bull.* **27** (2018) 2505.



J. Serb. Chem. Soc. 89 (5) 715–727 (2024)
JSCS–5751

Cadmium and lead flow analysis as a decisions support data for waste management

NIKOLINA Ž. TOŠIĆ¹, MARKO Z. MUHADINOVIĆ², MILJAN Z. ŠUNJEVIĆ^{1*},
ILIJA P. ČOSIĆ¹ and NEMANJA S. STANISAVLJEVIĆ¹

¹University of Novi Sad, Faculty of Technical Sciences, Department of Environmental Engineering and Occupational Safety and Health, Trg Dositeja Obradovića 6, Novi Sad, Serbia and ²Lafarge BFC Srbija d.o.o. Beočin, Trg Beočinske fabrike cementa 1, Beočin, Serbia

(Received 6 December 2023, revised 3 January, accepted 7 March 2024)

Abstract: Striving for EU membership, the Republic of Serbia must adjust its waste management practices to comply with EU directives, including targets to reduce biodegradable waste disposal in landfills, as outlined in its Waste Management Program 2022–2031. Cadmium and lead, two highly toxic heavy metals, that are present in municipal solid waste, can pose high environmental and human health threats if not properly managed. The research evaluates how different technologies for biodegradable waste treatment influence the transformation of cadmium and lead flows through waste management systems. Hence, two waste management scenarios were modelled and developed for the Republic of Serbia, where the flows of cadmium and lead are monitored. The results indicate the differences between quantities and concentrations of cadmium and lead emitted in environmental media, thus confirming the various impacts of different waste technologies on achieving the vital goal of waste management – protection of the human health and the environment. The research concludes the crucial role of the versatile approach, where the quality of waste management outputs is highlighted.

Keywords: heavy metals; materials; quality; flow scenarios; substance flow analysis.

INTRODUCTION

The importance of the quantitative aspect has been defined – the greater the amount of waste removed from natural habitats, the greater the benefits for both human health and the environment.¹ Nevertheless to achieve effective, goal-oriented waste management an equal emphasis on both quality and quantity of waste management is fundamental.^{2,3} It is crucial to treat waste in a way that pro-

*Corresponding author. E-mail: msunjevic@uns.ac.rs
<https://doi.org/10.2298/JSC231206027T>

protects the environment and human health, since even small amounts of hazardous substances can have serious adverse short and long term effects.¹ From the waste to resource point of view, the impurities in the circular waste management system can significantly affect the re-use of waste as a resource. This indicates the need for the approach that is also oriented towards understanding the vital substances through waste management systems. Hence, two waste management scenarios were developed for the Republic of Serbia, where the flows of cadmium and lead are monitored.

Republic of Serbia, in its capacity as a candidate country for European Union (EU) membership, is anticipated to adopt solid waste management strategies that align with the directives established by the EU. According to the Waste Management Program of the Republic of Serbia for the period 2022–2031, the target values for reducing the disposal of biodegradable waste at landfills are defined.⁴ The specific objective is to reduce the disposal of biodegradable waste in landfills by 75 % of the total amount generated in 2008 by the year 2028. The ultimate goal is to reach a 50 % reduction by the end of 2032 and a 35 % reduction by the end of 2039. The Program envisions the construction of a comprehensive biodegradable waste diversion infrastructure by 2037, and it is anticipated that a significant period of adjustment will be necessary to ensure these systems operate in compliance with the established standards.

The fulfilment of the goals related to reducing the quantity of biodegradable municipal waste deposited in landfills, according to the Landfill Directive (1999/31/EC), does not provide insight into the quality of waste management. Hence, given the misalignment between the objectives of the directive and waste management goals, an examination was conducted to assess the impact of waste management models in accordance with the directive. More specifically, the aim was to comprehend how these models affect the core objective of waste management. The key waste management goal is inter and intra disciplinary and encompass protection of human health and the environment.^{5,6} To fulfil this objective, a key focus on individual elements is essential, as they play a pivotal role in determining environmental impacts and resource potential. In the realm of waste management, effective decision-making necessitates well-defined objectives, suitable methodologies, and accurate data of known uncertainty. Having adequate and sufficient information regarding waste composition is essential to monitor and control the transformations that occur during waste treatment.⁷ The background knowledge is crucial, as certain substances play a significant role in determining whether waste holds resource potential or is considered hazardous material.⁸

Cadmium and lead rank as the most toxic heavy metals, representing substantial threats to both human health and the environment. Prolonged cadmium exposure can result in a spectrum of health complications, encompassing kidney disorders, hypertension, and lung emphysema. Lead can inflict severe damage

upon the central nervous system, activating a variety of symptoms, from irritability and cognitive impairment to the onset of encephalopathy.⁹ Burnley has shown that implementing an integrated waste management strategy effectively diverts lead and cadmium from the environment using appropriate treatment technologies.¹⁰ Products manufactured decades or even a century ago often contain legacy substances that are now considered toxic or banned, with cadmium and lead being the most significant among them, directing their proper management.⁸ Every year, a broad spectrum of new consumer products is being introduced, marked by multiplex chemical compositions and they may include novel hazardous substances not previously utilized. The role of waste management extends beyond the provision of resources derived from waste involving handling non-useful and hazardous substances by facilitating their proper transformation and directing them toward sustainable, long-term disposal solutions.^{11,12} Adequate waste management is achieved by “clean” recycling materials for substituting primary materials, inert residues suitable for safe disposal, and maintaining emissions into the environment at acceptable levels.¹³

The two original areas of material flow analysis (MFA) application are analysing city metabolism and analysis of pollutant pathways in regions. Over time, MFA has been widely adopted in various fields, such as process control, waste and wastewater treatment, agricultural nutrient management, water quality management, resource conservation and recovery and more.¹⁴ Stanisavljevic and Brunner developed waste management scenarios that were quantitatively assessed using substance flow analysis.¹⁵ Additionally, similar topics were addressed by Astrid *et al.*, presenting the Austrian waste management system, and Arena *et al.*, applying a substance flow analysis approach in Italian areas.^{16,17} This research models two potential future waste management systems in the Republic of Serbia and applies material flow analysis and substance flow analysis (Pb and Cd) to indicate the impact on waste management goal (protection of human health and the environment). Improved waste management systems were modelled in order to monitor the future flows of heavy metals through waste management systems and to indicate how different biowaste treatment technologies influence the fulfilment of the most important waste management goal.

EXPERIMENTAL

Materials and methods

MFA, based on the fundamental principle of mass balance, is a systematic assessment of material flows and stocks within a specified system, encompassing spatial and temporal boundaries. The MFA calculations were performed using modern and sophisticated tool STAN 2.6 software.¹⁸ Furthermore, in addition to MFA, the term substance flow analysis (SFA) is occasionally used.¹⁴ SFA represents a type of MFA that only applies to a specific substance within a system and is based on the input flow of a substance, the flow of which can be followed through system in order to define output flows. It is a comprehensive tool for

evaluation the effectiveness of a unit treatment or entire waste management system in achieving waste management goals. Information acquired through SFA is crucial for evaluating the flows of substances within the waste management system. SFA focuses on monitoring the transformations that occur to wastes during their treatment, encompassing both valuable and hazardous substances.¹⁵

The mass-balance principle applies to systems as well as processes. In accordance with the mass-balance principle, the total mass of inputs entering a process is equivalent to the combined mass of outputs from that process, along with a stock term accounting for the accumulation or depletion of materials within the process. It is elucidated through the following equation:

$$\sum_{ki} \dot{m}_{input} = \sum_{ko} \dot{m}_{output} + \dot{m}_{stock} \quad (1)$$

where ki – number of input flows, ko – number of output flows, \dot{m}_{input} – mass of input flows, \dot{m}_{output} – mass of output flows and \dot{m}_{stock} – mass of stocks.

The sink indicator, as elucidated by Kral *et al.*, serves as a powerful tool for quantifying the proportionate mass of a specific substance considered environmentally acceptable within the framework of waste and emission flows.¹¹ This indicator represents the ratio between the amount of environmentally acceptable and unacceptable flows and sinks and defines the best possible scenario outcome. The innovative concept is defined on a scale ranging from 0 %, representing the worst-case scenario, to 100 %, denoting the best-case scenario. Kral *et al.* developed and provided a detailed explanation of the sink indicator concept, laying the foundation for its application in environmental assessments. The sink indicator formula is expressed as the ratio of the sum of acceptable flows to the sum of actual flows, multiplied by 100 to represent the result as a percentage:

$$\lambda = \frac{100Fa}{F} \quad (2)$$

where λ – the sink indicator (%), Fa – the sum of acceptable flows and F – the sum of actual flows.

Calculating the sink indicator requires the following information:

- The actual flows which are determined by SFA results
- The critical flows refer to the specific levels of cadmium and lead, that are considered to be of significant concern due to their potential impact on human health. In accordance with legislative values for Pb and Cd for the leachate from landfills¹⁹ and for compost material,²⁰ these critical levels are defined by legislation and represent a threshold beyond which the risks are considered unacceptable. This is the level that regulatory authorities have determined to be safe for human health and the environment.
- The acceptable flows correspond to the lower of the actual flows and the critical flows.

Modelling approach

The Waste Management Program of the Republic of Serbia has set target values for reducing the disposal of biodegradable waste at landfills for various years, including 2028 and 2032. However, it is in 2039 that the program likely envisions achieving a substantial level of compliance with EU standards, suggesting that a more extended period of adjustment is needed to ensure the proper operation of waste allocation systems in accordance with EU requirements. Consequently, the year 2039 is chosen because it represents a significant milestone in the Republic of Serbia's efforts to align its solid waste management strategies with EU directives.

The research input data structure was defined by the analysis of the current state and the calculated projections of municipal solid waste (MSW) amounts and the content in the Republic of Serbia.²¹ A data-based prediction of municipal solid waste production for the year 2039 is estimated to be approximately 3.5 Mt. The input data for substance concentrations in waste fractions were modified and applied according to Stanisavljevic, Astrid *et al.* and Arena *et al.*^{16,17,22} Mass flows and comprehensive data on the presence of the heavy metals Pb and Cd within different waste components are presented in Table I.

TABLE I. Mass flows and substance flows (for lead and cadmium) in the input data

Input fractions	Mass flow, t year ⁻¹	Cadmium flow, mg kg ⁻¹	Lead flow, mg kg ⁻¹
Biodegradable waste ^a	1,220,000	1.05	15.05
Paper and cardboard	415,000	1.95	14
Glass	300,000	1.4	215
Metal	105,000	6.6	1437
Plastic	600,000	22.5	213
Other ^b	840,000	22,3	323
Total/average	3,480,000	10.2	184

^agarden, kitchen and green; ^btextiles, leather, diapers, batteries, fine elements, *etc.*

Based on comprehensive information from other studies, electronic waste, batteries and plastic are identified as primary contributors to the sources of Cd, while metals, primarily, and electronic waste and plastics to a lesser extent, are highlighted as the primary contributors to sources of Pb. While the concentrations of cadmium and lead in biodegradable waste are relatively low, with values of 1.05 mg kg⁻¹ for Cd and 15.05 mg kg⁻¹ for Pb, it's essential to acknowledge that these levels are not insignificant and warrant attention due to their potential environmental impact.

Scenarios development

Waste management consists of several functional units: waste generation, collection and transport, pre-treatment and treatment and waste disposal. The systems are limited in time and space, where consumer goods are defined as input into the system and become waste at the end of their life cycle. Emissions to air, water and soil after waste treatment and final disposal, compost after treatment of the biodegradable part of waste and recycling materials are defined as outputs of the system. A simplified graph of the scenarios by functional units is shown in the Fig 1.

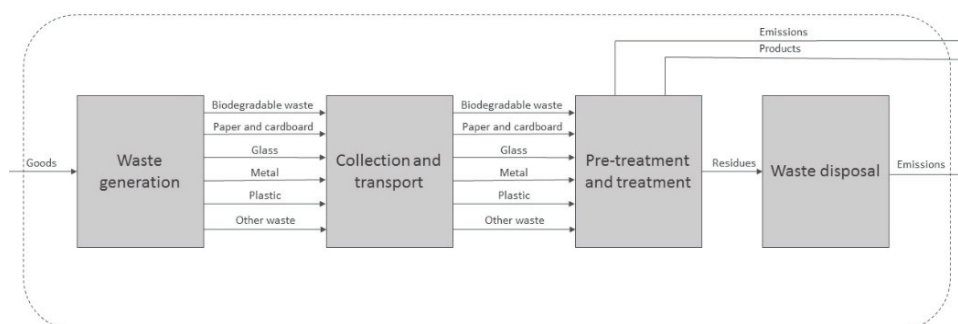


Fig. 1. Simplified representation of waste management system.

The developed waste management systems observe and compare how different ways of treating municipal solid waste affect waste management objectives. Two scenarios are outlined in the following sections.

Scenario I. Generated municipal solid waste is divided into following categories: biodegradable waste, paper and cardboard, glass, metal, plastic and other. Households utilize a three-bin system to separate MSW, comprising recyclable materials, wet waste and residual waste collections. In this case, separately collected wet waste is subjected to composting treatment processes, aimed at enhancing its environmental sustainability. Recyclable materials, upon collection, are omitted from the scope of this study as they no longer represent waste, but valuable resources for potential utilization in diverse recycling procedures. The remaining waste stream, unallocated to either recyclables or wet waste bins, is directed towards disposal in a sanitary landfill, indicating the management of non-recyclable and non-compostable waste components. Residues resulting from the composting treatment procedure are also deposited into the sanitary landfill.

Scenario II. This scenario with regard to the treatment of waste, compared to the previous scenario, primarily diverges in the treatment technology applied to wet waste. In this scenario, separately collected wet waste undergoes anaerobic digestion with subsequent post-composting as a distinct treatment process. Following the post-composting stage, any remaining residues are consigned to a sanitary landfill. The inclusion of Scenario II serves to emphasize the opposing approaches between composting and anaerobic digestion technologies in the context of wet waste treatment.

Transfer coefficients of the selected waste treatment processes describe the partitioning of a substance in a process and are defined for each output result. The most suitable transfer coefficients for the modeled scenarios were synchronized and set through the literature assessment. Data on the mass and substance balance for the composting process were derived from Allesch and Brunner, information regarding the landfill was obtained from Stanisavljevic *et al.*, while detailed data on anaerobic digestion process are presented by Jensen *et al.*^{15,16,23}

RESULTS AND DISCUSSION

Material flow analysis and substance flow analysis were applied to the previously described scenarios. Modelled scenarios for cadmium and lead flows are presented below in Figs. 2–5.

Values and concentrations of the observed heavy metals in various environmental mediums are presented in Tables II and III.

The concentration values of cadmium and lead in the obtained compost material were compared with the limit values of the Serbian standards.²⁰ The Serbian standard for compost has set the concentration values for Cd and Pb to 1.5 and 200 mg kg⁻¹, respectively. The compost reuse for Cd has shown in both scenarios' higher concentrations than the given standard limitations. The Pb is in both scenarios in compliance within standard. Due to differences in the functioning of the composting and anaerobic digestion processes, there are differences in the distribution of Cd and Pb into the environmental compartments. Considering scenarios results, it is evident that Cd and Pb concentration values are lower in the process of composting than after anaerobic digestion. Cadmium and lead concentration values in landfills body show similar results in both scenarios.

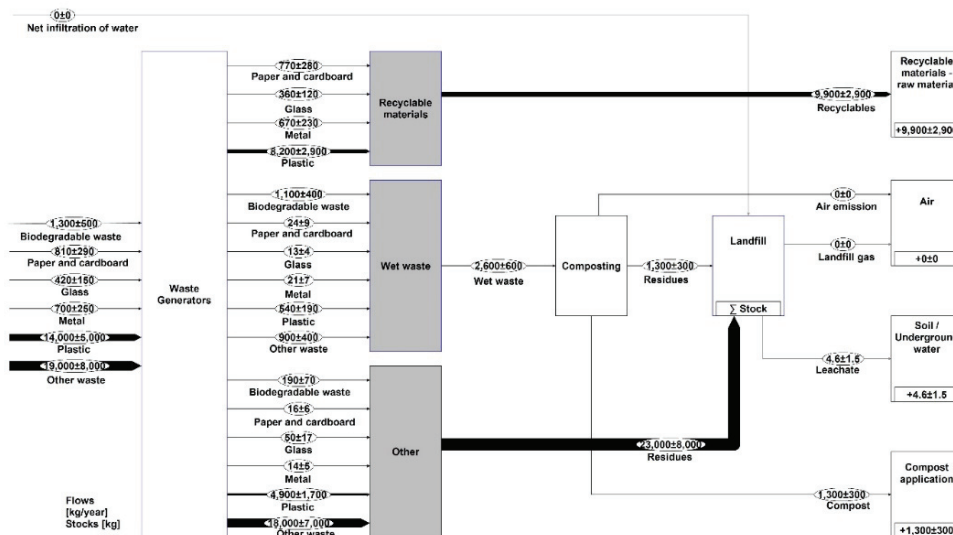


Fig. 2. Cadmium flow for Scenario I.

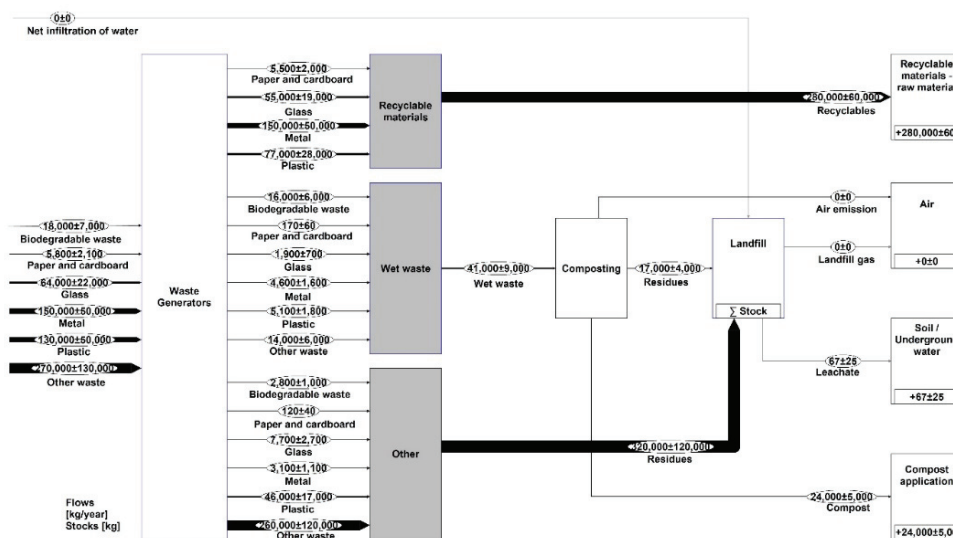


Fig. 3. Lead flow for Scenario I.

The high concentrations of heavy metals are sign of compost contamination and indicators of the potential environmental risks. Depending on the specific context and the levels of contamination, certain use of compost is possible for soil stabilization, landfill cover, remediation and landscaping.

While the mass balance for the scenarios includes emissions to air, soil and water, substance flow analysis reveals that Cd and Pb ultimately end up in com-

post and soil/underground water only. Heavy metals such as Cd and Pb undergo transformations, making them less mobile or volatile, thus preventing their release into the air. Emissions into the soil are slightly higher in scenario I.

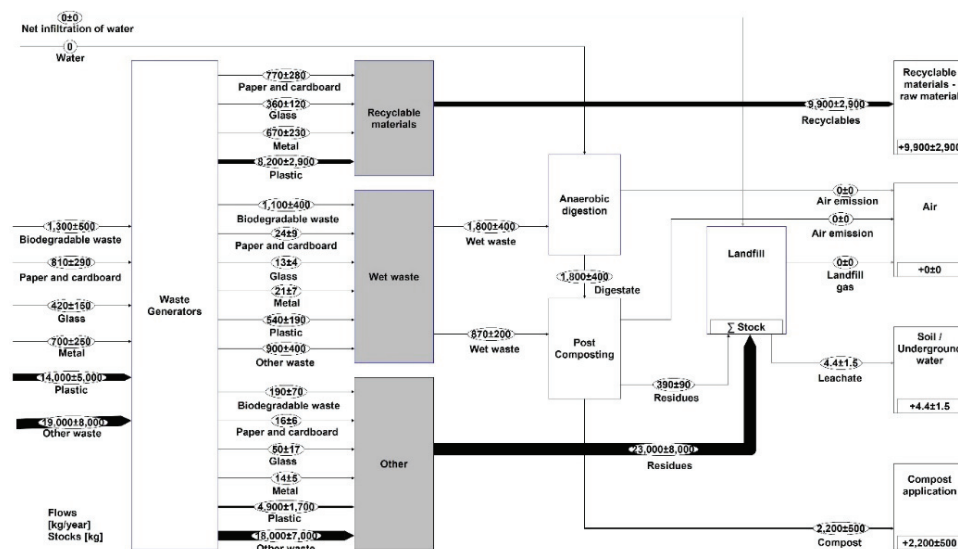


Fig. 4. Cadmium flow for Scenario II.

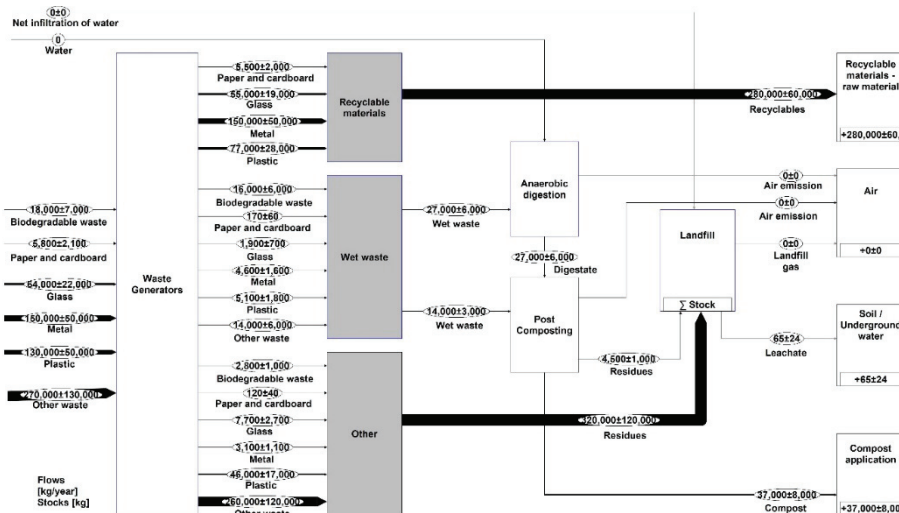


Fig. 5. Lead flow for Scenario II.

The composting scenarios presented in this study are largely consistent with previous studies.^{24,25} Zarkadas *et al.*'s research yielded slightly superior outcomes for heavy metals, since the collection was focused on biodegradable food

waste. Enhancing the biodegradable waste collection process and minimizing impurities introduced into the system can lead to improved results. Knoop *et al.*'s results also demonstrated similar concentrations of cadmium and lead after the anaerobic digestion process.²⁶ The study by Arena *et al.* presents comparable results for mass flow analysis, with no specific information on substance concentrations after the anaerobic digestion process.¹⁷

TABLE II. Values of Cd and Pb in environmental compartments expressed in kg year⁻¹

Environmental compartments	Scenario I		Scenario II	
	Cd	Pb	Cd	Pb
Air	0	0	0	0
Soil/underground water	4.6	67	4.4	65
Soil (compost reuse)	1300	24000	2200	37000
Landfill body	24000	340000	23000	320000

TABLE III. Concentrations of Cd and Pb in environmental compartments expressed in mg kg⁻¹

Environmental compartments	Scenario I		Scenario II	
	Cd	Pb	Cd	Pb
Air	0	0	0	0
Soil/underground water	0.01	0.08	0.01	0.08
Soil (compost reuse)	3.23	59.56	4.89	79.91
Landfill body	39.88	549.67	39.05	538.75

Sink indicator

The quantification of the sink indicator yielded the results depicted in Fig. 6.

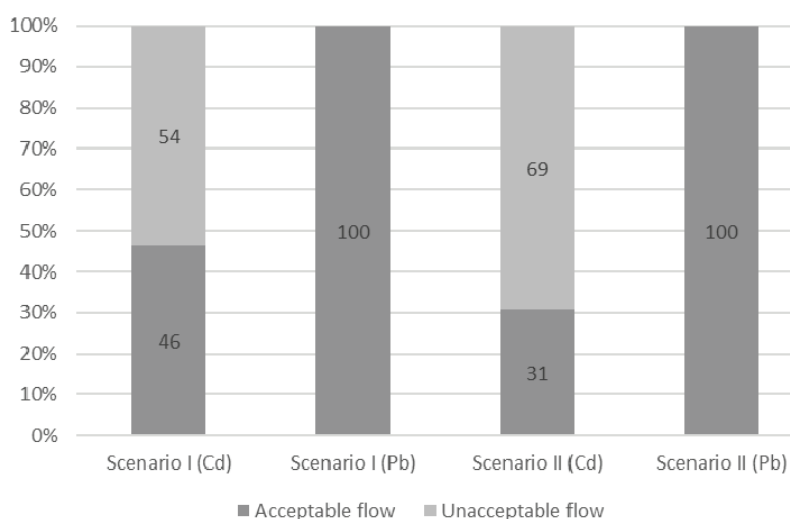


Fig. 6. Sink indicator results expressed in percentages.

The results for Pb indicated that in both scenarios, concentrations remained within the limit values (100% directed to the acceptable sink), due to the high allowable values of lead concentrations.

Analysing the modelled scenarios and Cd values within the anaerobic digestion context, 30.68 % of the input material is characterized as an acceptable flow. In the case of the composting process, 46.39 % is designated as an acceptable flow. These findings indicate a greater proportion of the input material undergoes a satisfactory transformation or stabilization during composting when compared to anaerobic digestion. Unacceptable levels arise from elevated cadmium concentrations in compost material, with the outcomes once again underscoring superior results achieved through the composting process.

CONCLUSION

Understanding the influence of the transformation of materials within waste management systems and how the specific application of various technologies in these systems can impact material transformation, directing substances to different sinks, is essential. All transformations within the system are based on the mass conservation law. The mass-balance principle applies to systems as well as processes. In accordance with the mass-balance principle, the total mass of inputs entering a process is equivalent to the combined mass of outputs from that process, along with a stock accounting for the accumulation or depletion of materials within the process. The material entering the system transforms into other forms and will definitely remain, it will not disappear. According to this law, the material entering the system undergoes transformation into different forms and is assured to persist rather than vanish.

Fulfilling the objectives linked to decreasing the quantity of biodegradable municipal waste disposed of in landfills, according to the Landfill Directive (1999/31/EC), doesn't provide insights into the impact on the main environmental compartments: atmosphere, hydrosphere and lithosphere. The emphasis is on recognizing the significance of considering waste management goals. Thus, a more comprehensive knowledge base for waste management development can be established.

The emissions of hazardous heavy metals, cadmium and lead in two modelled scenarios designed for the Republic of Serbia waste management systems provide us with a clearer insight into the quality-level waste management goals. There is no feasible means to reduce the amounts of Pb and Cd in waste flows. Nevertheless, through the application of suitable technologies, these heavy metals can be directed into appropriate final sinks to protect human health and the environment. Designed scenarios both show increased values of Cd, while the values of Pb are in accordance with Serbian legislative. Observation of the obtained data for lead indicates that limit values for lead are very high, and nec-

essity for it to be more strictly determined. Final modelled values distinguish Scenario I as better solution concerning share of cadmium and lead in possible waste management system. Importance of waste management system modelling perceives the possible pollution hotspots and allows for additional treatment to be introduced in structure, creating clean circular economy blueprint.

The results emphasize that cadmium and lead values and concentration levels need to be perceived separately. Total values of processed waste are considered to be key factor in waste management systems. The modelled data indicates that different approach should be taken into consideration, whereas concentration values are to be observed. The new approach is backed with the fact that some metals can have very adverse effect on both population health and the environment even in small doses, especially in long term exposure. The application of the MFA and SFA approaches has the potential to provide positive benefits for understanding cadmium and lead contamination, thereby decreasing the toxic hazard's impact on human health and the environment in the future waste management systems of the Republic of Serbia. Concerning the study's limitations and potential avenues for further research, modelling scenarios for additional substances would be advantageous. Future research should prioritize identifying critical and problematic substances, analysing their impact on waste management goals. Furthermore, this study did not explore the influence of Cd and Pb on the implications of the recycling process. Subsequent research could address this aspect, providing a more precise assessment of substance flows associated with the implementation of recycling technologies.

ИЗВОД

АНАЛИЗА ТОКОВА КАДМИЈУМА И ОЛОВА КАО ПОДРШКА ПОДАЦИМА ЗА УПРАВЉАЊЕ ОТПАДОМ

НИКОЛИНА Ж. ТОШИЋ¹, МАРКО З. МУХАДИНОВИЋ², МИЉАН З. ШУЊЕВИЋ¹, ИЛИЈА П. ЋОСИЋ¹
и НЕМАЊА С. СТАНИСАВЉЕВИЋ¹

¹Универзитет у Новом Саду, Факултет техничких наука, Департаман за инжењерство заштите животне средине и заштити на раду, Три Досијеја Обрадовића 6, Нови Сад и ²Lafarge БФЦ Србија д.о.о. Беочин, Три Беочинске фабрике цемента 1, Беочин

Као део процеса тежње ка чланству у ЕУ, Република Србија мора прилагодити своје праксе управљања отпадом како би се ускладила са директивама ЕУ, укључујући циљеве смањења одлагања биоразградивог отпада на депоније, како је дефинисано у Програму управљања отпадом. Кадмијум и олово, два високо токсична тешка метала који се налазе у комуналном чврстом отпаду, могу представљати велике претње по животну средину и људско здравље ако се са њима не управља правилно. Истраживање приказује како различите технологије за третман биоразградивог отпада утичу на трансформацију токова кадмијума и олова кроз системе управљања отпадом. Стога су развијена и моделована два сценарија управљања отпадом за Републику Србију, где су праћени токови кадмијума и олова. Резултати указују на разлике између количина и концентрација кадмијума

и олова емитованих у животну средину, потврђујући тако различите утицаје примењених технологија на постизање циљева управљања отпадом. Као резултат истраживања истиче се неопходност свестраног приступа, са нагласком на квалитет излазних токова приликом управљања отпадом.

(Примљено 6. децембра 2023, ревидирано 3. јануара, прихваћено 7. марта 2024)

REFERENCES

1. N. Stanisavljevic, P. H. Brunner, *Waste Manage. Res.* **37** (2019) 665 (<https://doi.org/10.1177/0734242X19853677>)
2. C. Roithner, H. Rechberger, *Waste Manage.* **105** (2020) 586 (<https://doi.org/10.1016/j.wasman.2020.02.034>)
3. B. Puyuelo, J. Colón, P. Martín, A. Sánchez, *Waste Manage.* **33** (2013) 1381 (<https://doi.org/10.1016/j.wasman.2013.02.015>)
4. The government of the Republic of Serbia, *Waste management program of the Republic of Serbia for the period 2022-2031*, 2018 (in Serbian)
5. P. H. Brunner, H. W. Ma, *J. Ind. Ecol.* **13** (2008) 11 (<https://doi.org/10.1111/j.1530-9290.2008.00083.x>)
6. G. Doberl, R. Huber, P. H. Bruner, M. Eder, R. Pierrard, W. Shconback, W. Fruhwirth, H. Hutterer, *Waste Manage. Res.* **20** (2002) 311 (<https://doi.org/10.1177/0734247X0202000402>)
7. M. L. Mastellone, P. H. Brunner, U. Arena, *J. Ind. Ecol.* **13** (2009) 735 (<https://doi.org/10.1111/j.1530-9290.2009.00155.x>)
8. U. Kral, *PhD Thesis*, Vienna University of Technology, Vienna, 2014 (https://publik.tuwien.ac.at/files/PubDat_229212.pdf)
9. *Heavy metals in the environment*, L. K. Wang, J. P. Chen, Y.-T. Hung, N. K. Shammas, Eds., Taylor & Francis Ltd., Oxfordshire, 2009 (ISBN 9781138112575)
10. S. J. Burnley, *Waste Manage.* **27** (2007) 327 (<https://doi.org/10.1016/j.wasman.2005.12.020>)
11. U. Kral, P. H. Brunner, P. C. Chen, S. R. Chen, *Ecol. Indic.* **46** (2014) 596 (<https://doi.org/10.1016/j.ecolind.2014.06.027>)
12. U. Kral, L. S. Morf, D. Vyzinkarova, P. H. Brunner, *J. Mater. Cycles Waste Manage.* **21** (2019) 1 (<https://doi.org/10.1007/s10163-018-0786-6>)
13. N. Stanisavljevic, P. H. Brunner, *Waste Manage. Res.* **39** (2021) 1437 (<https://doi.org/10.1177/0734242X211058344>)
14. P. H. Brunner, H. Rechberger, *Practical Handbook of Material Flow Analysis*, Lewis publishers, Boca Raton, FL, 2004 (<https://doi.org/10.1016/B978-1-85617-809-9.10003-9>)
15. N. Stanisavljevic, P. H. Brunner, *Waste Manage. Res.* **32** (2014) 733 (<https://doi.org/10.1177/0734242X14543552>)
16. A. Allesch, P. H. Brunner, *Environ. Sci. Technol.* **51** (2017) 540 (<https://doi.org/10.1021/acs.est.6b04204>)
17. U. Arena, F. Di Gregorio, *Resour. Conserv. Recycl.* **85** (2014) 54 (<https://doi.org/10.1016/j.resconrec.2013.05.008>)
18. O. Cencic, H. Rechberger, *J. Environ. Eng. Manage.* **18** (2008) 440
19. *Regulation on emission limit values of pollutants in water and deadlines for their achievement*, *Official Gazette of the Republic of Serbia*, No. 67/2011, 48/2012 and 1/2016, 2016 (in Serbian)

20. *Specification for composted materials*, Institute for standardization of Serbia, Belgrade, 2017
21. N. Stanisavljevic, J. W. Levis, M. A. Barlaz, *J. Ind. Ecol.* **22** (2018) 341 (<https://doi.org/10.1111/jiec.12564>)
22. N. Stanisavljević, *PhD Thesis*, University of Novi Sad, Novi Sad, 2012
23. M. B. Jensen, J. Møller, C. Scheutz, *Waste Manage.* **66** (2017) 23 (<https://doi.org/10.1016/j.wasman.2017.03.029>)
24. P. H. Brunner, A. Allesch, B. Färber, M. Getzner, G. Grüblinger, M. Huber-Humer, A. Jandric, G. Kanitschar, J. Knapp, G. Kreindl, P. Mostbauer, W. Müller, G. Obersteiner, A. Pertl, R. Pomberger, L. Plank, S. Salhofer, T. Schwarz, *Benchmarking für die österreichische Abfallwirtschaft*, Technische Universität Wien, Vienna, 2015 (https://publik.tuwien.ac.at/files/PubDat_247861.pdf)
25. I. Zarkadas, E. Angeli, I. Sainis, E. Voudrias, G. Pilidis, *Clean – Soil, Air, Water* **46** (2018) 1700622 (<https://doi.org/10.1002/clen.201700622>)
26. C. Knoop, M. Tietze, C. Dornack, T. Raab, *Bioresour. Technol.* **251** (2018) 238 (<https://doi.org/10.1016/j.biortech.2017.12.019>).



J. Serb. Chem. Soc. 89 (5) 729–742 (2024)
JSCS–5152

Effects of carbonation and chloride ingress on the durability of concrete structures

RADOMIR FOLIĆ^{1*}, DAMIR ZENUNOVIĆ² and ZORAN BRUJIĆ¹

¹University of Novi Sad, Faculty of Technical Sciences, Novi Sad, Serbia and ²University of Tuzla, Faculty of Mining, Geology and Civil Engineering, Tuzla, Bosnia and Herzegovina

(Received 2 January, revised 15 February, accepted 7 March 2024)

Abstract: The durability of concrete structures, which are designed for long-term use is predominantly determined by the resistance to chemical influences, *i.e.*, the concrete's ability to protect the reinforcement steel. The carbonation and the chloride ingress into concrete are the most significant causes of steel corrosion and the potential failure of the structure. The primary goal is to ensure that any significant damage does not occur during the structure's service life, primarily achieved by selecting an adequate thickness of the concrete cover. The issue is approached through calculations based on performance analyses, and the use of appropriate models for these chemical phenomena. The paper provides a brief overview and the methodology for analysing the impact on the durability of concrete structures in accordance with the leading international normative documents. The emphasis is on the recent changes introduced in second generation of European Eurocode standards. The consequences of the analysed phenomena are presented through the results of field tests conducted at salt factories, coke industries, and thermal power plants, and through laboratory tests. The tests were performed in order to develop a rapid prediction method for the measure of chloride ingress into concrete without the stimulating chloride ion migration by electricity, as an alternative to standardized tests.

Keywords: service life; deterioration, field tests; laboratory tests; Eurocodes; depassivation.

INTRODUCTION

Concrete structures are exposed to different environment conditions and are vulnerable to damage from corrosion. The progressing corrosion is the major cause of deterioration of concrete structures. The durability of concrete structures receives significant attention in many international normative documents and recommendations. The Euro-international Committee for Concrete (fib) has published a Design Guide,¹ while International Union of Laboratories and Experts in

* Corresponding author. E-mail: folic@uns.ac.rs
<https://doi.org/10.2298/JSC240102030F>

Construction Materials, Systems and Structures (RILEM) has published a monograph.² The theoretical foundations of durability design are presented in the monographs by Richardson (2002)³ and Alexander *et al.* (2017),⁴ while the fib's "Structural concrete" textbook,⁵ in Chapter 5, describes the durability of concrete structures. In some standards, durability is associated with the service life design of concrete structures,⁶ while it is treated separately in the American Concrete Institute's approach.^{7,8} European structural standards are based on a probabilistic approach,⁹ and for concrete structures, there are designated standards¹⁰ for specification, performance, production and conformity.¹¹ Like in ACI recommendations, in the fib's guide,¹² the provisions for service life are separated (in the Model Code,¹³ this is outlined in clauses 7.8.2 and 7.8.3). The fundamentals analysis of concrete durability design is a subject of the paper by Folic (2009),¹⁴ while modelling and structural assessment in durability design are considered by Folic *et al.* (2010).¹⁵ The method of designing service life according to the provisions of the fib Model Code MC 2010 and its implementation into ISO 16204 is analysed by Helland (2013).¹⁶ A comprehensive review of the literature on the introduction of carbonation and chlorides into the analysis of corrosion in reinforced concrete structures is the subject of the study by Zhou *et al.* (2014).¹⁷ A similar literature review on durability and service life, with a critical approach to modelling, is presented in the article by Alexander *et al.* (2019).¹⁸ Demis *et al.* (2019)¹⁹ consider the issues and perspectives of designing the durability of concrete structures while Helland (2022)²⁰ describes the performance-based service life as it is implemented in the 2021 Eurocodes. In Europe, the design for the durability of new reinforced concrete structures is currently based on a prescriptive approach. However, designers must understand the basic deterioration mechanisms and the potential types and rates of damage development, as it is given in next generation of European standards for different type of corrosion.²¹ Since 2014, EN1992¹⁰ and EN206¹¹ are under the main revision definition of exposure class for the new generation standards system to specify durability.^{20,22} The new tendencies in designing durability of concrete structures, and state of the art issues, are subject of paper by Folic and Brujic,²³ where pre-normative CEN documents,²⁴⁻²⁷ which will be adopted as the second-generation Eurocodes, are discussed.

The group of authors, Folic, Zenunović and Rešidbegović, published articles²⁸⁻³¹ related to the investigations of carbonation and chloride corrosion, in situ and in laboratories. Within the context of two case studies of complex industrial structures located in an aggressive environment, the issue of durability of concrete has been considered, the recommendations regarding structural durability analysis are considered by the means of verification of the limit state of depassivation and the reinforcement corrosion induced by chloride ingress, and the models for predicting chloride ingress in concrete samples and in existing concrete structures have been suggested.

In this paper, the theoretical foundations related to their implementation into the analysis of the durability of reinforced concrete structures were discussed. The primary goal of this study is to illustrate the examples of applying fundamental sciences, especially chemistry, in the practice of designing concrete structures, particularly in terms of their durability.

Carbonation and chloride ingres in standards (CODES)

In international standards, structural reliability is defined as the “ability of structure to fulfil the specific designed requirements during the design service life”. Degradation (mainly in structural materials), which affects the structural durability, accumulates slowly over time and gradually leads to the deterioration of structural performance. For the performance assessment, it is necessary to investigate the material degradation caused by long-term effects of chemical, physical and other factors, and their effects on structural resistance. In the case of concrete structures, the investigation of structural durability, and its testing, primarily involves the analysis of corrosion of reinforcing steel. The designers should have a comprehensive understanding of fundamental deterioration mechanisms, as well as the potential types and rates of damage development (different types of corrosion cause very different damage developments, some of which reduce the structural safety). The parameters which influence durability are the cement type and quality control of early age cracking, the limitation of crack width, the environmental aggressiveness, etc. The models for the description of the deterioration mechanisms must integrate knowledge from a wide range of different fundamental and applied disciplines.

In deterministic design of durability, actions (S), resistance (R) and service life are used as deterministic quantities. The design formula compares two quantities for the target service life, t_g :

$$R(t_g) - S(t_g) > 0 \quad (1)$$

In reality, S and R are time dependent functions. In the case of the service life the principal design formula is: $t_L - t_g > 0$, where t_L is the service life function.

In stochastic design method the distributions of S , R and service life are taken into account. Probability that the service life of a structure is shorter than the target life is smaller than a certain allowable failure probability is written as:

$$P\{\text{failure}\}_{t_g} = P\{t_L < t_g\} < P_{\text{fmax}} \quad (2)$$

The problem can be solved if the distribution of service life is known. The design service life is: $t_d = \gamma_t t_g$, where t_d is the design service life, while γ_t is the lifetime safety factor. The service life principle may be written:

$$R(t_g) - S(t_g) \geq 0, \quad t_L - t_g > 0 \quad (3)$$

The lifetime safety factor must be calibrated with the results of stochastic design methods and value depends on the maximum allowable failure probability.

The resistance $R(t)$ of a structure and the applied loads $S(t)$ both are stochastic time functions. At any time, t , the margin of safety $M(t)$ is:⁸

$$M(t) = R(t) - S(t) \quad (4)$$

The function $P_f(t)$ has the character of a distribution function. Considering the continuous distributions, the failure probability P_f at a certain moment of time can be determined using the convolution integral:

$$P_f(t) = [M(t) < 0] = \int_{-\infty}^{\infty} F_R(s) f_S(s) ds \quad (5)$$

in which $F_R(s)$ and $f_S(s)$ are probability distribution function of R and density function of S , while s is the common quantity or measure of R and S . It is important to establish a model describing action and the resistance with acceptable reliability. Steel in concrete is protected against corrosion by passivation, due to the alkalinity of concrete (the pH of the pore water runs up to greater than 12.5). If the pH of concrete around reinforcement drops below 9 or chloride content exceeds a critical value, the passive film and the corrosion protection will be lost.¹

The verification of design requires definition of the limit states, and identification of the required design service life and reliability. Recently, besides the serviceability limit state (*SLS*) and the ultimate limit state (*ULS*), some codes introduce the condition limit state (*CLS*), *i.e.*, “use of depassivation as a limit state of durability”.¹⁹ For the depassivation, the suggested probability for failure is 10^{-1} , and reliability coefficient is $\beta = 1.3$, while for *ULS* it is between 10^{-4} and 10^{-6} , depending on the consequences of potential failure.¹²

In *ACI*,⁸ the corrosion models for reinforced concrete are based on a general deterioration model (0) that has been developed to predict the service life of reinforcing steel (Tuutti, 1982). Time moment at the transition from the initial to the propagation phase is introduced as a depassivation point.

Instead, in *fib*, a multilinear dependence of corrosion on time is introduced for propagation (0).

The length of the initial period is controlled by the rate of the chloride ions in concrete. The one-dimensional diffusion process follows Fick's second law of diffusion,⁸ here presented in a modified form, as applied in the analysis of concrete structures in the industrial zone of Tuzla:

$$\frac{\partial C(x,t)}{\partial t} = D_c \frac{\partial^2 C(x,t)}{\partial t^2} \quad (6)$$

where C is a concentration of chloride ions, and D_c is a coefficient of diffusion at distance x from surface at time t . This is further discussed in ACI's Report on service life prediction,⁸ theoretical background are given,¹⁴⁻²² while its application is implemented in the next generation Eurocode text.²⁷

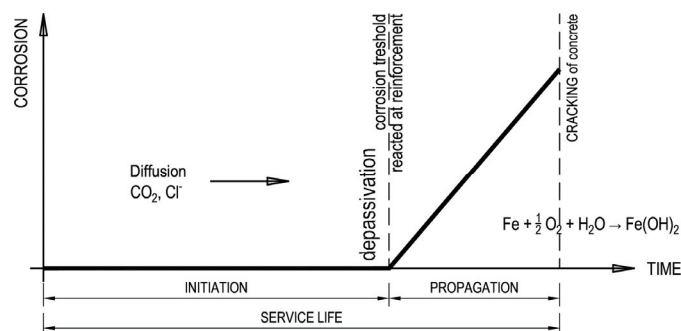


Fig. 1. Schematic of conceptual model of corrosion of steel reinforcement in concrete.

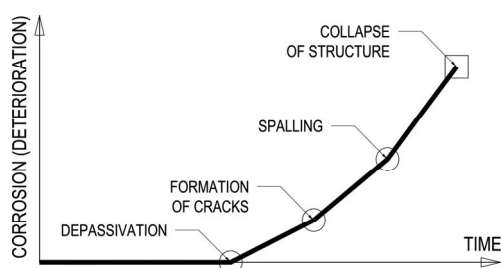


Fig. 2. Determination of service life and limit states with respect to reinforcement corrosion.

With the assumption of a constant chloride concentration on the surface, C_s , of concrete, the typical solution to the previous expression is in the form:

$$C(x,t) = C_s \left(1 - \operatorname{erf} \frac{x}{2\sqrt{D_t}} \right) \quad (7)$$

Carbonation

The passive ferric oxide film on embedded steel may be disrupted by a reduction in the alkalinity ($\text{pH} < 10.5$) of the concrete by carbonation (CO_2 penetrate in concrete) or by the presence of aggressive ions such as chlorides and sulphates. The chemical reaction may be described as:



The empirical formulae for depth of carbonation (x) may be adopted as:

$$x = k\sqrt{t} \quad (9)$$

where k is the factor depending on diffusivity, reserve alkalinity, carbon dioxide, concentration, and expose condition. Some formulae modification and theoretical verification of the square root relationship, and the application of models to service life prediction are introduced and discussed by Richardson.³

Penetration of chlorides into concrete

Chlorides (originating from sea water or de-icing salt used in winter) may penetrate through the pores to the interior of the concrete. The decrease in diffusion coefficient is due to the effects of penetrated chlorides, from de-icing salts, leading to an ion exchange with subsequent blocking of pores in the surface layer. The critical chloride content, indicating the incipient danger of corrosion and subsequent cracks and the spalling of concrete, depends on various parameters. In the region of cracks, carbonation and chlorides tend to penetrate faster towards the the reinforcement than in uncracked concrete. Fick model with apparent diffusion coefficient (Eq.(6) and Crank's solution (Eq.(7)) are given in the literature.³ During the 1980s, Schiessl examined the use of finite difference models, as well as other models.³ For the corrosion of reinforcement, as a simplification, two single processes may be separated: the cathodic and the anodic process (0).

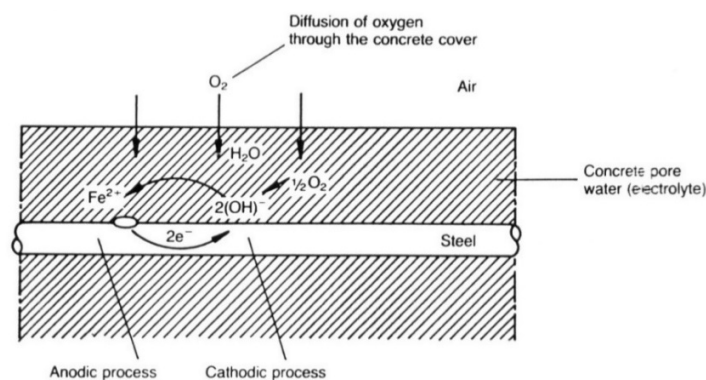


Fig. 3. Simplified model for corrosion of reinforcement in concrete.

In June 2010 fib Technical Council approve start of activities on the MC2020 project to undertake the provisions for the design of concrete structures and will provide them for new and for existing structures, including promotion of structural safety, service ability and durability (limit state of depassivation). Empirical models for corrosion initiation due the carbonation and chloride ingress are defined by fib^{12,16} (deemed to satisfy provision and the application of modelling methods). Providing partial factors for carbonation assuming normal

serviceability limit state reliability requirements. Like in EN¹⁰, fib¹³ introduces the limit state of depassivation – the following requirement shall be fulfilled:

$$P\{\} = P_{\text{dep}} = P\{c - x_c(t_{\text{SL}}) < 0\} < P_0 \quad (10)$$

where $P\{\}$ is the probability that depassivation occurs, c is the concrete cover; $x_c(t_{\text{SL}})$ is the carbonation depth at time t_{SL} in mm, t_{SL} is the design service life in years, while P_0 is the target failure probability. The variables c and $x_c(t_{\text{SL}})$ need to be quantified in a probabilistic approach.

The design model, the ingress of the carbonation front, may be assumed to obey the following:

$$x_c(t) = W(t)k'\sqrt{t} \quad (11)$$

where k' is a factor reflecting aspects like the execution, basic resistance of the chosen concrete mix (like water-cement ratio, cement type, additions) under the reference conditions and the influence of the basic environmental conditions (like mean relative humidity and CO₂ concentration) against the ingress of carbonation, and $W(t)$ is a weather function taking the meso-climatic conditions due to wetting events of the concrete surface into account. For the partial safety factor format the following limit state function shall be fulfilled:

$$c_d - x_{c,d}(t_{\text{SL}}) \geq 0 \quad (12)$$

where index c,d denotes the design value of the concrete cover (c_{nom} – safety margin), $x_{c,d}(t_{\text{SL}})$ is a design value of the carbonation depth at time t_{SL} in mm, while c_{nom} is nominal value for the concrete cover. The design value of the carbonation depth at time t_{SL} is calculated as follows:

$$x_{c,d}(t_{\text{SL}}) = x_{c,c}(t_{\text{SL}})\gamma_f \quad (13)$$

where $x_{c,c}(t_{\text{SL}})$ is characteristic value of the carbonation depth, *e.g.*, mean value of the carbonation depth, and γ_f is partial safety factor of the carbonation depth.

In Europe, design for the durability of new reinforced concrete structures is currently based on a prescriptive approach, *i.e.*, deemed-to-satisfy design: within this approach a trading-off of geometrical (concrete cover to reinforcement), material parameters (indirectly linked to the diffusion and binding characteristics) and execution aspects (compaction and curing) is applied.

The following limit state function shall be fulfilled (see Eq. (10)):

$$P\{\} = P_{\text{dep}} = P\{C_{\text{crit}} - C(c, t_{\text{SL}}) < 0\} < P_0 \quad (14)$$

where C_{crit} is the critical chloride content to achieve depassivation of the reinforcement, and $C(c, t_{\text{SL}})$ is the chloride content at depth c and time t_{SL} . The variables c , C_{crit} and $C(c, t_{\text{SL}})$ shall be quantified in a probabilistic approach.

The area of durability design is regulated by a number of normative documents applied in Europe⁹⁻¹¹ and USA,^{7,8} and the documents of the fib,^{12,13}

which are intended to represent the state-of-the-art in theory and practice. Traditionally, in Europe, as well as in most others leading codes worldwide (even in present Eurocodes related to concrete structures EN 1992-1-1 and EN 206), although ensuring durability is nominally based on performance-based approach, the durability design and verification of performance follows the, so called “prescriptive” or “deemed-to satisfy” (DtS) rules. In the literature²³ some selected aspects and their theoretical background related to the European perspective on performance-based durability design for reinforced concrete structures, which are implemented in new, second-generation, Eurocode FprEN 1992-1-1²⁶ are mentioned. The exposure classes in Eurocodes refer to categories that classify the anticipated environmental conditions to which a structure will be exposed over its intended design life. The exposure classes are defined for the most common environmental exposure conditions: 1) the corrosion of embedded steel induced by carbonation (XC), when reinforced concrete is exposed to air and moisture; 2) the corrosion of the embedded steel induced by chlorides (XD; de-icing salts usually) or 3) chlorides from sea water (XS); 4) chemical attack (XA1 to XA3). The environmental exposure classification has retained the same form as in present Eurocode 2, only some of the descriptions have been modified for the classes related to the corrosion of reinforcement. Since the selection of a specific exposure class is a designer’s decision, in the second-generation of Eurocodes, the definition of exposure classes has been copied from EN 206²⁵ to the main text.²⁶ The exposure Resistance Classes (ERC) are used to classify concrete with the respect to resistance against the corrosion induced by carbonation (class XRC) and by chlorides (class XRS) were covered only through limiting values for mix compositions (similar to DtS approach). Briefly, the exposure resistance classes link the minimum concrete cover required for durability, $c_{\min, \text{dur}}$, to exposure class and design service life. ERC is, thus, a set/group of requirements for concrete which are needed to resist the type of exposure associated to an exposure class. The adequate durability may be assumed against the corrosion caused by carbonation or chloride ingress, where cover to reinforcement is selected appropriate to the exposure class, exposure resistance class and the design service life and not less than the minimum cover for durability $c_{\min, \text{dur}}$.

EXPERIMENTAL INVESTIGATIONS ON SITE AND IN LABORATORY

The experimental investigations were conducted in the facilities of the Salt Factory, Coke Industry and the Thermal Power Plant in Tuzla. By examining the pollution of air and water in the area, the presence of chemical compounds aggressive in contact with concrete and reinforcement, such as CO, CO₂, SO₂, SO₃,..., has been determined. The comprehensive field research and laboratory testing have been conducted in order to determine the content of chlorides and sulphates, as well as the depth of carbonation. It has been established that the

primary cause of the corrosion process in concrete is the presence of chloride (consequences are shown in 0).

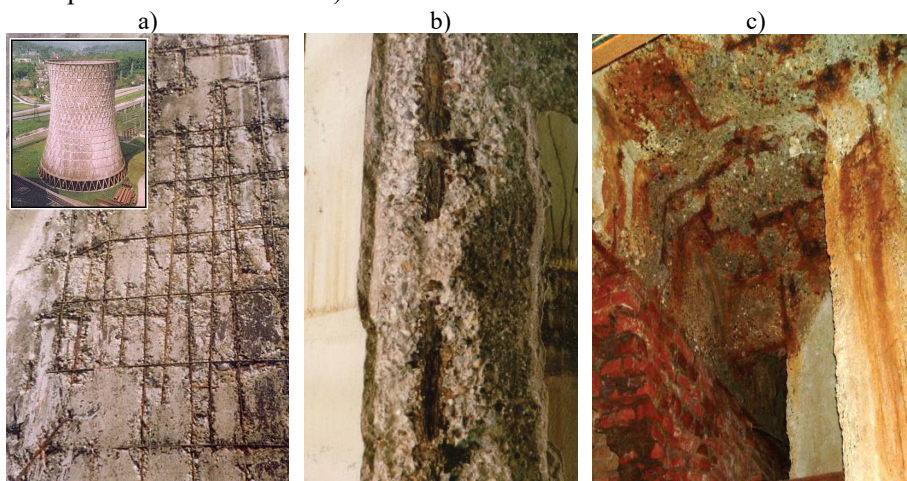


Fig. 4. Effects of chloride ingress: a) cooling tower in power plant; b) salt factory; c) nitrogen factory in the coke industry.

The reinforcement carbonation depth is determined by testing with 0.1 % alcohol phenolphthalein and 0.1 % alcohol thymolphthalein. The procedure is performed by making a cut on the concrete surface, on which the solution is sprayed. The healthy concrete depth is shown through the violet colour of the solution. The chloride concentration is determined by applying two substances, 1 % AgNO_3 and 5 % K_2CrO_4 , one after another. The indication of chloride presence is the brown colour of the substances.

The amount of chloride and sulphate in samples of concrete removed was determined by laboratory testing. The amount of chloride was determined by filtering the sample in distilled water with $\text{K}_2\text{Cr}_2\text{O}_7$ solution, which is subsequently added to the standard solution of AgNO_3 . The amount of sulphate was determined by filtering with additions to the solution HCl and BaCl_2 .

In order to define a rapid method for determining the chloride penetration profile in concrete without the initiation of chloride ions by electrical current, the laboratory research was conducted in the laboratories of the University of Tuzla. The chloride diffusion coefficients through the concrete surface layer exposed to salted water with and without pressure were analysed. Three concrete mix formulas were used. The samples were tested by immersing them into salty water (bulk diffusion test – BDT) and pressuring them with salted water (pressure penetration test – PPT). The term permeation coefficient was introduced, which represent a difference of the transport mechanisms during BDT and PPT. The PPT procedure was applied to define the chloride profile of sampled concrete

from the Salt Factory. The procedure of determination of the chloride content by depth is described in detail in the literature.^{29,30} The sampling was performed by grinding samples by depth for the purpose of determining chloride concentration and using the indicator colour to determine the chloride penetration depth. After the chloride content in the supplied concrete samples was determined, they were prepared for the PPT examination in the way presented in 0. The samples are named the stepped samples.

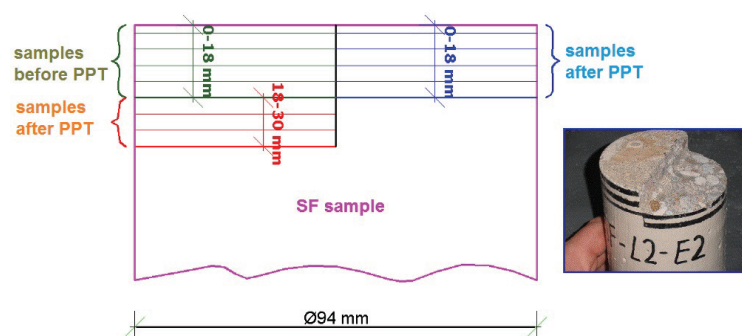


Fig. 5. Stepped samples.

The goals of testing the stepped sample are simultaneous determination of the residual capacity for the chloride absorption in the surface layers and the determination of the chloride penetration depth in the old concrete (0). The procedure is described in more detail in the literature.³¹

TABLE I. The pH value, chloride content, sulfate content and the depth of chloride penetration

Sample	pH	Content, %		Depth of chloride penetration, cm
		Chlorides	Sulfates	
1	11.5	0.113	0.90	1.0
2	11.0	0,098.	0.69	1.0
3	9.5	0.128	0.76	2.0
4	11.0	0.135	0.74	1.0
5	11.0	0.137	1.30	1.0
6	9.5	0.103	0.83	2.5
7	9.5	0.113	0.71	2.5
8	10.5	0.098	0.88	1.0
9	11.0	0.015	0.46	1.0
10	11.0	0.015	0.96	1.0

The investigation of concrete carbonation was conducted by the determination of the pH value of the concrete samples. Depending on the determined values, a 0.1 % alcohol phenolphthalein indicator solution was applied for pH 8.2–9.8, and a 0.1 % alcohol thymolphthalein indicator for pH 9.3–10.5. The

determined pH values ranged from 9.0 to 11.0. The depth of carbonation at selected locations of the deteriorated concrete ranged from 15 to 20 mm. The rates of carbonation are the highest in the range from 50 to 70 % of relative humidity. Above 75 % of the relative humidity the influence of water filling the pores becomes significant. The coefficient of variation for measuring the depth of carbonation $V = 30\%$ and the distribution function is shown in 0.

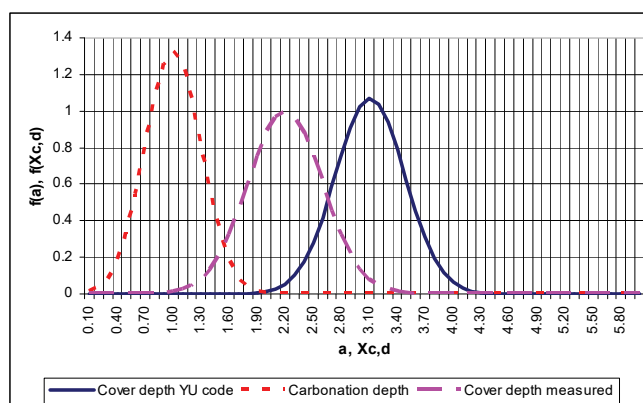


Fig. 6. Functions of distribution of cover concrete depth and carbonation depth.²⁸

In the Salt Factory, the predominant impact is notably from chloride, which has penetrated the structure up to the reinforcement. By extracting the samples, the amount of soluble chloride was determined to be between 0.14 and 0.3 %. However, it is important to note that the chloride and sulphate content is significantly higher in concretes where the concrete cover has been spalled due to the reinforcement corrosion, ranging up to 2 % for chlorides and sulphates. This high chloride content has caused significant damage and a decrease in concrete strength of 30 % or more. In the Thermal Power Plant, the chloride content was determined to be up to 0.15 %, and the sulphate content up to 1 %. A more detailed presentation of the results is given in the literature.²⁸ The sampled concrete from the Salt Factory was used to create a predictive model of chloride penetration using a stepwise sample (0). Here, a representation of one chloride profile determined in the affected concrete from the Salt Factory is provided (0). The obtained diagrams are described in detail in the literature.³¹

The aim of this investigation was to determine the possibility of chloride penetration at greater depths, where the concrete is firmer and less porous, and to assess the remaining capacity for chloride absorption.

CONCLUSIONS

Parameters which influence the durability of a concrete are the cement type and the quality control of early age cracking of concrete, water–cement ratio,

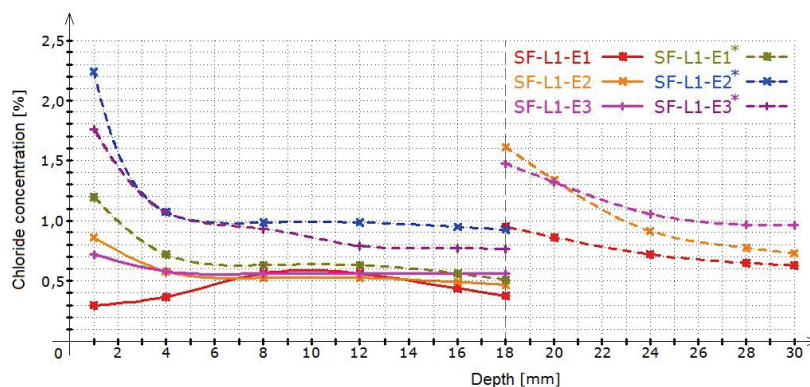


Fig. 7. Chloride profiles in stepped samples – location L1.

limitation of crack width, the environmental aggressiveness, etc. Even if in most cases durability concerns the serviceability, the resistance verification during the design of concrete structures, the inclusion of durability aspects and the deterioration mechanisms are a necessity. The deterioration is a result of external environmental exposure of a concrete, which is most often the carbonation of concrete and chloride corrosion of reinforcement, especially when using de-icing salt and near marine or industrial regions.

The European approach to durability design is in continuous development. To overcome the inconsistencies of the current European prescriptive approach, a new durability design concept has recently been proposed – the “exposure resistance classes”.²¹ While the exposure classes given in actual Codes^{10,11} refer to categories that classify anticipated environmental conditions, to which a structure will be exposed over its intended service life, the exposure resistance classes relate to the performance of concrete in such environments.

The models for describing the deterioration mechanisms have to integrate the knowledge from a wide range of different fundamental and applied disciplines, especially chemistry. They need to be founded in a reliable manner and to provide some appropriate testing options, which is essential for the design or the assessment of structures. The assessment of the existing concrete structures, which is important before rehabilitation, must be performed timely, by the combination of *in situ* testing and laboratory testing of samples taken from the structures.

The further research is directed towards the investigation and assessing the corrosion of prestressed concrete structures.

ИЗВОД

УТИЦАЈ КАРБЕНИЗАЦИЈЕ И ПРОДОРА ХЛОРИДА НА ТРАЈНОСТ БЕТОНСКИХ КОНСТРУКЦИЈА

РАДОМИР ФОЛИЋ¹, DAMIR ZENUNOVIĆ² и ЗОРАН БРУЈИЋ¹¹Универзитет у Новом Сагу, Факултет технолошких наука, Нови Саг и ²University of Tuzla, Faculty of Mining, Geology and Civil Engineering, Tuzla, Bosnia and Herzegovina

Трајност бетонских конструкција, које су предвиђене за дуготрајну употребу, пре свега зависи од отпорности на хемијске утицаје, односно од способности бетона да заштити челик за арматуру. Карбонација и улазак хлорида у бетон су најзначајнији узроци корозије челика и потенцијалног квара конструкције. Примарни циљ је да се у току радног века конструкције не појаве значајна оштећења, пре свега избором адекватне дебљине бетонског покривача. Овом питању се приступа кроз прорачуне засноване на анализама перформанси и коришћењем одговарајућих модела за ове хемијске феномене. У раду је дат кратак преглед и методологија за анализу утицаја на трајност бетонских конструкција у складу са водећим међународним нормативним документима. Акцент је на недавним променама уведеним у другу генерацију европских Eurocode стандарда. Последице анализираних појава приказане су кроз резултате теренских испитивања спроведених у фабрикама соли, коксаре и термоелектрана, као и кроз лабораторијска испитивања. Тестови су спроведени да би се развила метода брзог предвиђања за мерење уласка хлорида у бетон без стимулисања миграције јона хлорида електричном енергијом, као алтернатива стандардизованим тестовима.

(Примљено 2. јануара, ревидирано 15. фебруара, прихваћено 7. марта 2024)

REFERENCES

1. CEB, *Durable of Concrete Structures, Design Guide*, T. Thelford, London, 1992, p. 112
2. *Durability Design of Concrete Structures*, RILEM R. 14, A. Sarja, E. Vesikari, Eds., E&FN Spon, London, 1996
3. M. G. Richardson, *Fundamentals of durable reinforced concrete*, CRC Press, London, 2002 (<https://doi.org/10.1201/9781482272109>)
4. *Durability of Concrete – Design and construction*, M. Alexander, A. Bentur, S. Mindess, Eds., CRC Press, Boca Raton, FL, 2017 (<https://doi.org/10.1201/9781315118413>)
5. *Structural Concrete Textbook on behaviour, design and performance*, 2nd ed., Vol. 3: *Design of durable concrete structures*, Manual-textbook, Ch. 5 (ISBN 978-2-88394-093-2) (<https://doi.org/10.35789/fib.BULL.0053>)
6. ISO 16204:2012: *Durability-Service life design of concrete structures* (<https://www.iso.org/standard/55862.html>)
7. ACI (American Concrete Institute), *ACI 201. 2R-16: Guide to durable concrete*, ACI Committee, 2016 (ISBN: 9781945487392)
8. ACI (American Concrete Institute), *ACI 365.1R-17: Report on service life prediction*, ACI Committee 365, 2017 (ISBN: 9781945487743)
9. CEN, *European Standard EN 1990:2002: Eurocode – Basis of structural design*, European Committee for Standardization, 2002
10. CEN, *European Standard EN 1992:2004: Eurocode 2 – Design of Concrete Structures*, European Committee for Standardization, 2004

11. CEN, *European Standard EN 206-1:2000: Concrete: Specification, Performance, Production and conformity*, European Standard, 2000
12. fib (Federation international du beton), *Model Code for Service Life Design*, Bull. 34, 2006 (<https://doi.org/10.35789/fib.BULL.0034>)
13. fib (Federation international du beton), *Model Code for concrete structures 2010*, Ernst & Sohn, 2013 (ISBN: 978-3-433-03061-5)
14. R. Folić, *Facta Universitatis, Series: Architect. Civil Eng.* **7** (2009) 1 (<https://dx.doi.org/10.2298/FUACE0901001F>)
15. R. Folić, D. Zenunović, *Facta Universitatis, Series: Architect. Civil Eng.* **8** (2010) 45 (<https://dx.doi.org/10.2298/FUACE1001045F>)
16. S. Helland, *Struct. Concrete* **14** (2013) 10 (<https://dx.doi.org/10.1002/suco.201200021>)
17. Y. Zhou, B. Gencturk, K. Willam, A. Attar, *J. Mater. Civ. Eng.* **27** (2014) ([https://dx.doi.org/10.1061/\(ASCE\)MT.1943-5533.0001209](https://dx.doi.org/10.1061/(ASCE)MT.1943-5533.0001209))
18. M. Aleksander, H. Baushausen, *Cement and Concrete Research* **122** (2019) 17 (<https://dx.doi.org/10.1016/j.cemconres.2019.04.018>)
19. S. Demis, G. Vagelis, G. Papdakis, *J. Bridge Eng.* **26** (2019) 100876 (<https://dx.doi.org/10.1016/j.jobe.2019.100876>)
20. S. Helland, in *Proceedings of fib Int. Congress*, Oslo, June 12–16, 2022
21. M. R. Geiker, M. A. N. Hendriks, B. Elsener, *Sustain. Resilient Infrastruct.* **8** (2003) 169 (<https://dx.doi.org/10.1080/23789689.2021.1951079>)
22. JWG (JWG 250/104-N25) Durability Report 2014, *Durability Exposure Resistance Classes, a new system to specify durability in EN 206 and EN 1992*, Leivestad, 2014
23. R. Folić, Z. Brujić, in *Proceedings of MASE*, September 28-29, 2023
24. CEN, *European Standard prEN 1990:2021. Eurocode – Basis of structural and geotechnical design*, European Committee for Standardization, 2021
25. CEN, *European standard EN 206:2013 + A2:2021. Concrete - Specification, performance, production and conformity*, European Committee for Standardization, 2013
26. CEN, *European Standard FprEN 1992-1-1:2023. Eurocode 2 – Design of concrete structures – Part 1-1: General rules and rules for buildings, bridges and civil engineering structures*, European Committee for Standardization, 2023
27. CEN, *Background document to FprEN 1992-1-1:2023-04, Formal-Vote-Draft: Eurocode 2 - Design of concrete structures - Part 1-1: General rules and rules for buildings, bridges and civil engineering structures*, CEN/TC 250/SC 2 N2087, 2023
28. R. Folić, D. Zenunović, *Eng. Struct.* **32** (2010) 1346 (<https://dx.doi.org/10.1016/j.engstruct.2010.03.004>)
29. D. Zenunović, N. Rešidbegović, R. Folić, in *Proceedings of the 1st IC COMS 2017*, Zadar, Croatia, pp. 407–413
30. D. Zenunović, N. Rešidbegović, R. Folić, *Roman. J. Mater.* **49** (2019) 80 (<https://solacolu.chim.upb.ro/p80-87.pdf>)
31. D. Zenunović, N. Rešidbegović, R. Folić, in *Proceedings of 18th Int. Symp. MASE*, Oct. 2019, pp. 511–518.



J. Serb. Chem. Soc. 89 (5) 743–755 (2024)
JSCS–5753

Effects of urban vegetation on PM mitigation: The case of a street in Novi Sad, Serbia

MILJAN ŠUNJEVIĆ¹, DEJANA NEDUČIN^{1*}, RUŽICA BOŽOVIĆ², MAJA SREMAČKI¹,
BORIS OBROVSKI¹ and IRINA SUBOTIĆ¹

¹Faculty of Technical Sciences, University of Novi Sad, Trg Dositeja Obradovića 6, Novi Sad, Serbia and ²Faculty of Technical Sciences, University of Priština, Knjaza Miloša 7, Kosovska Mitrovica, Serbia

(Received 17 January, revised 2 February, accepted 7 March 2024)

Abstract: Experiencing rapid development and growth, cities worldwide face a surge in air pollution, primarily driven by the increased concentrations of the particulate matter (PM) originating from various anthropogenic sources, such as traffic, household fuel combustion, and industrial and construction activities. Urban green spaces can naturally filter PM through physicochemical processes, serving as effective urban planning instruments for the improvement of the air quality. Focusing on a street in Novi Sad, the second-largest city in Serbia, this study investigates the efficiency of vegetation in mitigating air pollution, specifically PM₁₀ emissions from traffic and construction activities. Using the contemporary monitoring and modelling techniques for measuring and predicting PM₁₀ concentrations, the focus of this research is to evaluate the efficacy of vegetation in affecting and minimizing detected PM concentrations. The results indicate a significant reduction in the monitored PM₁₀ concentrations behind the green barrier compared to the modelled concentrations near the pollution source (on the road) for both traffic and construction-related emissions. The paper highlights the capacity of green elements to act as natural air pollution mitigators and suggests better integration of strategic environmental management into urban planning to foster the development of healthier and more sustainable cities, providing recommendations to facilitate this objective.

Keywords: air pollution; particulate matter (PM); mitigation; urban green spaces; urban design.

INTRODUCTION

Developing and growing at an almost unprecedented pace, the cities worldwide are grappling with an upsurge in air pollution, primarily attributed to the elevated concentrations of the urban particulate matter (PM). The term refers to a

* Corresponding author. E-mail: d.neducin@uns.ac.rs
<https://doi.org/10.2298/JSC240117028S>

mixture of minute liquid droplets, solid fragments, and solid cores with liquid coatings suspended in the air and dispersed within urban environments. The particles vary in size, shape, and chemical composition and are classified based on the diameter, with a distinction between fraction PM_{10} ($\leq 10 \mu\text{m}$) and $PM_{2.5}$ ($\leq 2.5 \mu\text{m}$). Among diverse sources of PM emission in urban areas, which are mainly related to anthropogenic activities, traffic emerges as a primary contributor.^{1–3} According to the calculations, it is responsible for 25 % of urban ambient air pollution from $PM_{2.5}$ and PM_{10} , followed by household fuel combustion and industrial activities.^{4,5} Additionally, traffic releases various gaseous pollutants, including carbon monoxide, nitrogen oxides (NO_X) and sulphur dioxide.⁶ Construction activities, including road construction or reconstruction, as well as building projects, are also recognized as significant sources of air pollution in urban environments, releasing a substantial quantity of PM into the air.^{7–9} Due to their minute size, PM_{10} and $PM_{2.5}$ are inhalable and can thus induce adverse health effects, including severe acute and chronic diseases.^{2,10} With over half of the world's population residing in cities (a proportion expected to increase to 68 % by 2050 according to the UN),¹¹ urban air quality represents a paramount health concern. Therefore, monitoring and regulating urban PM levels are crucial for mitigating air pollution and safeguarding public health.

A large body of literature has explored the positive environmental impacts of urban green spaces (UGS) in terms of their ability to mitigate the effects of the ambient air pollution by naturally filtering PM, CO, NO_X and SO_2 .^{12–14} UGS thus serve as an effective urban planning tool for improving air quality, especially in urban areas with moderate to heavy traffic, while also contributing to the regulation of temperature, humidity, and air circulation, thereby improving microclimate conditions. In addition, they can reduce the urban heat island effect and offset greenhouse gas emissions by absorbing CO_2 , contributing to the efforts to address the impacts of climate change.^{15,16} Owing to the array of positive impacts on the urban environment they provide, which turn into benefits for public health, UGS can be considered a public good.¹⁷ They are regarded as one of the most valuable urban planning solutions for enhancing the sustainability and resilience of cities.

Novi Sad, the second-largest city in Serbia, was formerly recognized as the green city due to the abundance of lush vegetation that adorned its urban landscape. In alignment with global urbanization trends, it has recently experienced rapid urban development and growth, resulting in a significant increase in both vehicular traffic and construction activities. As outlined in the city's Strategy for the Development of the Green Spaces System 2015–2030, the novel urban development patterns that favour land-use conversion for new constructions have largely overlooked the development of UGS and diminished their share in many city neighbourhoods and along numerous streets.¹⁸ This type of transformation

has brought about significant environmental implications, contributing to the elevated concentrations of urban PM and thus exerting a notable impact on air quality in many city neighbourhoods, especially those that underwent extensive regeneration. However, in the neighbourhoods unaffected by extensive regeneration projects, UGS were preserved, although they were often inadequately maintained, because of the increased traffic pollution.

The paper investigates the efficacy of UGS in mitigating air pollution in a street in Novi Sad, focusing on PM₁₀ emissions from two different sources – traffic and construction activities. Employing monitoring and modelling techniques, it measures and predicts PM₁₀ concentrations and assesses the capacity of vegetation to reduce them. The monitoring involves measuring PM concentrations behind the green barrier using a sensor, while modelling uses COPERT v.5.7 software for the traffic emissions and the EPA tier 1 prediction model for the construction-related emissions near the source (on the road). Additionally, the paper describes the physicochemical interactions between urban PM and vegetation, and addresses current challenges in maintaining and developing UGS in Novi Sad. It underscores the potential of green elements to act as natural air pollution mitigators and suggests the integration of strategic environmental management into urban planning, in order to create healthier and more sustainable cities, offering recommendations that would aid in achieving this goal.

Physicochemical interactions mechanisms between urban PM and vegetation

Vegetation mitigates air pollution by capturing and interacting with urban PM through physicochemical processes. Leaves of trees and hedges act as physical barriers to PM through both adsorption and absorption mechanisms.¹⁹ Their surface properties influence the adsorption of PM, while their microscopic structures and chemical components facilitate the absorption of soluble components from PM into leaf tissues.²⁰ Upon the contact with leaves, the chemical composition of urban PM undergoes transformations. The reactive oxygen species (ROS), released by leaves during photosynthesis, may oxidize certain PM components, altering their toxicity and reactivity, while enzymatic activities within leaves contribute to the breaking of organic compounds present in PM.

Adsorption predominantly involves the physical adherence of particles to a surface, whereas absorption entails their uptake into the body of the absorbing material. Biochemical adsorption is a process in which particles adhere to a surface, playing a fundamental role in the interaction between urban PM and leaves (trichomes, cuticles and stomata are integral to this process). Trichomes, the hair-like structures on leaf surfaces, significantly contribute to the PM adsorption through their unique morphology enhancing the surface, acting as physical barriers, effectively trapping airborne particles and preventing their dispersion into the atmosphere.²¹ Cuticles, the waxy layers covering the leaf epidermis (hydro-

phobic barrier), and stomata, microscopic pores facilitating the gas exchange, are also integral to the process of PM adsorption.²² The absorption process involves the penetration of PM components through the cuticles and stomata, entering the leaf tissues, after which they may undergo chemical transformations.²³ ROS released during photosynthesis and enzymatic activities within leaves contribute to the PM transformations within the interaction with UGS. ROS-mediated oxidation can modify the chemical structure and the toxicity of PM components, potentially rendering them less harmful.²⁴ Furthermore, the enzymatic activities within tree leaves play a crucial role in breaking down organic compounds present in PM. This enzymatic degradation is a crucial step in the transformation of complex organic pollutants into potentially less harmful forms.

UGS in Novi Sad

According to the European Environment Agency (EEA) report, green infrastructure covers 18.7 % of Novi Sad's core area and 29.8 % of its commuting zone, both figures falling below the average of 42 % for urban areas in 38 EEA member and cooperating countries.²⁵ The UGS provision, also referred to as the UGS ratio, quantifies the total green space area within a city's administrative boundaries, expressed as m² per inhabitant (inhab), and various scientific papers and public policies commonly cite a minimum ranging between 9 and 11 m²/inhab.^{26–28} Novi Sad slightly exceeds this minimum, boasting 12 m²/inhab. The data obtained from the newly developed GIS of green areas reveals that grasslands cover 30 % of the city area, while shrubs make up 14 %. The EEA report further notes that urban tree cover, defined as the urban area "covered by tree crowns when seen from above", is 23 % in Novi Sad, which is lower than the average in cities of EEA member and cooperating countries, standing at 30 %.²⁵ UGS-related issues have also been outlined in local documents. In the UGS SWOT analysis presented in the city's Strategy for the Development of the Green Spaces System 2015–2030 identified weaknesses include inadequate maintenance, a lack of adequate UGS-related regulations (standards and norms), violations of planning documentation, shortages of greenery in some city neighbourhoods, inadequacy of certain UGS categories, and an incomplete UGS network.¹⁸ The main threats to UGS include the risk of land use conversion that may jeopardize the existing green areas and insufficient financial resources for both maintaining existing and creating new UGS. Similarly, the city's Sustainable Development Strategy identifies a lack of UGS as one of the main weaknesses in the urban development SWOT analysis.²⁹ The results from a 2021 survey, based on a sample of 1,500 residents, reveal that the public is well-aware of all these problems – 38.1 % of respondents rated UGS with a grade 3 (out of 5), while 39.1 % assigned them a grade of 1 or 2 – suggesting that the level of satisfaction with UGS in Novi Sad is generally low.³⁰ However, in the neighbourhoods that

were unaffected by urban regeneration projects and land-use conversions, which often diminished the share of UGS, the satisfaction is much higher than in the regenerated ones.

MATERIALS AND METHODS

The examination of the impact of vegetation on mitigating air pollution in a street in Novi Sad comprised two phases – monitoring and modelling of PM_{10} emissions from two different sources – traffic and construction activities. The monitoring focused on determining the PM_{10} concentration behind the green barrier, away from the source, while the modelling predicted the concentration values at the source (on the road).

The monitoring and modeling location

The examination took place in the Novo Naselje neighbourhood, which was predominantly developed in the late 1970s and during the 1980s (Figs. 1 and 2). This neighbourhood was chosen for two reasons: 1) it stands out as one of the few city districts that largely preserved its green infrastructure, *i.e.*, it remained relatively unaffected by the recent land-use conversion trends, which brought new residential, commercial, and mixed-use developments and typically resulted in a significant reduction of vegetation; 2) in the aforementioned public survey, the residents of Novo Naselje expressed much higher satisfaction with the quality of green spaces, compared to the residents of other city neighbourhoods. A segment of Jovana Dučića Blvd. was chosen as the monitoring and modelling location for three reasons (Figs. 2 and 3): 1) it represents the main and busiest street of this neighbourhood, characterized by moderate traffic, with heavy traffic peaks and frequent congestions during rush hours; 2) the selected segment features lush vegetation along both sides; 3) it underwent comprehensive road reconstruction that began in November 2022, enabling the measurement of both traffic and construction activities-related PM_{10} emissions.



Fig. 1. The position of Novo Naselje within Novi Sad. Source: GIS of Green Areas in Novi Sad (<https://gis.zelenilo.com/Map>).



Fig. 2. Jovana Dučića Blvd. within Novo Naselje and the analyzed segment. Source: GIS of Green Areas in Novi Sad (<https://gis.zelenilo.com/Map>).

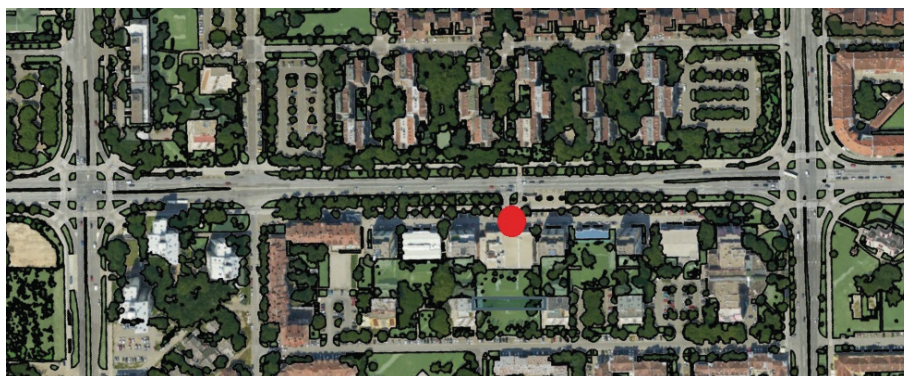


Fig. 3. The monitoring and modeling location and its green infrastructure, with the position of the monitoring sensor. Source: GIS of Green Areas in Novi Sad (<https://gis.zelenilo.com/Map>).

The monitoring phase

The monitoring of PM_{10} emissions was conducted in two different urban circumstances – road reconstruction (no traffic) and rush hour (morning and afternoon – heavy traffic). The monitoring for road reconstruction emissions was performed on the 2nd and 3rd of November 2022, coinciding with the road removal activities that generate higher PM_{10} emission levels. The morning and afternoon rush hour emissions (07:00–09:00 and 15:00–17:00) were measured before the reconstruction began, from the 24th to the 28th of October 2022, capturing baseline levels. A custom-designed PM monitoring sensor based on the optical particle counter OPC-N2 (produced by Alphasense) was used, positioned on the building facade (behind the green barrier) in the middle section of the street, distanced approximately 25 m from the road (Figs. 3 and 4).

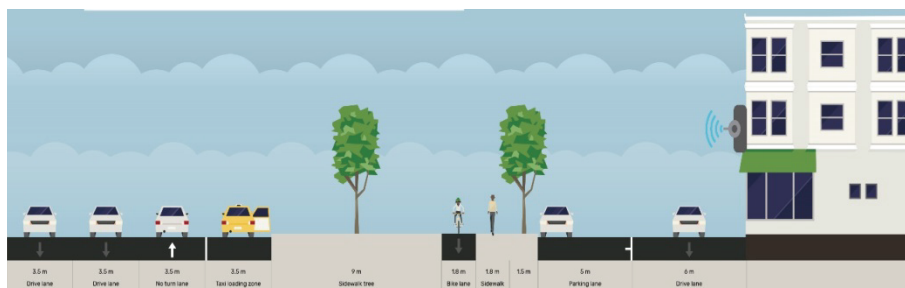


Fig. 4. Street section of the monitoring and modeling location, with the position of the monitoring sensor.

The modeling phase

Traffic-related PM_{10} emissions were modelled using COPERT v5.7 software (computer program to calculate emissions from road transport), used in EU member states for the official submission of road transport inventories. The spatial scale of the applied COPERT model can range from a street to a continental level. The modelling followed the COPERT methodology outlined in the EMEP/EEA Air Pollutant Emission Inventory Guidebook 2019 for the calculation of air pollutant emissions, which aligns with the 2006 IPCC Guidelines for National Greenhouse Gas Inventories.^{31,32} The modelling using COPERT v5.7 software required specific data. According to the National Traffic Safety Strategy 2023–2030, the average age of vehicles in Serbia is 17 years, with a petrol- and diesel-fuelled car ratio of 1:2.³³ The local meteorological data, including average wind speeds, humidity and temperatures necessary for the modelling process, were sourced from the website of the Republic Hydrometeorological Institute of Serbia (available at <https://www.hidmet.gov.rs/>), while the local traffic-related data were collected from the Traffic Study of the City of Novi Sad.³⁴ For PM_{10} emissions from the construction activities, the calculations relied on the EPA tier 1 prediction model, previously applied and tested in a study involving five construction sites in Novi Sad, which included a direct comparison of modelled and sensor-measured data, confirming the high efficiency of the prediction model.³⁵ Given that the location C1 in this study was undergoing road reconstruction, the silt content value of $35.4 \mu\text{g m}^{-3}$ has been adopted for the purpose of this research.

The limitations of this research relate to $PM_{2.5}$ concentrations, arising from insufficient data necessary for accurate modelling.

RESULTS AND DISCUSSION

The average PM_{10} concentrations obtained through the monitoring and modelling of pollutant emissions attributed to traffic and construction activities on Jovana Dučića Blvd. in Novi Sad are presented in Table I.

The data reveal a substantial reduction in PM_{10} concentrations behind the green barrier compared to those modelled at the source (on the road) for both traffic and construction-related emissions. Specifically, the PM_{10} concentration from traffic emissions decreased from 98.45 to $26.69 \mu\text{g m}^{-3}$, while the concentration from the construction activities exhibited a similar drop – from 145.17 to $51.36 \mu\text{g m}^{-3}$.

TABLE I. Average PM₁₀ concentration values () obtained from monitoring and modeling

PM ₁₀ concentration, $\mu\text{g m}^{-3}$	Traffic	Construction activities
Modelled (on the road)	98.45	145.17
Monitored (behind the green barrier)	26.69	51.36
Relative decrease (behind the green barrier), %	72.9	64.6

Considering the EPA's PM₁₀ breakpoints for assessing the health impact of PM₁₀ concentrations,³⁶ the modelled values for both sources fall within the moderate interval (55–154 $\mu\text{g m}^{-3}$). The green barrier (monitored values) lowers them down to the good interval (0–54 $\mu\text{g m}^{-3}$), thereby mitigating the risk of short or long-term health effects. Specifically, for traffic-induced emission, the monitored value (26.69 $\mu\text{g m}^{-3}$) falls in the middle of the good interval; however, in the case of construction activities (51.36 $\mu\text{g m}^{-3}$), the monitored value is close to the upper interval limit, nearing the “unhealthy for sensitive individuals” threshold. This highlights a potential health concern in relation to PM₁₀ concentrations, originating from construction activities.

The influence of construction activities on environmental pollution can be additionally analysed by comparing the PM₁₀ emission intensity from two sources. The absolute values of PM₁₀ concentrations, both modelled and monitored (Table I), indicate that construction activities need particular attention as a significant PM₁₀ pollution source.

The relative decrease in PM₁₀ concentrations behind the green barrier is moderately balanced (Table I), yet a more pronounced reduction is observed for traffic, when compared to construction activities as a pollution source. This difference in the effectiveness of UGS can be attributed to the nature of the pollution particles emitted from these two sources, and the mechanisms of their interaction with the surface of leaves – suggesting that vegetation might be more efficient in mitigating the traffic-originated particle species.

The average hourly PM₁₀ concentration values obtained through monitoring are presented in Fig. 5 for both traffic and construction activities. The frequency of traffic during working days is revealed, considering two distinct rush hours. They also highlight a slowdown in construction activities between 10 and 11 AM, corresponding to the breakfast break, and suggest that particles take approximately 2 h to settle after work cessation. The higher PM₁₀ values from construction activities may be attributed to the previously documented limited use of mitigation measures on building sites in Novi Sad.³⁷

The modelling of PM₁₀ concentrations simulated air pollution at the source (on the road), which would decrease on their path to buildings in the absence of vegetation to perform physicochemical processes and interact with air pollutants. The extent of that decrease would depend on meteorological factors, yet it would be much less significant than when street greenery is present. The notable dec-

rease in PM₁₀ concentrations observed behind the green barrier during the monitoring underscores the effectiveness of vegetation in mitigating urban air pollutants. This reduction in both traffic and construction-related PM₁₀ concentrations highlights the role of the green infrastructure in alleviating the adverse effects of the anthropogenic activities on air quality in urban environments. The intricate physicochemical processes involving PM and leaves, namely adsorption, absorption and chemical transformations, enable vegetation to function as natural filters, regulating the composition of PM, reducing its toxicity, and thereby improving air quality. It is important to emphasize that the protective role of street vegetation in these terms is contingent upon various factors, including street geometry and morphology,³⁸ traffic volume,⁶ the type of vegetation and its distribution,¹³ as well as ventilation conditions influenced by wind patterns.³⁹

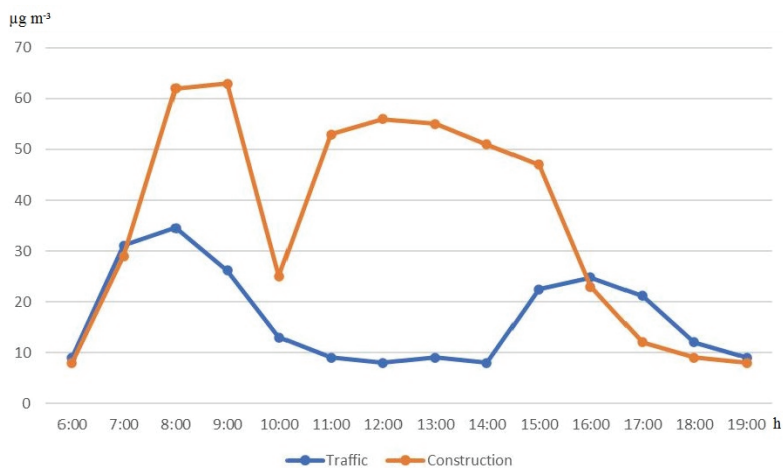


Fig. 5. Average hourly PM₁₀ concentration values obtained from monitoring.

The research findings highlight the broader challenges that Novi Sad faces in managing air pollution through urban green spaces (UGS). These results offer a valuable tool for sustainable urban planning and environmental management in the city, leading potential actions. Firstly, it is essential to identify the areas within the city with elevated air pollution levels where the strategic placement of vegetation can effectively mitigate pollutants. Secondly, there should be a priority on preserving and protecting existing vegetation, while also strategically planning for the creation of new UGS in urban regeneration projects. This approach will help maintain or enhance air quality in targeted neighbourhoods. Additionally, it is crucial to develop the UGS-related regulations that take into account factors such as traffic volume, residential density, and other urban planning parameters. Furthermore, efforts should be made to explore the strategies aimed at

optimizing traffic flow, reducing congestion, and promoting alternative transportation modes to minimize traffic-related emissions.

Consideration should also be given to the implementing measures that mitigate emissions during construction activities. This can be achieved by carefully selecting parameters, methodologies and indicators for monitoring and evaluating the effects of construction projects. Lastly, integrating the air quality monitoring programs into the city's infrastructure, incorporating the air pollution assessments into the city's land use planning process, and using monitoring data to inform the future urban planning decisions are vital steps to ensure the sustainable air quality management in Novi Sad. These recommendations are also closely tied to the the necessary measures to reduce the UGS-related issues outlined in local documents.

CONCLUSION

The research explored the effectiveness of vegetation in mitigating air pollution in a street in Novi Sad, with a focus on PM₁₀ emissions from traffic and construction activities. The research findings suggest that strategically implemented green infrastructure holds the significant promise for enhancing air quality in urban environments by successfully reducing the concentration of pollutants derived from anthropogenic activities. Future studies could assess the capacity of different plant species related to their physicochemical interactions with PM, in order to gain a better understanding of the physical and chemical impacts of pollutants on plants, which is essential for assessing their long-term viability as natural filters and air pollution mitigators. The research also highlighted the role of UGS as “environmental defenders” and underscored the importance of incorporating environmental management into urban planning to foster healthier and more sustainable cities. Regarding Novi Sad, its new Master Plan adopted in 2022 envisions substantial improvements and enhancements to the city's green infrastructure.⁴⁰ In addition to Novi Sad joining EBRD Green Cities in 2019, this signals the local government's shift toward adopting a proactive and environmentally responsible approach to addressing the current UGS-related issues, demonstrating the city's commitment to ensuring sustainable urban development. Therefore, the research findings, complimented by an overview of relevant literature in the field, can be regarded as a technical support to the city administrators and local stakeholders, which should be designed to facilitate the effective development and the implementation of UGS-related policy measures identified in the city's strategies and plans.

Acknowledgements. The paper was written within the project “Innovative Approaches and Advancement of Processes and Methods in Higher Education in Architecture, Urbanism and Scene Design” of the Department of Architecture and Urban Planning (Faculty of Technical Sciences, University of Novi Sad, Serbia). This research has been supported by the Min-

istry of Science, Technological Development and Innovation through project no. 451-03-47/2023-01/200156 “Innovative scientific and artistic research from the FTS (activity) domain”.

ИЗВОД

УТИЦАЈ УРБАНОГ ЗЕЛЕНИЛА НА СМАЊЕЊЕ КОНЦЕНТРАЦИЈЕ РМ ЧЕСТИЦА:
СЛУЧАЈ УЛИЦЕ У НОВОМ САДУ

МИЉАН ШУЊЕВИЋ¹, ДЕЈАНА НЕДУЧИН¹, РУЖИЦА БОЖОВИЋ², МАЈА СРЕМАЧКИ¹, БОРИС ОБРОВСКИ¹
и ИРИНА СУБОТИЋ¹

¹Факултет техничких наука, Универзитет у Новом Саду, Трг Доситеја Обрадовића 6, Нови Сад и

²Факултет техничких наука, Универзитет у Приштини са привременим седиштем у Косовској
Мишровици, Књаза Милоша 7, Косовска Мишровица

Услед брзог урбаног развоја и раста, градови широм света суочавају се са порастом загађења ваздуха, првенствено изазваним повећаним концентрацијама урбаних суспендованих честица (РМ), које потичу из различитих антропогених извора, као што су моторни саобраћај, грејање фосилним горивом и индустријске и грађевинске активности. Зеленило има капацитет да, путем физичко–хемијских процеса, природно филтрира суспендоване честице, служећи као ефикасан инструмент урбаног планирања за побољшање квалитета ваздуха. Кроз студију случаја улице у Новом Саду, другом по величини граду у Србији, истражује се ефикасност зеленила у смањењу честичног загађења које потиче од саобраћаја и грађевинских активности. Користећи методе мониторинга и моделовања, у раду се мере и предвиђају концентрације РМ₁₀ честица, а затим се евалуира ефикасност зеленила у њиховом смањењу. Резултати указују на значајно смањење измерених концентрација РМ₁₀ честица иза зелене баријере у поређењу са моделованим концентрацијама у близини извора загађења (на путу). Наглашава се значај зеленила као природног ублаживача загађења ваздуха у урбаним срединама и кроз формулисане препоруке се залаже за бољу интеграцију стратешког управљања животном средином у урбано планирање.

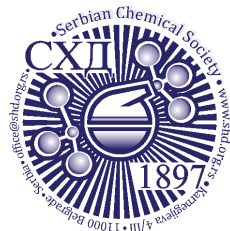
(Примљено 17. јануара, ревидирано 2. фебруара, прихваћено 7. марта 2024)

REFERENCES

1. T. M. T. Lei, M. F. C. Ma, *Sustainability* **15** (2023) 10993 (<https://doi.org/10.3390/su151410993>)
2. A. Mukherjee, M. Agrawal, *Environ. Chem. Lett.* **15** (2017) 283 (<https://doi.org/10.1007/s10311-017-0611-9>)
3. M. F. Zakaria, E. Ezani, N. Hassan, N. A. Ramli, M. I. A. Wahab, *IOP Conf. Ser.: Earth Environ. Sci.* **228** (2019) 012017 (<https://doi.org/10.1088/1755-1315/228/1/012017>)
4. F. Karagulian, C. A. Belis, C. F. C. Dora, A. M. Prüss-Ustün, S. Bonjour, H. Adair-Rohani, M. Amann, *Atmos. Environ.* **120** (2015) 475 (<https://dx.doi.org/10.1016/j.atmosenv.2015.08.087>)
5. J. Li, H. Chen, X. Li, M. Wang, X. Zhang, J. Cao, F. Shen, Y. Wu, S. Xu, H. Fan, G. Da, R. Huang, J. Wang, C. K. Chan, A. L. De Jesus, L. Morawska, M. Yao, *Atmos. Environ.* **212** (2019) 305 (<https://dx.doi.org/10.1016/j.atmosenv.2019.05.048>)
6. K. V. Abhijith, P. Kumar, J. Gallagher, A. McNabola, R. Baldauf, F. Pilla, B. Broderick, S. Di Sabatino, B. Pulvirenti, *Atmos. Environ.* **162** (2017) 71 (<https://dx.doi.org/10.1016/j.atmosenv.2017.05.014>)

7. D. Cheriyan, J. Choi, *J. Clean. Prod.* **254** (2020) 120077 (<https://dx.doi.org/10.1016/j.jclepro.2020.120077>)
8. E. Sekhavati, R. J. Yengejeh, *Front. Public Health* **11** (2023) 1130620 (<https://dx.doi.org/10.3389/fpubh.2023.1130620>)
9. H. Yan, G. Ding, H. Li, Y. Wang, L. Zhang, Q. Shen, K. Feng, *Sustainability* **11** (2019) 1906 (<https://dx.doi.org/10.3390/su11071906>)
10. T. Li, Y. Yu, Z. Sun, J. Duan, *Part. Fibre Toxicol.* **19** (2022) 67 (<https://doi.org/10.1186/s12989-022-00507-5>)
11. UN-Habitat, *World Cities Report 2022: Envisaging the Future of Cities*, United Nations Human Settlements Programme, Nairobi, 2022, <https://unhabitat.org/wcr/> (accessed November 3, 2023)
12. A. Diener, P. Mudu, *Sci. Total Environ.* **796** (2021) 148605 (<https://dx.doi.org/10.1016/j.scitotenv.2021.148605>)
13. S. Janhäll, *Atmos. Environ.* **105** (2015) 130 (<https://dx.doi.org/10.1016/j.atmosenv.2015.01.052>)
14. S. Wang, S. Cheng, X. Qi, *Front. Public Health* **8** (2020) 551300 (<https://dx.doi.org/10.3389/fpubh.2020.551300>)
15. M. Fadhil, M. N. Hamoodi, A. R. T. Ziboon, *IOP Conf. Ser.: Earth Environ. Sci.* **1129** (2023) 012025 (<https://doi.org/10.1088/1755-1315/1129/1/012025>)
16. A. Shishegaran, A. Shishegaran, M. Najari, A. Ghotbi, A. N. Boushehri, *Clean. Eng. Technol.* **1** (2020) 100002 (<https://dx.doi.org/10.1016/j.clet.2020.100002>)
17. A. Lee, H. Jordan, J. Horsley, *RMHP* **8** (2015) 131 (<https://doi.org/10.2147/RMHP.S61654>)
18. City of Novi Sad, *Strategy for the Development of the Green Spaces System of the City of Novi Sad 2015–2030*, Official Gazette of the City of Novi Sad, No. 22/2015, Novi Sad, 2015 (in Serbian)
19. A. Przybysz, A. Nawrocki, E. Mirzwa-Mróz, E. Paduch-Cichal, K. Kimic, R. Popek, *Environ. Sci. Pollut. Res.* (2023) (<https://dx.doi.org/10.1007/s11356-023-28371-6>)
20. J. Liu, Z. Cao, S. Zou, H. Liu, X. Hai, S. Wang, J. Duan, B. Xi, G. Yan, S. Zhang, Z. Jia, *Sci. Total Environ.* **616–617** (2018) 417 (<https://dx.doi.org/10.1016/j.scitotenv.2017.10.314>)
21. U. Weerakkody, J. W. Dover, P. Mitchell, K. Reiling, *Urban For. Urban Green.* **30** (2018) 98 (<https://dx.doi.org/10.1016/j.ufug.2018.01.001>)
22. S. Lu, X. Yang, S. Li, B. Chen, Y. Jiang, D. Wang, L. Xu, *Urban For. Urban Green.* **34** (2018) 64 (<https://dx.doi.org/10.1016/j.ufug.2018.05.006>)
23. S. Chen, H. Yu, X. Teng, M. Dong, W. Li, *Sci. Total Environ.* **853** (2022) 158656 (<https://dx.doi.org/10.1016/j.scitotenv.2022.158656>)
24. J. H. M. Schippers, *Adv. Bot. Res.* **105** (2023) 113 (<https://dx.doi.org/10.1016/bs.abr.2022.10.001>)
25. EEA, *Urban Green Infrastructure, 2018*, European Environment Agency, 2018, <https://www.eea.europa.eu/data-and-maps/dashboards/urban-green-infrastructure-2018> (Accessed October 28, 2023)
26. D. L. Badiu, C. I. Iojă, M. Pătroescu, J. Breuste, M. Artmann, M. R. Niță, S. R. Grădinaru, C. A. Hossu, D. A. Onose, *Ecol. Indic.* **70** (2016) 53 (<https://dx.doi.org/10.1016/j.ecolind.2016.05.044>)

27. F. de la Barrera, S. Reyes-Paecke, R. Truffello, H. De La Fuente, V. Salinas, R. Villegas, S. Steiniger, *Urban For. Urban Green.* **79** (2023) 127791 (<https://dx.doi.org/10.1016/j.ufug.2022.127791>)
28. S. Pouya, M. Aghlmand, *Environ. Monit. Assess.* **194** (2022) 633 (<https://dx.doi.org/10.1007/s10661-022-10298-z>)
29. City of Novi Sad, *Sustainable Development Strategy of the City of Novi Sad*, Official Gazette of the City of Novi Sad, No. 68/2017, Novi Sad, 2017 (in Serbian)
30. M. Petrović, L. Bajić, I. Stamenković, *Novi Sad - Strategic Framework of Urban Greenery in 2021*, BOŠ, Movement of the Highlanders of Novi Sad & Ministry for Human and Minority Rights and Social Dialogue, Novi Sad, 2021 (in Serbian)
31. EEA, *EMEP/EEA Air Pollutant Emission Inventory Guidebook 2019: Technical Guidance to Prepare National Emission Inventories (EEA Report No 13/2019)*, European Environment Agency, Luxembourg, 2019
32. National Greenhouse Gas Inventories Programme, *2006 IPCC Guidelines for National Greenhouse Gas Inventories*, Institute for Global Environmental Strategies, Hayama, 2006 (<https://www.ipcc-nggip.iges.or.jp/public/2006gl/>)
33. *Traffic Safety Strategy of the Republic of Serbia 2023-2030*, Official Gazette of the Republic of Serbia, No. 84/2023, Belgrade, 2023 (in Serbian)
34. PE Urbanizam, *Traffic Study of the City of Novi Sad with the Dynamics of Traffic Regulation*, Urban Planning, Development and Research Centre PE "Urbanizam" Novi Sad, Novi Sad, 2009 (in Serbian)
35. M. Šunjević, D. Reba, V. Rajs, B. Vujić, M. Ninkov, M. Vojinović-Miloradov, *Therm. Sci.* **27** (2023) 2275 (<https://dx.doi.org/10.2298/TSCI220215108S>)
36. EPA, *EPA Code Tables: AQI Breakpoints*, United States Environmental Protection Agency, 2024, https://aqs.epa.gov/aqswweb/documents/codetables/aqi_breakpoints.html (accessed January 3, 2024)
37. M. Šunjević, D. Reba, V. Rajs, B. Vujić, D. Nedučin, M. Vojinović-Miloradov, *FU Arch. Civ. Eng.* **20** (2022) 193 (<https://dx.doi.org/10.2298/FUACE221004015S>)
38. Y. Dai, A. Mazzeo, J. Zhong, X. Cai, B. Mele, D. Toscano, F. Murena, A. R. MacKenzie, *Atmosphere* **14** (2023) 1385 (<https://dx.doi.org/10.3390/atmos14091385>)
39. GLA, *Using Green Infrastructure to Protect People from Air Pollution*, Greater London Authority, London, 2019, <https://www.london.gov.uk/programmes-and-strategies/environment-and-climate-change/environment-publications/using-green-infrastructure-protect-people-air-pollution> (accessed October 28, 2023)
40. City of Novi Sad, *Master Plan of the City of Novi Sad until 2030*, Official Gazette of the City of Novi Sad, No. 33/2022, Novi Sad, 2022 (in Serbian).



J. Serb. Chem. Soc. 89 (5) 757–772 (2024)
JSCS–5754

Chemical engineering in technical and technological culture

LJUBICA POPOVIĆ¹•, NEMANJA SREMČEV¹*, DAMIR PURKOVIĆ²
and ILIJA ČOSIĆ¹••

¹University of Novi Sad, Faculty of Technical Sciences, Department of Industrial Engineering and Engineering Management, Trg Dositeja Obradovica 6, 21000 Novi Sad, Serbia and

²University of Rijeka, Department of Polytechnics, Sveučilisna avenija 4, 51000 Rijeka, Croatia

(Received 9 December, revised 19 December 2023, accepted 22 January 2024)

Abstract: Modern technologies continuously change humans and their relationship with the environment. They can achieve a lot in the field of chemical engineering, thereby improving and enhancing the quality of human life, but on the other hand, technologies can be used to destroy human lives. Technical and technological culture (hereinafter referred to as TTC) is the entirety of social achievements in the field of technical and technological sciences and their application, as well as of the all knowledge and skills needed to understand the achievements, use them correctly, transfer them to the younger generation and create new values in this field. This paper will present a pilot study aimed to examine the attitudes and beliefs of engineers, Technological (chemical engineering) and Technical faculties, regarding the development of TTC and to determine socio-demographic factors that may influence its development. The research was conducted in Serbia and Croatia. The results indicate that the most important aspects of TTC are: the development of awareness of sustainable development, the impact on environmental protection, *etc.* The respondents recognized the ethical challenges we face today, the need for the education of young engineers and the promotion of TTC in the media and professional public.

Keywords: environmental protection; ethical; attitudes; research; promotion; education.

INTRODUCTION

Engineering practice has been present since the beginning of humankind. The history of chemical engineering traces the historical and technological dev-

* Corresponding author. E-mail: nextesla@uns.ac.rs

• PhD candidate at University of Novi Sad, Faculty of Technical Sciences, Department of Industrial engineering and engineering management, Serbia.

•• Prof. emeritus at University of Novi Sad, Faculty of Technical Sciences, Department of Industrial engineering and engineering management, Serbia.

<https://doi.org/10.2298/JSC231209011P>

elopment of industry.¹ Today's modern technologies are not only a product of humans but also a prerequisite for their existence; they continuously change the mankind and their relationship to the environment.² A chemical engineer is a professional who researches, develops, advises and directs chemical processes at a commercial level.³ Developing a comprehensive skill set, including technical, professional, and technological expertise, is critical to success in an increasingly competitive global job market.⁴ At the turn of the millennium, there was a discrepancy between the trained engineers and the engineers that society needed, while there have been concerns about the ability of future professionals to act socially and to cope with the current global challenges, that are becoming much more complex and multidisciplinary.^{1,5} The engineering education is being urged to move towards student-centred teaching.¹ The competency-based curriculum represents a major paradigm shift in the conceptualization of the university education system.^{1,6} Professional competencies include three dimensions: knowledge, skills and attitudes.¹ To develop these skills, the global institutions have promoted and adapted teaching strategies aimed at preparing students to work in complex situations.¹ During the engineering education process, it is necessary to develop students' ability to perceive humanity and sociality, to bridge the gap between humanitarian and technical and technological culture, and to eliminate the traditional dehumanization of the engineering-technical education.⁷ The challenges for chemical engineers, at local, regional, national and global levels, require graduates to have strong training in technical skills and knowledge, but also in soft skills, and such as communication and teamwork, critical and creative thinking, ethics and sustainability, as well as in social responsibility.³ In 2019, Serbia and Macedonia held training called Escape Room, aimed to promote student engagement and motivation to master teaching content through playing, improve the communication skills *via* social interaction and fun, and develop creative, critical and logical thinking, self-regulation and a positive attitude towards chemistry lessons.⁸ The technological changes and the introduction of new technological concepts lead to the emergence of completely new needs regarding the behaviour and competencies of those who implement production processes.⁹ The introduction of technological innovations into everyday life, the readiness to recognize new solutions, the acquisition of the ability to exploit technological products is associated with a personal, organizational, and local culture, and should be analysed as a separate category – technical and technological culture.¹⁰ According to Wyrwicka, technical and technological culture is a system of permanent attitudes and efficiency, which enable the proper use of the existing technological products in order to change the pattern in the quality of life.¹⁰ It is expressed in relatively permanent and positive attitudes towards the phenomena of technology (design and product), in the possession of knowledge, and above all in the ethical behaviour and the attitude of people involved in different tech-

nological situations.¹⁰ Technical and technological culture manifests itself in relatively long-term activities and good ethical human attitudes, enabling the correct application of the existing technologies and the development of new ethical solutions aimed at the improvement of the efficiency of life's cooperative processes.¹¹ If we want to respond to the demands of future technological development, it is important to reinvest in the concept of technical and technological culture. It is also important for engineers, as they are the carriers of technical and technological culture, to ask themselves questions related to the impact of techniques and technology on society and the world we live in.¹² The social demands for greener products, a reduction in greenhouse gas emissions and more sustainable processes have also had an irreversible impact on the chemical industry.¹ The chemical engineering professionals must have the necessary skills and abilities to apply numerical solutions and understand their limitations and difficulties in approach, and also possess critical thinking, *etc.*¹ The role of engineers in the transformation of society is very clear. Engineers, throughout history, have been uniquely suited to provide new solutions to some of the humanity's greatest challenges.⁴ At present, the state of engineering has been assessed as critical, with a focus on four areas in particular: the taking over of engineering by unconventional design; the technological takeover of engineering; an awareness of the negative consequences of engineering; and a crisis in the traditionally scientific and engineering image of the world.¹³ In this context, technical and technological culture is a valuable aspect of modern and future education and includes the personal qualities that enable a technologically competent solution of any problems in the field of engineering and creative solutions to social and economic issues.¹³ The process of introducing technical and technological culture is sometimes very difficult and therefore it is necessary to overcome the inertia of technocratic thinking and a misunderstanding of the importance of the idea of developing technical and technological culture and the personal characteristics and qualities that are important for it.¹³ The European engineering education and academic networks in Europe should open up to cooperation with academic, student, industrial and professional partners worldwide and, in addition to lifelong learning, expand the inclusion of non-technical skills without lowering the technical level of the learning process and also improve the cooperation between companies and universities in the field of education.¹⁴ The mission of educators is to contribute not only to building a society of "knowledge" but also a society of "wisdom".¹⁴

This paper presents the pilot research on attitudes and beliefs about technical and technological culture, as well as socio-demographic factors that can have an impact on its development (gender, age, education, years of work experience, company size, ownership structure of the company and its activity, as well as satisfaction with the respondent's material status). The pilot research was conducted on a sample consisting of engineers from the Technical and Technological

Faculties (chemical engineering) in the Republic of Serbia and the Republic of Croatia. Professors/assistants, students and employees in the industry/IT sector/NGO also participated in the research. As part of the pilot research, a questionnaire was constructed to examine attitudes and beliefs about the development of technical and technological culture, which was created on the basis of a list of questions, related to the perception of the development of technical and technological culture (list of survey questions, Wyrwicka), supplemented with the indicators for popularization and the legislation of scientific and technical technological culture and the key competencies of polytechnic engineers.^{10,15,16}

METHODOLOGY

Pattern and procedure

A total of 105 respondents participated in the research, the majority of them were male (56.19 %), with a slightly higher number of respondents from Serbia (59.04 %) compared to respondents from Croatia (40.96 %). In relation to the engineering profile, a larger number of respondents were engineers of technical sciences (75.24 %) compared to engineers of technological sciences (chemical engineering) (24.76 %). The largest number of respondents were professors/assistants at faculties (54.29 %), followed by the employees in the economy/industry/IT/NGO (35.24 %), while the smallest number of respondents were students (10.48 %). The majority of respondents, from both countries, attended doctoral academic studies as their educational level (50.00 %). When it comes to differences between countries, and in the context of individual socio-demographic characteristics of the respondents, differences were present only in respect of company size. The respondents from Serbia are mostly employed in large companies (in excess of 250 employees), while respondents from Croatia are more often employed in medium-sized companies (from 50 to 250 employees). The complete socio-demographic characteristics of the sample, for the entire sample, as well as for each country individually, have been presented in Table I.

The data collection was carried out during September and October 2023, within the Republic of Serbia and the Republic of Croatia. The respondents were invited to participate in the research through various communication media (live, by phone, email, *etc.*) and were informed about the goals of the research, prior to filling out the questionnaire. The participation in the research was anonymous and the respondents needed about five minutes to answer the questionnaire. The data collection was carried out through the Google Forms platform.

Instrument

The questionnaire for the assessment of attitudes and beliefs on technical and technological culture (hereinafter: TTC), created for the purposes of this research, includes a total of 31 questions with a 5-point Likert-type response scale (from 1 – completely disagree to 5 – agree completely). The questionnaire items were devised in accordance with the subject of the measuring items, applied during the previous researches (for the use of which we obtained the author's consent), and are directly related to the research problem from this paper, as well as the assessment of several experts from the field.^{12,18,19} One question each was associated with the understanding of the meaning of the term TTC, as well as the development of TTC. The remaining questions were grouped into the sets of questions related to education on TTC (3 questions), promotion of TTC (3 questions), legal regulations related to TTC (2 questions), different attitudes and beliefs regarding TTC (18 questions) and cultural factors (3 questions).

TABLE I. Sociodemographic characteristics of the sample

Variable	Category	<i>N</i>	Total %	<i>N</i>	Serbia %	<i>N</i>	Croatia %	χ^2	<i>DF</i>	<i>p</i>
Gender	Male	59	56.19	30	48.39	29	67.44	3.74	1	.053
	Female	46	43.81	32	51.61	14	32.56			
Age (years)	20–24	4	3.81	2	3.23	2	4.65	7.43	6	.283
	25–29	11	10.48	5	8.06	6	13.95			
	30–34	20	19.05	10	16.13	10	23.26			
	35–39	12	11.43	9	14.52	3	6.98			
	40–49	38	36.19	27	43.55	11	25.58			
	50–59	15	14.29	6	9.68	9	20.93			
	60+	5	4.76	3	4.84	2	4.65			
Education	OAS	21	20.00	12	19.35	9	20.93	0.67	2	.714
	MAS	34	32.38	22	35.48	12	27.91			
	DAS	50	47.62	28	45.16	22	51.16			
Professional status	Students	11	10.48	7	11.29	4	9.30	2.17	2	.337
	Prof. and Ass. prof.	57	54.29	30	48.39	27	62.79			
	Employed in industry/IT/NGO	37	35.24	25	40.32	12	27.91			
Engineering profile	Technical	79	75.24	47	75.81	32	74.42	0.02	1	.871
	Technological	26	24.76	15	24.19	11	25.58			
Years of work experience	0–1	3	2.86	2	3.23	1	2.33	7.33	8	.501
	1–5	21	20.00	13	20.97	8	18.60			
	6–10	18	17.14	9	14.52	9	20.93			
	11–15	19	18.10	15	24.19	4	9.30			
	16–20	17	16.19	11	17.74	6	13.95			
	21–25	13	12.38	5	8.06	8	18.60			
	26–30	3	2.86	2	3.23	1	2.33			
	31–35	7	6.67	3	4.84	4	9.30			
	36+	4	3.81	2	3.23	2	4.65			
Company size (number of employees)	Micro (1–10)	4	3.81	3	4.84	1	2.33	14.59	3	.002
	Small (11–50)	15	14.29	8	12.90	7	16.28			
	Medium (51–250)	48	45.71	20	32.26	28	65.12			
	Large (250+)	38	36.19	31	50.00	7	16.28			
Company activity	Service	78	74.29	50	80.65	28	65.12	3.20	1	.073
	Production	27	25.71	12	19.35	15	34.88			
Ownership structure	Domestic public	70	66.67	39	62.90	31	72.09	6.85	3	.077
	Domestic private	26	24.76	14	22.58	12	27.91			
	Foreign	7	6.67	7	11.29	0	0.00			
	Shared ownership	2	1.90	2	3.23	0	0.00			
Satisfaction with material status	Very dissatisfied	1	0.95	1	1.61	0	0.00	3.69	4	.448
	Dissatisfied	11	10.48	7	11.29	4	9.30			
	Neider sat. nor dissat.	26	24.76	18	29.03	8	18.60			
	Satisfied	55	52.38	28	45.16	27	62.79			
	Very satisfied	12	11.43	8	12.90	4	9.30			

RESULTS AND DISCUSSION

The descriptive statistical analysis was performed using the SPSS program. The descriptive statistics and the correlations between variables have been presented in Tables II and III. Based on the value of the indicators of the shape of the distribution (skewness and kurtosis), we concluded that the distribution of all continuous measures were close to normal distribution. When it comes to correlation coefficients, the results pointed to the conclusion that the correlations were predominantly statistically significant, positive and of low to moderate intensity.

TABLE II. Descriptive statistical indicators; Min – minimum value; Max – maximum value; *AS* – arithmetic mean; *SD* - standard deviation; *Sk* – skewness; *Ku* – kurtosis

Indicator	Min	Max	<i>AS</i>	<i>SD</i>	<i>Sk</i>	<i>Ku</i>
Meaning of the term TTC (1)	1	5	3.89	0.93	-0.71	0.43
Development of TTC (2)	1	5	3.63	0.92	-0.24	-0.40
Edukation about TTC (3)	7	15	12.37	1.77	-0.56	0.03
Promotion of TTC (4)	7	15	11.57	1.64	-0.40	0.28
Legal regulations related to TTC (5)	2	10	6.38	1.49	-0.09	0.85
Development of awareness about TTC (6)	41	90	75.32	11.50	-0.85	0.44
Cultural factors (7)	6	15	11.55	2.31	-0.41	-0.44

TABLE III. Correlations between continuous measures; * $p < .05$; ** $p < .01$

Indicator	1	2	3	4	5	6	7
Meaning of the term TTC (1)	1						
Development of TTC (2)	.464**	1					
Edukation about TTC (3)	.648**	.562**	1				
Promotion of TTC (4)	.389**	.517**	.565**	1			
Legal regulations related to TTC (5)	.384**	.223*	.299**	.481**	1		
Development of awareness about TTC (6)	.240*	.211*	.279**	.342**	.123	1	
Cultural factors (7)	.248*	.070	.163	.195*	.089	.273**	1

The association and differences in socio-demographic variables, with the understanding of the meaning of the term TTC and the development of TTC, have been presented in Table IV. The satisfaction with material status achieves a statistically significant and positive correlation of low intensity with the question related to the development of TTC. The respondents from Croatia, and respondents/engineers of technical sciences, achieved higher scores than the respondents from Serbia, and the respondents/engineers of technological sciences (chemical engineering), with the respect to understanding the term TTC (Fig. 1). This data shows us that the technological faculties (chemical engineering) in Serbia should implement promotional activities (or education) for students, professors and employees in the economy/IT/NGO, about technical and technological culture, and contribute to its better understanding. The remaining correlations, as well as the differences between the groups, are not statistically significant.

TABLE IV. Association and differences in sociodemographic variables with the understanding of the meaning of the term TTC and the development of TTC. The results from the upper part of the table refer to the results obtained using the Pearson correlation coefficient r , while the results from the lower part of the table refer to the results obtained using t -test for independent samples/one-way analysis of variance

Variable	Meaning of the term TTC		Development of TTC	
	r /T/F-test	p	r /T/F-test	p
Age, years	.146	.137	.026	0.791
Education	-.181	.064	-.043	0.661
Years of work experience	.160	.103	.054	0.584
Company size	-.068	.491	-.097	0.327
Satisfaction with material status	.091	.358	.274	0.005
Gender	1.428	.156	-0.870	.386
Company activity	-0.736	.463	-0.248	.805
Country	-2.028	.045	-0.853	.396
Engineering profile	2.489	.014	1.314	.192
Professional status	0.932	.397	0.603	.549
Ownership structure	1.740	.164	2.622	.055

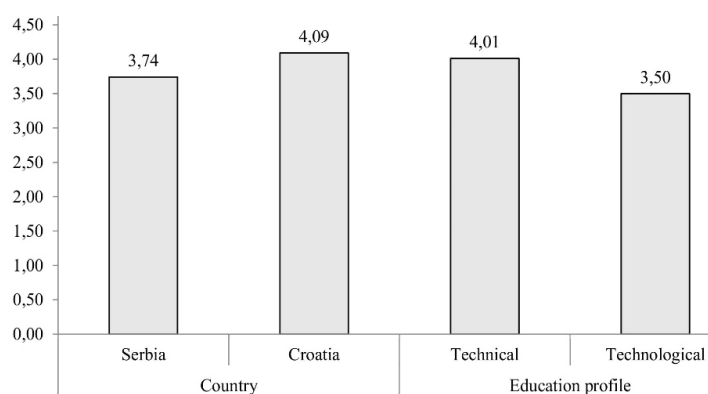


Fig. 1. Differences between countries and educational profiles in the context of understanding the meaning of the term TTC.

The association and the differences in socio-demographic variables with the understanding of the meaning of the term TTC and the development of TTC, especially by country and especially by engineering profile, have been presented in Tables V and VI. When it comes to correlations, there are significant and positive correlations between the satisfaction with material status and the development of TTC in the sub-sample of respondents from Serbia, as well as in the sub-sample of respondents/engineers of technological sciences (chemical engineering). This result indicates that the engineers of technological sciences (chemical engineering) in Serbia, who are more satisfied with their material status, have a more developed TTC in their environment. Age and work experience achieve significant and positive correlations with the meaning of the term TTC, on the

sub-sample of respondents/engineers of technical sciences. When it comes to the significance of the differences between the groups, the female respondents achieved higher scores on the understanding of TTC, on the sub-sample of respondents from Croatia, while male respondents from Serbia achieved higher scores from the companies that are jointly owned, compared to the respondents whose companies are from other categories of ownership structure. The remaining correlations and differences between groups are not statistically significant. The significant differences between groups have been presented in Fig. 2.

TABLE V. Association and differences in sociodemographic variables with the understanding of the meaning of the term TTC and the development of TTC, especially by country. The results from the upper part of the table refer to the results obtained using the Pearson correlation coefficient r , while the results from the lower part of the table refer to the results obtained using t -test for independent samples/one-way analysis of variance

Variable	Meaning of the term TTC				Development of TTC			
	Serbia		Croatia		Serbia		Croatia	
	r /T/F-test	p	r /T/F-test	p	r /T/F-test	p	r /T/F-test	p
Age, years	0.226	.077	0.064	.683	-0.005	.967	0.078	.618
Education	-0.185	.149	-0.206	.185	-0.138	.285	0.086	.584
Years of work experience	0.209	.103	0.042	.790	0.004	.973	0.101	.517
Company size	-0.066	.608	0.058	.713	-0.153	.235	0.058	.712
Satisfaction with material status	0.088	.497	0.046	.768	.311	.014	0.193	.214
Gender	0.928	.357	0.560	.578	0.287	.775	-2.212	.033
Company activity	-0.656	.515	0.167	.868	-0.671	.511	0.991	.327
Professional status	1.830	.169	0.093	.911	0.001	.999	1.269	.292
Ownership structure	2.189	.099	0.157	.694	3.104	.033	0.984	.327

The differences by country and engineering profile (technical and technological sciences), in the context of the remaining continuous measures, have been presented in Table VII and Fig. 3. Between the engineering profiles, the only statistically significant differences were identified on the dimensions education on TTC, where the respondents who belong to technical sciences achieve significantly higher scores than the respondents who belong to technological sciences. The remaining differences are not statistically significant, neither when it comes to the differences between countries, nor when it comes to the differences between engineering profiles (engineers of technical sciences and engineers of technological sciences (chemical engineering)).

When it comes to the degree of agreement between the respondents' statements related to attitudes and beliefs about what TTC refers to, the results (arithmetic means) have been presented in Table VIII. The results have been presented for the entire sample of respondents, subsamples by country and subsamples by engineering profile (technical and technological). Regardless of whether it refers

to the entire sample of respondents, or about sub-samples with the respect to country and engineering profile, the highest degree of agreement refers to the statements related to the development of the awareness of the environmental and social impact of engineering and technology, the development of the awareness of the impact of engineering and technology on sustainable development, encouraging the development of the awareness about the use of renewable energy sources, encouraging the interest and forming the positive attitudes among young people towards technique and technology, developing a responsible attitude towards work, work tools and one's own environment, and developing technical and information literacy.

TABLE VI. Association and differences in sociodemographic variables with the understanding of the meaning of the term TTC and the development of TTC, especially for engineering profiles (technical and technological). The results from the upper part of the table refer to the results obtained using the Pearson correlation coefficient r , while the results from the lower part of the table refer to the results obtained using t -test for independent samples/one-way analysis of variance

Variable	Meaning of the term TTC				Development of TTC			
	Serbia		Croatia		Serbia		Croatia	
	r /T/F-test	p	r /T/F-test	p	r /T/F-test	p	r /T/F-test	p
Age, years	.223	.049	0.202	.323	0.128	.262	-0.253	.212
Education	-0.072	.531	-0.373	.061	-0.022	.847	0.082	.691
Years of work experience	0.221	.050	0.230	.258	0.169	.136	-0.206	.312
Company size	-0.141	.216	0.030	.884	-0.181	.111	0.178	.384
Satisfaction with material status	-0.013	.913	0.200	.326	0.187	.098	.528	.006
Gender	0.342	.733	1.209	.238	-1.394	.167	0.111	.913
Company activity	-1.284	.203	1.480	.152	-1.443	.155	-1.357	.187
Professional status	0.286	.752	1.638	.213	0.850	.431	1.766	.196
Ownership structure	1.045	.378	1.153	.294	2.144	.102	0.053	.820

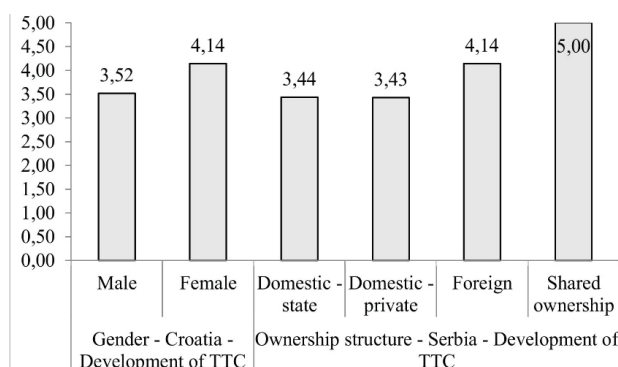


Fig. 2. Differences between TTC development in relation to gender (Croatia) and ownership structure (Serbia).

TABLE VII. Differences in relation to the country and engineering profile, and in the context of the remaining continuous measures

Item	Country		Engineering profile	
	<i>t</i> -Test	<i>p</i>	<i>t</i> -Test	<i>p</i>
Education about TTC	-1.932	0.056	2.715	0.008
Promotion of TTC	-1.638	0.104	0.118	0.907
Legal regulations related to TTC	-0.614	0.541	0.895	0.373
Development of awareness about TTC	0.067	0.946	0.813	0.418
Cultural factors	0.836	0.405	-0.549	0.584

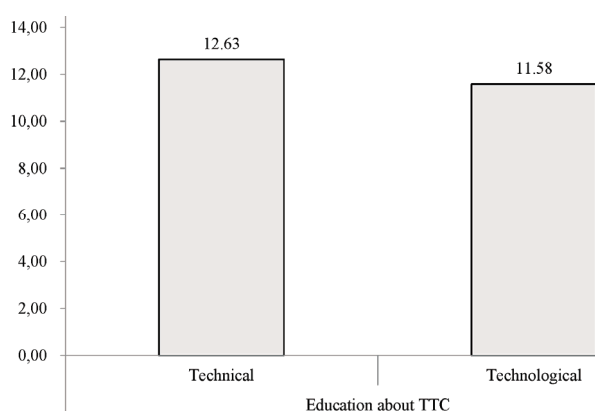


Fig. 3. Distinguishing engineers' profiles based on the cumulative score of three items pertaining to the significance of education about TTC.

TABLE VIII. The degree of agreement of respondents with the statements related to attitudes and beliefs about what TTC refers to

No.	Statement	Total	Technical engineers	Technological engineers	Serbia	Croatia
11.1.	Obeying to the norms for the successful performance of the work process	3.96	4.08	3.62	4.05	3.84
11.2.	Establishment of work procedures	4.11	4.22	3.81	4.10	4.14
11.3.	Creation of quality standards (standardization)	4.16	4.27	3.85	4.08	4.28
11.4.	Unification of the approach to technological problems	3.90	3.86	4.00	3.94	3.84
11.5.	Prevention (anticipating future needs for successful work performance)	3.98	4.08	3.69	4.00	3.95
11.6.	Thriftiness (not spending more than is needed)	3.90	3.90	3.92	3.84	4.00
11.7.	Paying greater attention to work efficiency (economy, rationality...)	4.13	4.19	3.96	4.15	4.12
11.8.	Solidarity in the work environment and cooperation (teamwork)	4.07	4.15	3.81	4.18	3.91

TABLE VIII. Continued

No.	Statement	Total	Technical engineers	Technological engineers	Serbia	Croatia
11.9.	Reliability in people when performing work tasks	3.98	4.08	3.69	4.06	3.86
11.10.	Work discipline	4.01	4.04	3.92	4.02	4.00
11.11.	Commitment to work (involvement in one's work)	3.97	4.04	3.77	4.02	3.91
11.12.	Developing an awareness of the environmental impact of technique and technology (importance of environmental protection)	4.38	4.42	4.27	4.32	4.47
11.13.	Developing an awareness of the social impact of technique and technology (human aspect)	4.42	4.47	4.27	4.37	4.49
11.14.	Developing an awareness of the impact of technique and technology on the sustainable development of society	4.52	4.49	4.62	4.48	4.58
11.15.	Encouraging the development of awareness about the use of renewable energy sources	4.44	4.35	4.69	4.45	4.42
11.16.	Encouraging interest and forming an affirmative attitude, among young people, towards technique and technology	4.45	4.37	4.69	4.35	4.58
11.17.	Developing a responsible attitude towards work, means of work and own environment	4.33	4.29	4.46	4.42	4.21
11.18.	Developing technical and IT literacy	4.60	4.57	4.69	4.56	4.65

Based on the research conducted in Poland, the author implies that technical and technological culture will be more important in future business environments and that it should be nurtured in every company, through organizational learning and continuous improvement.¹⁰ The development of students' professional competences can be developed through the implementation of technical and technological culture at faculties.¹² The results of the research conducted in Russia indicate that the introduction of content, for the formation of technical and technological culture among students, as future engineers, enables an increase in the level of development of technical and technological cultural indicators.¹³ In addition, it ensures the integration of special, professional and technological training that contributes to the formation of a certain technological view of the world, and the mastery of technical and technological culture.¹³ The results of the pilot research presented in this paper, which we conducted among the eng-

ineers of technological (chemical engineering) and technical faculties in Serbia and Croatia, confirmed that educating young people about technical and technological culture is perceived as very important. The empirical research was conducted in Hungary with the aim of examining the competencies of undergraduate engineering informatics students.¹⁷ Based on the obtained results, optional courses were introduced into the curricula for engineering studies aimed at developing their communication skills and preparing them for the globalized and competitive labour market.¹⁷ This research data has also highlighted the importance of teamwork and cooperation. The lack of required skills for the engineering sectors, which reduces the scope of employment for engineering graduates, is particularly pronounced in India where only 7 % of engineers are suitable for basic engineering jobs.¹⁸ Based on the research results, it has been suggested that the professional skills, as well as social skills, are equally important for future engineers, and their synergy in higher education can ensure more efficient learning and teaching processes, and improve the quality of education.¹⁷ This is also confirmed by the results of our pilot research, which also stresses the development of technical and information literacy, encouraging interest and forming positive attitudes among young people towards technique and technology. An intervention implemented, as part of an undergraduate course among chemical engineering students at Columbia, led to an increase in the students' perceptions of the development of teamwork and collaborative skills.⁴ The approach implemented in Macedonia and Serbia, called Escape Room, based on teamwork, communication, cooperation and problem solving, contributed to the promotion of creativity, critical and logical thinking, a positive attitude towards chemistry and encouraging student engagement and motivation.⁸ The project-based learning and the use of educational projects in science are also some of the powerful tools for the promotion, the motivation, and the inspiration of scientific and technical and technological culture.¹⁹ The promotional activities are very important for the development of technical and technological culture, and the results we obtained through the pilot research indicate that technical and technological culture has been insufficiently represented in the media, and that it should be promoted, in particular among experts and engineers. Godin and Gingras present a multidimensional model in which scientific and technical and technological culture is defined as having two dimensions: individual and collective.¹⁵ They discuss how this model can be used to define the indicators of scientific and technical and technological culture, and to understand the role of scientists in the dissemination of scientific and technical and technological culture.¹⁵ They also state that the scientific and the technical and technological culture is related to the promotional and diffusion activities aimed at the general public. Therefore, they point out that the ability to design and present relevant policies, for the executives and the managers in the industry, is the capacity to invest wisely in research; to evaluate

and select new technologies and ensure adequate training of employees and the proper maintenance of equipment.¹⁵ The results of this research indicate the importance of developing an awareness of the impact of technique and technology on sustainable development, developing a responsible attitude towards work, work tools and one's own environment, all of which is also a part of a technical and technological culture. A constructivist approach centred on chemical engineering students, applied to modernize the chemical engineering curriculum at the level of the faculty, defines the so-called sensitivities, capacities and competencies (SCC) as a set of attitudes, skills and knowledge necessary for the integral work of an engineer.³ They were considered from two points of view: general and disciplinary training. At the disciplinary level, the historic traditional pillars of chemical engineering have been preserved using the advantage of academic research, development and innovation (R+D+I), and the expertise required by industry across the university, in addition to the transversal priority areas for modern professional chemical engineering.³ The pilot research results obtained in this paper have presented the following views: developing an awareness of the ecological and social impact of technique and technology, developing an awareness of the impact of technique and technology on sustainable development, *etc.*

CONCLUSION

Technology is changing the world, and engineers are the ones who create, design, and produce everything in our environment, and that is the reason why their attitudes and beliefs are of importance, because of how the world will look tomorrow depends on them. In this pilot research, we used a questionnaire designed to examine the attitudes and beliefs of the engineers of technical and technological sciences (chemical engineering) about the technical and technological culture, which we believe has been unfairly overshadowed by the innovation and which is of great importance for the future directions of technical and technological development, and the engineers as their creators. The results obtained in this pilot research indicate that our respondents – engineers of technological sciences (chemical engineering) and technical sciences have positive attitudes towards the statements related to technical and technological culture, but state that they do not understand the meaning of the term technical and technological culture, which can be the result of insufficient representation of this topic in the media, as well as the lack of promotional activities among the general and professional public. The greatest misunderstanding of the term technical and technological culture was expressed by the respondents of technological sciences (chemical engineering) from Serbia, which could be significant for thinking about the education of young people, and the organization of promotional activities at faculties and among the general public. Given that our respondents were engineers, all interested parties should be involved in the promotion of technical

and technological culture: from universities, government, the private sector, and non-governmental organizations. A better understanding of the meaning of the term technical and technological culture, of the respondents from Croatia, can be linked to the legal regulations and the existence of laws of technical culture in Croatia. It is interesting that, although they express a lack of understanding of the term technical and technological culture, some significant and positive correlations were achieved between the satisfaction with material status, and the development of technical and technological culture in the working environment on the sub-sample of respondents from Serbia, as well as on the sub-sample of respondents/engineers of technological sciences (chemical engineering). It is indicated that the engineers of technological sciences (chemical engineering) in Serbia, who are more satisfied with their material status, have a more developed technical and technological culture in their environment. Based on an analysis of the obtained data, it can be concluded that all respondents agree that young people should be educated about technical and technological culture, that it is important to promote it among scientists and engineers, and that the topic of technological culture should be more represented in the media, and also, the legislation and the law on technical and technological culture should be adopted in Serbia as well. We hope that these results will stimulate thinking and will be followed by the specific actions regarding education and the promotion of the technical and the technological culture, so that all engineers develop positive and ethical attitudes when creating and applying techniques and technologies in the future.

The possible limitations of this pilot research are that the research was done only at the level of two countries, from the same region, so we think that the research should be extended to all the countries that are mentioned in this paper, which possess the technical and the technological culture. Therefore, the number of respondents should be increased in order to obtain more data.

What would be important for further research is to connect with the universities from all over the world, who have devoted the attention to the education of future engineers of technical and technological sciences, as well as to the promotion of technical and technological culture among scientists, experts, engineers and the general public, and the legal regulation of technical and technological culture.

Acknowledgement. This research (paper) has been supported by the Ministry of Science, Technological Development and Innovation through project no. 451-03-47/2023-01/200156 "Innovative scientific and artistic research from the FTS (activity) domain".

ИЗВОД

ХЕМИЈСКО ИНЖЕЊЕРСТВО У ТЕХНИЧКО-ТЕХНОЛОШКОЈ КУЛТУРИ

ЉУБИЦА ПОПОВИЋ¹, НЕМАЊА СРЕМЧЕВ¹, DAMIR PURKOVIĆ² и ИЛИЈА ЋОСИЋ¹

¹Факултет техничких наука Нови Сад, Универзитет у Новом Саду, Три Досићеја Обрадовића 6, 21000 Нови Сад и ²University of Rijeka, Department of Polytechnics, Sveučilisna avenija 4, 51000 Rijeka, Croatia

Савремене технологије континуирано мењају човека и његов однос са околином. Оне могу много постићи у области хемијског инжењерства, чиме се побољшава и унапређује квалитет људског живота, али са друге стране, технологије се могу користити и за уништавање људских живота. Техничко-технолошка култура (у даљем тексту ТТК) је свеукупност друштвених достигнућа у области техничко-технолошких наука и њихове примене, као и сва знања и вештине потребне за разумевање достигнућа, њихово правилно коришћење, пренос на млађе генерације и стварање нових вредности у овој области. У овом раду ће бити представљено пилот истраживање спроведено у циљу испитивања ставова и уверења инжењера технолошких (хемијско инжењерство) и техничких факултета у погледу развоја ТТК и утврђивања социо-демографских фактора који могу имати утицаја на њен развој. Истраживање је спроведено у Србији и Хрватској. Резултати указују да су важни аспекти ТТК: развој свести о одрживом развоју, утицај на заштиту животне средине, итд. Испитаници су препознали етичке изазове са којима се данас суочавамо, потребу за увођење ТТК у садржај образовања младих инжењера и промоцију ТТК у медијима и стручној јавности.

(Примљено 9. децембра, ревидирано 19. децембра 2023, прихваћено 22. јануара 2024)

REFERENCES

1. L. F. M. Franco, A. C. da Costa, A. F. de Almeida Neto, A. M. Moraes, E. B. Tambourgi, E. A. Miranda, G. J. de Castilho, G. Doubek, J. V. H. Dangelo, L. V. Fregolente, L. M. F. Lona, L. G. de La Torre, L. A. Alvarez, M. C. da Costa, P. F. M. Martinez, R. Ceriani, R. J. Zemp, R. P. Vieira, R. M. Filho, S. S. V. Vianna, S. M. A. Bueno, M. G. A. Vieira, R. S. Suppino, *Educ. Chem. Eng.* **44** (2023) 21 (<https://dx.doi.org/10.1016/j.ece.2023.04.001>)
2. J. Didier, in *Science, Technology and Innovation Culture*, M. Chouteau, J. Forest, C. Nguyen, Eds., ISTE Ltd., London, 2018 (<https://dx.doi.org/10.1002/9781119549666.ch7>)
3. D. Gomez-Rios, H. Ramirez-Malule, N. Marriaga-Cabrales, *Educ. Chem. Eng.* **44** (2023) 181 (<https://dx.doi.org/10.1016/j.ece.2023.06.002>)
4. M. A. Ballesteros, J. S. Sanchez, N. Ratkovich, J. C. Cruz, L. Reyes, *Educ. Chem. Eng.* **35** (2021) 8 (<https://dx.doi.org/10.1016/j.ece.2020.12.004>)
5. D. G. Broo, O. Kaynak, S. M. Sait, *J. Ind. Inf. Integr.* **25** (2022) 100311 (<https://dx.doi.org/10.1016/j.jii.2021.100311>)
6. A. Lunev, I. Petrova, V. Zaripova, *Eur. J. Eng. Educ.* **38** (2013) 543 (<https://dx.doi.org/10.1080/03043797.2013.824410>)
7. M. G. Evdokimova, in *IEEHGIP*, Z. Anikina, Ed., LNNS volume 131, Springer Nature, 2022, pp. 558–568 (https://dx.doi.org/10.1007/978-3-030-47415-7_59)
8. A. Naumoska, H. Dimeski, M. Stojanovska, *J. Serb. Chem. Soc.* **88** (2023) 563 (<https://doi.org/10.2298/JSC211228088N>)

9. M. K. Wyrwicka, A. Chuda, *Logforum* **15** (2019) 279
(<https://dx.doi.org/10.17270/J.LOG.2019.319>)
10. M. K. Wyrwicka, *Hum. Factor. Ergonom. Man. Service Ind.* **21** (2011) 178
(<https://dx.doi.org/10.1002/hfm.20254>)
11. D. E. Leidner, T. Kayworth, *MIS Q.* **30** (2006) 357 (<https://dx.doi.org/10.2307/25148735>)
12. Lj. Popovic, Dj. Cosic, S. Popov, *J. Mechatron. Autom. Identif. Technol.* **7** (2022) 1
(<http://jmait.org/wp-content/uploads/JMAIT-Vol-7-1-1-7.pdf>)
13. E. Rubtsova, I. Bogolyubova, G. Starodubtseva, S. Lyubaya, *IOP Conference Series: Earth and Environmental Science* **315** (2019) 022002, San Francisco, CA
(<https://dx.doi.org/10.1088/1755-1315/315/2/022002>)
14. C. Borri, E. Guberti, F. Maffioli, in *Proceedings of the SEFI 37th Annual Conference*, Rotterdam, Netherlands, 2009, Code: 112544
15. B. Godin, Y. Gingras, *Pub. Understand. Sci* **9** (2000) 43
(<https://dx.doi.org/10.1088/0963-6625/9/1/303>)
16. D. Purkovic, *STEMp technique: Occupational standards and qualification standards*, University of Rijeka, Polytechnic Study, Rijeka, Croatia, 2022 (ISBN 978-953-7720-57-5, available at: <https://www.bib.irb.hr/1185690>)
17. I. Holik, I. D. Sanda, *Int. J. Eng. Pedagog.* **10** (2020) 20
(<https://dx.doi.org/10.3991/ijep.v10i5.13727>)
18. S. Mekala, C. Harishree, R. Geetha, *JEET* **34** (2020) 76
(<https://dx.doi.org/10.16920/jeet/2020/v34i2/150740>)
19. N. Mendez, C. Castillo, D. Suarez, M. A. Castilla-Bolanos, in *Proceedings of the International Astronautical Congress*, IAC, 2022, Paris, France (ISSN 00741795, available in: (<https://iafastro.directory/iac/paper/id/72277/summary/>)).



J. Serb. Chem. Soc. 89 (5) 773–783 (2024)
JSCS–5755

Cultural heritage in the face of climate change: From protection to decolonisation

IRINA SUBOTIĆ¹, VIŠNJA KISIĆ^{2*} and DEJANA NEDUČIN¹

¹Faculty of Technical Sciences, University of Novi Sad, Serbia and ²Faculty of Sport and Psychology, EDUCONS University, Novi Sad, Serbia

(Received 9 February, revised 1 March, accepted 18 March 2024)

Abstract: The risks climate change poses to cultural heritage have garnered increased attention in recent decades, prompting reactions from organizations such as UNESCO and ICOMOS. While there is a consensus among heritage actors that the climate crisis requires a departure from “business as usual”, there is no unanimity regarding which aspects of heritage protection should remain unchanged and which necessitate transformation, nor what level of action and transformation is required. Such disagreements may not always be immediately apparent, as different approaches are often mentioned within the same policy paper or call for action. They offer different interpretations of the climate crisis impacts, different framings of what is at stake, and different political visions regarding the necessary steps, thus creating tensions. This paper utilizes maximum variation sampling to identify and analyse groups of approaches through which climate change has been addressed within the cultural heritage field, ranging from technical protection to decolonisation. It highlights the significance of grasping their political and eco-social underpinnings, crucial for fostering transdisciplinary dialogues that draw upon the expertise of natural and social sciences, engineering and humanities to alleviate tensions, jointly shape future actions and develop sustainable solutions that respect and protect heritage while fostering regenerative socio-ecological relations.

Keywords: climate crisis; approaches; tensions; transdisciplinarity; underpinnings.

INTRODUCTION

The global climate is undergoing an unprecedented and rapid change, primarily driven by anthropogenic activities that release greenhouse gases. These gases trap heat in the Earth’s atmosphere, resulting in a warming (greenhouse) effect and causing ice to melt, sea levels to rise, and weather extremes to increase.^{1,2} The climate crisis is intricately linked with numerous global challenges,

* Corresponding author. E-mail: visnja.kisic@tims.edu.rs
<https://doi.org/10.2298/JSC240209034S>

extending beyond environmental dimensions to impact economic, geopolitical and social spheres. As a result, there are growing calls for comprehensive and transformative actions that prioritize regenerative and sustainable practices and policies in addressing multifaceted issues linked to climate change.

The cultural heritage field has not been left out of such calls. The risks climate change poses to heritage sites in terms of accelerated degradation or potential loss have garnered increased attention over the past two decades.^{3,4} This heightened awareness has prompted relevant international organizations, such as United Nations Educational, Scientific and Cultural Organization (UNESCO) and International Council on Monuments and Sites (ICOMOS), to initiate various efforts aimed at assessing the anticipated impacts. However, the protection of cultural heritage from climate-related hazards still faces challenges in integrating specially designed measures into national plans for climate change adaptation.⁵ For instance, a 2022 EU report titled “Strengthening Cultural Heritage Resilience for Climate Change” highlights that only 12 EU member states include cultural heritage in their climate change policies.⁶

The integration of climate change discourse into cultural heritage research, policy, and practice has taken various forms and is becoming increasingly diverse. Spanning disciplines connected to social sciences, humanities and technical sciences, the heritage field finds itself at the intersection of complementary and conflicting research theories, methodologies and policy agendas related to addressing the impacts of the climate crisis.^{7,8} Critical heritage studies have drawn attention to tensions between humanities-based approaches to heritage protection and those primarily grounded in technical sciences, as well as between normative Western canons governing heritage policy and its global applications, prompting calls for pluralizing approaches.^{9,10}

The range of responses to the climate crisis within the heritage sector is expanding, encompassing both dominant and marginalized voices. It is evident that the heritage field is undergoing transformation, with many changes being driven by concerns related to climate change and its impacts. However, uncertainties persist regarding how the heritage field will address the climate crisis. Will the focus primarily be on technical adaptations to climate change? Will heritage simply adopt environmentally friendly practices and “go green”? Or could climate change and its associated challenges spur a more profound re-evaluation and transformation of our societies – consequently reshaping our understanding of heritage and altering our relationship with the past and the future? In this article, five groups of approaches to climate change within the heritage field are analysed and discussed, highlighting the diverse heritage politics they embody and enact.

METHODOLOGY

The climate crisis introduced novel approaches to heritage protection, each carrying different transformative implications. Despite the variety of approaches within the heritage field, they are often perceived as part of a unified response to the crisis and the differences often remain underexplored in heritage research, policy, and practice. The objective of this paper is to analyse several approaches that address climate change in different manners and elucidate their implications. The central questions posed are: What approaches can be identified within the cultural heritage field that address the climate crisis? What themes and interpretations regarding the connection between cultural heritage and climate change emerge from these approaches? What are the political implications of these approaches and what visions of cultural heritage and its future are either fostered or hindered by them? To illustrate the diversity of approaches, the analysis is based on a methodology known as heterogeneous sampling or maximum variation sampling, deliberately selecting phenomena that exhibit wide variations from one another.^{11,12} Consequently, the analysis does not encompass all possible attitudes, approaches and nuances related to the responses to climate change, but focuses on several illustrative and diverse phenomena. The aim is to identify their central themes, shedding light on the diversity of approaches and strategies resulting from the integration of climate change and broader ecological discourse within the cultural heritage field. In the following section, five distinct groups of approaches to climate change within the heritage field are identified and analysed.

FIVE GROUPS OF APPROACHES TO FRAMING CLIMATE CHANGE WITHIN THE CULTURAL HERITAGE FIELD

1. Protecting heritage against climate change: transformation through technical adaptation and risk mitigation

Climate change can impact buildings in numerous ways.^{13,14} The increased frequency and intensity of extreme weather events, such as hurricanes and floods, can directly damage buildings. Rising temperatures and more frequent heatwaves may subject building materials to thermal stress, causing deterioration. Coastal areas experiencing sea level rise are at risk of flooding and erosion, which can result in structural damage. Shifts in humidity levels can foster the growth of mold and fungi, compromising the structural integrity. Altered precipitation patterns may increase exposure to moisture, leading to rot and corrosion. In regions with permafrost, warmer temperatures can induce thawing, causing ground instability and affecting foundations. These effects are particularly pronounced in the case of historic buildings and structures. The majority of historic buildings and structures were not designed to resist 'new' climate conditions, which makes those with aged and fragile materials particularly vulnerable to climate change, while various legal constraints aiming to preserve their original features often limit the application of advanced climate adaptation techniques commonly used for modern buildings and structures.¹⁵ According to ICOMOS, in technical terms, "climate change will have an unprecedented impact on what is now considered to be good conservation practice. Modifications will be required, both to

better position heritage as an asset in climate action and to address the anticipated impacts of climate change".¹⁶

Over the past two decades, research on the observed and projected impacts of the climate crisis on cultural heritage has led to significant advancements in damage quantification and risk assessment, which are crucial for making informed decisions and implementing effective protection measures.¹⁷ A dedicated scientific field has emerged within cultural heritage studies and practice, focusing on the optimal ways to technically safeguard heritage amidst climate change.^{18,19} They encompass a range of measures and actions, including vulnerability and risk assessments, implementations of risk and disaster mitigation measures, climate change adaptation strategies, as well as preparedness, response and recovery actions.^{20,21} It is important to note that the conservation profession has long utilized scientific techniques to monitor and assess the impact of temperature, moisture, and winds, but also earthquakes, floods and droughts on cultural heritage sites.²²

The group of approaches advocating for the protection of heritage amidst the climate crisis through technical adaptation and risk mitigation provides valuable guidelines for enhancing conservation practices. It prioritizes objectivity and scientific grounding, focuses on the technical conditions of cultural heritage, and utilizes technical data to comprehensively assess the impacts of climate change. However, while these approaches recognize the reality of the climate crisis, they tend to neglect the broader economic, political, social, cultural and systemic dimensions underlying it. Instead, they often view the climate crisis solely as a threat that requires mitigation, posing challenges to heritage conservation efforts. Consequently, these approaches frequently overlook the deeper societal transformations needed to effectively respond to the climate crisis, including the potential role heritage might play in facilitating such transformations. This is where tensions between humanities-based approaches to heritage protection and those primarily grounded in natural sciences and engineering arise. In addition, some voices within this group advocate for the involvement of local communities in risk mitigation, recognizing heritage as a resource that can enhance community resilience and rootedness in the face of climate change.²³ They also emphasize the importance of "finding alternative ways and means of sustaining heritage significance amidst a changing climate" and ensuring that heritage responses to climate change are "holistic" and that they "include the social, environmental and cultural dimension of sustainability".²⁴

2. Re-interpreting heritage for climate action: raising public awareness and inspiring transformation by representing „climate-responsible“ past practices

Climate change science and policy often fail to provide ideas and imaginaries for post-carbon ways of living. This lack of imagination and alternatives is

increasingly being addressed within the heritage field. The fundamental questions are: What lessons can contemporary societies learn from ancient civilizations that thrived in pre-carbon eras to enhance resilience, adaptability, and environmental consciousness? Simultaneously, what insights can we glean from the *petrocultures* and heritage of the anthropocene to guide us forward? For instance, Interpret Europe's (European Association for Heritage Interpretation) workshops "Heritage Interpretation for Climate Cooling" drew attention to 'the power of the past' in terms of evoking how humans lived before the fossil fuel era and exploring how "heritage interpretation could be a way to engage more people with the issues surrounding the climate chaos we are facing".²⁵ This exemplifies a group of approaches that focus on the interpretative, educational, and awareness-raising potential of heritage to help societies react to climate change. In such approaches, prominent themes include leveraging the attachment to a place that heritage fosters to galvanize climate action, utilizing cultural heritage to underscore the urgency of responding to climate change, and learning about adaptation and mitigation strategies from cultural heritage.²⁶ Furthermore, these approaches stress that "traditional knowledge, buildings, and landscapes" predating the fossil fuel era can illuminate the path to "post-carbon living".²⁷

This group of approaches acknowledges a fundamental critique inherent in the anthropocene narrative: that the industrial revolution and reliance on coal and fossil fuels have triggered unprecedented environmental destruction and have significantly influenced climate change.²⁸ However, what they often overlook are the colonial and anthropocentric historical practices that facilitated the emergence of the global "capitalist world-ecology".²⁹ The primary challenge faced by these approaches is political in nature, *i.e.*, how the narrative of climate change is constructed and how pre-carbon societies are interpreted will shape the political visions promoted through heritage.

3. *Greening heritage: embracing transformations in line with green policies*

Heritage advocates often highlight the sustainability of existing buildings, emphasizing that "the greenest building is... one that is already built".³⁰ They also stress the mitigation benefits of minimizing the introduction of new materials that contribute to additional carbon emissions during production.³¹ However, many practices deeply engrained in the heritage sector are now under scrutiny due to climate change. This includes examining the energy requirements of heritage and museum buildings, as well as evaluating lighting, cooling and humidity standards for their safeguarding. Therefore, the pressing question is how to make heritage (and museums) "green" and transition to post-carbon modes of functioning. The "greening" group of approaches offers a variety of strategies to address this challenge, such as ecological footprint calculations, ongoing monitoring, improving energy efficiency, transitioning to green energy sources, red-

ucing waste, promoting reuse and recycling, implementing new legal regulations, as well as introducing principles and practices of the circular economy.

In its political underpinnings, this group of approaches aligns with green policies and assumes public funding for structural transformations, while predominantly relying on market-led solutions for the implementation of renewable technologies. However, despite being labelled as *green*, these approaches are firmly rooted in anthropocentric world relations.³² The danger lies in the possibility that “green transformations” of heritage may further exacerbate existing geopolitical and economic inequalities, including climate injustices, as green deal-type investments and transitions are primarily affordable in the wealthiest countries of the Global North.

4. *Opposing extraction and exploitation through heritage safeguarding*

The discourse on climate change is increasingly intertwined with efforts to preserve both natural and cultural heritage, aiming to prevent further extraction, exploitation, and destruction of urban and rural areas and landscapes. However, many “sustainable development” and “green” agendas have prioritized economic goals over social and ecological concerns, often tolerating cultural and territorial destruction in the pursuit of economic progress.³³ In response, a group of approaches has emerged, involving individuals and groups within the heritage sector, as well as local communities, who view heritage safeguarding as a political opposition to the dominant capitalist system characterized by extraction, exploitation and destruction. These actors advocate for a reconsideration of approaches to heritage amidst climate change by defending heritage on a local level against the “development” plans of large corporations and speculative investor-led projects. The case of Rosia Montana, a mining town nestled in the mountains of Romania, exemplifies this group of approaches. The Rosia Montana Project, initiated in the 1990s, aimed to establish Europe’s largest open-pit gold mine, spearheaded by a Canadian mining company. As local opposition to the project grew, it was joined by environmental and cultural heritage organizations, leading to the framing of Rosia Montana as a mining cultural landscape. Themes of safeguarding versus extraction and destruction, localized relations *versus* globalized capital interests, community versus profit and environmental protection *versus* pollution were evident in protests, media coverage and legal battles.³⁴ While climate change was not the central focus, concerns about biodiversity loss and territorial destruction were present. After two decades of struggle, Rosia Montana was ultimately inscribed on the UNESCO World Heritage List.³⁵

The approaches exemplified by Rosia Montana embrace an inclusive and democratic vision of heritage, broadening its scope to encompass more communal and localized aspects. These approaches are transformative in a critical and oppositional manner, mobilizing local communities to safeguard their herit-

age in the face of potential destruction. They situate climate change within the Capitalocene discourse, opposing the narrative of the “Anthropocene era” and its underlying logic of perpetual exploitation. However, there is a risk that some of these approaches may be co-opted within the capitalist logic of heritage-led regeneration, thus it is crucial to distinguish between heritage-making actions that foster commoning and those that commodify heritage.³⁶

5. Decolonizing heritage and conservation for climate action

While a significant number of policy texts and guidelines on climate action and heritage make references to indigenous wisdom and ancestral knowledge, there is a lack of meaningful effort to truly reconsider and reimagine the heritage sphere from indigenous ontological and epistemic perspectives. However, there is a distinct group of approaches aiming to revive what has been erased, marginalized and colonized through promoting regenerative, interspecies practices of care. These initiatives start from the premise that prevailing modern heritage is a product and reflection of colonial, anthropocentric and capitalist histories and politics. They primarily originate from indigenous communities in the Global South, seeking to reclaim their local knowledge as part of efforts to decolonize heritage and conservation practices.³⁷ Unlike the aforementioned approaches that are grounded in anthropocentric ontologies and epistemological positions, this group addresses heritage and climate change through the lens of “Epistemologies of the South”.³⁸ The central focus of these approaches is the revival of indigenous cosmovisions grounded in interspecies care, kinship and local ancestral practices. In this context, heritage is conceptualized as intricately tied to the territory and encompassing all spiritual and material relationships spanning generations, varying from place to place and from community to community. Examples of these approaches, which seek to interlink biological, cultural, ancestral, territorial and spiritual aspects of heritage, include the practice of “sacred agriculture” by the Xukuru do Ororubá Indigenous people in the state of Pernambuco, Brazil, and the establishment of the Indigenous Devenir University in the Inga territories of the Andean Amazon, Colombia, which fosters land-based learning, ancestral wisdom and multispecies care. These approaches frame climate change within a call for radical eco-social transformation and decolonization. Their essence is deeply political, insisting on rethinking heritage in conjunction with challenging dominant global economic and social relations and structures.

CONCLUSION

In this paper, various lenses have been identified for analysing and categorizing the multitude of approaches to climate change within the heritage field. The presented categorization is not exhaustive, while also concealing potential interconnectedness between approaches belonging to different groups. For instance, some approaches focusing on heritage transformation through technical adapt-

ation and risk mitigation can complement the goals of green transformation or align with local and indigenous efforts to decolonize heritage and conservation practices. The greening of heritage can intersect with broader questions of colonialism and capitalist extraction, while local and indigenous communities may draw from the technical or greening toolbox to achieve energy autonomy. Reinterpreting the heritage of pre-carbon societies can involve both green transformation of heritage and its examination through decolonial and anti-capitalist lenses. These interconnections demonstrate that tensions between the approaches to climate change within the heritage field are not necessarily inherent and suggest that collaborative and holistic approaches could help alleviate them, while also leveraging the diverse strengths of each approach.

While climate change is often depicted as an all-encompassing and uncontrollable crisis necessitating unprecedented actions, dominant discourses on the subject tend to perpetuate the status quo. Notions of “humanity as a whole” and universal “techno-optimistic” solutions prevalent in these discourses often obscure important political questions. According to Swyngedouw, the emphasis on the “Spectre of Climate Change” serves to normalize the current neoliberal order and economic practice, thereby hindering calls for radical transformations.³⁹ Given this context, it is plausible that the heritage field may also adopt these dominant discourses. What remains obscured in such narratives are the issues of climate injustices and their colonial, capitalist and anthropocentric roots. Therefore, it becomes increasingly vital to recognize heritage studies and practices as political and as bearing significant eco-social implications.

This article demonstrates that responses to the climate crisis within the heritage field are diverse. Each group of approaches is deeply rooted in specific ideas about heritage and necessary changes, shedding light on their eco-social and political underpinnings. A comprehensive understanding of these underpinnings is essential for fostering transdisciplinary and inter-sectoral dialogues, drawing upon the expertise of natural and social sciences, engineering, as well as humanities, to collaboratively shape future transformative actions that are responsive to the complexities of climate change and its intersection with heritage. Ultimately, the goal is to develop sustainable solutions that respect and protect heritage while fostering regenerative socio-ecological relations.

Acknowledgement. This research has been carried out as part of the project “EPICA – Encouraging Participation in Architecture and Culture: Activating Public Resources for and with Communities” (ID 7744648), supported by the Science Fund of the Republic of Serbia.

ИЗВОД

КУЛТУРНО НАСЛЕЂЕ ПРЕД ИЗАЗОВИМА КЛИМАТСКИХ ПРОМЕНА: ОД ЗАШТИТЕ ДО ДЕКОЛОНИЗАЦИЈЕ

ИРИНА СУБОТИЋ¹, ВИШЊА КИСИЋ² и ДЕЈАНА НЕДУЧИН¹¹Факултет техничких наука, Универзитет у Новом Сагу и ²Факултет за спорти и психологију, ЕДУКОНС Универзитет, Нови Саг

Ризици које климатске промене представљају за културно наслеђе изазвали су велики интерес, током претходних деценија, и подстакли организације као што су UNESCO и ICOMOS на реакцију. Иако су актери у области културног наслеђа једногласни да климатске промене захтевају одступање од „уобичајеног начина деловања“, међу њима не постоји консензус око тога који аспекти заштите културног наслеђа могу да се одвијају по уобичајеним процедурама, а које треба трансформисати, као ни око потребних нивоа деловања и трансформација. Таква неслагања нису увек видљива на први поглед из разлога што се различити приступи често помињу у оквиру истог документа или позива на акцију. Ови приступи имају различита тумачења утицаја климатске кризе, различита разумевања онога што је улог, као и различите политичке визије о томе које кораке треба предузети, што резултира тензијама. У овом раду користи се узорковање максималних варијација да би се идентификовало и анализирано пет група приступа кроз које су климатске промене обухваћене у области културног наслеђа, од техничке заштите до деколонизације. Указује се на значај разумевања њихових политичких и еко-друштвених основа, што је кључно за подстицање трансдисциплинарних дијалога који се ослањају на експертизу природних, инжењерских и друштвених наука и инжењеринга како би се ублажиле тензије, заједнички обликовале будуће акције и креирала одржива решења која поштују и штите наслеђе.

(Примљено 9. фебруара, ревидирано 1. марта, прихваћено 18. марта 2024)

REFERENCES

1. Z. Bassam, J. Shkhashiri, Jerry, A. Bell, *Arab. J. Chem.* **7** (2014) 5 (<https://dx.doi.org/10.1016/j.arabjc.2013.10.004>)
2. A. E. Stagrum, E. Andenæs, T. Kvande, J. Lohne, *Sustainability* **12** (2020) 1721 (<https://dx.doi.org/10.3390/su12051721>)
3. E. Sesana, A. S. Gagnon, C. Ciantelli, J. Cassar, J. J. Hughes, *WIREs Clim. Change* **12** (2021) (<https://dx.doi.org/10.1002/wcc.710>)
4. H. Fluck, M. Dawson, *Policy Pract.* **12** (2021) 263 (<https://dx.doi.org/10.1080/17567505.2021.1990492>)
5. C. Daly, C. E. Purcell, J. Donnelly, C. Chan, M. MacDonagh, P. Cox, *J. Cult. Heritage Manage. Sustain. Dev.* **11** (2021) 313 (<https://dx.doi.org/10.1108/JCHMSD-04-2020-0053>)
6. European Commission Directorate-General for Education, Youth, Sport and Culture, *Strengthening Cultural Heritage Resilience for Climate Change: Where the European Green Deal Meets Cultural Heritage*, Publications Office of the European Union, Luxembourg, 2022 (<https://data.europa.eu/doi/10.2766/44688>)
7. M. Strlič, *Angew. Chem. Int. Ed.* **57** (2018) 7260 (<https://dx.doi.org/10.1002/anie.201804246>)

8. E. Waterton, S. Watson, *Int. J. Herit. Stud.* **19** (2013) 546 (<https://dx.doi.org/10.1080/13527258.2013.779295>)
9. T. Winter, *Int. J. Herit. Stud.* **19** (2013) 532 (<https://dx.doi.org/10.1080/13527258.2012.720997>)
10. T. Winter, *Int. J. Herit. Stud.* **20** (2014) 556 (<https://dx.doi.org/10.1080/13527258.2013.798671>)
11. C. Robson, *Real World Research: A Resource for Social Scientists and Practitioner-Researchers* (2nd ed.), Blackwell Publishers Ltd., Oxford, 2002 (ISBN 10 0631213058)
12. M. Q. Patton, *Qualitative research and evaluation methods* (3rd ed.), Sage, Thousand Oaks, CA, 2002 (ISBN 10 0761919716)
13. D. Crichton, N. Fergus, S. Roaf, *Adapting Buildings and Cities for Climate Change: A 21 Century Survival Guide* (2nd Ed.), Elsevier, Oxford, UK, 2009 (ISBN 9780080961279)
14. IPCC, *Climate Change 2022 – Impacts, Adaptation and Vulnerability: Working Group II Contribution to the Sixth Assessment Report of the Intergovernmental Panel on Climate Change*, Cambridge University Press, Cambridge, 2023 (<https://dx.doi.org/10.1017/9781009325844>)
15. A. Haugen, C. Bertolin, G. Leijonhufvud, T. Olstad, T. Broström, *Geosci.* **8** (2018) 370 (<https://dx.doi.org/10.3390/geosciences8100370>)
16. Climate Change and Cultural Heritage Working Group of ICOMOS, *The Future of Our Pasts: Engaging cultural heritage in climate action. Outline of Climate Change and Cultural Heritage*, ICOMOS, Paris, 2019 (<https://openarchive.icomos.org/id/eprint/2459/>)
17. A. Bonazza, A. Sardella, *Heritage* **6** (2023) 3578 (<https://dx.doi.org/10.3390/heritage6040190>)
18. L. Kotova, J. Leissner, M. Winkler, R. Kilian, S. Bichlmair, F. Antretter, J. Moßgraber, J. Reuter, T. Hellmund, K. Matheja, M. Rohde, U. Mikolajewicz, *Her. Sci.* **11** (2023) (<https://dx.doi.org/10.1186/s40494-022-00853-9>)
19. D. Bienvenido-Huertas, M. León-Muñoz, J. J. Martín-del-Río, C. Rubio-Bellido, *Build. Environ.* **200** (2021) 107959 (<https://dx.doi.org/10.1016/j.buildenv.2021.107959>)
20. S. Fatorić, C. Daly, *Wiley Interdiscip. Rev. Clim. Change* **14** (2023) (<https://dx.doi.org/10.1002/wcc.855>)
21. R. Jigyasu, *J. Int. Aff.* **73** (2019) 87 (<https://www.jstor.org/stable/26872780>)
22. J. M. Madariaga, *Anal. Methods* **7** (2015) 4848 (<https://dx.doi.org/10.1039/C5AY00072F>)
23. H. E. Kim, *Int. J. Cult.* **18** (2011) 259 (<https://dx.doi.org/10.1017/S094073911100021X>)
24. ICOMOS, *Resolution 20GA/15: Cultural Heritage and the Climate Emergency. Agenda item 6-6-1*, 2020, p. 2, https://www.icomos.org/images/DOCUMENTS/Secretariat/2020/Cultural_Heritage_and_the_Climate_Emergency-Resolution_20GA_15_.pdf (accessed on 20 November 2023)
25. Interpret Europe, *Hot topic – Heritage interpretation for climate cooling*, <https://interpret-europe.net/news/2021/hot-topic-heritage-interpretation-for-climate-cooling/> (accessed on 11 November 2023)
26. *The Future of Our Pasts: Engaging cultural heritage in climate action. Outline of Climate Change and Cultural Heritage*, p. 11
27. Climate Heritage Network, *Empowering People to Imagine and Realise Climate Resilient Futures Through Culture – from Arts to Heritage: The Climate Heritage Network 2022-24 Action Plan*, p. 4, <https://www.climateheritage.org/s/CHN-Action-Plan-Final.pdf> (accessed on 20 November 2023)

28. W. Steffen, J. Grinevald, P. Crutzen, J. McNeill, *Phil. Trans. R. Soc., A* **369** (2011) 842 (<https://dx.doi.org/10.1098/rsta.2010.0327>)
29. *Anthropocene or Capitalocene? Nature, history, and the crisis of capitalism*, J. W. Moore (Ed.), PM Press, New York, 2016 (ISBN 9781629631486)
30. C. Elefante, *Forum J.* **27** (2012) 62 (<https://dx.doi.org/10.1353/fmj.2012.a494514>)
31. A. P. González, *The Heritage Machine: Fetishism and Domination in Maragateria, Spain*, Pluto Press, London, 2019, p. 214 (<https://dx.doi.org/10.2307/j.ctv86dhrk>)
32. D. Vela Almeida, V. Kolinjivadi, T. Ferrando, B. Roy, H. Herrera, M. Vecchione Gonçalves, G. Van Hecken, *Polit. Geogr.* **105** (2023) 102925 (<https://dx.doi.org/10.1016/j.polgeo.2023.102925>)
33. M. Hemmingsen, in *The Nature of Peace and the Peace of Nature*, A. Fiala, Ed., Brill, Leiden, 2016, p. 81 (https://dx.doi.org/10.1163/9789004299597_010)
34. I. Velicu, *Globalizations* **12** (2015) 846 (<https://dx.doi.org/10.1080/14747731.2015.1100858>)
35. M. Dawson, *Hist. Environ.: Policy Pract.* **8** (2017) 25 (<https://dx.doi.org/10.1080/17567505.2017.1291593>)
36. P. A. González, in *Globalized World*, P. F. Biehl, D. C. Comer, C. Prescott, H. A. Soderland, Eds., Springer, Cham, 2015, p. 27 (ISBN 978-3-319-09688-9)
37. *Decolonize Conservation: Global Voices for Indigenous Self-Determination, Land, and a World in Common*, A. Dawson, F. Longo, (Eds.), Common Notions, New York, 2023 (ISBN 9781942173762)
38. B. de Sousa Santos, *Epistemologies of the South: Justice Against Epistemicide*, Routledge, London, 2014 (ISBN 9781612055459)
39. E. Swynedouw, *Theory Cult. Soc.* **27** (2010) 213 (<http://dx.doi.org/10.1177/0263276409358728>).